KU LEUVEN

FACULTY OF SCIENCE

Holographic RG flows in gauged supergravity

Thibeau WOUTERS

Supervisor: Prof. N. Bobev
Institute for Theoretical Physics, KU Leuven

Thesis presented in
fulfillment of the requirements
for the degree of Master of Science
in Physics

Academic year 2021-2022

Abstract

We study renormalization group flows of three-dimensional superconformal Chern-Simons field theories using holography. The gravity duals of the flow solutions are constructed in four-dimensional maximally supersymmetric gauged supergravity theories which are known to embed into string theory or M-theory. We work within a $\mathbb{Z}_2^3$-invariant truncation which keeps 14 real scalar fields out of the 70 scalar fields of the maximal four-dimensional supergravity. Our work brings forward new RG flows in the ABJM, SU(N) Chern-Simons and J-fold CFTs which are dual to domain wall solutions interpolating between supersymmetric vacua of, respectively, de Wit-Nicolai SO(8), dyonically gauged ISO(7) and dyonically gauged $[\mathrm{SO}(6) \times \mathrm{SO}(1,1)] \ltimes \mathbb{R}^{12}$ supergravity. Moreover, our results reveal that RG flows can break the continuous symmetry group along the flow within the $\mathbb{Z}_2^3$-truncation. Our solutions are constructed from a novel numerical algorithm which is designed, developed and tested in this work. As this algorithm is inspired by basic concepts of machine learning, our positive results indicate that combining theoretical physics with machine learning promises to be a fruitful direction of future research.

Acknowledgements

As you open the first page of this thesis, a chapter of my life comes to an end. Five years of physics education have culminated in this manuscript in front of you. It is only appropriate to thank everyone and everything that supported me throughout my education and in the preparation of this thesis in particular.

First of all, I would like to give lots and lots of thanks to my parents and my brother for their infinite amount of love, support and motivation. Without them, I would have never started my studies, and because they believed in me, they sparked the motivation to give the best of me throughout these five years. There are a lot of people that made my studies a great experience with many great stories. I thank my dear fellow master students HannaH, Cassandra, Seppe and Alex for sharing our struggles and for upgrading the ITF office of the crumbling physics building to a cosy place to hang out. Thanks for our pizza nights at the office which made the final, intense weeks of writing a joy. Additional thanks to Hannah and Cassandra for all the fun we had: the teatimes, dinners, our two hour long 'coffee breaks', the prom, our weekend trip, for enduring my *Harry Potter* imitations, karaoke mania and unbeatable (except by Cassandra) *Just Dance* skills – and more memories to come! You made working on the master thesis an incredibly fun experience which I'll never forget. Thanks Hannah for being such a joyful office buddy. Thanks Cassandra for our discussions on strings and branes – I am not sure if, without them, I would have realized that branes are, in fact, *not* magical flying carpets. Going from 200D to 200B, I'd like to thank my math friends with particular mention of Robbe and Rune. Our beer tasting sessions last year made the combination of a pandemic and tons of deadlines more manageable. Additional thanks to Rune for helping me out with group theory in this thesis, and to Robbe for joining our wonderful prom night. I'd also like to thank my best friends, the *#2804,6* gang, for their many years of wonderful friendship and all good laughs, with a particular emphasis on the long nights of *Mario Kart* in the past academic year as support for this thesis. I would like to thank Lucas, because he asked me to mention him in the acknowledgements.

I would like to thank my supervisor, Nikolay Bobev, for his guidance in this project and all advice and help offered along the way. Your way of teaching is inspiring, just like your wit and general attitude towards life. Thanks for the book recommendations and the Easter chocolate! I would like to thank the entire ITF for their hospitality and warm welcome of master students. Thanks for our office, thanks Anneleen and Filip for the coffee and cookies and everyone for the enjoyable coffee breaks. Thanks to Val and Brandon for occasionally answering some of my questions. Thanks Toine for signing my copy of the *Supergravity* book. Thanks to the ITF for organizing the holography workshop. Also *dankuwel*, Thomas and *grazie*, Enrico, for reading this thesis. I hope you enjoy it and apologies for the large number of pages! Don't be discouraged: there are

many pictures to look at!

Thanks to Leuven for being such a wonderful city to live in. Thanks to *Café Belge* for the supply of *Gulden Draak 9000 Quadruple*. Thanks to my dogs Oscar and Fien and our cat Fidel. Thanks to my *Spotify* playlist *Groovy Tunes* for giving me focus while writing the thesis.

And finally, I want dedicate this last, most significant part of my acknowledgements section to thanking the most important person in my life, my love and my soulmate, Eline. This silly acknowledgements section is far too short to express my eternal gratitude and does not even come close to conveying how lucky I am for having you in my life. You are my sunshine, you make me happy when skies are gray. I thank you for standing next to me and supporting me at every moment of this five year long journey. Thanks for the uncountable laughs and all our moments of joy. Thanks for enduring my many phases in preparation of the thesis, from my grumpy and frustrated mood up to the exhilarated-by-exhaustion mood. You fill my heart with an immeasurable amount of love, you are the true hero behind this piece of work!

Thanks everyone!

Summary in layman's terms

Imagine that we lived in a world much like our own, with many cultures and languages, but lacking any means of translation. Different communities would be unable to exchange any information when they encounter each other. We would never learn to be humble from the story of Daedalus and Icarus, we would never get inspired to be as heroic as Hercules and we would never grasp the profound life lessons of Dostoevsky. In some sense, this artificial world portrays the landscape of theoretical physics established at the end of the 20^{th} century.

Physics of the 20^{th} century is marked by two intellectual revolutions. On the one hand, the famous theory of general relativity, formulated by Einstein, provided a new description of space, time and gravity. Einstein's theory allows us to understand phenomena on the scale of large and heavy objects, such as planets, stars, and galaxies. On the other hand, during the previous century, it was observed that a quantum nature of reality emerges once we probe Nature at the smallest possible length scale, even smaller than the atom. The subsequent development of particle physics required a new theoretical framework, known to physicists as quantum field theory, in order to explain this behaviour. These two theories, general relativity and quantum field theory, are both formulated in their own language and, like the hypothetical world we fantasized above, lack any means to talk to each other. This is a conceptual problem in theoretical physics, as some situations require us to deal with large matter densities at small scales. For example, at the dawn of our universe, an event known as the Big Bang, the entire observable universe was compressed into a size comparable to that of an atom. Describing this 'primeval atom' is impossible with general relativity or quantum field theory alone. Hence, we need a new theory, called quantum gravity, to provide us with an accurate description of such phenomena.

Currently, the most viable candidate for quantum gravity is string theory. Out of studies of string theory came a remarkable discovery, which plays the role of the *deus ex machina* in our story. That is, string theory brought forward a dictionary that allows us to translate expressions from the language of gravity theories to the language of quantum field theory and vice versa. This link, known as the AdS/CFT correspondence, gives physicists new computational tools that provide a window into the phenomena of so-called strongly coupled quantum field theories. The term 'strong coupling' signifies that it is hard or even impossible to do computations in the theory. An exciting feature of the AdS/CFT dictionary is that it translates these 'hard problems' of a quantum field theory into 'easier problems' formulated in a gravity theory, enabling us to compute and solve these problems. In this thesis, we explore applications of this interesting aspect of the AdS/CFT dictionary. In particular, we gain insight on the dependence of strongly coupled quantum field theories on the energy scale with the help of calculations performed in a gravity theory.

Beknopte samenvatting

Stel je voor dat we in een wereld zouden leven gelijkend op de onze, met verschillende culturen en talen, maar zonder enige manier om te vertalen. We zouden nooit leren om nederig te zijn vanuit het verhaal van Daedalus en Icarus, we zouden nooit geïnspireerd worden om zo heroïsch te zijn als Hercules, en we zouden nooit in staat zijn de diepe levenslessen van Dostojevski te vatten. In zekere zin weerspiegelt deze fictieve wereld het landschap van de theoretische fysica aan het einde van de 20^{ste} eeuw.

De fysica van de 20^{ste} eeuw is gekenmerkt door twee intellectuele revoluties. Aan de ene kant gaf de befaamde algemene relativiteitstheorie van Einstein ons een nieuwe beschrijving van ruimte, tijd en gravitatie. Einstein's theorie laat ons toe om fenomenen te vatten op de schaal van erg grote en zware objecten zoals planeten, sterren en sterrenstelsels. Aan de andere kant observeerde men in de vorige eeuw dat er een kwantum versie van de realiteit naar voren treedt wanneer we de Natuur onderzoeken op de kleinste schaal, zelfs kleiner dan een atoom. De daaropvolgende ontwikkeling van de deeltjesfysica had nood aan een nieuw theoretisch kader, dat fysici kwantumveldentheorie noemen, om dit gedrag te verklaren. Deze twee theoriën, de algemene relativeit en de kwantumveldentheorie, zijn geformuleerd in hun eigen taal en, net als de fantasiewereld van hierboven, hebben geen manier om met elkaar in conversatie te treden. Dit is een conceptueel probleem in de theoretische fysica, aangezien we in bepaalde situaties geconfronteerd worden met grote materiedichtheden op kleine schalen. Bij het ontstaan van ons universum, de oerknal, bijvoorbeeld, was het hele heelal samengeperst in een volume vergelijkbaar met dat van een atoom. Het beschrijven van dit 'oeratoom' is onmogelijk met alleen maar algemene relativiteit of kwantumveldentheorie. Daarom hebben we nood aan een nieuwe theorie, genaamd kwantumgravitatie, om zulke fenomenen accuraat te beschrijven.

Momenteel is de meest geschikte kandidaat voor een theorie van kwantumgravitatie de snaartheorie. Uit onderzoek in de snaartheorie kwam een opmerkelijke ontdekking, die de rol speelt van de *deus ex machina* in ons verhaal. Dat wilt zeggen, snaartheorie heeft een woordenboek naar voren gebracht dat ons toelaat om vertalingen te maken van de taal van de gravitatie naar de taal van een kwantumveldentheorie en omgekeerd. Deze link, gekend als de AdS/CFT correspondentie, geeft fysici een nieuw rekenkundig werktuig dat een blik werpt in zogenaamde sterk gekoppelde kwantumveldentheoriën. De term 'sterk gekoppeld' wijst erop dat berekeningen moeilijk of zelfs onmogelijk zijn. Een stimulerend aspect van het AdS/CFT woordenboek is dat het de 'moeilijke problemen' van een kwantumveldentheorie vertaalt naar 'makkelijkere problemen' in een gravitatie theorie, zodat we deze problemen kunnen berekenen en oplossen. In deze thesis onderzoeken we toepassingen van dit interessante aspect van het AdS/CFT woordenboek. We verwerven inzicht in de wijze waarop sterk gekoppelde kwantumveldentheoriën afhangen van de energieschaal dankzij berekeningen in een gravitatie theorie.

Contribution statement

The project and goals were defined by Nikolay Bobev (supervisor). We thank him for addressing all key points of this thesis and guiding the project to its end.

All figures and tables are our own creations. All code written for this thesis (both Python and Mathematica code) is our own creation. Advice on the code and optimisation of computations were given by the supervisor. Explorations on new loss functions, as mentioned in Section 9.6.3, are inspired by conversations with the supervisor. Our first few lines of Mathematica code are inspired by an introductory notebook created by Brandon Robinson. We invented the toy model from Section 4.2 as illustration. Preliminary tests of working with Mathematica were done together with the supervisor related to his earlier work on holographic RG flows. Original, analytic calculations (*i.e.*, not directly adapted from references) in this thesis are: the calculation following equation (6.54), the calculation following (7.17) and the calculations in Chapter 8. For the latter, we thank Antoine Van Proeyen for checking these calculations and his recommendations on improvements.

Chapter 9 mostly consists of independent, original work, which we now summarize. Generally speaking, we work in a larger truncation compared to the literature, and as such, our work directly verifies and extends earlier results from the literature. More details on earlier work are provided in each of the separate sections. We verified the locations of all critical points in the larger truncation and give these locations in Appendix A. We computed the linearized BPS equations around each of the vacua and give these in Appendix A. We constructed all the flows given in the figures throughout this chapter and we give details on the initial conditions used in our work in Appendix A.

We found a mistake in one of the papers of the supervisor, and we reported the correct version in equation (9.3). We designed and developed the numerical algorithm from Section 9.1.2. We implemented this algorithm in Mathematica. We tested and optimized the working of this algorithm up until its final state, which we believe to be free of bugs. In Section 9.2, we computed the location of the `P1200000` critical point, guided by an older note from the supervisor which detailed a $\mathrm{U}(1) \times \mathrm{U}(1)$-invariant truncation which enabled us to find the location. We computed the values given in Table 9.2. We found new holographic RG flows which were not reported in the literature before, which are discussed in detail in this section. We came up with a way of estimating the number of solutions in an orbit of a critical point, discussed in Section 9.2.5, and computed these estimates in Table 9.3.

In Section 9.3, we provide more accurate numerical values for the locations of the `P25697101` and `P35610235` vacua compared to the literature, specified in Appendix A. We computed the values given in Table 9.5. The final two rows of this table were already computed in the literature by Guarino, Tarrio and Varela, but we report the same values with a higher numerical accuracy. We constructed all holographic RG flows that are

shown in this section and found new flows to the P25697101 vacuum. We computed the estimates given in Table 9.5.

In Section 9.4, we computed the values given in Table 9.8. The flow from Figure 9.23 is obtained from a linearized BPS equation and corresponding initial conditions by Guarino and Sterckx. We found two new holographic RG flows. We found a new initial condition that, with the linearized BPS equation from Guarino and Sterckx, resulted in Figure 9.24. We found a new linearized BPS equation and initial condition for the flow of Figure 9.25. In Section 9.5, we computed the values of Table 9.10. We found a mistake in a paper of the supervisor and we have provided the correct location of the P07582970 vacuum in Appendix A. We computed all the values that are given in Appendix B.

Nomenclature

List of Abbreviations

ABJM Aharony-Bergman-Jafferis-Maldacena

BPS Bogomol'nyi–Prasad–Sommerfield

CFT conformal field theory

EH Einstein-Hilbert

FP fixed point

GR general relativity

IR infrared, used to denote low energy/large distance behaviour

KK Kaluza-Klein

ML machine learning

OPE operator product expansion

QCD quantum chromodynamics

QED quantum electrodynamics

RG renormalization group

SCA superconformal algebra

SCFT superconformal field theory

sugra supergravity

susy supersymmetry

SYM super Yang-Mills

UV ultraviolet, used to denote high energy/short distance behaviour

List of Symbols

AdS_d anti-de Sitter space-ti,e in d dimensions

α' Regge slope, equal to ℓ_s^2

ℓ_s string length

$\eta_{\mu\nu}$ Minkowski space-time metric in D dimensions with mostly plus convention, *i.e.* $\eta_{\mu\nu} = \mathrm{diag}(-1, 1, 1, \ldots, 1)$

κ^2 $8\pi G$, with G the gravitational constant

Λ cosmological constant, or cut-off scale in Sections 3.4 and 4.3

$\mathcal{D}_\alpha$ Kähler covariant derivative

$\mathcal{K}$ Kähler potential

$\mathcal{K}_{\alpha\overline{\beta}}$ Kähler metric

$\mu, \nu, \ldots$ coordinate indices

∇_μ covariant derivative with respect to diffeomorphisms

$a, b, \ldots$ local frame indices

D_μ covariant derivative with respect to local Lorentz transformations

g gauge coupling

$g_{\mu\nu}$ space-time metric

g_s string coupling

L length scale of AdS

S^n The n-sphere.

$T_{\mu\nu}$ energy-momentum tensor

V scalar potential

W superpotential

We use natural units ($\hbar = c = 1$) and the mostly plus convention for the metric.

List of Figures

2.1 Visual representation of a chart ϕ on a manifold M, with domain U such that $\phi(U)$ is an open set in $\mathbb{R}^n$. 9
2.2 Illustration of the tangent space T_pM (grey) at a point p on the manifold. Also shown is a curve γ on the manifold going through p, and its velocity vector at p is an element of T_pM. 10

3.1 Visual representation of the exponential mapping from a Lie algebra $\mathfrak{g}$ to a Lie group G, with $T_\gamma G$ represented as tangent space of the manifold G. . 19

4.1 Illustrative example of fine-tuning a flow between critical points, involving saddle points. The streamlines of the system of equations of (4.6) are shown (red) along with the critical points (black dots) and some solutions, explained in detail in the text. 30
4.2 Illustration of RG flows in a theory space $\mathcal{T}$ around a fixed point (CFT) at couplings $\boldsymbol{g}^\star$. Blue (red) arrows denote deformations by irrelevant (relevant) operators and show how a QFT will flow from the UV to the IR. Generic flows, starting from deformations from both irrelevant and relevant operators, are shown in black. 32

5.1 One-loop diagrams involving fermions f and their scalar superpartners S. Their contributions cancel out and solves the hierarchy problem. 35
5.2 Branes in string theory. (a) A point-particle or 0-brane. (b) Two inequivalent 1-branes: an open string (left) and a closed string with a visualization of its $2d$ world-sheet (right). (c) Dp-brane visualized as a plane, with an open string attached to the brane. 38
5.3 Links between the Standard Model, supersymmetry and -gravity, and superstring theories discussed in this chapter. They are organized according to energy regimes at which they are (believed to be) valid descriptions of Nature. 39

6.1 Lie (super)algebras encountered in this thesis and their corresponding generators. Bold ellipses denote Lie algebras, while dashed ellipses denote superalgebras. 44
6.2 Overview of the gauged supergravities and the $\mathbb{Z}_2^3$-truncation appearing in this thesis. A detailed discussion is given in the text. 53

7.1 Illustration of the argument leading to the Maldacena conjecture. Details are given in the text. Left: open string point of view at $g_sN \ll 1$. Right: closed string point of view at $g_sN \gg 1$. 59
7.2 Relation between the two different points of view, taking the supergravity limit, and dualities relating the different descriptions. 61

8.1 Sketch of the single scalar toy model. (a) Scalar potential with two critical points, giving two AdS vacua lying at the UV and the IR. (b) Generic scalar and scale factor profiles as a function of r. The slopes of the scale factor (red) are related to the length scales of AdS. 67

9.1 Higher-dimensional origin of the four-dimensional gauged supergravities (with gauge groups G) discussed in this chapter, along with their dual field theories. 77
9.2 Visualization of the step descent algorithm in a one-dimensional parameter space. Starting from an initial parameter $A^{(1)}$ (black dot), the parameter space is explored in the direction of decreasing loss function values towards the minimum of the loss function (red dot). 81
9.3 Overview of holographic RG flows in the SO(8) theory discussed in this section. 84
9.4 Top: Direct flow from the SO(8) vacuum (origin) in the UV to the G_2 vacuum in the IR. Bottom: Direct flow from the SO(8) vacuum (origin) in the UV to the SU(3) × U(1) vacuum in the IR. The arrows denote the direction in which the physical solution will flow: from the UV towards the IR. 86
9.5 Triangular flow from the SO(8) vacuum (origin) in the UV to the G_2 vacuum (crosses) and eventually reaching the SU(3) × U(1) vacuum (dots) in the deep IR. 86
9.6 Plot of the profile $A'(r)$ related to the solution shown in Figure 9.5. Dashed lines show the value of $1/L$, with L the length scale of the corresponding AdS space-time. 87
9.7 Flow from the SO(8) vacuum (origin) in the UV to the U(1) × U(1) vacuum (dots) in the IR, which was found in [93]. 88
9.8 Flow from the SO(8) vacuum (origin) in the UV to the U(1) × U(1) vacuum (dots) in the IR, where the continuous symmetry is broken along the flow. 88
9.9 Flow from the SO(8) vacuum (origin) in the UV to the G_2 vacuum (crosses) and eventually reaching the U(1) × U(1) vacuum in the IR and preserving the U(1) × U(1) symmetry. 89
9.10 Triangular flow from the SO(8) vacuum (origin) in the UV to the G_2 vacuum (crosses) and to the U(1) × U(1) vacuum (dots) in the deep IR. . . . 89
9.11 An inequivalent triangular flow from the SO(8) vacuum (origin) in the UV to the G_2 vacuum (cross) and to the U(1) × U(1) vacuum (dots) in the deep IR. 90
9.12 Flow from the SO(8) vacuum (origin) in the UV to the SO(3) vacuum (dots) in the IR which preserves the SO(3) symmetry. 91
9.13 Flow from the SO(8) vacuum (origin) in the UV to the SO(3) vacuum (dots) in the IR, where the continuous symmetry is broken along the flow. 91

9.14 Flow from the SO(8) vacuum (origin) in the UV to the G_2 vacuum (cross) and eventually reaching the SU(3) × U(1) vacuum (dots) in the IR which preserves the SO(3) symmetry. 91
9.15 Flow from the SO(8) vacuum (origin) in the UV to the G_2 vacuum (cross) and eventually reaching the SU(3) × U(1) vacuum (dots) in the IR, where the continuous symmetry group is maximally broken. 92
9.16 An attempt to construct a flow from the SU(3) × U(1) vacuum in the UV to the U(1) × U(1) vacuum in the IR. 93
9.17 Visualization of the scalar potential V and the SO(8) and G_2 vacua. Since the G_2 breaks the continuous symmetry, it has a continuous orbit (red) within the 70-dimensional scalar manifold. However, since we only consider a 14-dimensional subspace of the scalar manifold (black line), only a few points of this orbit are vacua within our truncation (black dots). Figure adapted from [94]. 93
9.18 Overview of known holographic RG flows in the ISO(7) theory. 97
9.19 Flow from the G_2 vacuum (cross) in the UV to the U(1) vacuum `P2569710` (dots) in the IR. The flow itself preserves U(1) symmetry. 98
9.20 Flow from the G_2 vacuum (cross) in the UV to the U(1) vacuum `P2569710` (dots) in the IR. The flow itself breaks the U(1) symmetry. 98
9.21 Flow from the G_2 vacuum (cross) in the UV and reaching the SU(3) × U(1) vacuum (dots) in the IR. 99
9.22 Flow from the G_2 vacuum (cross) in the UV and reaching the SO(4) vacuum (dots) in the IR. 99
9.23 Flow from the $\chi_{1,2,3} = 0$ vacuum in the UV with SU(3) symmetry to the $\chi = 0$ vacuum with SU(2) × U(1) symmetry in the IR. 103
9.24 Flow from the $\chi^{\star}_{1,2,3}$ vacuum with SU(2) × U(1) symmetry in the UV to the $\chi = 0$ vacuum with SU(2) × U(1) symmetry in the IR. 103
9.25 Flow from a vacuum with U(1) × U(1) symmetry in the UV to the $\chi = 0.01$ vacuum with U(1) × U(1) symmetry in the IR. 104
9.26 Visualization of a major drawback of gradient descent algorithms. The algorithm converges to a local minimum (red) lying close to the initial guess (black) and is unable to find the true minimum (blue). 107

List of Tables

3.1 Dimensions of the simple Lie algebras. 21

6.1 Weyl weights of the generators of the superconformal algebra. 44
6.2 Four gauge groups of $4d$ gauged supergravities considered in this thesis and their values of $a, b, \tilde{a}, \tilde{b}$ which parametrize the superpotential via equations (6.49) and (6.50). 52

9.1 Supersymmetric vacua in the SO(8) gauged supergravity. Potential values are at $g = 1$. 84
9.2 Values of δ_a for the susy vacua in SO(8) gauged supergravity, with the multiplicity given in brackets. The integer n denotes the number of parameters of the loss function. 84
9.3 Lower bounds on number of distinct copies of each of the critical points. . 94
9.4 Supersymmetric vacua in the ISO(7) gauged supergravity. Potential values are at $g, m, c = 1$. 96
9.5 Values of δ_a for the susy vacua in ISO(7) gauged supergravity, with multiplicity given in brackets. For `P2569710` and `P3561023`, all δ_a have multiplicity one. The integer n denotes the number of parameters of the loss function. 96
9.6 Lower bounds on number of distinct copies of each of the critical points in the ISO(7) theory. 100
9.7 Supersymmetric vacua of the $[\mathrm{SO}(6) \times \mathrm{SO}(1,1)] \ltimes \mathbb{R}^{12}$ gauged supergravity. Potential values are at $g = c = 1$. Symmetry enhancements occur at special values for the parameters $\chi, \chi_{1,2,3}$ and φ given in the appendix. 102
9.8 Values of δ_a for the susy vacua, with multiplicity given in brackets. The integer n denotes the number of parameters of the loss function. 102
9.9 Supersymmetric vacua in $[\mathrm{SO}(6) \times \mathrm{SO}(2)] \ltimes \mathbb{R}^{12}$ gauged supergravity. Potential values are at $g = c = 1$. 105
9.10 Values of δ_a for the susy vacua. All values have multiplicity 1. The integer n denotes the number of parameters of the loss function. 105
9.11 Comparison between algorithms to construct holographic RG flows currently being used in the literature and the algorithm designed in this thesis. 107

B.1 Masses of the 14 scalar fields at vacua of SO(8) gauged supergravity. The two roots $\Delta_\pm$ are obtained using equation (B.2). Grey-coloured values of Δ_- are below the unitarity bound and hence do not correspond to scaling dimensions in the dual theory. Boldface values of $\Delta_\pm$ denote modes that are selected by the linearized BPS equations. 119

B.2 Masses of the 14 scalar fields at vacua of ISO(7) gauged supergravity. The two roots $\Delta_\pm$ are obtained using equation (B.2). Grey-coloured values of Δ_- are below the unitarity bound and hence do not correspond to scaling dimensions in the dual theory. Boldface values of $\Delta_\pm$ denote modes that are selected by the linearized BPS equations. 120
B.3 Masses of the 14 scalar fields at vacua of $[\mathrm{SO}(6) \times \mathrm{SO}(1,1)] \ltimes \mathbb{R}^{12}$ gauged supergravity. The two roots $\Delta_\pm$ are obtained using equation (B.2). Grey-coloured values of Δ_- are below the unitarity bound and hence do not correspond to scaling dimensions in the dual theory. Boldface values of $\Delta_\pm$ denote modes that are selected by the linearized BPS equations. The values of $\chi^\star_{123}$ are given in equation (9.18). 121
B.4 Masses of the 14 scalar fields at vacua of $[\mathrm{SO}(6) \times \mathrm{SO}(2)] \ltimes \mathbb{R}^{12}$ gauged supergravity. The two roots $\Delta_\pm$ are obtained using equation (B.2). Grey-coloured values of Δ_- are below the unitarity bound and hence do not correspond to scaling dimensions in the dual theory. Boldface values of $\Delta_\pm$ denote modes that are selected by the linearized BPS equations. 122

Contents

Abstract i

Acknowledgements ii

Summary in layman's terms iv

Beknopte samenvatting v

Contribution statement vi

Nomenclature ix

List of Figures xii

List of Tables xiv

Contents xvii

1 Introduction 1
- 1.1 The landscape of theoretical physics . . . 1
- 1.2 AdS/CFT and the holographic dictionary . . . 3
- 1.3 Renormalization group flows and their holographic translation . . . 4
- 1.4 Outline . . . 6

I Preliminaries 8

2 General relativity 8
- 2.1 Manifolds, vectors, tensors and forms . . . 8
- 2.2 Metrics and connections . . . 11
- 2.3 Curvature and Einstein equation . . . 13
- 2.4 Anti-de Sitter space-time . . . 14

3 Quantum field theory 17
- 3.1 Groups & symmetries . . . 17
  - 3.1.1 Lie algebras and Lie groups . . . 17
  - 3.1.2 Representations . . . 19
  - 3.1.3 Simple Lie algebras and Lie groups . . . 20
  - 3.1.4 The conformal group . . . 22

3.2 Fields and Lagrangians . . . 23
3.3 Gauge symmetries . . . 23
3.4 Renormalization . . . 25
3.5 Conformal field theory . . . 25

4 Dynamical systems and RG flows 28
4.1 Fixed points and linearization . . . 28
4.2 Fine-tuned flows: an illustrative example . . . 29
4.3 Renormalization group flows . . . 31

II Supergravity and holography 33

5 Interlude: why new theories? 33
5.1 The hierarchy problem, dark matter and supersymmetry . . . 34
5.2 String theory and supergravity . . . 35
5.2.1 Basics of string theory . . . 35
5.2.2 Branes . . . 37
5.2.3 The supergravity limit . . . 38
5.2.4 Dualities and M-theory . . . 38

6 Supersymmetry and supergravity 40
6.1 Global supersymmetry . . . 40
6.1.1 Spinors in higher dimensions . . . 40
6.1.2 Supersymmetry algebras and representations . . . 41
6.2 Superconformal field theory . . . 43
6.2.1 $\mathcal{N} = 4$ super Yang-Mills . . . 45
6.3 Supergravity . . . 45
6.3.1 Frame fields and spinors in curved space-times . . . 46
6.3.2 Eleven-dimensional supergravity and dimensional reduction . . . 47
6.3.3 Scalar geometry and Kähler manifolds . . . 49
6.3.4 Chiral multiplets in $\mathcal{N} = 1, d = 4$ supergravity . . . 50
6.3.5 Gauged supergravity and consistent truncation . . . 51
6.3.6 AdS vacua and BPS equations . . . 54

7 Gauge/gravity duality 57
7.1 Large N field theories and holography . . . 57
7.2 The Maldacena conjecture . . . 58
7.3 Holographic dictionary . . . 61
7.4 Evidence and prospects of AdS/CFT . . . 64

III Holographic RG flows 66

8 Toy models for holographic RG flows 66
8.1 Single scalar field . . . 66
8.1.1 Equations of motion . . . 68
8.1.2 Irreversibility of holographic RG flows . . . 71

8.1.3 Gradient flow equations . . . 72
8.2 Multiple scalar fields . . . 73

9 Holographic RG flows in gauged supergravity 76
9.1 Set-up and numerical methods . . . 76
9.1.1 General set-up of the problem . . . 76
9.1.2 A new algorithm to construct holographic RG flows . . . 80
9.2 SO(8) gauged supergravity . . . 82
9.2.1 Supersymmetric vacua . . . 83
9.2.2 Reconstructing known flows . . . 85
9.2.3 New flows to the U(1) × U(1) vacuum . . . 87
9.2.4 New flows to the SO(3) vacuum . . . 90
9.2.5 On conjectured flows and the plethora of vacua . . . 92
9.3 ISO(7) gauged supergravity . . . 95
9.3.1 Supersymmetric vacua . . . 96
9.3.2 New flows to the `P2569710` vacuum . . . 97
9.3.3 Plethora of vacua . . . 100
9.4 $[\mathrm{SO}(6) \times \mathrm{SO}(1,1)] \ltimes \mathbb{R}^{12}$ gauged supergravity . . . 100
9.4.1 Supersymmetric vacua . . . 101
9.4.2 New holographic RG flows . . . 102
9.5 $[\mathrm{SO}(6) \times \mathrm{SO}(2)] \ltimes \mathbb{R}^{12}$ gauged supergravity . . . 104
9.6 Discussion and outlook . . . 105
9.6.1 Discussion of results . . . 105
9.6.2 Future work . . . 106
9.6.3 Comparison of numerical methods and future algorithms . . . 106
9.6.4 Machine learning meets theoretical physics . . . 108

A Critical points and linearized BPS equations 109
A.1 SO(8) gauged supergravity . . . 109
A.1.1 Locations of critical points . . . 109
A.1.2 Linearized BPS equations . . . 110
A.2 ISO(7) gauged supergravity . . . 111
A.2.1 Locations of critical points . . . 111
A.2.2 Linearized BPS equations . . . 112
A.3 $[\mathrm{SO}(6) \times \mathrm{SO}(1,1)] \ltimes \mathbb{R}^{12}$ gauged supergravity . . . 114
A.3.1 Locations of critical points . . . 114
A.3.2 Linearized BPS equations . . . 115
A.4 $[\mathrm{SO}(6) \times \mathrm{SO}(2)] \ltimes \mathbb{R}^{12}$ gauged supergravity . . . 116
A.4.1 Locations of critical points . . . 116
A.4.2 Linearized BPS equations . . . 117

B Scalar masses and scaling dimensions 118

Bibliography 123

Index 132

Chapter 1

Introduction

Imagine that we lived in a world much like our own, with many cultures and languages, but lacking any means of translation. Different communities would be unable to exchange any information when they encounter each other. We would never learn to be humble from the story of Daedalus and Icarus, we would never get inspired to be as heroic as Hercules and we would never grasp the profound life lessons of Dostoevsky. Clearly, having a method to convey information between one another enriches our understanding of abstract subjects. In some sense, this artificial world portrays the landscape of theoretical physics established at the end of the 20^{th} century.

1.1 The landscape of theoretical physics

Physics in the 20^{th} century culminated in two new revolutionizing insights into our description of Nature. The first one is the famous theory of general relativity, formulated by Albert Einstein. The term 'relativity' refers to the idea that the concepts of space and time, originally thought to be merely the woodwork of the static stage of the universe, depend on the relative motion of observers. That is, observers travelling at different speeds with respect to each other will disagree on their notions of space and time. Moreover, space and time are coordinates which should be treated on the same footing, and together, they combine into what is known as space-time. Einstein took his groundbreaking idea of space-time one step further and formulated an entirely new theory of gravity. Instead of describing gravity as a Newtonian force, attracting apples and moons, Einstein stated that space-time is not static, but rather something dynamical that can deform, stretch and even curve. Gravity, Einstein said, is merely the manifestation of the fact that the fabric of our space-time is curved. This curvature originates from all the sources of matter and energy. When poured into a proper mathematical framework, this new description of gravity turned out to be highly successful. It correctly explained why the planet Mercury draws odd rosette shapes as it traces its orbit, predicted several phenomena which were experimentally verified and even continues to triumph to this day while we are taking the first-ever pictures of black holes. In short, general relativity is currently our most accurate description of the universe on the largest of scales: planets, stars, galaxies and even the birth of the universe, the Big Bang.

On the other hand, the 20^{th} century is also the epoch in which the quantum revolution took place. After failed attempts at a theoretical explanation of the spectrum of radiation coming from a blackbody, Planck conceived the idea that the energy levels of atoms would

not form a continuous spectrum, but rather constitute a set of discrete values. That is, the energy spectrum would be quantised. Because of its success, this hypothesis was formalized and eventually led to the theory of quantum mechanics, where quantised energy levels emerge from all physical systems studied at very small scales. However, quantum mechanics is irreconcilable with the principles of relativity. Indeed, the Schrödinger equation, the evolution equation of quantum mechanics, involves an explicit time derivative but no space derivatives, thereby violating the tenet of relativity that all space-time coordinates should be treated on equal footing. By requiring that both the ideas of quantum mechanics and the principles of relativity are valid, physicists developed quantum field theory. In quantum field theory, the fundamental objects of the theory are not particles, but fields that permeate all of space-time and of which the excitations are interpreted as particles. The framework of quantum field theory turned out to provide a successful description of particle physics: the three fundamental interactions besides gravity (the electromagnetic, weak and strong interactions) join together in a quantum field theory called the Standard Model. Moreover, the Standard Model incorporates all fundamental particles that have been observed in Nature so far, such as electrons, the constituents of protons and neutrons (quarks) and the mysterious neutrinos. The ultimate triumph of the Standard Model was the successful prediction of the Higgs boson, the 'God-particle' that gives mass to all known, massive particles. The Higgs boson was conjectured to exist merely based on principles of an abstract type of symmetry known as a gauge symmetry. Its observation validated quantum field theory as the theoretical blueprint of the three interactions of particle physics and provides an extremely accurate description of Nature on the smallest of scales.

The established landscape of theoretical physics therefore has two completely distinct theories that reign in different regimes. On the largest of scales, the theory of general relativity describes the gravitational interaction and the motion of stars, galaxies and even offers a model for cosmology. On the smallest of scales, the framework of quantum field theory accounts for the three interactions of particle physics and the behaviour of Nature's fundamental constituents of matter. Both theories have their own language associated to them. We certainly expect that these theories will meet each other in some exotic places in the universe. In the vicinity of black holes, for example, quantum effects may produce strange incidents. More importantly, at the origin of our universe, we have to deal with enormous space-time curvatures and immense matter densities located essentially at a single point. In these examples, we therefore expect that some hybrid theory, named quantum gravity, must come into play as fundamental description of Nature, unifying all known interactions.

Unfortunately, these two theories are very much like the dystopian world that opened this introduction. They resemble two characters that lack any means of communicating with each other. Indeed, if we attempt to describe gravity as a quantum field theory with a spin-2 particle, known as the graviton, which mediates the gravitational interaction, the theory is ill-defined and our calculations yield infinities. These infinities are a signal that our equations to work with are simply wrong, and therefore, that we are missing an essential piece of the puzzle.

A new approach has to be found to resolve this issue, and theoretical research in the past decades has culminated in a viable candidate of quantum gravity known as string theory. The way string theory attempts to resolve the above infinities is by 'smearing out', an idea that turned out to be fruitful in the past. Indeed, the infinities that made the Fermi

theory of weak interactions ill-defined were cured by introducing bosons which smeared out the interactions. In string theory, on the other hand, all point-particles themselves are smeared out into one-dimensional objects resembling strings. While string theory harbors the potential of unifying all interactions, understanding its mathematics and the implications for experiments turned out to be quite difficult. In a way, we have traded incorrect answers for finite results, but paid the price of having to deal with a much more complicated theory. Therefore, it remains to be seen whether experiments can confirm that string theory is indeed our desired, unifying 'theory of everything'. Unfortunately, current prospects indicate that such a verification will likely not be realized in the near future.

However, even without this confirmation, string theory is able to deliver new advancements into our understanding of theories of gravity and quantum field theories. The most exciting development in this regard is the AdS/CFT correspondence, also known as gauge/gravity duality or holography. This correspondence plays the role of the *deus ex machina* in our story. That is, AdS/CFT offers us a dictionary that allows us to translate all terminology of a gravity theory to expressions in the completely different language of quantum field theory. In this thesis, we will neglect phenomenological aspects of string theory and its relation to quantum gravity. Instead, we take this AdS/CFT dictionary as an independent tool with a life of its own and focus on the new insights into physics that we can gain from it.

1.2 AdS/CFT and the holographic dictionary

To properly introduce AdS/CFT, we have to enter deeper into the domain of string theory. As mentioned, the fundamental quantum objects in string theory are one-dimensional spatially extended strings. They can be either closed or open, in the sense that they either form a closed loop or have two free endpoints. The philosophy behind string theory is that the vibrational modes of these strings incorporate the particles observed in Nature, the three gauge interactions and even gravity, thereby (possibly) providing a description of quantum gravity. In essence, string theory unifies all of Nature into one musical magnum opus. The length of these strings is extremely small (on the order of the Planck length) and as such, today's experiments are unable to probe and verify this stringy-like nature of particles. As a consequence of requiring mathematical consistency, string theories can be interpreted as theories that are formulated in ten dimensions of space-time rather than the usual four that we experience in our everyday lives. Like the string nature of particles, these extra dimensions of space-time escaped detection in experiments so far as they are 'curled up' into small spaces. The extra freedom gained by additional space-time directions allows us to generalize the notion of the string. Indeed, we can consider higher-dimensional extended objects that move through space-time, and due to this description resembling that of a membrane, these objects are called branes. In some circumstances, strings with free endpoints can 'anchor' on these branes, and the vibrations of the strings give dynamics to the branes.

It is because of these branes that we are able to formulate a dictionary between gauge and gravity theories. In 1997, the Argentinian cosmologist Juan Maldacena considered a collection of coincident branes in string theory. By tuning g_s, the coupling parameter of string theory, he identified two different regimes which produced completely different

pictures. On the one hand, at small coupling g_s, gravity is essentially switched off and strings can easily anchor to the branes. The vibrational modes of the branes then describe a gauge quantum field theory. For the case that Maldacena studied, this quantum field theory is invariant under scale transformations, such that the field theory is a conformal field theory or CFT for short. On the other hand, at large g_s, gravity becomes relevant. The branes will curve the geometry of the space-time, resulting in a well-known solution of general relativity: an anti-de Sitter, or AdS, space-time. Hence we have, at different values of g_s, completely different pictures emerging: a quantum field theory on the one hand, and a gravity theory on the other. However, since nothing fundamentally changed in the original set-up of the theory, there is no reason why we should consider these pictures to be at odds with each other. Hence, Maldacena concludes, the two pictures should in fact be completely equivalent to each other. Therefore, there must be an exact correspondence between the CFT emerging at small g_s and the AdS appearing at large g_s, which became known as the AdS/CFT correspondence.

Research flourished after Maldacena published his groundbreaking idea, and his argument was extended to other cases. It was quickly realized that the correspondence would offer a dictionary between gauge quantum field theories and theories of gravity in general. As such, it would provide an entirely new theoretical instrument. Moreover, two additional features of AdS/CFT implied that this instrument could provide a window into currently inaccessible physics, and uncover deep truths on the nature of quantum gravity.

The latter is related to the remarkable observation that in Maldacena's AdS/CFT, the quantum field theory is defined on a space-time which has one dimension less compared to the gravity theory. It seems as if all phenomena occurring at the gravity side of the correspondence can equally be formulated in a lower-dimensional space-time without losing any information. In some sense, this resembles the mechanism behind a hologram, where information is encoded on a two-dimensional surface and gets projected into a three-dimensional volume. For this reason, Maldacena's correspondence is also referred to as holography and the dictionary offered by AdS/CFT is said to be 'holographic'.

Both sides of the correspondence have their own coupling parameter which dictates the regime where perturbative calculations (which is, unfortunately, the only way to perform calculations in most cases) are valid and meaningful. The other appealing feature of AdS/CFT is the fact that this correspondence is in particular a strong/weak duality. This means that both sides of the correspondence are necessarily at a different regime of coupling: whenever the quantum field theory is strongly coupled, the gravity theory is weakly coupled and vice versa. Therefore, the AdS/CFT correspondence can offer us a glimpse into the physics of strongly coupled field theories via computations performed in a gravity theory. This is precisely our aim in this thesis.

1.3 Renormalization group flows and their holographic translation

In this thesis, we explore how AdS/CFT offers us a window into strongly coupled phenomena in physics. More specifically, we study the evolution of strongly coupled quantum field theories through calculations in the appropriate dual gravity theories. This 'evolution' originates from the observation that physics depends on the energy scale, or equivalently, on the magnification, under which we study systems. For example, when considering a

free electron, its charge is not a fixed number in Nature, but rather depends on the scale at which the electron is being probed. Indeed, the vacuum surrounding the electron is not completely empty, as quantum field theory tells us. In vacuum, quantum fluctuations imply that it is possible to create an electron-positron pair out of photons, which will annihilate again at a later time. Due to these fluctuating pair creations, the vacuum surrounding an electron gets polarized and the charge of the electron gets partially screened. If we get closer to the electron, we will 'see' less electron-positron pairs and hence less screening due to vacuum polarization. Therefore, particles will feel a more negative charge of the electron. For this reason, the electric charge of particles, seen as the coupling constant of the underlying quantum field theory, is said to be a 'running coupling', as its value depends on the energy scale.

The above hand-waving explanation can be made mathematically precise and is a general phenomenon of quantum field theory, related to the concept of renormalization. As such, the evolution of parameters of the theory is known as the renormalization group evolution (or flow). While the effect of this evolution is not dramatic for quantum electrodynamics, the theory describing electrons, it is a crucial way of gaining insight into other field theories such as quantum chromodynamics, the quantum field theory of the strong interaction. Indeed, the renormalization group tells us that the coupling of quantum chromodynamics goes to zero at high energy (or equivalently, small distance separations). This implies that the theory essentially becomes non-interacting, a feature known as asymptotic freedom. However, as we decrease the energy, or equivalently increase the distance separation between particles, the interaction becomes much stronger. Understanding the renormalization group evolution provides us key insights into the nature of the interaction at all energy scales.

In some sense, the renormalization group shows that energy can be interpreted as an extra dimension. This idea is also asserted by the AdS/CFT correspondence. Indeed, as we will argue in more detail later on, the holographic nature of AdS/CFT manifests itself in the identification of one of the space-time coordinates of the gravity theory with the energy scale of the field theory. Moreover, AdS/CFT provides us a new device to tackle the problem of finding these renormalization group flows by translating it into the language of a gravity theory. This is precisely our goal in this thesis: to gain knowledge on the evolution of quantum field theories by studying their gravity duals, known as holographic renormalization group flows.

However, in order to make calculations feasible, we have to take a step back from string theory in which AdS/CFT was originally formulated. That is, we have to consider a low-energy limit of string theory known as supergravity, where we again approximate strings by point-particles. In practice, we will deal with a supergravity theory that itself is invariant under a gauge symmetry and is therefore called gauged supergravity. By introducing this gauge group, we couple the vector fields of the supergravity theory to the scalars of the theory. This will introduce a highly non-trivial potential for the scalar fields. In fact, 'highly non-trivial' is a serious understatement, as this scalar potential will be a complicated function of 70 real variables. However, we are able to perform calculations by restricting our attention, in a mathematically well-defined sense, to a subsector of the scalar fields, such that the potential depends on only 14 real variables. The extrema of this scalar potential are solutions of the theory which correspond to empty AdS space-times. As such, AdS/CFT dictates that these solutions are dual to conformal vacua of the dual quantum field theory. Since the scalar potential has multiple extrema, we can look

for a solution starting from a vacuum located "high" up on the mountain of this potential landscape, and subsequently travels downwards, according to a gradient descent rule, until it settles into another vacuum solution at a lower value of the scalar potential. As such, we have an interpolating solution between two empty AdS space-times, and the holographic dictionary allows us to interpret these solutions as dual to renormalization group flows in the dual quantum field theory. Our work in this thesis is focused on constructing precisely such interpolating solutions in various gauged supergravity theories.

1.4 Outline

Now that we have situated this thesis within the larger framework of theoretical physics, we will give a detailed overview of the contents of this thesis and how we will arrive at the goal established above. The thesis is divided into three parts.

In Part I, we provide the preliminary concepts required to follow the main content of this thesis. Since this work is aimed at second-year master students, 'preliminary' in this case refers to concepts that are covered in detail in the theoretical physics courses of KU Leuven. In Chapter 2, we give the basics of general relativity, our most accurate description of gravity so far. Section 2.4 also introduces anti-de Sitter space-times, the first actor of AdS/CFT. In Chapter 3, we briefly discuss some basic ingredients of quantum field theory which are relevant for the thesis, such as gauge symmetries and renormalization. In this chapter, we also introduce conformal field theory, the second actor of AdS/CFT. In Chapter 4, we spend more time on renormalization group flows of quantum field theories. Moreover, we review basic concepts of dynamical systems in this chapter, as these will be of central importance to our calculations presented at the very end of the thesis.

In Part II, we go beyond general relativity and quantum field theory and initiate readers into string theory and, more importantly, supersymmetry and supergravity. The aims of Chapter 5 are twofold. First of all, it provides a more technical motivation for the development of an entirely new framework for quantum gravity. On the other hand, it serves as a detailed introduction to string theory and supergravity, without burdening readers with equations which may mystify the core concepts required to understand the remainder of the thesis. As such, it is intended as a bridge between Part I and Part II. From that point onward, we open Pandora's box of mathematics and will no longer spare the technical details of the story. Chapter 6 introduces a new symmetry of space-time, supersymmetry, and subsequently discusses the main scene of our work, supergravity. We consider gauged supergravity theories and introduce the notion of a consistent truncation, which make it feasible for us to perform our calculations. Chapter 7 offers a more technical introduction to the AdS/CFT correspondence, and formulates the holographic dictionary we employ in the final part of the thesis.

In Part III, we present the main topic of the thesis, the holographic renormalization group flows. By matter of introduction to the topic, Chapter 8 considers toy models which, as a simplified version of the problem, allow us to highlight the most prominent features based on analytic calculations. In Chapter 9, we take the holographic renormalization group flows beyond these toy models and develop them in gauged supergravity theories in four dimensions of space-time, which are the supergravity theories that are also studied extensively in the literature. As such, we reiterate concepts and ingredients which are introduced in detail in earlier chapters, such that this chapter can be read independently

from all others by experts in the field. Our aim is to present this chapter on the level of recent publications with respect to the topic of holographic RG flows and to include 'state-of-the-art' research on this matter. Hence, this final chapter also delivers our new results which give new insights into the dual field theories. To conclude the thesis, we reflect on our work and on possible continuations and extensions for the future.

Part I

Preliminaries

Chapter 2

General relativity

The theory of general relativity (GR), first formulated by Albert Einstein in 1915, revolutionized our view on space and time and provided a sophisticated description of gravity. Einstein himself proposed three experimental tests of his theory of relativity [1]: the deflection of light rays, the precession of perihelia of planets and the gravitational redshift of light, all of which validated Einstein's theory. Afterwards, GR continued to withstand even more astonishing tests. Gravitational waves originating from mergers of black holes or neutron stars are consistent with GR [2–4]. In the past years, humankind was even able to photograph the elusive black holes for the very first time, and recently, we even got a view of the black hole 'in our own backyard' [5, 6]. Also here, the equations of GR hold to an outstanding accuracy.

The essence of GR is neatly summarized by a famous quote by John Wheeler: *"Space-time tells matter how to move, matter tells space-time how to curve"* [7]. Hence, if relativity were a play, its actors would be massive objects such as stars and galaxies, and its stage a curved manifold, changing from scene to scene. To describe curved manifolds, we will borrow concepts from the mathematical field of differential geometry. In this chapter, we will summarize the most important mathematical tools and give a brief overview of the theory of GR, based on [1, 8]. Moreover, this chapter serves as an introduction to the more complicated theory of supergravity, which directly builds on the framework of GR.

2.1 Manifolds, vectors, tensors and forms

Since gravity is essentially the manifestation of curved geometry, we start by introducing manifolds. A *manifold*, intuitively speaking, is a smooth space which locally looks like a flat Euclidean space and on which our notion of coordinates still holds. Rigorously, a *coordinate system* or *chart* on a subset U of a topological space M is a bijective map $\phi : U \to \mathbb{R}^n$ such that the image $\phi(U)$ is an open set in $\mathbb{R}^n$. A C^∞ *atlas* is then a collection of charts $\{(U_i, \phi_i)\}$ such that

1. The U_i cover M, that is, their union equals M,
2. The charts are *compatible*: if $U_i \cap U_j \neq \emptyset$, then the map $(\phi_i \circ \phi_j^{-1}) : \mathbb{R}^n \to \mathbb{R}^n$ is infinitely times differentiable.

An atlas is said to be *maximal* if it contains every possible compatible chart. Given these ingredients, a C^∞ *manifold* M of dimension n is defined as a topological space M with a

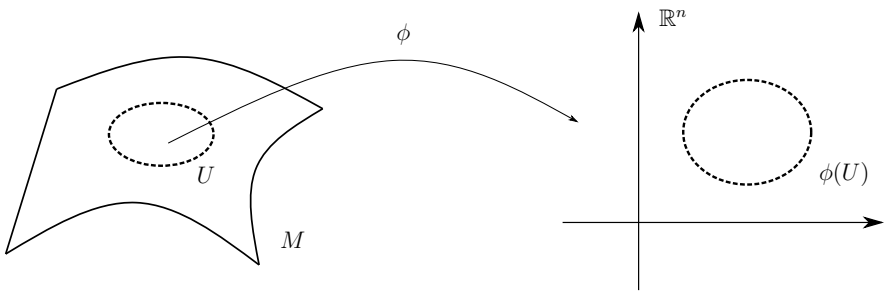

Figure 2.1: Visual representation of a chart ϕ on a manifold M, with domain U such that $\phi(U)$ is an open set in $\mathbb{R}^n$.

maximal atlas.

As physicists, we want to describe how particles, initially sitting at a point $p \in M$, move around on the manifold. One can imagine a (hyper)plane tangent to the manifold at p, containing all possible velocity vectors, which can equivalently be seen as directional derivatives of curves (paths) on the manifold. The set of all these tangent vectors at p, or all directional derivative operators along curves through p, is called the *tangent space*, denoted by T_pM and visualized in Figure 2.2. One can show that T_pM is a vector space of equal dimension as M. There exists a natural basis for T_pM: if we use a patch with coordinates x^μ to cover p, then curves that vary along only one of the coordinates are the most simple to consider, *e.g.* the 'north-south' and 'east-west' directions on a two-sphere. The directional derivatives are then ordinary partial derivatives, which indeed form a basis of T_pM called the *coordinate basis*. Partial derivatives will be written as

$$\partial_\mu \equiv \frac{\partial}{\partial x^\mu} \,. \tag{2.1}$$

Note that using the coordinate basis implies that any coordinate transformation necessarily induces a basis transformation of T_pM. While the coordinate basis is useful in GR, supergravity requires the use of another basis of T_pM, which we will introduce in Section 6.3.1. Since the partial derivatives form a basis, any vector $V \in T_pM$ can be written as a linear combination of the n basis vectors ∂_μ:

$$V = V^\mu \partial_\mu \equiv V^0 \partial_0 + \cdots + V^{n-1} \partial_{n-1} \,, \tag{2.2}$$

where we introduced the *Einstein summation convention*: a repeated index implies a summation over all possible index values. For example, the chain rule in this notation reads

$$\partial_{\mu'} = \frac{\partial x^\mu}{\partial x^{\mu'}} \partial_\mu \,, \tag{2.3}$$

with μ' labeling a different set of coordinates $x^{\mu'}$. The abstract vector V does not depend on the choice of basis, but its components V^μ do. To guarantee consistency when changing basis, *i.e.* $V = V^\mu \partial_\mu = V^{\mu'} \partial_{\mu'}$, the components of a vector obey

$$V^{\mu'} = \frac{\partial x^{\mu'}}{\partial x^\mu} V^\mu \,. \tag{2.4}$$

With a slight abuse of terminology, we will often refer to V^μ as vectors, even though they are actually the components of a vector.

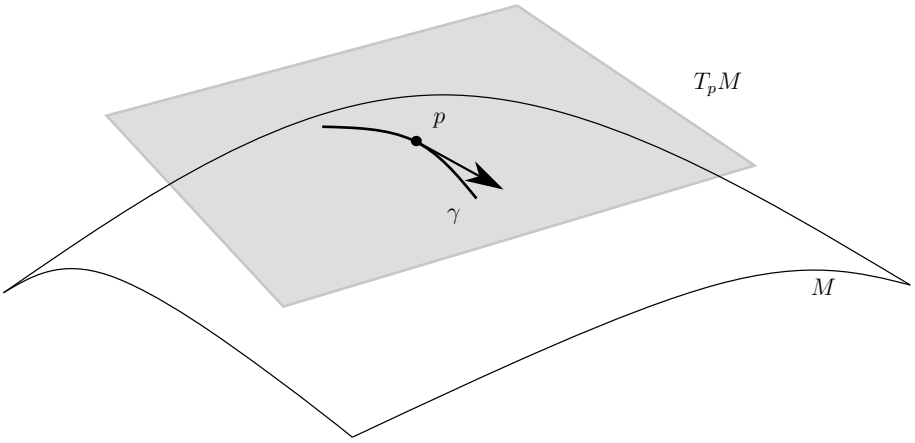

Figure 2.2: Illustration of the tangent space T_pM (grey) at a point p on the manifold. Also shown is a curve γ on the manifold going through p, and its velocity vector at p is an element of T_pM.

It is a basic fact from algebra that every vector space V has a so-called *dual vector space* $V^\star$, which is the vector space of all linear maps from V to $\mathbb{R}$ and has the same dimension as V. We can hence naturally define the dual vector space $T_p^\star M$ of the tangent space, called the *cotangent space*. A natural basis of $T_p^\star M$ is the basis dual to the coordinate basis of T_pM, and its basis vectors are the differentials $\{\mathrm{d}x^\nu\}$. Their action on the basis vector ∂_μ is

$$\mathrm{d}x^\nu(\partial_\mu) = \frac{\partial x^\nu}{\partial x^\mu} = \delta^\nu_\mu \,, \tag{2.5}$$

where δ^ν_μ is the Kronecker delta symbol. Since the differentials $\mathrm{d}x^\nu$ also depend explicitly on the coordinate system, a change of basis will modify them as

$$\mathrm{d}x^{\nu'} = \frac{\partial x^{\nu'}}{\partial x^\nu}\,\mathrm{d}x^\nu \,. \tag{2.6}$$

We can expand dual vectors ω in the basis $\{\mathrm{d}x^\nu\}$:

$$\omega = \omega_\nu\,\mathrm{d}x^\nu \,, \tag{2.7}$$

and similar to vectors, the components of dual vectors transform under coordinate transformations non-trivially:

$$\omega_{\nu'} = \frac{\partial x^\nu}{\partial x^{\nu'}}\omega_\nu \,. \tag{2.8}$$

Introducing tensors is now simply an exercise in index gymnastics. A *tensor* of *rank* (k,l) is a map T [8]

$$T : T_p^\star M \times \cdots \times T_p^\star M \times T_pM \cdots \times T_pM \to \mathbb{R} \,, \tag{2.9}$$

where $T_p^\star M$, respectively T_pM, appears k, respectively l, times in the above product. The components of a tensor are found from the expansion

$$T = T^{\mu_1\cdots\mu_k}{}_{\nu_1\ldots\nu_l}\,(\partial_{\mu_1}\otimes\cdots\otimes\partial_{\mu_k}\otimes\mathrm{d}x^{\nu_1}\otimes\cdots\otimes\mathrm{d}x^{\nu_l}) \,. \tag{2.10}$$

Again, we will abuse terminology and refer to the components $T^{\mu_1\cdots\mu_k}{}_{\nu_1\ldots\nu_l}$ as a tensor. The transformation law of the components of T under a change of basis is

$$T^{\mu'_1\cdots\mu'_k}{}_{\nu'_1\ldots\nu'_l} = \frac{\partial x^{\mu'_1}}{\partial x^{\mu_1}}\cdots\frac{\partial x^{\mu'_k}}{\partial x^{\mu_k}}\frac{\partial x^{\nu_1}}{\partial x^{\nu'_1}}\cdots\frac{\partial x^{\nu_l}}{\partial x^{\nu'_l}}T^{\mu_1\cdots\mu_k}{}_{\nu_1\ldots\nu_l} \tag{2.11}$$

A useful operation on tensors is the *contraction*, which takes a (k, l) tensor and transforms it into a $(k-1, l-1)$ tensor by summing over one of its indices. For example, starting from a tensor $R^{\rho}{}_{\mu\sigma\nu}$, we can create a tensor $R_{\mu\nu}$ by summing over the ρ and σ indices: $R_{\mu\nu} = R^{\lambda}{}_{\mu\lambda\nu}$. A tensor is said to be symmetric in its indices μ and ν if it is invariant under swapping μ with ν, while it is anti-symmetric if this produces a minus sign. From an arbitrary tensor $T_{\mu_1\cdots\mu_n}$, one can construct a completely symmetric tensor (*i.e.*, symmetric in all its indices) by the *symmetrization* procedure:

$$T_{(\mu_1\cdots\mu_n)} = \frac{1}{n!}\sum_{\sigma\in\mathcal{S}(n)} T_{\sigma(\mu_1)\cdots\sigma(\mu_n)}\,, \tag{2.12}$$

where the sum goes over all permutations σ of the indices. Similarly, we define the *anti-symmetrization* procedure as:

$$T_{[\mu_1\cdots\mu_n]} = \frac{1}{n!}\sum_{\sigma\in\mathcal{S}(n)} \mathrm{sgn}(\sigma) T_{\sigma(\mu_1)\cdots\sigma(\mu_n)}\,, \tag{2.13}$$

where now each term carries the sign of its permutation. Theories in higher dimensions of space-time often involve differential forms. A differential *p-form* is defined by

$$\omega^{(p)} = \frac{1}{p!}\omega_{\mu_1\cdots\mu_p}\,\mathrm{d}x^{\mu_1}\wedge\mathrm{d}x^{\mu_2}\wedge\cdots\wedge\mathrm{d}x^{\mu_p}\,, \tag{2.14}$$

where the *wedge product* $\wedge$ is anti-symmetric. Hence, each p-form corresponds to an anti-symmetric tensor $\omega_{\mu_1\cdots\mu_p}$. One can define the *exterior derivative* of a p-form, giving a $(p+1)$-form, via

$$\mathrm{d}\omega^{(p)} = \omega^{(p+1)} = \frac{1}{p!}\partial_\mu\omega_{\mu_1\cdots\mu_p}\,\mathrm{d}x^{\mu}\wedge\mathrm{d}x^{\mu_1}\wedge\mathrm{d}x^{\mu_2}\wedge\cdots\wedge\mathrm{d}x^{\mu_p}\,. \tag{2.15}$$

For example, a p-form gauge field has its exterior derivative as field strength. Such higher-dimensional field strengths will appear in our discussion of p-branes and the AdS/CFT correspondence.

2.2 Metrics and connections

Manifolds that appear in GR are special in the sense that their tangent spaces are endowed with a positive-definite inner product. Any manifold in GR hence has a *metric*, which is a symmetric $(0,2)$ tensor $g_{\mu\nu}$ and a crucial tool to describe the geometry of the manifold. The inverse metric $g^{\mu\nu}$ is defined by $g^{\mu\nu}g_{\nu\rho} = \delta^{\mu}_{\rho}$. The metric and its inverse are used to raise or lower indices of tensors, *e.g.* $g_{\mu\nu}V^{\nu} = V_{\mu}$. Importantly, the metric allows us to define distances on the manifold via the *line element*, defined by

$$\mathrm{d}s^2 = g_{\mu\nu}\,\mathrm{d}x^{\mu}\,\mathrm{d}x^{\nu}\,. \tag{2.16}$$

For example, for the Euclidean space $\mathbb{R}^3$ with Cartesian coordinates (x, y, z), the line element is

$$\mathrm{d}s^2 = \mathrm{d}x^2 + \mathrm{d}y^2 + \mathrm{d}z^2\,, \tag{2.17}$$

where the metric is $g_{\mu\nu} = \mathrm{diag}(1, 1, 1)$. However, we can make a change of variables to spherical coordinates (r, θ, φ), such that the line element becomes:

$$\mathrm{d}s^2 = \mathrm{d}r^2 + r^2(\mathrm{d}\theta^2 + \sin^2\theta\,\mathrm{d}\varphi^2) \equiv \mathrm{d}r^2 + r^2\,\mathrm{d}\Omega_2^2\,, \tag{2.18}$$

where $g_{\mu\nu} = \mathrm{diag}(1, r^2, r^2\sin^2\theta)$ is no longer constant. We also defined $\mathrm{d}\Omega_2^2$, the line element on the two-sphere S^2. Generalizing this metric to an arbitrary number of dimensions, one finds the n-sphere, which in this thesis will be denoted by S^n.

Every metric can be put in its *canonical form*, such the metric becomes a diagonal matrix:

$$g_{\mu\nu} = \mathrm{diag}\left(-1, -1, \ldots, -1, +1, +1, \ldots, +1\right)\,. \tag{2.19}$$

For example, performing this operation on the metric from the line element in equation (2.18) would yield the metric from equation (2.17). The canonical form also determines the *signature* (p, q) of the metric, where p, respectively q, is the amount of minus, respectively plus, signs in the canonical form. In GR, all manifolds of interest have *Lorentzian signature*[1] $(1, d-1)$, and are called space-time manifolds. The simplest space-time is the *Minkowski space-time*, which is a flat (zero curvature) space-time. Its $4d$ line element is

$$\mathrm{d}s^2 = -\,\mathrm{d}t^2 + \mathrm{d}x^2 + \mathrm{d}y^2 + \mathrm{d}z^2\,, \tag{2.20}$$

where t is the time coordinate. The metric of this space-time is often denoted by $\eta_{\mu\nu}$.

Besides distances on the manifold, we are interested in its curvature. For this, we first have to introduce connections. From the transformation law of tensors, one can show that partial derivatives are not appropriate tensor operators in the sense that *e.g.* $\partial_\mu V^\nu$ is not a tensor. To remedy this, we define the *covariant derivative* which is denoted by ∇_μ and acts as

$$\nabla_\mu V^\nu = \partial_\mu V^\nu + \Gamma^\nu_{\mu\rho} V^\rho\,, \tag{2.21}$$

$$\nabla_\mu V_\nu = \partial_\mu V_\nu - \Gamma^\rho_{\mu\nu} V_\rho\,. \tag{2.22}$$

The action of a covariant derivative on a (k, l) tensor is then generalized by including a term similar to equation (2.21) for each of the k upper indices of the tensor, and including a term similar to equation (2.22) for each of the l lower indices of the tensor. For simple scalar functions, the covariant derivative of a scalar quantity reduces to the ordinary partial derivative: $\nabla_\mu f = \partial_\mu f$. The extra Γ terms are known as *connection coefficients* and they specify a *connection* on a manifold. They are not tensors, which is why we put their indices carelessly on top of each other. A connection generalizes the notion of parallel transport of tensors to curved manifolds, but for our purpose, it suffices to consider it a tool to construct covariant derivates. From the connection coefficients, one can define the *torsion tensor*

$$T^\lambda_{\ \mu\nu} \equiv \Gamma^\lambda_{\mu\nu} - \Gamma^\lambda_{\nu\mu} \tag{2.23}$$

It turns out that the connection is uniquely specified if we impose two additional constraints:

1. The connection is 'torsion-free', that is, the torsion tensor vanishes identically. This is equivalent to requiring that the connection coefficients are symmetric in the lower indices ($\Gamma^\lambda_{\mu\nu} = \Gamma^\lambda_{\nu\mu}$),

[1] The signature can also be denoted as $(-+++)$ and is known as the 'mostly plus' convention. A different convention takes the signature to be $(+---)$, or 'mostly minus'.

2. The connection is *metric compatible*, meaning that $\nabla_\rho g_{\mu\nu} = 0$. This implies that the inverse metric also has a vanishing covariant derivative: $\nabla_\rho g^{\mu\nu} = 0$.

This unique connection is the one used in GR and is known as the *Christoffel connection* or the *Levi-Civita connection*. For this reason, the connection coefficients are frequently called the *Christoffel symbols*. They can be expressed in terms of derivatives of the metric:

$$\Gamma^\sigma_{\mu\nu} = \frac{1}{2} g^{\rho\sigma} \left(\partial_\mu g_{\nu\rho} + \partial_\nu g_{\rho\mu} - \partial_\rho g_{\mu\nu} \right) . \tag{2.24}$$

Note that the Christoffel symbols vanish for the Minkowski space-time as its metric is constant. We will see later that curvature can be expressed in terms of the Christoffel symbols, such that the label of 'flat' for this space-time is justified.

The connection allows us to define the equation of parallel transport of a tensor along a path $x^\mu(\lambda)$, which for a vector V^μ reads:

$$\frac{\mathrm{d}V^\mu}{\mathrm{d}\lambda} + \Gamma^\mu_{\sigma\rho} \frac{\mathrm{d}x^\sigma}{\mathrm{d}\lambda} V^\rho = 0 \, . \tag{2.25}$$

The interesting application is, of course, parallel transport along trajectories $x^\mu(\lambda)$ of particles in space-time, also known as the *world-line* of a particle. Substituting the velocity vector $V^\mu = \mathrm{d}x^\mu(\lambda)/\,\mathrm{d}\lambda$ in the above equation gives

$$\frac{\mathrm{d}^2 x^\mu}{\mathrm{d}\lambda^2} + \Gamma^\mu_{\sigma\rho} \frac{\mathrm{d}x^\rho}{\mathrm{d}\lambda} \frac{\mathrm{d}x^\sigma}{\mathrm{d}\lambda} = 0 \, , \tag{2.26}$$

which is the *geodesic equation*. A *geodesic* is the path of shortest distance between two points in a space-time, with distances measured by the line element $\mathrm{d}s^2$. As an extension of the principle of least action from classical mechanics, particles are required to travel on paths which minimize distance, *i.e.* on geodesics. Note that, for flat space-times, we recover Newton's first law of motion, stating that particles travel along straight lines. The geodesic equation gives a precise meaning to the first part of John Wheeler's quote: "*space-time tells matter how to move*".

2.3 Curvature and Einstein equation

Einstein's theory states that gravity is not a Newtonian force. Rather, it is simply the manifestation of space-time being curved. Let us therefore introduce the concept of curvature of a manifold.

Intuitively speaking, curvature modifies a tensor as it is being moved along a closed loop. We can quantify this change using the *commutator* of covariant derivatives, which gives the *Riemann tensor* or *curvature tensor*:

$$[\nabla_\mu, \nabla_\nu] V^\rho = R^\rho{}_{\sigma\mu\nu} V^\sigma \, . \tag{2.27}$$

The Riemann tensor can be expressed in terms of the Christoffel symbols:

$$R^\rho{}_{\sigma\mu\nu} = \partial_\mu \Gamma^\rho_{\nu\sigma} - \partial_\nu \Gamma^\rho_{\mu\sigma} + \Gamma^\rho_{\mu\lambda} \Gamma^\lambda_{\nu\sigma} - \Gamma^\rho_{\nu\lambda} \Gamma^\lambda_{\mu\sigma} \, . \tag{2.28}$$

From the Riemann tensor, we obtain the *Ricci tensor* by contracting a pair of indices:

$$R_{\mu\nu} = R^\lambda{}_{\mu\lambda\nu} \, . \tag{2.29}$$

Taking the trace of this tensor gives the *Ricci scalar*:

$$R = R^{\mu}{}_{\mu} = g^{\mu\nu} R_{\mu\nu} \,. \tag{2.30}$$

The John Wheeler quote hints that the source of this curvature is mass and energy present in the space-time, which is stored mathematically in the *energy-momentum tensor* $T_{\mu\nu}$. The interplay between curvature and energy is expressed by the famous *Einstein equation*:

$$R_{\mu\nu} - \frac{1}{2} R g_{\mu\nu} = 8\pi G T_{\mu\nu} \,, \tag{2.31}$$

where G is Newton's gravitational constant. The Einstein equation is the mathematical translation of the second part of John Wheeler's quote: "*matter tells space-time how to curve*".

There exists a generalization of the above equation which accounts for space-times with a *cosmological constant* Λ:

$$R_{\mu\nu} - \frac{1}{2} R g_{\mu\nu} + \Lambda g_{\mu\nu} = 8\pi G T_{\mu\nu} \,. \tag{2.32}$$

This Λ-term is somewhat puzzling, as one could choose to write it on either side of the above equation. That is, one can interpret Λ as an intrinsic quantity of the space-time geometry, as its value determines whether the space-time is flat, open or closed. In this regard, it seems natural to write Λ on the left hand side as above. However, one could write the Λ-term on the right hand side and view it as another contribution to the energy-momentum tensor, which is somehow present even when no 'ordinary' matter or energy sources are present. The second interpretation calls this extra contribution a *vacuum energy*. The cosmological constant is of utmost importance in cosmology, since observations reveal that our universe has a very small but non-zero, positive value of Λ [9]. The generalized Einstein equation can be obtained by extremizing the *Einstein-Hilbert* (EH) action:

$$S_{\text{EH}} = \frac{1}{2\kappa^2} \int \mathrm{d}^d x \sqrt{-g} (R - 2\Lambda) \,, \tag{2.33}$$

where $\kappa^2 \equiv 8\pi G$ and $\sqrt{-g} \equiv \sqrt{-\det g_{\mu\nu}}$. For this thesis, an important solution of the Einstein equation with a non-zero cosmological constant is the anti-de Sitter space-time.

2.4 Anti-de Sitter space-time

The *anti-de Sitter* (AdS) space-time is an example of a *maximally symmetric space-time*, which are space-times for which the Riemann tensor with all indices down (*i.e.*, $R_{\rho\sigma\mu\nu} = g_{\rho\alpha} R^{\alpha}{}_{\sigma\mu\nu}$) and the Ricci tensor satisfy the non-trivial relations

$$R_{\rho\sigma\mu\nu} = \beta \left(g_{\rho\mu} g_{\sigma\nu} - g_{\rho\nu} g_{\sigma\mu} \right) \,, \tag{2.34}$$

$$R_{\mu\nu} = \beta (d-1) g_{\mu\nu} \,. \tag{2.35}$$

where d is the number of space-time dimensions and β is a constant to be specified later on for AdS. Taking the trace, the second equation implies the Ricci scalar is constant across the manifold for a maximally symmetric space-time and equal to

$$R = \beta d (d-1) \,, \tag{2.36}$$

A metric for which equation (2.35) is satisfied is known as an *Einstein metric*, and the corresponding space-time is then called an *Einstein space-time*. Every maximally symmetric space-time is hence an Einstein space-time.

Besides flat Minkowski space-time, there exist two curved maximally symmetric space-times of interest: positively curved ($\beta > 0$) de Sitter space-time and negatively curved ($\beta < 0$) anti-de Sitter space. The former is the space-time analogue of a sphere, while the latter is the space-time analogue of hyperbolic space. AdS space-times in d dimensions, denoted by AdS_d, can be constructed via an embedding into the $(d+1)$-dimensional space-time $\mathbb{R}^{2,d-1}$ with signature $(-++\cdots+-)$ and coordinates $(X_0, X_1, \ldots, X_d)$. That is, AdS is identified with the hyperboloid determined by the equation

$$\sum_{i=1}^{d-1} X_i^2 - X_0^2 - X_d^2 = -L^2\,, \tag{2.37}$$

where L is called the *length scale* of AdS. One can show that the AdS space-times indeed obey equation (2.34) and one finds that $\beta = -1/L^2$. The above embedding makes it manifest that AdS_d has a $\mathrm{SO}(2, d-1)$ global symmetry group, a fact which is crucial for the AdS/CFT correspondence. From the defining equation, one finds that the line element on the hyperboloid yields

$$\mathrm{d}s^2 = -\,\mathrm{d}X_0^2 - \mathrm{d}X_d^2 + \mathrm{d}X_1^2 + \cdots + \mathrm{d}X_{d-1}^2\,. \tag{2.38}$$

As mentioned earlier, AdS space-times are solutions of the generalized Einstein equations with a non-vanishing, negative cosmological constant, which can be written as

$$\Lambda = -\frac{(d-1)(d-2)}{2L^2}\,. \tag{2.39}$$

Let us introduce new coordinate systems which illuminate important aspects of AdS spaces [10]. First, we define coordinates

$$X_i = r\bar{x}_i \quad X_0 = \sqrt{L^2+r^2}\sin(t/L) \quad X_d = \sqrt{L^2+r^2}\cos(t/L)\,, \tag{2.40}$$

where $\bar{x}_i$ are coordinates parametrizing S^{d-1} and the range of the time coordinate t is $0 \le t \le 2\pi L$. The metric becomes

$$\mathrm{d}s^2 = -\left(1+\frac{r^2}{L^2}\right)\mathrm{d}t^2 + \left(1+\frac{r^2}{L^2}\right)^{-1}\mathrm{d}r^2 + r^2\,\mathrm{d}\Omega_{d-2}^2\,. \tag{2.41}$$

By extending this solution to the range $-\infty < t < +\infty$, we get the so-called covering space of AdS, which, with abuse of terminology, we will still refer to as AdS. Other interesting coordinate systems can be found by a change of radial variable. Going from r to y, defined by $\cosh(y/L) = \sqrt{1+r^2/L^2}$, one finds

$$\mathrm{d}s^2 = -\cosh^2(y/L)\,\mathrm{d}t^2 + \mathrm{d}y^2 + L^2\sinh^2(y/L)\,\mathrm{d}\Omega_{d-2}^2\,. \tag{2.42}$$

Important insights into the global structure of AdS can be found if we define ρ via $\cosh(y/L) = 1/\cos\rho$ with range $0 \le \rho < \pi/2$ and rescale time via $t = L\tau$. This results in

$$\mathrm{d}s^2 = \frac{L^2}{\cos^2\rho}\left[-\,\mathrm{d}\tau^2 + \left(\mathrm{d}\rho^2 + \sin^2\rho\,\mathrm{d}\Omega_{d-2}^2\right)\right]\,. \tag{2.43}$$

This metric is of the form $g_{\mu\nu} = e^{2\omega}\tilde{g}_{\mu\nu}$, where $\tilde{g}_{\mu\nu}$ in this case describes a higher-dimensional cylinder $\mathbb{R} \times S^{d-1}$, with $\mathbb{R}$ being the time axis. Therefore, it is said that the conformal boundary of an AdS space-time is $\mathbb{R} \times S^{d-1}$. Light rays, or any type of information, coming from spatial infinity can reach the origin in finite time. Therefore, we have to specify the relevant boundary conditions. It will turn out that these boundary conditions are an important step towards the holographic dictionary of AdS/CFT in Section 7.3.

Finally, we also introduce the coordinates on AdS in the *Poincaré patch*, which cover a region of AdS that is conformal to half of Minkowski space-time. The coordinates are defined via

$$X_0 = Lrx_0\,, \quad X_i = Lrx_i\,, \tag{2.44}$$

$$X_{d-1} = \frac{1}{2r}\left(-1 + r^2(L^2 - x^2)\right)\,, \quad X_d = \frac{1}{2r}\left(1 + r^2(L^2 + x^2)\right)\,, \tag{2.45}$$

where x^2 was defined as $\eta_{\mu\nu}x^\mu x^\nu$. The line element is

$$\mathrm{d}s^2 = L^2\left[\frac{\mathrm{d}r^2}{r^2} + r^2\eta_{\mu\nu}\,\mathrm{d}x^\mu\,\mathrm{d}x^\nu\right]\,, \tag{2.46}$$

By defining $z = 1/r$, the line element becomes

$$\mathrm{d}s^2 = \frac{L^2}{z^2}\left(\mathrm{d}z^2 + \eta_{\mu\nu}\,\mathrm{d}x^\mu\,\mathrm{d}x^\nu\right)\,, \tag{2.47}$$

where the boundary region is now located at $z = 0$. This coordinate system is especially useful for the AdS/CFT correspondence. In these coordinates, AdS has a *horizon*, in the same sense as an event horizon of a black hole, located at $z = \infty$ ($r = 0$). This aspect will return in our discussion of Maldacena's original derivation for the AdS/CFT correspondence in Section 7.2.

Chapter 3

Quantum field theory

Quantum field theory (QFT) is one of the modern cornerstones of theoretical physics. This framework dawned from the unification of the theory of special relativity with quantum mechanics. Eventually, it became the blueprint for the Standard Model, the most successful theoretical framework for the description of particles and their interactions to date. In this chapter, we first introduce the necessary mathematical language to describe symmetries and discuss the basic ingredients of QFT. Next, we explain a few specific aspects of QFT which are relevant for the thesis in more detail, such as gauge symmetries, renormalization and conformal field theories. This chapter is largely inspired by [10–12].

3.1 Groups & symmetries

Symmetries are the beating heart of mathematics and physics. They simplify complicated problems and allow us to uncover fundamental laws from experiments. More abstract symmetries, known as gauge symmetries, play an important role in the formulation of the Standard Model as well as new theories that go beyond the Standard Model discussed later on in the thesis. Therefore, we provide readers with a thorough refresher on mathematical concepts related to symmetries.

3.1.1 Lie algebras and Lie groups

Symmetries are intimately linked to transformations applied to physical systems. Indeed, we can think of a *symmetry* as a mapping of the physical state of a system which leaves its dynamics invariant. Hence, symmetries can be combined into a deeper underlying structure. We will introduce the necessary mathematical tools to facilitate our description of these structures. First, let us recall the following two basic definitions:

- A *group* $(G, *)$ is a set endowed with a product $* : G \times G \to G$ which is associative, has a unit element e, and each element x has an inverse element x^{-1} such that their product is the unit element.

- An *algebra* $(\mathcal{A}, +, *)$ is a vector space with an additional bilinear, binary operation $* : \mathcal{A} \times \mathcal{A} \to \mathcal{A}$. Bilinear means that for all x, y, z in $\mathcal{A}$ and all a, b in the field F

over which the algebra is defined, we have:

$$(x+y)*z = x*z + y*z\,, \quad x*(y+z) = x*y + x*z\,, \tag{3.1}$$
$$(ax)*(by) = (ab)(x*y)\,. \tag{3.2}$$

An algebra is said to be *abelian* (or commutative) if its binary operation satisfies $x*y = y*x$. We limit our discussion to algebras defined over $F = \mathbb{C}$, and in a few cases which are explicitly stated $F = \mathbb{R}$. Of particular importance in theoretical physics are Lie algebras. A *Lie algebra* $\mathfrak{g}$ is an algebra for which the bilinear operation is a *Lie bracket* $* = [\cdot,\cdot]$, meaning it has the additional properties

1. Antisymmetry: $[x,y] = -[y,x]$,
2. Jacobi identity: $[x,[y,z]] + [y,[z,x]] + [z,[x,y]] = 0$.

Well-known examples are the Poisson bracket in the Hamiltonian formulation of classical mechanics and the commutator bracket in quantum mechanics. A textbook example of a Lie algebra is $\mathfrak{gl}(n)$, which as a set contains all $n \times n$ complex matrices. This set can be turned into an algebra by endowing it with the ordinary matrix multiplication as product. By introducing the bracket $[M_1, M_2] = M_1M_2 - M_2M_1$, one can turn this algebra into a Lie algebra.

The dimension of a Lie algebra $\mathfrak{g}$ is its dimension when considered as a vector space. Hence, there exists a basis[1] $\mathcal{B} = \{T^a \mid a = 1,\dots,d\}$, with $d = \dim\mathfrak{g}$. The Lie bracket is known once its action on a basis is identified. Therefore, each basis comes with their defining relations

$$[T^a, T^b] = f^{ab}{}_c T^c\,, \tag{3.3}$$

where again the Einstein summation convention is used. The expansion coefficients $f^{ab}{}_c$ are called the *structure constants* of the Lie algebra. For example, the algebra $\mathfrak{sl}(2)$, representing angular momentum, has generators L_1, L_2, L_3 which satisfy

$$[L_i, L_j] = i\sum_k \varepsilon_{ijk} L_k\,, \tag{3.4}$$

with ε_{ijk} the completely anti-symmetric Levi-Civita symbol.

If a subspace $\mathfrak{h} \subset \mathfrak{g}$ in itself satisfies the above properties, with Lie bracket induced by $\mathfrak{g}$, then $\mathfrak{h}$ is said to be a *subalgebra* of $\mathfrak{g}$. An important subalgebra, the *Cartan subalgebra*, is constructed from the *semisimple elements* x of the algebra. These are elements for which there exists a basis $\{\tilde{T}^a\}$ of $\mathfrak{g}$ such that $[x, \tilde{T}^a] \propto \tilde{T}^a$ for all a. The Cartan subalgebra is the maximal abelian subalgebra consisting of such semisimple elements. The *rank* of a Lie algebra $\mathfrak{g}$ is defined as the dimension of its Cartan subalgebra.

From Lie algebras, one can construct corresponding Lie groups. A Lie group G is a hybrid structure in the sense that it is both a group as well as a differentiable manifold, as introduced in Chapter 2. As discussed there, we can define the tangent space $T_\gamma G$ at a point $\gamma \in G$. For any pair of vector fields A, B, a Lie bracket (or Lie derivative) can be defined and in local coordinates ξ^a written as

$$([A,B])^a = B^b\partial_b A^a - A^b\partial_b B^a\,. \tag{3.5}$$

[1] We restrict our attention to finite-dimensional algebras and groups.

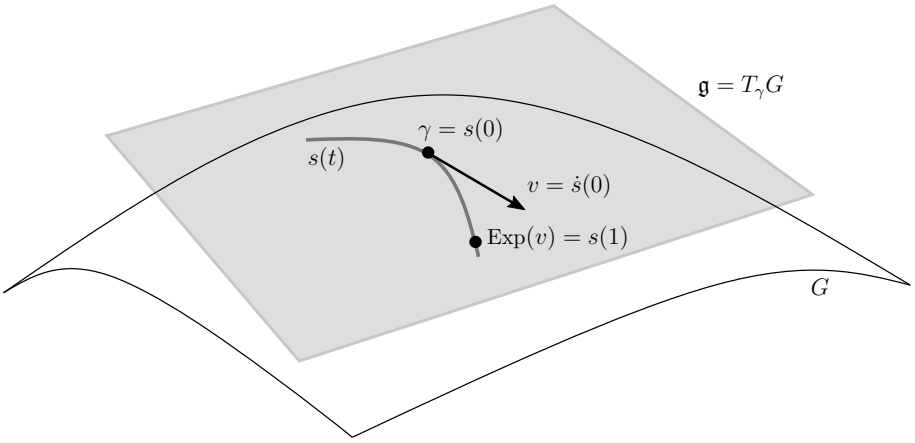

Figure 3.1: Visual representation of the exponential mapping from a Lie algebra $\mathfrak{g}$ to a Lie group G, with $T_\gamma G$ represented as tangent space of the manifold G.

In short, $T_\gamma G$ carries the structure of a Lie algebra. We define $\mathfrak{g} \equiv T_e G$, with e the unit element of G, as 'the' Lie algebra corresponding to the Lie group G.

We can define an exponential mapping from the tangent space $T_\gamma G$ to the manifold G, which gives us a link between the a Lie algebra and its Lie group. Any geodesic $s(t)$ in the manifold that passes through γ is uniquely characterized by its velocity v at γ, which is an element of the tangent space. Conversely, to any vector $v \in T_\gamma G$, we can associate a geodesic $s(t)$ which satisfies $s(0) = \gamma$ and $\frac{\mathrm{d}s}{\mathrm{d}t}|_{t=0} = v$. Given this one-to-one correspondence between geodesics and vectors, the *exponential mapping* is defined as

$$\mathrm{Exp} : T_\gamma G \to G : v \mapsto \mathrm{Exp}(v) = s(1) \in G\,. \tag{3.6}$$

In a way, the exponential map provides coordinates in the neighbourhood of γ from the tangent space $T_\gamma G$. The idea behind the exponential map is shown in Figure 3.1. For Lie algebras and groups involving matrices, the exponential map reduces to the usual exponential power series.

3.1.2 Representations

For physical applications, one is interested in the representation theory of Lie algebras. Let us consider as example the angular momentum algebra with generators L_1, L_2, L_3. We first introduce the step operators

$$L_\pm = L_1 \pm i L_2\,, \quad L_0 = 2L_3\,, \tag{3.7}$$

defined from $L_{1,2,3}$ given in equation (3.4) and which satisfy the Lie brackets

$$[L_+, L_-] = L_0\,, \quad [L_0, L_\pm] = \pm 2 L_\pm\,. \tag{3.8}$$

Hence, L_0 generates the Cartan subalgebra. We can now build a *representation* by starting from some eigenvector (quantum state) v_Λ with maximal eigenvalue (quantum number) Λ with respect to the Cartan subalgebra generator L_0:

$$L_0 v_\Lambda = \Lambda v_\Lambda\,. \tag{3.9}$$

One can think of this as a nuclear spin being fully aligned along the positive z-axis. If we now apply the L_- operator, we transition to another state with a lower eigenvalue of L_0. Indeed, we have

$$L_0 (L_- v_\Lambda) = L_- (L_0 v_\Lambda) + [L_0, L_-] v_\Lambda = (\Lambda - 2) v_\Lambda \,, \tag{3.10}$$

where we used equations (3.8) and (3.9). By repeatedly applying L_-, we obtain a chain of states until eventually the spin is fully aligned with the negative z-axis, and the representation is complete (*i.e.*, the final state is annihilated by L_-). Such a representation is called a *highest-weight representation* and is important for the representation theory of (super)conformal algebras. These algebras (and corresponding groups) lie at the basis of (super)conformal field theories and are frequently encountered in applications of AdS/CFT. Representations can be decomposed into smaller ones, and their 'atomic building blocks' are called *irreducible representations*. Often, physicists use the term *multiplet* for an irreducible representation.

3.1.3 Simple Lie algebras and Lie groups

Mathematicians have classified the most common Lie algebras, and one class of interest to physicists are the *simple* Lie algebras. These are Lie algebras without a proper ideal[2] and which are non-abelian[3]. Simple Lie algebras are divided into the classical and exceptional algebras. The *classical* Lie algebras come in infinite sequences A_n, B_n, C_n and D_n, with n denoting the rank of the algebra. They can be represented by matrices, which is why they are also referred to as matrix Lie algebras.

For their construction, we can start from the Lie algebra $\mathfrak{gl}(n)$ introduced above which, however, is itself not a simple Lie algebra. Indeed, all matrices proportional to the unit matrix form an (abelian) ideal of $\mathfrak{gl}(n)$. We can get rid of this ideal by requiring the matrices to be traceless. This gives the Lie algebra $A_{n-1} = \mathfrak{sl}(n)$. The other three classical algebras are simple subalgebras of $\mathfrak{gl}(n)$:

1. The *symplectic Lie algebras* $C_n = \mathfrak{sp}(n)$ are $2n \times 2n$ matrices M satisfying $M^T = JMJ$, where $J \in \mathfrak{gl}(2n)$ is the matrix
$$J = \begin{pmatrix} \mathbf{0}_n & \mathbb{1}_n \\ -\mathbb{1}_n & \mathbf{0}_n \end{pmatrix} . \tag{3.11}$$

2. The *orthogonal Lie algebras* are divided into even and odd dimension. First of all, $D_n = \mathfrak{so}(2n)$ consists of matrices M which obey $M^T K + KM = 0$, with $K \in \mathfrak{gl}(2n)$ the matrix
$$K = \begin{pmatrix} \mathbf{0}_n & \mathbb{1}_n \\ \mathbb{1}_n & \mathbf{0}_n \end{pmatrix} . \tag{3.12}$$

3. Similarly, the algebra $B_n = \mathfrak{so}(2n+1)$ contains matrices M obeying $M^T K' + K' M = 0$, with $K' \in \mathfrak{gl}(2n+1)$ the matrix
$$K' = \begin{pmatrix} 1 & 0 & 0 \\ 0 & \mathbf{0}_n & \mathbb{1}_n \\ 0 & \mathbb{1}_n & \mathbf{0}_n \end{pmatrix} . \tag{3.13}$$

[2] An *ideal* $\mathfrak{h}$ of a Lie algebra $\mathfrak{g}$ is a Lie subalgebra such that for all $x \in \mathfrak{h}$ and $y \in \mathfrak{g}$, we have $[x, y] \in \mathfrak{h}$. The term 'proper' excludes the obvious ideals $\{0\}$ and $\mathfrak{g}$.

[3] A d-dimensional abelian Lie algebra $\mathfrak{g}$ is isomorphic to $\bigoplus_{i=1}^{d} \mathfrak{u}(1)$.

Equivalently, we can write the above as $M^T = -KMK$, respectively $M^T = -K'MK'$.

All of the aforementioned algebras have, via the exponential mapping introduced above, corresponding Lie groups $G = \mathrm{Exp}(\mathfrak{g})$ which are all denoted by ordinary, uppercase letters and will likely be familiar to most readers. We mention that these groups are easily generalized to other signatures. For instance, one can define the group $\mathrm{SO}(p,q)$ as matrices M for which $M^T = -gMg$, where g is a diagonal matrix with signature (p,q).

Besides the classical Lie algebras, there are five other 'isolated' simple Lie algebras known as the *exceptional Lie algebras*: $\mathfrak{e}_6, \mathfrak{e}_7, \mathfrak{e}_8, \mathfrak{f}_4$ and $\mathfrak{g}_2$, where the subscript again denotes the rank of the Lie algebra. By exponentiating, we find corresponding Lie groups E_6, E_7, E_8, F_4 and G_2. They are harder to visualize compared to the classical Lie algebras, and are best understood using Dynkin diagrams: see [12] for details. In this thesis, we will encounter the E_7 and G_2 algebras. The dimensions of the simple algebras are provided in Table 3.1.

We also briefly discuss *real forms* of algebras, which are obtained from the above complex algebras by restricting the field to the real numbers. As a consequence, the Cartan-Killing metric given by ${f_{AC}}^D {f_{BD}}^C$ is well-defined. After diagonalizing this metric, we have compact generators corresponding to a negative eigenvalue and non-compact generators with a positive eigenvalue. The *character* of a real form is defined as the difference between the number of non-compact and number of compact generators. For example, $\mathfrak{sl}(n,\mathbb{R})$ and $\mathfrak{su}(n,\mathbb{R})$ are two distinct real forms of the A_{n-1} complex algebra and hence differ in number of (non-)compact generators. The algebra $\mathfrak{su}(n,\mathbb{R})$, containing the $n \times n$ traceless hermitian matrices, corresponds to the well-known Lie group $\mathrm{SU}(n)$. This group is frequently encountered as the symmetry group of field theories: important examples include the SU(3) of quantum chromodynamics and the $\mathcal{N} = 4$ SYM of the Maldacena AdS/CFT conjecture with gauge group $\mathrm{SU}(N)$ to be introduced in Section 6.2.1. Another real form we will encounter is $\mathfrak{e}_{7,7}$, *i.e.* the real form of $\mathfrak{e}_7$ with character equal to 7. Indeed, it turns out that the group $E_{7,7}$ is the isometry group of the scalar manifold of $4d$ maximal supergravity.

$\mathfrak{g}$	G	d
$A_n \cong \mathfrak{sl}(n+1)$	$\mathrm{SL}(n+1)$	n^2+2n
$B_n \cong \mathfrak{so}(2n+1)$	$\mathrm{SO}(2n+1)$	$2n^2+n$
$C_n \cong \mathfrak{sp}(n)$	$\mathrm{Sp}(n)$	$2n^2+n$
$D_n \cong \mathfrak{so}(2n)$	$\mathrm{SO}(2n)$	$2n^2-n$
$\mathfrak{e}_6$	E_6	78
$\mathfrak{e}_7$	E_7	133
$\mathfrak{e}_8$	E_8	248
$\mathfrak{f}_4$	F_4	52
$\mathfrak{g}_2$	G_2	14

Table 3.1: Dimensions of the simple Lie algebras.

3.1.4 The conformal group

Let us now introduce an important space-time symmetry group for the application of AdS/CFT, the conformal group. As the name suggests, this will be the symmetry group of conformal field theories. The conformal group extends the *Poincaré group*, which consists of space-time translations, rotations and Lorentz boosts. *Conformal symmetry* can be defined as the symmetries of space-time which leave the angles between vectors invariant. That is, if we have two vectors x^μ and y^μ, then the quantity

$$\frac{x \cdot y}{\sqrt{x \cdot x \; y \cdot y}}\,, \tag{3.14}$$

with $x{\cdot}y \equiv x^\mu y^\nu g_{\mu\nu}$ is left invariant by conformal transformations. Equivalently, conformal symmetries map the space-time metric to itself up to a prefactor which can depend on the space-time coordinates, *i.e.*

$$g_{\mu\nu} \to \Omega^2(x) g_{\mu\nu}\,. \tag{3.15}$$

The Lie algebra containing the infinitesimal transformations of the conformal group in d dimensions of space-time is generated by

1. the translations, with d generators P_μ,
2. the Lorentz transformations, with $d(d-1)/2$ generators $M_{\mu\nu}$,
3. the *scale transformations* $x^\mu \to \lambda x^\mu$, with 1 generator D called the *dilatation operator* and
4. the *special conformal transformations*

$$x^\mu \to \frac{x^\mu + a^\mu x^2}{1 + 2x^\nu a_\nu + a^2 x^2}\,, \tag{3.16}$$

   with d generators K_μ.

The non-zero commutation relations between the generators of the conformal algebra read

$$[M_{\mu\nu}, M_{\rho\sigma}] = 4\eta_{[\mu[\rho} M_{\sigma]\nu]}\,, \tag{3.17}$$

$$[P_\mu, M_{\nu\rho}] = 2\eta_{\mu[\nu} P_{\rho]}\,, \qquad [K_\mu, M_{\nu\rho}] = 2\eta_{\mu[\nu} K_{\rho]}\,, \tag{3.18}$$

$$[P_\mu, K_\nu] = 2(\eta_{\mu\nu} D + M_{\mu\nu})\,, \tag{3.19}$$

$$[D, P_\mu] = P_\mu\,, \qquad [D, K_\mu] = -K_\mu\,. \tag{3.20}$$

In fact, one can show that the algebra of equations (3.17) – (3.20) is isomorphic to $\mathfrak{so}(2,d)$ [10]. Therefore, the conformal group is isomorphic to $\mathrm{SO}(2,d)$. Note that, because of our discussion of Section 2.4, this is precisely the isometry group of an AdS space-time in $d+1$ dimensions. This simple yet remarkable observation is our first hint towards the AdS/CFT correspondence and its holographic nature.

3.2 Fields and Lagrangians

Now that the relevant terminology of symmetries is discussed, we recapitulate concepts of (quantum) field theory, where symmetries turn out to be of vital importance. We restrict our attention to theories that admit a Lagrangian. One starts with defining the fundamental fields in the theory, of which, when quantized, the excitations are interpreted as particles. Their interactions are encoded in an *action* obtained from a *Lagrangian density* (or simply Lagrangian) $\mathscr{L}$:

$$S = \int \mathrm{d}^d x \mathscr{L}\left(\phi_r, \partial_\mu \phi_r\right) , \tag{3.21}$$

where ϕ_r represents a collection of fields. The field equations (equations of motion) are derived from employing Hamilton's principle of least action. Extremizing the action yields the relativistic *Euler-Lagrange equations*

$$\frac{\partial \mathscr{L}}{\partial \phi_r} - \frac{\partial}{\partial x^\mu}\left(\frac{\partial \mathscr{L}}{\partial(\partial_\mu \phi_r)}\right) = 0 . \tag{3.22}$$

Interaction terms in the Lagrangian can be visualised as interaction vertices from which Feynman diagrams are built. Each Feynman diagram represents a contribution to the perturbative Dyson series expansion of the scattering S-matrix.

For field theories involving fermions, fermionic fields are required to anti-commute, *i.e.* their *anti-commutator*, defined as

$$\{A, B\} = AB + BA \tag{3.23}$$

has to vanish. Another indispensable tool for theories involving fermions are the *gamma matrices* γ^μ. These are $d \times d$ matrices that are solutions of the *Clifford algebra*, which means they satisfy the anti-commutation relations

$$\{\gamma_\mu, \gamma_\nu\} = 2\eta_{\mu\nu}\mathbb{1} . \tag{3.24}$$

Fermionic fields are often called *spinor fields* and are generically multi-component vectors. As such, spinor fields and gamma matrices carry additional indices, *spinor indices*, which are often suppressed in equations. We delay the subtle technicalities involving spinors in higher dimensions and in curved backgrounds to Chapter 6.

3.3 Gauge symmetries

Given the Lagrangian of a theory, one can look for symmetry transformations acting on the fields that leave the action invariant. Depending on whether the parameters of these transformations depend on the space-time coordinates or not, these transformations are said to be global or local. The latter is also frequently called a *gauge symmetry* and will be of vital importance to supergravity. By means of introducing gauge symmetries in this regard, we shall briefly review the main highlights of quantum electrodynamics (QED), as it is the simplest example of a gauge theory.

One way of obtaining a gauge symmetry in QED is by promoting a global symmetry to a local one. For this, first consider the free Dirac Lagrangian

$$\mathscr{L} = \overline{\Psi}(x)(i\gamma^\mu \partial_\mu - m)\Psi(x) , \tag{3.25}$$

where Ψ is a spinor field and overlines denote the Dirac conjugate. We remark that the Lagrangian is invariant under global phase transformations on the fermion fields, *i.e.*

$$\Psi(x) \to e^{iqf}\Psi(x)\,, \tag{3.26}$$

where q represents the electric charge and f is the parameter of the transformation. This symmetry is violated if we allow the argument of the phase to depend on the space-time coordinates, as the partial derivative will introduce an additional term. Therefore, if we want to promote this symmetry to a local one, we have to introduce a *gauge field* $A_\mu(x)$, which transforms as

$$A_\mu(x) \to A'_\mu(x) = A_\mu(x) + \partial_\mu f(x)\,, \tag{3.27}$$

which will cancel the offending extra term. We can introduce interaction terms between the matter and gauge fields via the principle of *minimal substitution*: all partial derivatives in the Lagrangian density are replaced by *covariant derivatives* D_μ, defined by

$$D_\mu(\cdot) = \partial_\mu(\cdot) + (iqA_\mu)(\cdot)\,. \tag{3.28}$$

QED is said to be an abelian gauge theory, since two consecutive phase transformations commute as they are ordinary numbers. Indeed, the transformations generate a U(1) gauge group. On the other hand, quantum chromodynamics (QCD), the QFT describing the strong interaction, is the most famous example of a *non-abelian gauge theory*, also frequently called *Yang-Mills (YM) theory*. In QCD, fermion fields carry either a red, green or blue color charge and are organized in a single vector $\Psi = \begin{pmatrix}\psi^R & \psi^G & \psi^B\end{pmatrix}$. The free fermion Lagrangian density is then invariant under the global transformations

$$\Psi(x) \to \Psi'(x) = U(\alpha)\Psi(x) = e^{i\sum_k \alpha_k \lambda_k}\Psi(x)\,, \tag{3.29}$$

where α_k are numbers and λ_k are eight matrices (see Table 3.1) that generate the $\mathfrak{su}(3)$ algebra. Hence, we have a global SU(3) symmetry group, which can be promoted to a gauge symmetry by invoking the principle of minimal substitution with covariant derivative

$$D_\mu\Psi(x) = \left(\partial_\mu + ig\sum_{k=1}^{8}\lambda_k A_\mu^{(k)}(x)\right)\Psi(x)\,. \tag{3.30}$$

This introduces eight gauge fields $A_\mu^{(k)}(x)$, the gluon fields, which transform along with the matter fields when a gauge transformation is performed. The parameter g is called the *gauge coupling*. Beyond QCD, gauge invariance is crucial in the formulation of the Standard Model of particle physics, which is based on a SU(3) $\times$ SU(2) $\times$ U(1) gauge group.

From a set of gauge fields, we can construct a *field strength* which is essentially similar to the curvature tensor from GR, as one can find its expression by taking the commutator of two covariant derivatives. Using form notation from Section 2.1, a field strength can schematically be written as $F = \mathrm{d}A + A \wedge A$. In string theory, which is a theory in ten dimensions of space-time, one encounters p-form gauge fields with $(p+1)$-form field strengths, where p can easily be larger than one. An example is the five-form field strength of type IIB string theory which appears in the Maldacena AdS/CFT conjecture.

Finally, we remark that GR can be seen as a gauge theory as well. Indeed, GR should be independent of the coordinate system and hence is manifestly invariant under the general coordinate transformations (also called diffeomorphisms), which can be seen as a gauged version of translations.

3.4 Renormalization

Above, we have briefly mentioned the perturbative expansion of QFT with Feynman diagrams. However, in some theories such as QED and QCD, evaluating loop integrals coming from higher-order terms can yield infinite answers, which is clearly undesirable in a theory of physics. To solve this issue, we can regularize and renormalize the theory. While this may merely seem a way of sweeping the infinities under the rug at first sight, it turns out that renormalization reveals a deep fact on QFTs.

First of all, the theory is modified via *regularization*, such that it remains finite in all orders of perturbation theory. For example, if the divergences originate from the behaviour of loop integrals at high energies, one can introduce a cut-off energy scale Λ (not to be confused with the cosmological constant) and only integrate over the momentum k running in the loop up until Λ. One can then multiply the integrand with a convergence factor $f(k, \Lambda)$ which causes the integral to be well-defined and convergent for large k. If this convergence factor tends to unity as Λ tends to infinity, we can restore the original theory by taking the limit $\Lambda \to \infty$.

Secondly, when adding the modified integral to the tree-level diagram of the perturbative expansion, one notices that these modifications can be absorbed into the coupling constants and masses of the particles of the theory. This admits the following interpretation. When writing down the Lagrangian density, one essentially treats all particles as 'bare' or free particles with masses m_0 and, for example, electric charge q_0. However, in Nature, we observe 'physical' particles with masses m and charges q, which can be related to the bare quantities through the absorption of the counterterms we obtained from the regularization procedure. The result is that the originally divergent integrals now remain finite even in the limit $\Lambda \to \infty$, whereas the divergences now appear in the relation between the bare and physical quantities. However, this is no longer an issue, as these relations are unobservable through experiments. This process of absorbing infinities through redefining parameters of the Lagrangian is called *renormalization*. A field theory is said to be *renormalizable* if its predictions, expressed via a finite set of parameters, remain finite after we remove all cut-offs introduced in the regularization procedure.

The concept of renormalization eventually leads us to the consideration that all QFTs depend on the energy scale at which our theories are defined. Computing this behaviour as a function of the energy scale leads us to renormalization group flows and the idea of running coupling constants. As this is an important part of the thesis, we will dedicate more time on this topic in the next chapter.

3.5 Conformal field theory

We will now introduce the second important player in the AdS/CFT correspondence, namely *conformal field theory* (CFT), which is a QFT that has the conformal group, introduced in Section 3.1.4, as symmetry group. Perhaps the most well-known example of a CFT is the critical Ising model. In fact, this is only an example of the more general fact that the fixed points of the renormalization group flow are CFTs, as we will discuss in more detail in the next chapter.

While it is not proven in general yet, it is believed that a scale-invariant, unitary and interacting field theory is automatically invariant under the complete conformal group

[13]. However, only the case $d = 2$ is proven, which is a special case since the conformal algebra is infinite-dimensional for $d = 2$. For the thesis, however, we are interested in CFTs in $d > 2$.

A CFT has no asymptotic states or S-matrix, as there are no scales in the theory, and the natural objects to consider are operators. The observables of interest to us are the correlation functions (n-point functions) of operators, with the expectation value taken with respect to the conformal vacuum. The interesting representations consist of operators $\mathcal{O}_\Delta$ which are eigenstates of the dilatation operator with eigenvalue Δ, *i.e.*

$$[D, \mathcal{O}_\Delta] = \Delta \mathcal{O}_\Delta \,. \tag{3.31}$$

The eigenvalue Δ is known as the *scaling dimension* of the operator. Applying the translations P_μ, respectively special conformal transformations K_μ, on $\mathcal{O}_\Delta$ creates an operator with scaling dimension $\Delta + 1$, respectively $\Delta - 1$. This is an immediate consequence of the commutation relations of the conformal group and the Jacobi identity. Indeed, one can compute that

$$\begin{aligned} [D, [P_\mu, \mathcal{O}_\Delta]] &= -[\mathcal{O}_\Delta, [D, P_\mu]] - [P_\mu, [\mathcal{O}_\Delta, D]] \\ &= -[\mathcal{O}_\Delta, [D, P_\mu]] + [P_\mu, [D, \mathcal{O}_\Delta]] \\ &= -[\mathcal{O}_\Delta, P_\mu] + \Delta [P_\mu, \mathcal{O}_\Delta] = (\Delta + 1)[P_\mu, \mathcal{O}_\Delta] \,, \end{aligned} \tag{3.32}$$

and hence $[P_\mu, \mathcal{O}_\Delta]$ is an operator with scaling dimension $\Delta + 1$. A similar proof shows that $[K_\mu, \mathcal{O}_\Delta]$ has scaling dimension $\Delta - 1$. Representations of the conformal group can now be built similar to the highest-weight representation of angular momenta introduced in Section 3.1.2. We start from a *conformal primary operator*, which is an operator $\widehat{\mathcal{O}}_\Delta$ that is annihilated by the special conformal transformations K_μ, *i.e.*

$$[K_\mu, \widehat{\mathcal{O}}_\Delta] = 0 \,, \quad \mu = 1, \ldots, d \,. \tag{3.33}$$

As the special conformal transformations lower a scaling dimension, the highest-weight in this case corresponds to the lowest scaling dimension. From a conformal primary, we get *descendant operators* by applying space-time translations P_μ:

$$\widehat{\mathcal{O}}_{\Delta+n} = P_{\mu_1} \cdots P_{\mu_n} \widehat{\mathcal{O}}_\Delta \,, \tag{3.34}$$

and the operators obtained in this way have scaling dimension $\Delta + n$. Hence, in the language of highest-weight representations, the operators P_μ and K_μ are the ladder operators of this representation.

The scaling dimension of an operator is bounded from below by the *unitarity bound*, which for scalars is [14]

$$\Delta \geq \frac{d-2}{2} \,. \tag{3.35}$$

This bound can be derived from requiring that the scalar product of primaries and descendants are positive definite. The unitarity bound implies that a representation must have an operator with lowest scaling dimension, and hence guarantees the existence of primary operators. The above discussion can be generalized to primary operators with non-zero spin. However, as we will focus on scalar operators in later chapters, we do not go into the details.

The presence of conformal symmetry greatly simplifies the 2-point and 3-point correlation functions. One can show that they are given by [10]

$$\langle \mathcal{O}_{\Delta_1}(x)\mathcal{O}_{\Delta_2}(y)\rangle = \frac{\delta_{\Delta_1,\Delta_2}}{|x-y|^{2\Delta_1}}\,, \tag{3.36}$$

$$\langle \mathcal{O}_{\Delta_1}(x)\mathcal{O}_{\Delta_2}(y)\mathcal{O}_{\Delta_3}(z)\rangle = \frac{c_{123}}{|x-y|^{\Delta_{12}}|y-z|^{\Delta_{23}}|x-z|^{\Delta_{13}}}\,, \tag{3.37}$$

where c_{123} is a constant to be computed and we have defined $\Delta_{12} = \Delta_1 + \Delta_2 - \Delta_3$ et cetera. A deep fact on CFTs is that correlation functions involving more than three interaction vertices can be reduced to combinations of the above two expressions by using the *operator product expansion* (OPE). Schematically, the expansion reads[4] [15]:

$$\mathcal{O}_1(x_1)\mathcal{O}_2(x_2) \xrightarrow{x_1\to x_2} \sum_i C_{12}^{(i)}(x_1,x_2)\mathcal{O}_i(x_2)\,. \tag{3.38}$$

The above expression is convergent for x_1 sufficiently close to x_2 and must be interpreted as being valid inside correlation functions. This allows us to reduce n-point correlation functions to $(n-1)$-point correlation functions, at the price of introducing the OPE coefficients $C_{12}^{(i)}$. Hence, we can use the OPE to iteratively reduce n-point correlation functions until we reach 2-point correlation functions. The OPE reminds us of the definition of an algebra, where the OPE coefficients are interpreted as structure constants. In essence, conformal symmetry simplifies the n-point correlation functions and makes calculations easier.

[4]We again restrict our attention to scalar operators for simplicity. For operators with spin, the spirit remains the same, but the algebra becomes more complicated.

Chapter 4

Dynamical systems and RG flows

In an attempt to describe the world around us as accurately as possible, science relies on models which allow us to interpret observations and make testable predictions. Many models study evolutions through time and rely on dynamical systems theory. A well-known example is the Lotka-Volterra population model of prey and predators. The concept of renormalization of a QFT, as introduced in Section 3.4, reveals the deep fact that physics changes with the energy scale. This implies that coupling constants of interactions vary as we change the energy scale of a theory. Naturally, we want to determine this evolution. We will find it useful to import tools from dynamical systems theory and apply them in our study of (holographic) RG flows.

In this chapter, we first remind readers of basic concepts on dynamical systems. This will also introduce the tools we employ in Part III and provide intuition on the major complications faced in Chapter 9 through simple examples which can easily be visualized. Next, we discuss the renormalization group flow of QFTs and their relation with dynamical systems in more detail.

4.1 Fixed points and linearization

In this section, we will review the most important definitions from dynamical systems theory [16]. To start, we define the *phase space* $\mathcal{P} \subset \mathbb{R}^n$ where $(x_1, \ldots, x_n)$ represent variables of interest to us. *Dynamical systems* have a first-order ordinary differential equation specifying the evolution of these n variables through phase space. Restricting our attention to homogeneous systems, this differential equation reads

$$\dot{\boldsymbol{x}} = \boldsymbol{f}(\boldsymbol{x})\,, \tag{4.1}$$

where from now on, bold font denotes column n-vectors. Dots are used to denote derivatives with respect to the evolution parameter, which in most dynamical systems will be time t. However, for renormalization group flows, this evolution parameter is the energy scale, while for their holographic dual, this parameter is the AdS coordinate r. In this chapter, we will stick to t for simplicity.

A *flow* is a solution $\boldsymbol{x}(t)$ of equation (4.1). Analytic solutions are hard to find if the functions $\boldsymbol{f}(\boldsymbol{x})$ are non-linear and complicated, such that numerical techniques are used to find flow solutions. Starting from an initial condition $\boldsymbol{x}(0)$, solutions can be constructed by updating the phase point along the phase velocity from equation (4.1) by small time steps.

Interesting phase points are those where the phase velocity vanishes, such that a flow will stay at this phase point forever. Such a *fixed point* (FP) $\boldsymbol{x}^\star$ is hence a solution to the equations $\boldsymbol{f}(\boldsymbol{x}^\star) = \boldsymbol{0}$. For a point $\boldsymbol{x}$ close to the fixed point, we can approximate equation (4.1) via a Taylor series:

$$\dot{\boldsymbol{x}} = \boldsymbol{f}(\boldsymbol{x}) \approx \boldsymbol{f}(\boldsymbol{x}^\star) + \mathcal{J} \cdot (\boldsymbol{x} - \boldsymbol{x}^\star) + \dots \,, \tag{4.2}$$

where the dots denote higher-order contributions which we will omit. Here, we introduced the *Jacobian matrix* $\mathcal{J}$ evaluated at the fixed point:

$$(\mathcal{J})_{ij} = \frac{\partial f_i(\boldsymbol{x})}{\partial x_j}\Big|_{\boldsymbol{x}=\boldsymbol{x}^\star} . \tag{4.3}$$

Since $\boldsymbol{f}(\boldsymbol{x}^\star) = \boldsymbol{0}$ by definition, the *linearization* of the dynamical system from equation (4.1) around $\boldsymbol{x}^\star$ gives

$$\dot{\boldsymbol{u}} = \mathcal{J} \cdot \boldsymbol{u} \,, \tag{4.4}$$

with $\boldsymbol{u} = \boldsymbol{x} - \boldsymbol{x}^\star$. This linearization allows us to gain information about the nature of the FP and the behaviour of flows originating from initial conditions close to the fixed point. Indeed, the general solution close to $\boldsymbol{x}^\star$ is

$$\boldsymbol{x}(t) = \boldsymbol{x}^\star + \sum_{i=1}^{n} A_i e^{\lambda_i t} \boldsymbol{v}_i \,, \tag{4.5}$$

where $\lambda_i, \boldsymbol{v}_i$ are the eigenvalues and their corresponding eigenvectors of $\mathcal{J}$. Loosely stated, positive eigenvalues $\lambda_i > 0$ will 'repel' flows away from the FP in the direction of $\boldsymbol{v}_i$, while negative ones $\lambda_i < 0$ will 'attract' flows towards the FP in the direction of $\boldsymbol{v}_i$.

A *saddle point* is a FP for which the Jacobian matrix has both positive as well as negative eigenvalues. Hence, a saddle will repel flows in some directions, but attract them in other directions. In our study of AdS vacua of supergravity theories in Chapter 9, all vacua will turn out to be saddle points.[1] We will be interested in finding holographic RG flows between two AdS vacua, meaning two saddle points of a dynamical system. The major complication in the numerical construction of such a flow solution is the fine-tuning of the expansion coefficients A_i. We will illustrate this in a simple model in the next section.

4.2 Fine-tuned flows: an illustrative example

In Part III, we will construct holographic RG flows which are essentially flows of dynamical systems in a 14-dimensional phase space. A major difficulty comes from the fact that almost all critical points are saddle points. Let us explain this issue in an overly simplified situation to provide intuition to readers. Consider the $2d$ dynamical system in the variables (x, y) with flow equations

$$\begin{cases} \dot{x} &= -1 + x^3 \,, \\ \dot{y} &= 1 - y^2 \,. \end{cases} \tag{4.6}$$

[1] The only exception is the vacuum located at the origin of the de Wit-Nicolai supergravity from Section 9.2, which is a star node.

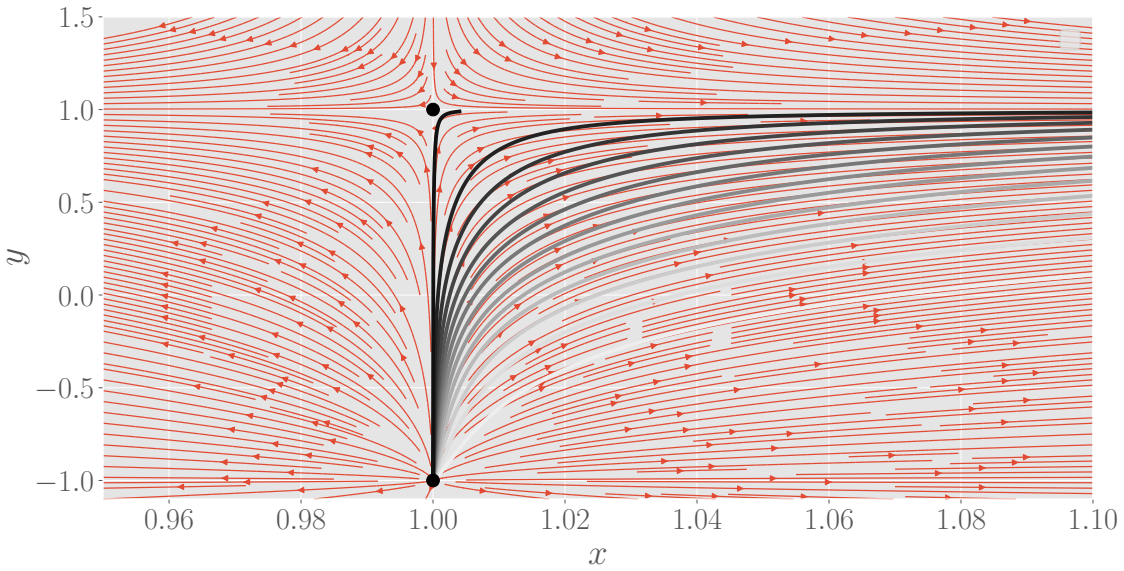

Figure 4.1: Illustrative example of fine-tuning a flow between critical points, involving saddle points. The streamlines of the system of equations of (4.6) are shown (red) along with the critical points (black dots) and some solutions, explained in detail in the text.

While we can easily obtain closed-form analytic expressions for solutions starting from any initial condition, let us, in line with the situation we will encounter in Part III, only make use of the linearization procedure and employ numerical techniques to construct solutions. We find that the above system has two fixed points at $(1, -1)$ and $(1, 1)$. The Jacobian matrix is

$$\mathcal{J}(x, y) = \begin{pmatrix} 3x^2 & 0 \\ 0 & -2y \end{pmatrix} . \tag{4.7}$$

The point $(1, -1)$ is a star node, and as the eigenvalues of the Jacobian are 3 and 2, solutions will flow away from it in all directions. This is a toy version of the SO(8) vacuum of the de Wit-Nicolai supergravity of Section 9.2. The other critical point $(1, 1)$ is a saddle point, as its eigenvalues are 3 and -2, and represents for example the G_2 vacuum of the same supergravity theory. In both cases, the eigenvectors point along the x- and y-axis, respectively. The saddle point therefore attracts flows in the vertical directions, but repels flows in the horizontal directions.

Suppose that we are interested in finding a flow that starts from $(1, -1)$ at $t = -\infty$ and ends up in $(1, 1)$ at $t = +\infty$. To construct such a flow, we start from the initial condition from equation (4.5) where we put $A_i \neq 0$ for eigenvalues $\lambda_i > 0$. We evaluate this expression at an initial time $t_{\text{in}} < 0$, *e.g.* $t_{\text{in}} = \ln(10^{-2})$, to induce a small perturbation on top of the fixed point. The linear expansion around the critical point gives

$$\begin{cases} x(t_i) = 1 + A_1 e^{3t_{\text{in}}} , \\ y(t_i) = -1 + A_2 e^{2t_{\text{in}}} . \end{cases} \tag{4.8}$$

In this toy example, we therefore have two arbitrary coefficients (A_1, A_2) that determine the initial condition. The task at hand is to find values such that the flow $(x(t), y(t))$ at a "late time" gets as close as possible to the saddle point. Since the dynamical system is homogeneous, we have a freedom in redefining the coordinate t, and this freedom allows

us to fix the value of one of the coefficients, say $A_1 = 1$. Hence, we have to scan a one-dimensional parameter space and try to find the optimal parameter value. An example of such a scan is given in Figure 4.1, showing 15 estimates with equidistant values for A_2 ranging from 0.713 (white) to 9.975 (black). Another generic feature of fine-tuning flow solutions is that often, due to numerical errors, solutions will inevitably diverge away from the target at very late times. Hence, the numerical solution has to be cut off at some late time.

This toy example raises an important issue that we need to overcome when constructing holographic RG flows. The real issue arises from the fact that we will work in a 14-dimensional space, implying that we will have to solve a much more complicated version of the above issue.

4.3 Renormalization group flows

We have discussed the issue of divergent loop integrals in perturbative calculations in QFT and how to remedy them in Section 3.4. While regulating these infinities, one inevitably introduces a mass or energy scale, such as the scale Λ in the cut-off method. As a consequence, after renormalization is performed, the parameters of the renormalized Lagrangian (*i.e.*, masses and coupling constants) depend on this scale Λ, while the parameters of the bare Lagrangian do not. This insight allows us to find the evolution of the renormalized Lagrangian parameters as we change the scale Λ, and the equations that govern this evolution are known as the *renormalization group* (RG) equations. Therefore, a coupling constant in the Lagrangian is a function of the energy scale Λ and is therefore called a *running coupling constant* $g(\Lambda)$.

The evolution of a running coupling[2] $g(\Lambda)$ is captured by the *beta-function*, which can be derived from the Callan-Symanzik equation [17]:

$$\beta(g) = \frac{\partial g}{\partial \ln \Lambda} = \Lambda \frac{\partial g}{\partial \Lambda} \,. \tag{4.9}$$

Now, we can make the link with dynamical systems. A running coupling constant lives in a phase space, which can be viewed as a 'theory space' $\mathcal{T}$, and its evolution is governed by the dynamical system $\dot{g} = \beta(g)$, where the dot now denotes a derivative with respect to $\ln \Lambda$. The fixed points of the RG equations correspond to CFTs. Indeed, whenever $g = g^\star$ such that $\beta(g^\star) = 0$, the coupling constant 'does not run' and the strength of the interaction is identical on all scales, such that the QFT enjoys scale invariance. A running coupling can approach a FP at high energy ($\Lambda \to \infty$), which is called a UV fixed point, or approach an IR fixed point as the energy is decreased. Equivalently stated, the UV behaviour is probed at short-distance interactions, while IR behaviour corresponds to large-distance interactions. As convention, we consider the evolution of RG flows going from the UV (high energy) to the IR (low energy). A famous example of a running coupling is the strong coupling of QCD: its interaction strength decreases as we increase energy, or equivalently, decrease distances of interactions.

Theories involving several parameters, such as the Standard Model with three coupling constants for each product of its gauge group, can then be studied using dynamical systems theory. In general, we expect the beta functions to be complicated, such that we can gain

[2]We restrict our attention to a single coupling constant for simplicity for now.

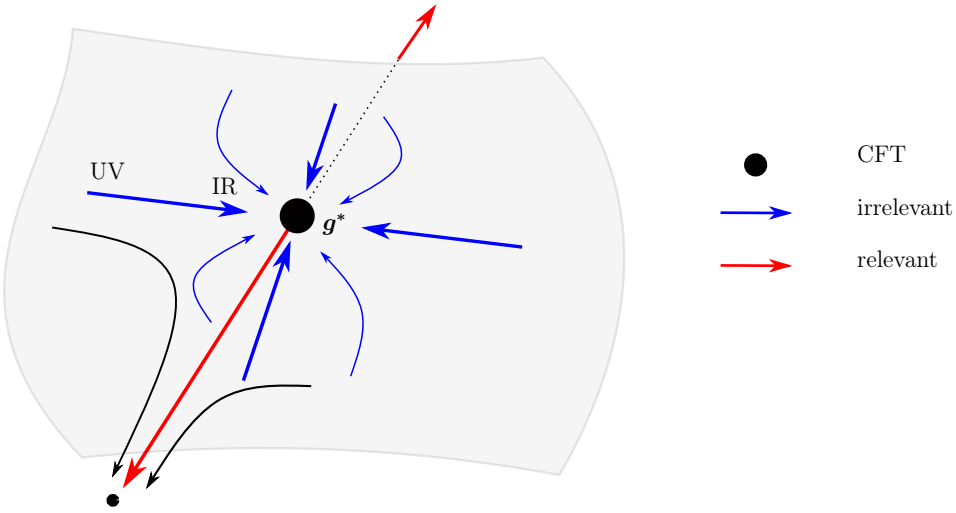

Figure 4.2: Illustration of RG flows in a theory space $\mathcal{T}$ around a fixed point (CFT) at couplings $\boldsymbol{g}^\star$. Blue (red) arrows denote deformations by irrelevant (relevant) operators and show how a QFT will flow from the UV to the IR. Generic flows, starting from deformations from both irrelevant and relevant operators, are shown in black.

information from linearizing the RG equations around fixed points. Suppose $\boldsymbol{g}^\star$ is a FP of the RG equations and the eigenvectors $\boldsymbol{v}_i$ and eigenvalues $\lambda_i = \Delta_i - d$ of the Jacobian of the beta function are known. As before, the general solution close to $\boldsymbol{g}^\star$ can then be written as

$$\boldsymbol{g}(\Lambda) = \boldsymbol{g}^\star + \sum_{i=1}^{n} A_i \boldsymbol{v}_i \left(\frac{\Lambda}{\Lambda_0}\right)^{\Delta_i - d}, \tag{4.10}$$

where Λ_0 is some reference scale. Here, the perturbation terms correspond to operators which are introduced in the Lagrangian of the CFT and deform it. The numbers Δ_i correspond to the scaling dimensions of these operators. The net effect of this deformation depends on the value of λ_i, as we mentioned in Section 4.1, and this in turn depends on the value of the scaling dimension Δ_i [17]:

- $\Delta_i > d$: As we go from the UV to the IR, the couplings will flow back towards the fixed point values $\boldsymbol{g}^\star$. The corresponding operator is then said to be an *irrelevant operator*.
- $\Delta_i < d$: Now, the opposite situation occurs. As the energy scale goes into the IR, the RG flow will be repelled away from $\boldsymbol{g}^\star$. The corresponding operator is then said to be a *relevant operator*.
- $\Delta_i = d$: In this case, the eigenvector has vanishing eigenvalue, and the corresponding operator is said to be a *marginal operator*. Higher-order quantum corrections can induce a weak dependence on the scale.

The RG flows around a CFT are visualized in Figure 4.2. Deformations coming from irrelevant operators will quickly die out, and RG flows will hence be centered along the same trajectories determined by the relevant operators, which is related to critical universality. Irrelevant operators, on the other hand, provide information which is, in the literal sense of the word, irrelevant for the physics at low energies.

Part II

Supergravity and holography

Chapter 5

Interlude: why new theories?

Before we delve into the mathematical details of the theories central to this thesis, let us slow down to get the bigger picture in view again. In the introductory part of this thesis, we briefly discussed two successful theories of 20^{th} century physics: Einstein's theory of GR and the Standard Model of particle physics. Why do we need theories beyond them? There are two ways of motivating new theories: either bottom-up or top-down. In the bottom-up or 'experimentally oriented' approach, we look for holes in our current description and try to fill those up with invoking as little new physics as possible. In the top-down approach, which is the 'theoretical approach', ambitious physicists attempt to find a mathematically well-defined theory of everything and try to fit current theories and our own universe into this larger framework.

In the bottom-up perspective, even those most fanatical about the Standard Model must admit that several reasons indicate that it is not a final, complete theory. One of those reasons is an issue known as the hierarchy problem. However, a more severe problem of the Standard Model is the observation that it only accounts for about 4% of the energy-matter content of the universe [9]. Indeed, besides the vacuum energy mentioned in Chapter 2, our universe contains dark matter which cannot consist of Standard Model particles. These issues are covered in more detail in Section 5.1. One way of resolving both issues is by introducing a new space-time symmetry known as supersymmetry.

The top-down approach, on the other hand, arises from the observation that GR and the principles of quantization are intrinsically incompatible with each other. Our current methods fail to create a consistent theory of quantum gravity out of GR. Obtaining such a unified theory is the main motivation for string theory, which is introduced in detail in Section 5.2. Supergravity theories, which are limits of string theories, provide an important bridge between GR and string theory.

As mentioned in the outline of this thesis, this chapter provides a more technical motivation for supergravity and string theory. However, at the same time, we will introduce readers to the essential concepts from those theories without any of the mathematical details. As such, this chapter serves as an introduction to the bulk content of Part II.

5.1 The hierarchy problem, dark matter and supersymmetry

The fact that none of the particles of the Standard Model are viable candidates for dark matter is an obvious motivation for the search of beyond the Standard Model physics. Another, subtler issue of the Standard Model is known as the hierarchy problem [18]. This issue is related to the sensitivity of the Higgs potential to new physics. It is well-known that the breaking of the electroweak sector of the Standard Model causes the Higgs field to acquire a vacuum expectation value and that, through interactions with the Higgs boson, the Standard Model particles acquire their masses in a gauge invariant manner. The mass of the Higgs receives quantum corrections from virtual particles coupled to the Higgs that run in loops of Feynman diagrams. These corrections can become enormous, especially if the energy scale at which new physics appears lies around the Planck scale $M_P \sim 10^{18}$ GeV. This is certainly expected to be the case, as some sort of quantum gravity theory should reign in this regime. These quantum corrections will therefore also affect the masses of quarks, leptons and the gauge bosons, through their coupling to the Higgs boson. In essence, it seems as if the entire mass spectrum of the Standard Model depends on the energy scale of new physics and is in that sense finely tuned, which is an undesirable aspect of a theory. The problem exists in various scenarios, including those where new, heavy particles indirectly couple to the Higgs and scenarios in which the scale of new physics lies beneath the Planck scale. In essence, theories are consistent with a natural mass of the fundamental Higgs scalar which is on the order of the Planck scale, while its effective, experimental value is around 125 GeV, which is why this issue is known as the hierarchy problem.

One proposed explanation of this problem adds an additional space-time symmetry, known as *supersymmetry* (susy), to the theory. The main idea is that susy connects bosonic and fermionic states by an operator Q which acts schematically as

$$Q\,|\text{Boson}\rangle = |\text{Fermion}\rangle\ , \quad Q\,|\text{Fermion}\rangle = |\text{Boson}\rangle\ . \tag{5.1}$$

In fact, under certain circumstances, theories can have multiple xerox copies of this operator, with $\mathcal{N}$ denoting the number of copies. As a consequence of the action of the Q operator, representations (multiplets) of bosons and fermions will be unified in larger representations, called *supermultiplets*. If susy is present in Nature, then Standard Model particles will have so-called superpartners, which differ in spin by 1/2 and carry names as selectrons, squarks, gluinos, photinos and so on. If susy is an unbroken symmetry, superpartners have equal masses.

Susy solves the hierarchy problem via the Feynman rule that fermions running through a loop of a Feynman diagram carry an additional minus sign. Consider for example the one-loop diagrams that contribute to the Higgs mass given in Figure 5.1. If the spin-1/2 fermions running in the loop on the left have bosonic superpartners (scalars) with an identical mass that run in a loop as well, such as in the diagram on the right, then there must be a relative minus sign between the two contributions. In essence, their contributions to the Higgs mass will cancel out, such that it remains on the order of GeV rather than the Planck scale.

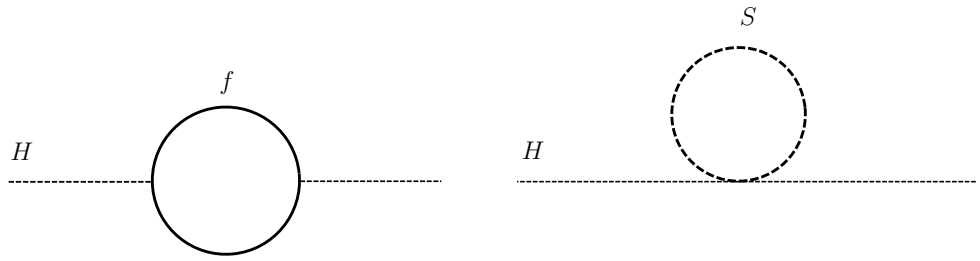

Figure 5.1: One-loop diagrams involving fermions f and their scalar superpartners S. Their contributions cancel out and solves the hierarchy problem.

Of course, one needs to ensure that this cancellation also persists at higher orders. Besides, if superpartners have the same mass, then particle colliders should have already discovered these superparticles, which is not the case. Therefore, the superpartners must be much heavier, which implies that susy must be a broken symmetry in Nature. This is actually also favourable from the perspective of the dark matter problem, given the following scenario. The lightest supersymmetric particle is a possible candidate for a dark matter particle. In the early, hot universe, superparticles were in thermal equilibrium with Standard Model particles. As the universe cooled down, this equilibrium was lost, and the superparticles annihilated or decayed to the lightest supersymmetric particle. The freeze-out abundance of this lightest superpartner could be an important contribution to dark matter sources.

The above discussion shows that susy is a promising way to deal with problems of the Standard Model, and provides a motivation to study susy in more detail in the next chapter.

5.2 String theory and supergravity

Einstein's theory of gravity is a classical field theory. As explained earlier, QED arose from the quantization of the electromagnetic field and resulted in the first successful and consistent QFT. One can wonder whether a similar approach can be used to develop a quantum theory of gravity by quantizing the metric, the dynamical field of GR. In this case, the quanta of the gravitational field are spin-2 particles known as *gravitons*, which are massless and travel at the speed of light. The action of a free, massless spin-2 particle turns out to be unique and is known as the Pauli-Fierz action [19]. Sadly, it turns out that the gravitational interaction is an irrelevant interaction and therefore, this QFT is non-renormalizable and UV-incomplete [20]. We are forced to maintain GR only as a low-energy effective field theory and as of today, we lack a quantum theory of gravity. One proposed UV-complete theory of quantum gravity is *string theory*.

5.2.1 Basics of string theory

We will present a short introduction to string theory based on [21, 22]. String theory treats one-dimensional extended objects, the strings, as the fundamental objects in the theory. Strings can be either open or closed, depending on whether or not its embedding into the higher-dimensional manifold is periodic in the spatial coordinate. The only two parameters appearing in the theory are the string coupling g_s and the length of the string ℓ_s, or equivalently, the *Regge slope* $\alpha' = \ell_s^2$. The vibrational modes of these strings

correspond to different particles. Historically, string theory was invented as an attempt to describe strong interactions, since hadrons resemble 'stringy objects' and the excitations of the strings could account for the vast amount of observed hadrons. However, with the advent and success of QCD, string theory fell out of favor as a fundamental theory of the strong interaction. Later, it was observed that string theories always contain a spin-2 particle, which became identified with the graviton. Ever since, string theory is studied as a favourable candidate of a theory of quantum gravity. Two other generic features of string theories support this goal. First, string theories containing fermions automatically require supersymmetry to be built in the theory and are therefore known as *superstring theories*. Second, Yang-Mills gauge groups, such as the gauge group of the Standard Model, naturally arise in the framework of (super)string theory.

A remarkable feature of superstring theories is that mathematical consistency automatically requires them to be formulated only in ten dimensions of space-time.[1] Hence, the remaining six dimensions have to be 'curled-up', or compactified, on an *internal manifold* whose size is small enough such that it escaped detection in experiments so far. Nevertheless, the structure of internal manifolds, such as their topology, has implications for the particle content of the $4d$ theory. In essence, the world looks effectively four-dimensional at low energy scales, or equivalently, large distance scales. These scales are relative to the scales built out of fundamental constants of Nature, such as the *Planck length*

$$\ell_P = \left(\frac{\hbar G}{c^3}\right)^{1/2} \sim 10^{-35}\ \mathrm{m}\,, \tag{5.2}$$

and the *Planck mass*

$$m_P = \left(\frac{\hbar c}{G}\right)^{1/2} \sim 10^{19}\ \mathrm{GeV}\,. \tag{5.3}$$

Hence, the size of the strings ℓ_s as well as the length scale of the internal manifolds is expected to be on the order of the Planck length. Similar to how the resolution of microscopes depends on the wavelength of light, experiments at energies below m_P (such as particle accelerators operating at the TeV-scale) cannot resolve distances on the order of the Planck length. Therefore, they are unable to probe the internal manifold or resolve the stringy nature of particles. This is why the four-dimensional Standard Model has been successful in explaining particle physics phenomena in our everyday lives.

There are five distinct superstring theories which are all formulated in ten dimensions of space-time: type I, type IIA, type IIB and two heterotic theories. Type IIA and IIB arise from using the superstring formalism for both left- and right-moving modes and have $\mathcal{N} = 2$ supersymmetry. The two possibilities are related to giving the supersymmetries either the same or an opposite chirality. Type I string theory can be obtained from type IIB by modding out the left-right symmetry and has $\mathcal{N} = 1$ supersymmetry. Besides superstring theories, there exist bosonic string theories which necessarily are formulated in 26 dimensions for mathematical consistency and which do not contain fermions. Nevertheless, a 'hybrid' theory, named *heterotic string theory*, can be obtained by using the

[1] In fact, string theory consists of a $2d$ CFT on the world-sheet of the string, and mathematical consistency requires that the central charge of this CFT vanishes. For this, additional scalar fields have to be introduced on the world-sheet in order to have an anomaly-free theory. However, these scalars can be interpreted as extra dimensions of space-time. We will not go into the details and stick to this interpretation.

bosonic $26d$ formalism for left-movers, and the $10d$ superstring formalism for right-movers and has $\mathcal{N} = 1$ susy. There are two possibilities related to two possible Lie algebras $\mathfrak{so}(32)$ and $\mathfrak{e}_8 \times \mathfrak{e}_8$ in the construction.

5.2.2 Branes

String theory contains other higher-dimensional objects besides strings, which are shown in Figure 5.2 and are known as p-branes, where p denotes the number of spatial dimensions of the object. A point-particle, for example, is a 0-brane, whereas a string is a 1-brane. The p-branes sweep out a $(p + 1)$-dimensional volume during their evolution, which is called the *world-volume*, as generalisation of the concept of a world-line of a point particle from GR. For a string, the world-volume is two-dimensional and hence referred to as *world-sheet*. As in QFT, one can perform perturbation theory in string theories. Diagrams in a QFT are built out of mergers of world-lines of particles in the theory. The analogue in string theory are diagrams where world-sheets of strings merge and is hence an expansion in Riemann surfaces. The loop expansion thus becomes an expansion in the genus of surfaces, with each increasing order introducing an additional factor of g_s. Certain superstring theories have a unique world-sheet topology at each order of the perturbation expansion which comes with a UV-finite contribution. This is in huge contrast with the enormous proliferation of Feynman diagrams from higher-order terms in QFT with infinities which have to be regulated. However, whether or not this perturbation theory is meaningful depends, of course, on the value of the string coupling g_s.

The p-branes with $p \neq 1$ do not belong to perturbative string theory, as they become infinitely heavy in the limit $g_s \to 0$. Rather, they are seen as non-perturbative excitations. The study of branes led to a remarkable amount of discoveries and demonstrates the power of string theory. For instance, it allowed for a microscopic description of the Bekenstein-Hawking entropy of black holes [23]. The AdS/CFT correspondence and its generalization to gauge/gravity dualities likewise arose out of studies of branes, as we will argue in more detail in Section 7.2. In type I and type II superstring theory, there exist *Dp-branes* on which open strings can end, where D stands for Dirichlet boundary conditions. In type IIB (IIA), only Dp-branes with odd p (even p) are allowed [24]. The D3-branes play an important role in the original AdS/CFT correspondence, formulated in type IIB string theory. Here, the gauge side of the correspondence comes from the massless modes of the open strings. When anchored to Dp-branes, these modes describe oscillations of the Dp-brane which, in the low-energy limit, result in the dynamics of a YM gauge theory living on the world-volume of the brane. The gravity side is related to a curved geometry which arises as follows. As mentioned, branes provide a higher-dimensional generalization of the notion of a point particle. Similar to how particles can be charged under gauge fields and generate fluxes, such as in electromagnetism, Dp-branes can be charged under $(p + 1)$-form gauge fields which have $(p + 2)$-form field strengths. Therefore, adding Dp-branes in the solution sources the field strengths and generates fluxes which, as a source of energy, curve the geometry. Such brane configurations also yield solutions in the low-energy limit (see below). These solutions have an event horizon and can be seen as higher-dimensional generalizations of the Reissner-Nördstrom black hole solution of GR. For this reason, they are also referred to as *black branes*. For example, the D3-branes of Maldacena's original AdS/CFT curve the geometry due to a five-form flux.

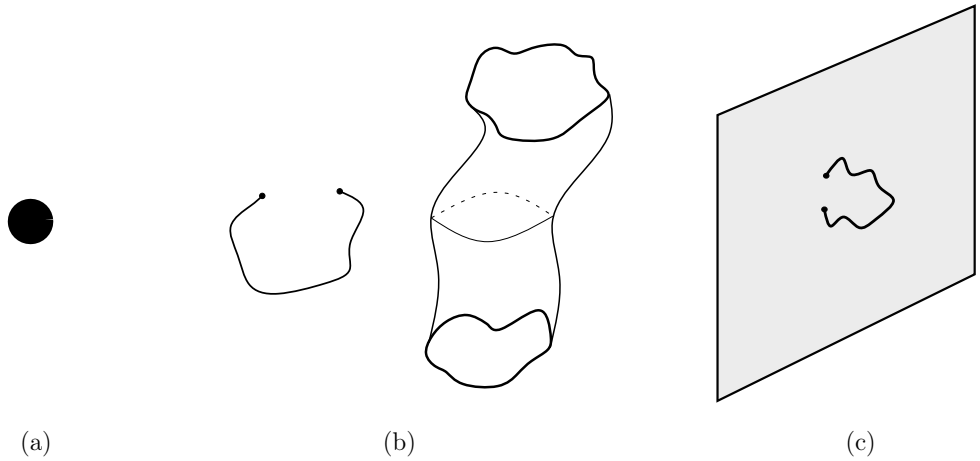

(a) (b) (c)

Figure 5.2: Branes in string theory. (a) A point-particle or 0-brane. (b) Two inequivalent 1-branes: an open string (left) and a closed string with a visualization of its $2d$ world-sheet (right). (c) Dp-brane visualized as a plane, with an open string attached to the brane.

5.2.3 The supergravity limit

While each of the string theories is a consistent quantum theory, the calculations become more tractable in a classical, low-energy limit of string theory. This limit is also known as the *supergravity limit*, as one approximates the string theory by a supergravity (sugra) theory. Besides an expansion in the coupling parameter of string theory g_s, in string theory, one also performs an expansion related to 'stringy effects'. That is, one can perform an expansion in terms of a dimensionless quantity made out of the length of the string ℓ_s (or equivalently, the Regge slope α'). By letting the size of the string tend to zero, we reduce the strings back to ordinary point particles. As we can only excite modes below the string energy scale, roughly stated equivalent to ℓ_s^{-1}, the limit $\ell_s \to 0$ means we omit all higher-energy excitation modes which arise from a finite length of the strings.

While these effective supergravity theories are non-renormalizable, this is of no issue since they are intended to describe low-energy phenomena of a more fundamental theory (the string theory) which itself is renormalizable in the UV. An independent way of obtaining supergravity theories is to promote susy from a global symmetry to a local one, *i.e.* by gauging susy. Supergravity cures the UV divergences of classical GR to some extent: while GR is only one-loop finite, pure sugra theories are finite up to two loops [25, 26].

5.2.4 Dualities and M-theory

One can wonder why there are five distinct superstring theories, rather than one single, fundamental theory. It turns out that there are various dualities linking the five string theories we have mentioned earlier. A *duality* in this context is an equivalence between different field and/or string theories [27]. There exist different well-known dualities in theoretical physics, such as the Montonen-Olive duality [28]. This is an example of a *strong/weak duality* or *S-duality*, as two distinct formulations are related to each other by replacing the coupling g by $1/g$, hence changing the strength of the coupling.

The various superstring theories are similarly related by S- and T-dualities. The S-

duality again amounts to replacing g_s with $1/g_s$. The T-duality, on the other hand, relates theories with different geometries for the internal manifold. Note that these dualities link different string theories to each other. In this regard, the AdS/CFT is a completely new kind of duality, as it provides a link between a quantum field theory and a string theory, which at first sight are two entirely inequivalent theories.

The dualities linking the various string theories seem to suggest that they are only different manifestations of a more fundamental theory. Another surprising result is that the type IIA and heterotic string theories at large coupling "grow an eleventh dimension" with size $g_s\ell_s$, which is either a circle or a line. Stated otherwise, a new quantum theory, known as *M-theory*, is conjectured to exist in eleven dimensions. According to Witten, M "stands for magic, mystery, or membrane, according to taste" [29]. Not much is known yet about M-theory, but like the superstring theories, it admits a low-energy supergravity theory. It turns out that the action of this $11d$ supergravity and its field content are uniquely fixed. Moreover, other supergravity theories in $d < 11$ dimensions can be obtained by compactifying some of the space-time dimensions on an internal manifold. In some sense, the quantum M-theory and its classical $11d$ supergravity limit incorporate many different theories in one. Hence, one could suggest to Witten to interpret M as standing for "mother of all theories".

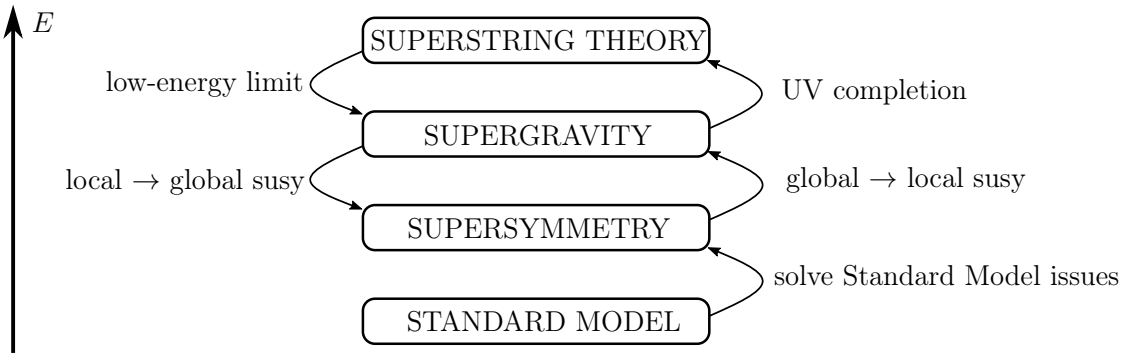

Figure 5.3: Links between the Standard Model, supersymmetry and -gravity, and superstring theories discussed in this chapter. They are organized according to energy regimes at which they are (believed to be) valid descriptions of Nature.

To summarize this chapter, whether one wants to solve flaws in the Standard Model or formulate a theory of quantum gravity, supersymmetry inevitably enters the stage. Supergravity theories are a next stop along the way, which can be reached either by gauging supersymmetry or by considering low-energy limits of superstring theories. The relations between the various theories we have discussed in this chapter are summarized by Figure 5.3. While we motivated the study of more fundamental theories from a phenomenological point of view, we want to emphasize that a large fraction of research in string theory is disconnected from phenomenology. Nevertheless, we can gain deep insights into the theoretical framework of physics from these studies. Indeed, a prime example is the discovery of the gauge/gravity duality, a revolutionizing idea which originated from the study of brane solutions. Following this line of thought, we will leave the cherished Standard Model behind, and, wading deeper into the waters of the great unknown, set sail for the terra incognita.

Chapter 6

Supersymmetry and supergravity

After the motivation given in the previous chapter, we will now discuss the mathematics of both supersymmetry and supergravity and focus on important aspects for holographic RG flows. After explaining theories with global (also called rigid) supersymmetry, we combine conformal symmetry with supersymmetry, leading to superconformal symmetry. An important example of a superconformal field theory is the $\mathcal{N} = 4$ super-Yang-Mills which appears in Maldacena's original AdS/CFT conjecture. Next, we discuss supergravity, obtained by promoting global supersymmetry to a local symmetry. This chapter is largely based on [10].

6.1 Global supersymmetry

Since supersymmetry involves spinors and we would like our discussion to be valid for any number of space-time dimensions, we begin this chapter with a discussion of spinors in an arbitrary number of dimensions of space-time.

6.1.1 Spinors in higher dimensions

Spinors in d space-time dimensions are treated in detail in [10]. We will assume spinor components are anti-commuting Grassmann numbers. As in $d = 4$, the key tools at our disposal are the gamma matrices, which satisfy the algebra

$$\{\gamma_\mu, \gamma_\nu\} = 2\eta_{\mu\nu}\mathbb{1}\,, \tag{6.1}$$

which is known as the Clifford algebra. This algebra has an irreducible representation in terms of square matrices of dimension $2^{\lfloor d/2 \rfloor}$, where $\lfloor\cdot\rfloor$ denotes the integer part. New elements of the algebra which are constructed from the γ^μ matrices must necessarily be anti-symmetric products, as symmetric products can be decomposed using equation (6.1). Recalling the anti-symmetrization of indices, as in equation (2.13), we define the notation

$$\gamma^{\mu_1\cdots\mu_r} \equiv \gamma^{[\mu_1\cdots\mu_r]}\,, \tag{6.2}$$

such that for example $\gamma^{\mu\nu} = \frac{1}{2}(\gamma^\mu\gamma^\nu - \gamma^\nu\gamma^\mu)$. We call r the *rank* of the gamma matrix. These products of gamma matrices serve as generators for the representation. In even dimensions $d = 2m$, we can define the matrix $\gamma_\star$ by

$$\gamma_\star = (-i)^{m+1}\gamma_0\gamma_1\cdots\gamma_{d-1}\,, \tag{6.3}$$

where indices are raised and lowered using the Minkowski metric. This matrix is used in left- and right-hand or *chiral projection* operators

$$P_L = \tfrac{1}{2}\left(\mathbb{1} + \gamma_\star\right) , \quad P_R = \tfrac{1}{2}\left(\mathbb{1} - \gamma_\star\right) . \tag{6.4}$$

In $d = 2m$ dimensions, a Dirac fermion field Ψ is a reducible representation and can be written in terms of two *Weyl fields* φ and χ, which are *chiral fermions* as they are defined as

$$\begin{pmatrix} \varphi \\ 0 \end{pmatrix} = P_L \Psi , \quad \begin{pmatrix} 0 \\ \tilde{\chi} \end{pmatrix} = P_R \Psi , \tag{6.5}$$

where the tilde denotes the Dirac conjugate[1]. Gamma matrices have an interesting symmetry property. There exists a unitary matrix, the charge conjugation matrix C, such that for any matrix of the Clifford algebra $\Gamma^{(r)}$ with rank r, we have

$$\left(C\Gamma^{(r)}\right)^T = -t_r C\Gamma^{(r)} , \quad t_r = \pm 1 , \tag{6.6}$$

which is then said to be (anti-)symmetric, depending on the sign of t_r. For the applications of susy and sugra, we replace the Dirac conjugate of a spinor λ by the *Majorana conjugate*:

$$\overline{\lambda} \equiv \lambda^T C . \tag{6.7}$$

We define the charge conjugate λ^C of a spinor as

$$\lambda^C \equiv B^{-1}\lambda^* , \quad B = it_0 C\gamma^0 , \tag{6.8}$$

where an asterix denotes ordinary complex conjugation. Using charge conjugation, we can define a *Majorana spinor* ψ as Dirac spinor that satisfies the reality condition

$$\psi = \psi^C , \tag{6.9}$$

and hence Majorana spinors have half as many degrees of freedom as a Dirac fermion. Majorana spinors are the most natural spinors to consider in the formulation of supergravity theories and are therefore central to our story. However, the reality condition from equation (6.9) can only consistently be applied if $t_1 = -1$, where t_1 is defined in equation (6.6), which holds in[2] $d = 4, 8, 9, 10$ and 11. Majorana spinors have $2^{\lfloor d/2 \rfloor}$ number of components. However, for $d = 10$, the Majorana and Weyl conditions can be imposed simultaneously, and this reduces the number of components by an additional factor 2. Hence, in $d = 10$, fundamental spinors have $2^{\lfloor d/2 \rfloor - 1} = 16$ components.

6.1.2 Supersymmetry algebras and representations

There exists a famous no-go theorem in theoretical physics, the Coleman-Mandula theorem [30], which states that, under reasonable assumptions, the Lie symmetry group of an interacting QFT is a direct product of the Poincaré group and an internal symmetry group (*i.e.*, of which the generators commute with the generators of the Poincaré

[1] We reserve overlines to denote the Majorana conjugate, to be defined later on, as this is the more natural conjugation to consider in supergravity.

[2] The condition $t_1 = -1$ also holds for $d = 8, 9$, but since then $t_0 = -1$, these spinors are called pseudo-Majorana. We will not consider them in more detail in this thesis. We will also not discuss symplectic spinors, which are used in $d = 5, 6, 7$.

algebra). Susy provides a loophole to this theorem. Because the supercharges Q are fermionic generators rather than bosonic, the symmetry algebra becomes a generalisation of a Lie algebra, for which the Coleman-Mandula theorem does not hold. Another no-go theorem, the Haag–Łopuszański–Sohnius theorem [31], further restricts the possibilities of supersymmetry algebras of an interacting QFT.

In global susy, the Poincaré symmetries with generators $P_\mu, M_{\mu\nu}$ are joined by the spinor supercharges Q^i_α, where α is an explicit spinor index and $i = 1, \ldots, \mathcal{N}$ labels the distinct supercharges in the algebra. The generators form a new algebraic structure known as a *superalgebra*, which is a $\mathbb{Z}_2$-graded Lie algebra. That is, the algebra has even and odd elements, which in physics terminology are called bosonic B and fermionic F, respectively. The bracket relations consist of a mixture of commutation and anti-commutation relations, depending on whether the bracket is between even or odd elements. Schematically, we have

$$[B, B] = B\,, \quad [B, F] = F\,, \quad \{F, F\} = B\,. \tag{6.10}$$

The Poincaré algebra is a Lie subalgebra of the susy algebra. Therefore, the commutation relations between its generators are still valid in the susy algebra: see equations (3.17) and (3.18). In global susy, the minimal extension requires the additional bracket relations

$$\{Q_{i\alpha}, Q^{\dagger j\beta}\} = \tfrac{1}{2}\delta_i{}^j \left(\gamma_\mu \gamma^0\right)_\alpha{}^\beta P^\mu\,, \tag{6.11}$$

$$[M_{\mu\nu}, Q_{i\alpha}] = -\tfrac{1}{2} i (\gamma_{\mu\nu})_\alpha{}^\beta Q_{i\beta}\,, \tag{6.12}$$

$$[P_\mu, Q_{i\alpha}] = 0\,, \tag{6.13}$$

and other brackets vanish. In particular, Q anti-commutes with itself and hence "squares to zero", which is important for representations of the susy algebra. From the bracket relation in equation (6.11), one can show that the energy of any state in the Hilbert space of a global susy field theory is positive. Moreover, it can be used to show that supermultiplets contain an equal amount of bosonic and fermionic degrees of freedom. This relation is why Q is sometimes loosely stated to be the "square root" of the translations. The second line above reinforces that the generators Q^i_α are spinors and carry angular momentum $1/2$. Equation (6.13) implies that superpartners have the same mass. We refer to $\mathcal{N} = 1$ susy as *simple supersymmetry*, while susy theories with $\mathcal{N} > 1$ are said to have *extended supersymmetry*.

The space of states can be formulated using ideas of highest-weight representations, discussed in Section 3.1.2. Here, the highest weight corresponds to the maximal helicity h_m of a particle in the representation. Other states in the representation are obtained by acting with the creation and annihilation operators $Q, Q^\dagger$, which raise or lower the helicity by $1/2$. Due to the required anti-symmetry in products of supercharges, states with helicity $h_0 - \frac{1}{2}m$ have multiplicity equal to the binomial coefficient $\binom{\mathcal{N}}{m}$.

In extended susy in $d = 4$, the above structure of representations limits the integer $\mathcal{N}$ to the range $\mathcal{N} \leq 8$. Since the supercharges change the helicity of a particle by $1/2$, theories with $4 < \mathcal{N} \leq 8$ necessarily contain a spin-$3/2$ particle. Such particles can only sit in the supergravity multiplet, and hence these field theories must necessarily correspond to supergravity theories. Therefore, field theories with global susy obey the stricter constraint $\mathcal{N} \leq 4$. Theories with $\mathcal{N} \geq 9$ are excluded because they necessarily contain particles of spin $s \geq 5/2$, for which no consistent interacting field theory is known. Note that these bounds apply to $d = 4$, such that we have up to maximally $N = 32$ independent components for the supercharges, and only $N = 16$ for global susy theories.

These bounds on N hold in all dimensions of space-time. Note, however, that supercharges have more components in higher dimensions, such that the bound on $\mathcal{N}$ changes. Recalling that irreducible spinors have $2^{\lfloor d/2 \rfloor}$ components in d dimensions, a single spinor in $11d$, for example, has 32 components. Hence, only $\mathcal{N} = 1$ supersymmetry is allowed in $11d$, and moreover, this must necessarily be incorporated as a supergravity theory. A supergravity theory is said to be *maximally supersymmetric* (or simply 'maximal') if it is invariant under the action of supercharges with $N = 32$ independent components in total. Examples are the $\mathcal{N} = 8, d = 4$ and $\mathcal{N} = 1, D = 11$ theories.

Extended supersymmetries can have an additional symmetry, called *R-symmetry*, which essentially rotates supercharges into each other. As such, these symmetries commute with Lorentz and translation generators and only act on the supercharges:

$$[T_A, Q_{i\alpha}] = (U_A)_i^{\ j} \, Q_{j\alpha} \,, \tag{6.14}$$

where T_A is a generator of the R-symmetry, and U_A its corresponding rotation matrix. Moreover, extended susy algebras can have additional charges, known as *central charges* $\mathcal{Z}$, which modify the anti-commutator of supercharges of the same chirality. The simplest example is for $\mathcal{N} = 2, d = 4$, where we can have the additional bracket relation

$$\{Q_{i\alpha}, Q_{j\beta}\} = -\tfrac{1}{2}\varepsilon_{ij} \, (P_L)_{\alpha\beta} \, \mathcal{Z} \,, \tag{6.15}$$

and the bracket for the opposite chirality follows from charge conjugation.

Supersymmetric field theories start from an action with a specified Lagrangian in terms of fields. One postulates the *supersymmetry transformations* of the fields, which can generically be written as

$$\delta_\epsilon \phi(x) = -i[\bar{\epsilon}^\alpha Q_\alpha, \phi(x)] \,, \tag{6.16}$$

where the parameters of the transformation ϵ_α are spinors. The theory is said to be supersymmetric if the susy transformations on the fields leave the action invariant. When looking for solutions of an extended susy theory, central charges are crucial for massive solutions. Indeed, one can show directly from the algebra that the mass M is restricted by

$$M \geq |\mathcal{Z}| \,, \tag{6.17}$$

for the above example of $\mathcal{N} = 2$ and multiple, similar bounds can be derived for $\mathcal{N} > 2$. The bound in equation (6.17) is known as the Bogomol'nyi–Prasad–Sommerfield bound or *BPS bound*. An important point to stress is that a solution of a supersymmetric field theory is not necessarily itself invariant under the supersymmetry transformations. However, one can show that whenever the BPS bound from equation (6.17) is satisfied, the solution is supersymmetric and in this case is known as a *BPS solution*. Hence, equality in the BPS bound is a fingerprint of a remaining amount of supersymmetry in the solution. However, it can happen that invariance under some supercharges is broken and the solution carries less supersymmetry compared to the theory we started with. If n_Q independent supercharges leave a solution invariant, the solution is referred to as $\frac{n_Q}{\mathcal{N}}$-BPS.

6.2 Superconformal field theory

Now that we highlighted the main points of supersymmetric field theories, we can extend the susy symmetry algebra even further. For example, in RG flows of susy field

theories, we also have additional conformal symmetry at the critical points of the beta functions. Hence, conformal symmetry and supersymmetry join into the *superconformal algebra* (SCA), and a QFT invariant under this symmetry group is called a *superconformal field theories* (SCFT). The SCA is again a superalgebra which contains the conformal algebra $\mathfrak{so}(2,d)$ as Lie subalgebra. Moreover, there appear new supercharges, the *conformal supercharges*, denoted by S^i_α. Intuitively speaking, just as Q is seen the "square-root" of P_μ, S can be seen as the "square-root" of K_μ. Figure 6.1 below summarizes the various Lie (super)algebras that have been encountered in this thesis so far.

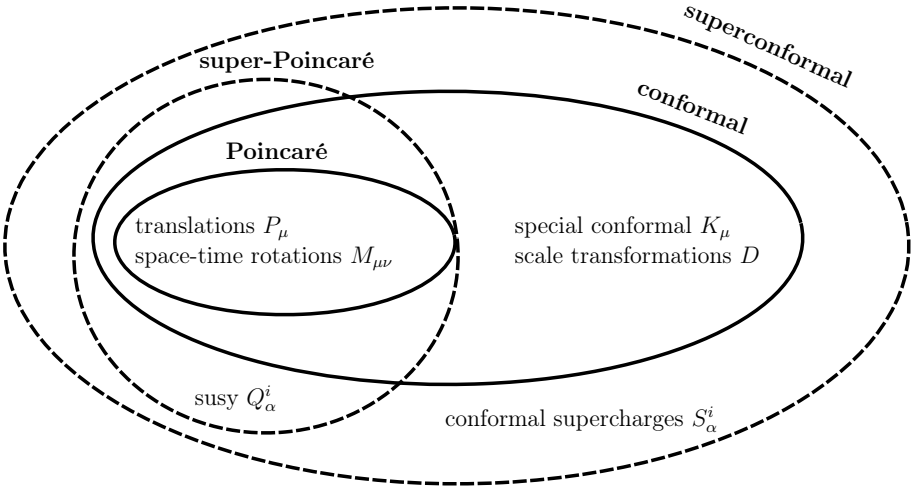

Figure 6.1: Lie (super)algebras encountered in this thesis and their corresponding generators. Bold ellipses denote Lie algebras, while dashed ellipses denote superalgebras.

Superconformal algebras only exist for $d \leq 6$ [13], and a classification can be found in [32]. On top of the commutators of the conformal algebra, which were specified in equations (3.17) – (3.20), and those of the super-Poincaré algebra, given by equations (6.11) – (6.13), the SCA has additional bracket relations. These depend on d and the R-symmetry group, but schematically, they have the general structure [13]

$$[D,Q] \propto \tfrac{1}{2}Q\,, \quad [D,S] \propto \tfrac{1}{2}S\,, \quad [P,S] \propto Q\,, \tag{6.18}$$

$$\{S,S\} \propto K\,, \quad \{Q,S\} \propto M + D + R\,. \tag{6.19}$$

The representation theory of the SCA mimics that of the conformal algebra, discussed in Section 3.5. Again, the dilatation operator generates the Cartan subalgebra and we can define the *Weyl weight* w_x of an element x of the SCA as the eigenvalue under the action of D, *i.e.* $[D,x] = w_x x$. The Weyl weights of all generators of the superconformal algebra are given in Table 6.1. Similar to how we defined a conformal primary operator,

$\boldsymbol{w_x}$	1	1/2	0	−1/2	−1
$\boldsymbol{x}$	P_μ	Q^i_α	$D, M_{\mu\nu}, T_A$	S^i_α	K_μ

Table 6.1: Weyl weights of the generators of the superconformal algebra.

we can define a *superconformal primary operator* as a state which is annihilated by all supercharges S^i_α. Other states, again called *descendant operators*, arise by acting with the supercharges Q^i_α on a superconformal primary. Note that this representation is finite,

as supercharges square to zero. Moreover, a representation can contain states which are annihilated by a (combination of) supercharges Q, such that the representation is said to be a *short representation*, and the primary operator is known as a *chiral primary operator*. Since the conformal algebra is a subalgebra of the SCA, the representations of the SCA will include representations of the conformal algebra. Note, for instance, that a superconformal primary is also a conformal primary. Besides, by acting with supercharges Q on a superconformal primary, we find additional states which are conformal primaries.

6.2.1 $\mathcal{N} = 4$ super Yang-Mills

Many applications of AdS/CFT involve superconformal field theories. An important example is the $\mathcal{N} = 4, d = 4$ *super Yang-Mills* (SYM) field theory, which combines a Yang-Mills SU(N) symmetry with susy. This particular theory appears in Maldacena's original AdS/CFT conjecture, to be discussed in Section 7.2. We briefly provide a few more details on this theory, but readers are referred to [10, 13] for a more extensive discussion. This theory has a gauge potential A_μ, four chiral fermion fields $P_L\lambda$ and six real scalars X^i in representations of the R-symmetry group SU(4) $\cong$ SO(6) as traceless, hermitian matrices. The Lagrangian is [10]

$$\begin{aligned}\mathscr{L} = \mathrm{tr}\big(&\tfrac{1}{2}F_{\mu\nu}F^{\mu\nu} + 2\overline{\lambda}^{\alpha}\gamma^{\mu}D_{\mu}P_L\lambda_{\alpha} + D_{\mu}X^iD^{\mu}X^i \\ &+ \left(g\left((C^{\alpha}{}_{\beta})^i\overline{\lambda}_{\alpha}P_L[X^i,\lambda_{\beta}]\right) + \text{ h.c.}\right) + \tfrac{1}{2}g^2\sum_{i,j}[X^i,X^j]^2\big)\,,\end{aligned} \tag{6.20}$$

where D_μ is the covariant derivative, g is the gauge coupling and the matrices C^i are given in terms of the Pauli matrices:

$$C^1 = \begin{pmatrix} 0 & \sigma_1 \\ -\sigma_1 & 0 \end{pmatrix}, \quad C^2 = \begin{pmatrix} 0 & -\sigma_3 \\ \sigma_3 & 0 \end{pmatrix}, \quad C^3 = \begin{pmatrix} i\sigma_2 & 0 \\ 0 & i\sigma_2 \end{pmatrix}, \tag{6.21}$$

$$C^4 = \begin{pmatrix} 0 & i\sigma_2 \\ i\sigma_2 & 0 \end{pmatrix}, \quad C^5 = \begin{pmatrix} 0 & 1 \\ -1 & 0 \end{pmatrix}, \quad C^6 = \begin{pmatrix} -i\sigma_2 & 0 \\ 0 & i\sigma_2 \end{pmatrix}. \tag{6.22}$$

The trace operation appearing in the Lagrangian ensures gauge-invariance of the constructed operators.

Of particular importance for AdS/CFT are the *single-trace operators*, which belong to short multiplets [21]. They can be written as

$$\mathcal{O} = \mathrm{tr}\left(\phi^{I_1}\cdots\phi^{I_n}\right). \tag{6.23}$$

Since commutators of scalar fields appear in the susy algebra of this theory, if some of the indices are anti-symmetrized, the state can be written as $\{Q,\psi\}$ for some field ψ and (combination of) supercharge(s) Q and is therefore a descendant state. Hence, only when the indices $I_1,\ldots,I_n$ are symmetrized does the state correspond to a primary operator, and their scaling dimension is equal to n [13].

6.3 Supergravity

We still require a few additional tools for the formulation of supergravity. Since supergravity heavily depends on both fermions and curved space-time, we have to introduce the frame field in order to combine these two concepts in supergravity.

6.3.1 Frame fields and spinors in curved space-times

For the application of supergravity, it is convenient to introduce a new basis for the tangent space T_pM of the space-time manifold which will allow us to work with spinors in curved space-times. In GR, one often works with the coordinate basis $\hat{e}_\mu = \partial_\mu$ for the tangent space, as mentioned in Chapter 2. However, there exists another basis which turns out to be more favorable if one wants to couple fermions to gravity. This is certainly required in supergravity, as the graviton will have a superpartner, the spin-3/2 gravitino. The new basis of T_pM is based on the input that locally, at a space-time point, the curvature of the manifold can be negated in the sense that there exists coordinates such that space-time looks flat in a neighbourhood surrounding that point [1]. Therefore, one can choose an orthonormal basis $\hat{e}_a$ with respect to the Minkowski metric. That is, their inner product satisfies

$$\hat{e}_a \cdot \hat{e}_b = \eta_{ab} \,. \tag{6.24}$$

If we denote the coordinate basis, introduced in Chapter 2, by $\hat{e}_\mu = \partial_\mu$, then one can expand the coordinate basis vectors $\hat{e}_\mu$ in terms of the orthonormal basis vectors

$$\hat{e}_\mu = e^a_\mu \hat{e}_a \,, \tag{6.25}$$

and one can similarly define the components e^μ_a. The orthonormal basis vectors $\hat{e}_a$ are known as the tetrad or vielbein (in $4d$ also vierbein), but we will call them *frame fields*. As before, we will, by abuse of terminology, refer to their components e^a_μ as frame fields as well. If we expand the inner product in equation (6.25), we find that

$$g_{\mu\nu} = e^a_\mu e^b_\nu \eta_{ab} \,, \tag{6.26}$$

such that, loosely speaking, frame fields are the "square root" of the metric. Note that frame fields hence depend on the space-time coordinates. The idea is that every point in space-time has a *local frame*, which is characterized by *local frame indices* which in our convention will be denoted by Latin letters $a, b, \ldots$ while Greek letters $\mu, \nu, \ldots$ are used for *coordinate indices*. These local frames are not unique, but they are equivalent up to local Lorentz transformations [10]. Such local Lorentz transformations act only on the frame indices and leave coordinate indices inert. We can still perform diffeomorphisms (coordinate transformations), which then act on coordinate indices while leaving frame indices invariant.

Since spinors are characterized by their properties under Lorentz transformations, it is evident that one needs a way to encode how spinors transform under these local Lorentz transformations. The defining relation of the Clifford algebra of gamma matrices, equation (6.1), uses the Minkowski metric. To adapt this to curved space-times, we therefore interpret this equation as valid in the local frame, *i.e.* we should, given the above conventions, rewrite equation (6.1) as $\{\gamma_a, \gamma_b\} = 2\eta_{ab}\mathbb{1}$. As before, the matrices γ^a are numerical, constant matrices. The frame fields are then used to transition between the local and the coordinate basis, *i.e.* we construct new gamma matrices $\gamma^\mu(x) = e^\mu_a(x)\gamma^a$, which are now space-time dependent, for the curved space-time.

In the language of frame fields, the connection is specified by $\omega^{ab} = \omega_\mu{}^{ab}\, \mathrm{d}x^\mu$, known as the *spin connection*. In GR, we required invariance under general coordinate transformations, seen as local (gauged) translations. As a consequence, the principle of minimal substitution dictated that ordinary derivatives of vectors and coordinate tensors should

be replaced by covariant derivatives ∇_μ using the Christoffel connection. Spinors ψ in gravitational theories must be described by local frame components, and invariance under local Lorentz transformations (generated by the matrices γ^{ab}) similarly dictates that partial derivatives acting on spinor fields are replaced by a covariant derivative D_μ which is created from the spin connection, *i.e.*

$$D_\mu\psi(x) = \left(\partial_\mu + \tfrac{1}{4}\omega_{\mu ab}(x)\gamma^{ab}\right)\psi(x)\,, \tag{6.27}$$

suppressing the spinor indices. The spin-3/2 gravitino field Ψ_μ, to be defined later on as the gauge field of local supersymmetry, therefore has a combined covariant derivative, as they carry a vector as well as spinor index, *i.e.*:

$$\nabla_\mu\Psi_\nu = D_\mu\Psi_\nu - \Gamma^\rho_{\mu\nu}\Psi_\rho = \left(\partial_\mu + \tfrac{1}{4}\omega_{\mu ab}(x)\gamma^{ab}\right)\Psi_\nu - \Gamma^\rho_{\mu\nu}\Psi_\rho\,. \tag{6.28}$$

6.3.2 Eleven-dimensional supergravity and dimensional reduction

We have already remarked several times that supergravity is the gauged version of global susy, such that the susy parameters ϵ_α now depend on the space-time coordinates $\epsilon_\alpha(x)$. A brief, hand-waving argument explains why gauging susy implies gravity is present. Starting from the generic transformation rule on fields, see equation (6.16), the commutator of two susy transformations δ_1, δ_2 with parameters[3] ϵ_1, ϵ_2 is given by

$$[\delta_1, \delta_2]\phi(x) = -\tfrac{1}{2}\bar{\epsilon}_1\gamma^\mu\epsilon_2\left(\partial_\mu\phi(x)\right)\,, \tag{6.29}$$

which is a translation (as expected) with parameter $-\frac{1}{2}\bar{\epsilon}_1\gamma^\mu\epsilon_2$. Therefore, if we want to promote susy to a local symmetry, this implies that translations become promoted to local symmetries. Such transformations are precisely the diffeomorphisms and imply that gravity is present in the theory. As we remarked in Section 3.3, the consistent gauging of a global symmetry requires the introduction of a gauge field, which in this case is a spin-3/2 field known as the *gravitino* $\Psi_{\mu\alpha}$. If we gauge $\mathcal{N}$-extended susy, this introduces $\mathcal{N}$ gravitini fields.

The simplest supergravity is[4] $\mathcal{N} = 1, D = 11$ supergravity [33], as its action and field content are completely fixed. The maximal number of space-time dimensions in which sugra theories can be formulated is 11, because a fundamental spinor in $D = 12$ is a Majorana spinor[5] and hence has $2^6 = 64$ components. Therefore, this would violate the constraint that sugra theories must have $N \leq 32$ components of supercharges. The field content of $11d$ sugra is as follows [10]. The graviton field is, of course, present and contains 44 bosonic degrees of freedom. There is one gravitino, which has 128 fermionic degrees of freedom. As the bosonic and fermionic degrees of freedom must be equal there are 84 bosonic degrees of freedom left, which are accounted for by a 3-form gauge field A_{MNP}.

Most of the maximally supersymmetric sugra theories in $d < 11$ can be obtained from $11d$ supergravity by compactification, with type IIB sugra in $10d$ being the only exception. Compactification means that we obtain a lower-dimensional theory, say in

[3] We suppress the spinor indices.

[4] We denote the number of space-time dimensions using capital D, since we will construct d-dimensional ($d < D$) theories via compactification.

[5] It cannot be a Majorana-Weyl spinor, as such spinors only exist in $D = 2 \bmod 8$ [10].

d dimensions, from a D-dimensional theory by reducing $D-d$ space dimensions to a compact space. Hence we write the D-dimensional space-time as a product space-time: $M_D = M_d + X_{D-d}$, where X_{D-d} is a compact space, referred to as the *internal manifold*. This process is known as *Kaluza-Klein (KK) compactification*.

When compactifying fields in the theory, we get so-called towers of massive states, which we can motivate using the simplest example of a free scalar field living in $\mathbb{R}^{1,d-1}\times S^1$, such that the compact space is a circle. The scalar field satisfies the Klein-Gordon equation $(\Box - m^2)\phi = 0$, with the d'Alembertian operator given by $\Box = g^{\mu\nu}\nabla_\mu\nabla_\nu$. Writing the space-time coordinates as (x^μ, y), with y the coordinate on the circle, we can decompose the d'Alembertian as $\Box_{d+1} = \Box_d + \partial_y^2$, and the Klein-Gordon equation becomes

$$\left(\Box_d + \partial_y^2 - m^2\right)\phi(x^\mu, y) = 0\,. \tag{6.30}$$

Since we require ϕ to be single-valued along the circle, y must be periodic and hence we can expand ϕ in Fourier modes as

$$\phi(x^\mu, y) = \sum_{k\in\mathbb{Z}} e^{iky/L}\phi_k(x^\mu)\,, \tag{6.31}$$

where L is the radius of the circle and k labels the different Fourier modes. Hence equation (6.30) becomes

$$\left[\Box_d - \left(\frac{k}{L}\right)^2 - m^2\right]\phi_k(x^\mu) = 0\,. \tag{6.32}$$

Hence, from the d-dimensional space-time point of view, we have an infinite amount of scalar fields, namely the Fourier modes $\phi_k(x^\mu)$, with masses $m_k^2 = m^2 + (k/L)^2$, which is an infinite tower of massive modes for each value of k. In *dimensional reduction*, a procedure related to Kaluza-Klein compactification, we perform a *consistent truncation* of this tower of states and retain only a finite subset of the Fourier modes. Usually, these include only the massless and/or some of the lightest modes. The heavier Fourier modes are omitted in a consistent way, that is, such that field equations are satisfied on the smaller subset and the omitted, heavier modes are not sourced by the lighter modes which are kept.

As mentioned above, dimensional reduction allows us to create maximally symmetric theories in $d < 11$ dimensions starting from the $11d$ sugra theory, of which the field content was specified above. Of particular interest for the thesis is the $\mathcal{N} = 8, d = 4$ sugra theory. Via dimensional reduction, one can find the following field content. The $11d$ gravitino gives rise to eight gravitinos and 56 spin-1/2 fields in $4d$. Using Greek letters to denote $4d$ coordinates, and Latin letters for coordinates on the internal manifold, the $11d$ metric yields the $4d$ metric $g_{\mu\nu}$, 7 spin-1 particles $g_{\mu i}$ and 28 scalars g_{ij}. The 3-form components give 21 vectors $A_{\mu ij}$ and 42 scalars of which 35 come from A_{ijk} and the remaining 7 from $A_{\mu\nu i}$. In total, there are 28 vector fields and 70 scalar fields in the $\mathcal{N} = 8, d = 4$ theory, which will turn out to be important for our story later on. In particular, we remark that the compactifications mentioned above are on a torus T^7 and as a result, the vectors turn out to gauge a $\mathrm{U}(1)^{28}$ gauge group. Moreover, the scalar potential in this supergravity vanishes. One can deform the gauge group into a less trivial group, and this results in a so-called gauged supergravity, where the coupling between vectors and scalars introduces a non-trivial scalar potential. This will be discussed in more detail in Section 6.3.5.

6.3.3 Scalar geometry and Kähler manifolds

The previous section discussed how to obtain four-dimensional supergravities from higher dimensions through compactification. Due to this compactification, the four-dimensional maximally supersymmetric supergravity contains 70 scalar fields. An important feature is the fact that the kinetic terms of these scalar fields are non-trivial. That is, instead of the usual term $-\frac{1}{2}\partial_\mu\phi_i\partial^\mu\phi^i$, where i labels the scalars, the kinetic terms are of the form $\mathcal{K}_{ij}(\phi)\partial_\mu\phi^i\partial^\mu\phi^j$. The matrix $\mathcal{K}_{ij}(\phi)$, which depends on the scalars, can be interpreted as a metric on a new manifold, the *scalar manifold* $\mathcal{M}_{\text{scalars}}$. This manifold and its geometry is part of the data of a theory and, unlike the space-time metric $g_{\mu\nu}$, is not a dynamical quantity. It turns out that these scalar manifolds are completely characterized by their isometries. For example, the scalar manifold of the $\mathcal{N}=8, d=4$ sugra is the symmetric space $\mathcal{M}_{\text{scalars}} = E_{7,7}/\text{SU}(8)$.

However, in order to make calculations feasible, we will only consider a subsector of this manifold which is related to only 14 out of the 70 scalar fields of the theory. Therefore, after having performed a consistent truncation (see Section 6.3.5), we will work in a $\mathcal{N}=1, d=4$ supergravity theory. The scalar manifold for such a supergravity is a specific type of manifold known as a Kähler manifold. Kähler manifolds are complex manifolds, which can be considered real manifolds of even dimension $2n$ parametrized by n complex coordinates $z^\alpha = x^\alpha + ix^{\alpha+n}$, with $\{x^\alpha, x^{\alpha+n}\}$ real coordinates on the manifold. The complex metric tensor can be expanded into

$$\mathrm{d}s^2 = 2g_{\alpha\overline{\beta}}\,\mathrm{d}z^\alpha\,\mathrm{d}\overline{z}^{\overline{\beta}} + g_{\alpha\beta}\,\mathrm{d}z^\alpha\,\mathrm{d}z^\beta + g_{\overline{\alpha}\overline{\beta}}\,\mathrm{d}\overline{z}^{\overline{\alpha}}\,\mathrm{d}\overline{z}^{\overline{\beta}}\,. \tag{6.33}$$

Kähler manifolds have additional constraints on their metric. One constraint requires the metric to be hermitian, which means it can be put in the form

$$\mathrm{d}s^2 = 2g_{\alpha\overline{\beta}}\,\mathrm{d}z^\alpha\,\mathrm{d}\overline{z}^{\overline{\beta}}\,. \tag{6.34}$$

For a hermitian metric, one can define the fundamental 2-form $\Omega = -2ig_{\alpha\overline{\beta}}\,\mathrm{d}z^\alpha \wedge \mathrm{d}\overline{z}^{\overline{\beta}}$. A *Kähler manifold* is then a complex manifold with a hermitian metric for which its 2-form is closed (*i.e.*, its exterior derivative vanishes). Following the conventions from the literature, we denote the metric on a Kähler manifold by $\mathcal{K}_{\alpha\overline{\beta}}$ rather than $g_{\alpha\overline{\beta}}$. This *Kähler metric* $\mathcal{K}_{\alpha\overline{\beta}}$ can be written as

$$\mathcal{K}_{\alpha\overline{\beta}} = \partial_\alpha\partial_{\overline{\beta}}\mathcal{K}\,, \tag{6.35}$$

where $\mathcal{K} = \mathcal{K}(z,\overline{z})$ is the *Kähler potential*. We adopt the notation that Greek subscripts $\alpha, \beta, \ldots$ denote derivatives with respect to complex scalars, while barred subscripts $\overline{\alpha}, \overline{\beta}, \ldots$ denote derivatives with respect to their complex conjugates, *i.e.*

$$\partial_\alpha \equiv \frac{\partial}{\partial z^\alpha}\,, \quad \partial_{\overline{\alpha}} \equiv \frac{\partial}{\partial \overline{z}^\alpha}\,. \tag{6.36}$$

In our work, we will encounter the *Poincaré plane* (or hyperbolic upper half-plane) as Kähler manifold. As a symmetric space, the Poincaré plane is the coset space[6]

[6]Since $\text{SU}(1,1) \cong \text{SL}(2,\mathbb{R})$, this is also $\text{SL}(2,\mathbb{R})/\text{U}(1)$. The group $\text{SL}(2,\mathbb{R})$ are the Möbius transformations with real parameters.

$\mathrm{SU}(1,1)/\mathrm{U}(1)$. Considered as a real manifold, it has two coordinates x, y with $y > 0$. The metric is

$$\mathrm{d}s^2 = \frac{1}{y^2}\left(\mathrm{d}x^2 + \mathrm{d}y^2\right) . \tag{6.37}$$

Therefore, distances become infinite as one approaches the line $y = 0$. We introduce the complex coordinate $z = x + iy$ which is therefore restricted to the upper half-plane since $\mathrm{Im}(z) > 0$. The metric can be written as

$$\mathrm{d}s^2 = \frac{1}{(\mathrm{Im}(z))^2}\,\mathrm{d}z\,\mathrm{d}\overline{z}\,. \tag{6.38}$$

For the Poincaré plane, the most common[7] Kähler potential used in the literature is

$$\mathcal{K} = -\log(-i(z-\overline{z}))\,, \tag{6.39}$$

such that the Kähler metric is

$$\mathcal{K}_{z\overline{z}} = -\frac{1}{(z-\overline{z})^2}\,. \tag{6.40}$$

This hyperbolic space is equivalent to the well-known[8] *Poincaré disk* $|z| < 1$. Both spaces are related to each other by a conformal transformation. In particular, the line $y = 0$ of the plane gets mapped into the boundary of the disk $|z| = 1$. We will not discuss further details of this transformation. The most common Kähler potential used in the literature for the Poincaré disk is

$$\mathcal{K} = -\log(1 - z\overline{z})\,, \tag{6.41}$$

such that the Kähler metric in this case is equal to

$$\mathcal{K}_{z\overline{z}} = \frac{1}{(1-z\overline{z})^2}\,. \tag{6.42}$$

As mentioned, Kähler manifolds appear in $\mathcal{N} = 1, d = 4$ supergravities coupled to chiral multiplets, which we introduce in the next section.

6.3.4 Chiral multiplets in $\mathcal{N} = 1, d = 4$ supergravity

Fields in sugra theories are organized into supermultiplets. Naturally, the supermultiplet which is always present, and which is the only possible supermultiplet for $N > 16$ real supercharges, is the supergravity multiplet, containing the graviton and $\mathcal{N}$ gravitinos. However, supergravity theories with $N \leq 16$ supercharges can have additional supermultiplets known as *matter multiplets*. We only discuss the *chiral multiplets* in $\mathcal{N} = 1, d = 4$, as this will be of relevance to the thesis. Each chiral multiplet contains a spin-1/2 Weyl spinor χ and a complex scalar z. The kinetic terms of the complex scalars are given by a Kähler metric, introduced in the previous section. The action of a supergravity coupled to a chiral multiplet is not unique and depends on a completely arbitrary holomorphic function called the *holomorphic superpotential* $W(z)$. Clearly, there are hence in principle an infinite amount of $\mathcal{N} = 1, d = 4$ sugra theories coupled to chiral multiplets. However,

[7] The Kähler potential is not unique. Given a Kähler potential $\mathcal{K}(z,\overline{z})$, the potential $\mathcal{K}(z,\overline{z}) + f(z) + \overline{f}(\overline{z})$ is another Kähler potential giving rise to the same Kähler metric, due to equation (6.35).

[8] If not from physics or mathematics, then certainly from the works by M.C. Escher [34].

the choices are limited in our work as we restrict our attention to the interesting subset of theories for which a higher-dimensional origin out of string theory is known.

Since we will be interested in classical solutions, in which fermions vanish, we can limit ourselves to the bosonic part of the action involving the metric $g_{\mu\nu}$ (or frame fields e^a_μ) and the scalars z_α, where $\alpha = 1, \ldots, n$ labels the different chiral multiplets in our theory. If the supergravity is coupled to n chiral multiplets, the bosonic part of the Lagrangian is

$$e^{-1}\mathscr{L}_{\text{bosonic}} = \frac{1}{2\kappa^2}\left(R(e) - \mathcal{K}_{\alpha\overline{\beta}}\partial_\mu z^\alpha \partial^\mu z^{\overline{\beta}} - 2V(z,\overline{z})\right) , \tag{6.43}$$

where $e \equiv \det e^a_\mu$ should not be confused with the Euler number. The first term contains the Ricci scalar, obtained from the frame fields, and corresponds to the Einstein-Hilbert part of the action. The second term are the kinetic terms of the scalars which, as mentioned, live on a Kähler manifold with Kähler metric $\mathcal{K}_{\alpha\overline{\beta}}$. The final term, which is the most important one for Part III of the thesis, is the *scalar potential*. For a supergravity coupled to chiral multiplets, this scalar potential is completely determined by the Kähler potential, the Kähler metric and the holomorphic superpotential W:

$$V(z,\overline{z}) = e^{\mathcal{K}}\left(\mathcal{K}^{\alpha\overline{\beta}}\mathcal{D}_\alpha W \overline{\mathcal{D}}_{\overline{\beta}}\overline{W} - 3W\overline{W}\right) , \tag{6.44}$$

Here, we have introduced the *Kähler covariant derivative* $\mathcal{D}_\alpha$, which acts as

$$\mathcal{D}_\alpha(\cdot) = \partial_\alpha(\cdot) + (\partial_\alpha \mathcal{K})(\cdot) , \quad \overline{\mathcal{D}}_{\overline{\alpha}}(\cdot) = \partial_{\overline{\alpha}}(\cdot) + (\partial_{\overline{\alpha}}\mathcal{K})(\cdot) . \tag{6.45}$$

We emphasize that the superpotential, by definition, is a function of the scalars z_α only, while this is not the case for the Kähler potential and consequently V depends on both z_α and $\overline{z}_\alpha$.

6.3.5 Gauged supergravity and consistent truncation

Our discussions above have been introducing the so-called *basic supergravity* theories. That is, while the super-Poincaré group is gauged, other symmetries, on the other hand, are not gauged in the theory. In particular, the 28 vector fields of the maximally supersymmetric $4d$ supergravity form a $\mathrm{U}(1)^{28}$ symmetry group. A next step towards our work in Part III is to deform this basic supergravity into a *gauged supergravity*. The details of this gauging procedure are involved and go beyond the scope of this thesis. We will merely state the essential ingredients and provide references for further reading. Moreover, we restrict our attention to the $\mathcal{N} = 8, d = 4$ theory. Recall that the scalar manifold of this theory is $E_{7,7}/\mathrm{SU}(8)$.

There are two ways of obtaining a gauged supergravity theory. One option is to gauge the vectors in the theory into a Yang-Mills group. The other option is to promote the isometries of the scalar manifold to symmetries of the complete action of the theory, which is known as the embedding tensor formalism [35–37]. In the latter approach, the generators X_M of the algebra of the gauge group G are hence written as linear combinations of the generators t_α of the $\mathfrak{e}_{7,7}$ algebra:

$$X_M = \Theta_M{}^\alpha t_\alpha , \tag{6.46}$$

where Θ is known as the embedding tensor. We further restrict our attention to gaugings where the Θ tensor is built from $\mathbf{36} \oplus \mathbf{36'}$ representations of a $\mathfrak{sl}(8,\mathbb{R})$ basis for $\mathfrak{e}_{7,7}$,

discussed in detail in [38, 39]. As a consequence of this, there are only four inequivalent gauged supergravity theories of interest to us which arise from the ungauged, basic $\mathcal{N} = 8, d = 4$ supergravity. They are given in Table 6.2 and will be discussed in more detail in Chapter 9. We restrict our attention to these gauged supergravities because they can be obtained from higher-dimensional theories. The gauge group of the $4d$ theory depends on the internal manifold on which we perform the dimensional reduction. Hence, we denote this internal space by X_G. We delay further discussions on the details of X_G to Chapter 9.

Gauge group G	$\boldsymbol{a}$	$\boldsymbol{b}$	$\tilde{\boldsymbol{a}}$	$\tilde{\boldsymbol{b}}$
SO(8)	1	1	0	0
ISO(7)	1	0	0	1
$[\mathrm{SO}(6) \times \mathrm{SO}(1,1)] \ltimes \mathbb{R}^{12}$	0	0	1	-1
$[\mathrm{SO}(6) \times \mathrm{SO}(2)] \ltimes \mathbb{R}^{12}$	0	0	1	1

Table 6.2: Four gauge groups of $4d$ gauged supergravities considered in this thesis and their values of $a, b, \tilde{a}, \tilde{b}$ which parametrize the superpotential via equations (6.49) and (6.50).

As mentioned before, the ungauged supergravity theories have a vanishing scalar potential V. For our work, the most important feature of gauging a supergravity is the fact that the vector fields become coupled to the scalar fields. This introduces a scalar potential to the theory, which is a function of 70 scalar fields for the $4d$ theories we consider in this thesis. However, it is rather difficult to work with the complete scalar potential and to consider all 70 real variables. Therefore, one often restricts the attention, in a mathematically well-defined way, to a subset of the scalar fields. That is, we perform a *consistent truncation*, meaning that we only retain fields which are invariant under a subgroup of the $E_{7,7}$ isometry group. We will again not discuss the details of these truncations, and only cover the most important aspects and results for our story. It turns out that there are three $\mathbb{Z}_2$ symmetry operations within $\mathrm{SL}(8,\mathbb{R})$ which can be represented as [38]:

$$\begin{aligned} S_1 &: (x_1, x_2, x_3, x_4, x_5, x_6, x_7, x_8) \mapsto (x_1, \quad x_2, \quad x_3, -x_4, -x_5, -x_6, -x_7, \quad x_8)\,, \\ S_2 &: (x_1, x_2, x_3, x_4, x_5, x_6, x_7, x_8) \mapsto (x_1, -x_2, -x_3, \quad x_4, \quad x_5, -x_6, -x_7, \quad x_8)\,, \\ S_3 &: (x_1, x_2, x_3, x_4, x_5, x_6, x_7, x_8) \mapsto (x_1, -x_2, \quad x_3, -x_4, \quad x_5, -x_6, \quad x_7, -x_8)\,. \end{aligned} \tag{6.47}$$

By imposing invariance under one, two or all three of the above S_i, one can obtain consistent truncations of the gauged supergravities which retain respectively 38, 22 or 14 real scalar fields [38]. In this thesis, we will only consider the latter, which we will refer to as the $\mathbb{Z}_2^3$-*invariant truncation* (or simply $\mathbb{Z}_2^3$-truncation). The major advantage is that the truncated theory can be recast in the language of a $\mathcal{N} = 1, d = 4$ supergravity theory coupled to 7 chiral multiplets, which introduces 7 complex scalars z_α. Therefore, we can use the results from Section 6.3.4 to compute the scalar potential explicitly. It turns out that the 7 complex scalars parametrize the Kähler manifold

$$\left[\frac{\mathrm{SL}(2,\mathbb{R})}{\mathrm{U}(1)}\right]^7\,, \tag{6.48}$$

which are 7 'commuting' copies of the Poincaré plane or Poincaré disk, which we discussed in detail in Section 6.3.3.

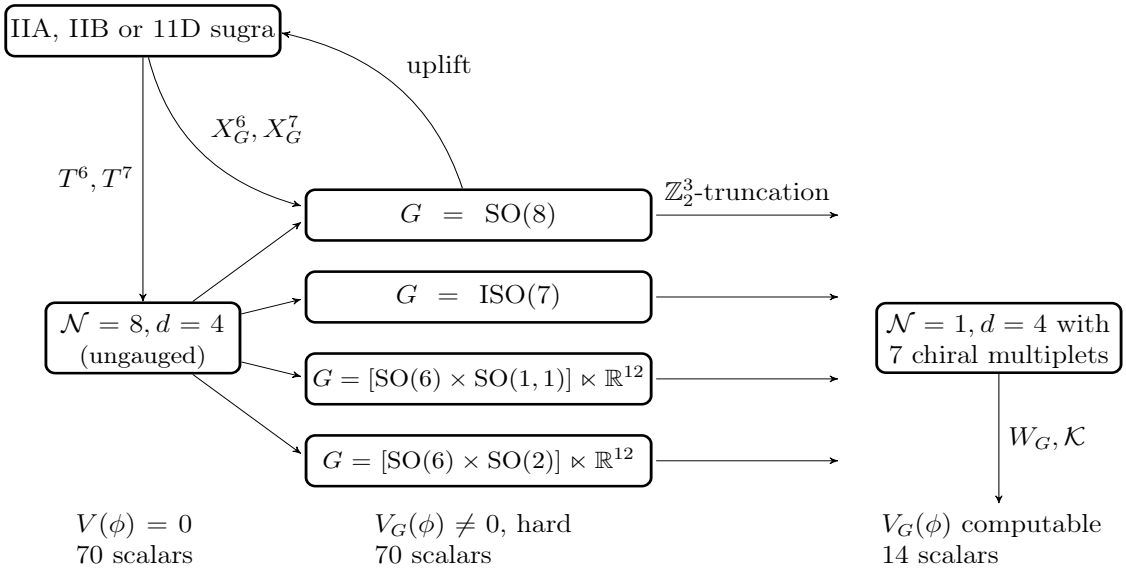

Figure 6.2: Overview of the gauged supergravities and the $\mathbb{Z}_2^3$-truncation appearing in this thesis. A detailed discussion is given in the text.

As mentioned before, the action of chiral multiplets depends on a holomorphic superpotential W. For the four truncated supergravities of this thesis, this superpotential is characterized by constants $a, b, \tilde{a}, \tilde{b}$. Indeed, the superpotential can be written as the sum of a universal part W_0 (*i.e.* shared by all four different gauge groups) given by

$$W_0 = 2g(z_1 z_5 z_6 + z_2 z_4 z_6 + z_3 z_4 z_5 + z_1 z_4 z_7 + z_2 z_5 z_7 + z_3 z_6 z_7)\,, \tag{6.49}$$

and a G-dependent part such that the the full superpotential becomes

$$W_G = W_0 + 2g(\tilde{a} z_4 z_5 z_6 z_7 + \tilde{b} + z_1 z_2 z_3 (a + b z_4 z_5 z_6 z_7))\,, \tag{6.50}$$

where g is the gauge coupling. The constants $a, b, \tilde{a}, \tilde{b}$ must satisfy $a\tilde{a} = b\tilde{b} = 0$, a constraint coming from consistency requirements on the embedding tensor. These values are given in Table 6.2. With the above information on the truncated theories, one is able to explicitly compute the scalar potential V_G by using equation (6.44).

To summarize the discussion up to now, we refer readers to Figure 6.2. On the left hand side, we give the basic (*i.e.*, ungauged) supergravities of interest in this thesis, which are formulated in $10d$, $11d$ and $4d$. The $4d$ ungauged supergravity is obtained from the $10d$ or $11d$ theories via dimensional reduction on a torus and is maximally supersymmetric. By dimensionally reducing on more complicated manifolds X_G, or equivalently, by gauging the vector fields of the $4d$ theory, one obtains a gauged supergravity theory. We find four inequivalent gauged supergravities, given in the middle of the figure. The scalar potential has become non-zero due to the gauging. To make calculations feasible, we work in a $\mathcal{N} = 1, d = 4$ supergravity coupled to 7 chiral multiplets obtained from the $\mathbb{Z}_2^3$-truncation, shown at the right of the figure. This allows us to compute the scalar potential explicitly as a function of 14 out of the 70 scalar fields. Our work presented in Chapter 9 is situated precisely in these truncated theories.

6.3.6 AdS vacua and BPS equations

Since we will work in a $\mathcal{N} = 1, d = 4$ supergravity coupled to chiral multipets, we are of course interested in its solutions. In particular, we are interested in classical (*i.e.*, with vanishing fermions), vacuum background solutions, also called *vacua*. Classical solutions are solutions of the bosonic part of the action, given in equation (6.43). The vacuum solutions correspond to extrema of the scalar potential V. That is, the scalar fields $z_\alpha^\star$ at a vacuum satisfy

$$\partial_\alpha V(z,\overline{z})|_{z_\alpha^\star} = 0\,, \tag{6.51}$$

for all α. Looking back at the action in equation (6.43) and comparing with equation (2.33), we see that these background solutions are space-times with a cosmological constant $\Lambda = V$. In our case, the scalar potential is negative and hence we will work with AdS vacua. Vacuum configurations can correspond to saddle points or even maxima of the scalar potential. One can wonder whether this implies that such vacua are unstable with respect to small, local perturbations to the scalar fields. It turns out that, due to the curved AdS background, these extrema can still be stable provided that the masses of the scalar fields satisfy the Breitenlohner-Freedman (BF) bound [40, 41]

$$m^2L^2 \geq -\frac{(d-1)^2}{4}\,, \tag{6.52}$$

where L is the length scale of the AdS space-time (see Section 2.4). We will refer to the dimensionless numbers m^2L^2 as squared masses for simplicity. Hence, the BF bound tells us that *tachyonic modes* (which have negative squared masses) are allowed up to a certain extent in a negatively-curved, AdS background space-time. Note that, in a flat space-time, this is not the case, and the squared masses must be positive.

An interesting result is that the *Kähler covariant extrema* $z_\alpha^\star$ of the superpotential, defined by

$$\mathcal{D}_\alpha W(z)|_{z_\alpha^\star} = 0\,, \tag{6.53}$$

for all α, are also extrema of the scalar potential, as we will now show explicitly in more detail compared to most references on this material. Indeed, if we act with a partial derivative on V from equation (6.44), we get

$$\begin{aligned}
\partial_\gamma V|_{z_\alpha^\star} &= e^{\mathcal{K}}\Big[(\partial_\gamma\mathcal{K})(\mathcal{K}^{\alpha\overline{\beta}}\mathcal{D}_\alpha W\overline{\mathcal{D}}_{\overline{\beta}}\overline{W} - 3W\overline{W}) + \partial_\gamma\Big(\mathcal{K}^{\alpha\overline{\beta}}\mathcal{D}_\alpha W\overline{\mathcal{D}}_{\overline{\beta}}\overline{W} - 3W\overline{W}\Big)\Big] && (6.54)\\
&= e^{\mathcal{K}}\Big[-3(\partial_\gamma\mathcal{K})W\overline{W} + \partial_\gamma(\mathcal{K}^{\alpha\overline{\beta}})\mathcal{D}_\alpha W\overline{\mathcal{D}}_{\overline{\beta}}\overline{W}\\
&\qquad + \mathcal{K}^{\alpha\overline{\beta}}\big(\partial_\gamma(\mathcal{D}_\alpha W)\overline{\mathcal{D}}_{\overline{\beta}}\overline{W} + \mathcal{D}_\alpha W\partial_\gamma(\overline{\mathcal{D}}_{\overline{\beta}}\overline{W})\big) - 3\partial_\gamma(W\overline{W})\Big] && (6.55)\\
&= -3e^{\mathcal{K}}\Big[(\partial_\gamma\mathcal{K})W\overline{W} + \partial_\gamma(W\overline{W})\Big] && (6.56)\\
&= -3e^{\mathcal{K}}\overline{W}\Big[(\partial_\gamma\mathcal{K})W + \partial_\gamma W\Big]\,, && (6.57)
\end{aligned}$$

where we have made heavily use of equation (6.53) and in the final step used the fact that the superpotential is a function of z_α only, such that $\partial_\gamma\overline{W}(\overline{z}) = 0$. In the final equation, we recognize the Kähler covariant derivative, and hence we find

$$\partial_\gamma V|_{z_\alpha^\star} = -3e^{\mathcal{K}}\overline{W}\mathcal{D}_\gamma W = 0\,, \tag{6.58}$$

again because of equation (6.53). This shows that Kähler covariant extrema of the superpotential are indeed extrema of the scalar potential.

These extrema of the superpotential are important to our story, as they correspond to supersymmetric vacua. Similar to global susy, a solution of a sugra theory is not necessarily itself invariant under susy transformations. Whenever a solution carries a residual amount of global susy, the solution is again called a *BPS solution*. There exists a prescription to determine such solutions using *Killing spinors*, which are the "square roots" of Killing vectors familiar from GR.[9] These are a finite subset of the spinor functions for which the susy transformations leave the solution invariant. Therefore, they form a set of constant parameters and hence determine the residual (global) susy of the solution. One can derive the Killing spinor conditions from the fermion transformation rules [10]. One can write the local susy transformations schematically as

$$\delta_\epsilon B(x) = \bar{\epsilon}(x) f(B)\ F(x) + \dots\,, \quad \delta_\epsilon F(x) = g(B)\epsilon(x) + \dots\,, \tag{6.59}$$

where $B(x)$ and $F(x)$ represent boson and fermion fields, respectively. The dots denote higher-order terms involving fermion fields only. If the solution has residual susy, this means that the set of equations $\delta_\epsilon F(x) = 0$, $\delta_\epsilon B(x) = 0$ has a non-trivial solution for some spinor ϵ. Since fermion fields vanish in a classical solution, the equation $\delta_\epsilon B(x)$ is trivially satisfied and the higher-order terms vanish. Only the linear term in the $\delta_\epsilon F(x)$ equation remains. Hence, a BPS solution is a classical solution for which the linearized fermion susy transformations vanish, *i.e.*

$$\delta_\epsilon F(x)|_{\text{lin}} = 0\,. \tag{6.60}$$

If there are n_Q linearly independent solutions to this set of equations, then we say the solution preserves n_Q supercharges and is said to be $\frac{n_Q}{\mathcal{N}}$-BPS. An important point to keep in mind is that the original symmetries are local, while the preserved ones are global.

As we have outlined above, we will be working in a $\mathcal{N} = 1, d = 4$ sugra theory coupled to chiral multiplets. It is therefore instructive to consider the susy transformations of the gravitini Ψ_μ and the spin-1/2 chiral fermions[10] χ^α. They are [42]

$$\delta_\epsilon P_L \Psi_\mu = \left(\partial_\mu + \frac{1}{4}\omega_\mu{}^{ab} - \frac{3}{2} i\mathcal{A}_\mu\right) P_L\epsilon + \frac{1}{2}\gamma_\mu e^{\mathcal{K}/2} W P_R\epsilon\,, \tag{6.61}$$

$$\delta_\epsilon P_R \Psi_\mu = \left(\partial_\mu + \frac{1}{4}\omega_\mu{}^{ab} + \frac{3}{2} i\mathcal{A}_\mu\right) P_R\epsilon + \frac{1}{2}\gamma_\mu e^{\mathcal{K}/2} \overline{W} P_L\epsilon\,, \tag{6.62}$$

$$\delta_\epsilon P_L \chi^\alpha = P_L\left(\gamma^\mu \partial_\mu z^\alpha - e^{\mathcal{K}/2}\mathcal{K}^{\alpha\overline{\beta}}\overline{\mathcal{D}}_{\overline{\beta}}\overline{W}\right)\epsilon\,, \tag{6.63}$$

$$\delta_\epsilon P_R \chi^{\overline{\beta}} = P_R\left(\gamma^\mu \partial_\mu \overline{z}^{\overline{\beta}} - e^{\mathcal{K}/2}\mathcal{K}^{\alpha\overline{\beta}}\mathcal{D}_\alpha W\right)\epsilon\,, \tag{6.64}$$

where $\mathcal{A}_\mu$ is the Kähler connection

$$\mathcal{A}_\mu = \tfrac{1}{6} i\left(\partial_\mu z^\alpha \mathcal{K}_\alpha - \partial_\mu \overline{z}^{\overline{\alpha}}\mathcal{K}_{\overline{\alpha}}\right)\,. \tag{6.65}$$

For an AdS vacuum, the scalars take constant values and hence their derivatives as well as the Kähler connection vanish. In order to have residual susy, we have to require that

[9] More precisely, for any pair of Killing spinors ϵ, ϵ', the bilinear $\bar{\epsilon}'\gamma^\mu\epsilon$ is a Killing vector.

[10] The index α runs over the different chiral multiplets and is not to be confused with a spinor index, which is suppressed here.

there exist four-component Killing spinors which solve all of the above equations. For this, equations (6.63) and (6.64) are satisfied if the scalars are a Kähler covariant extremum of the superpotential, *i.e.* they satisfy equation (6.53). Equations (6.61) and (6.62) can then, schematically speaking, be recast in the form $D_\mu\epsilon = c\gamma_\mu\epsilon$, with some constant c depending on the values of the scalar fields. The linearly independent solutions to these equations then determine the residual supercharges in the solution.

Finally, we remark that, due to a Higgs-like breaking mechanism, non-zero values of the scalar fields imply that the gauge symmetry of the theory is broken and the vacuum is invariant under a residual symmetry group which is contained within G. Hence, when we discuss the vacua of gauged supergravities in Chapter 9, we will specify the number of residual supercharges n_Q (denoted simply by $\mathcal{N}$ in Chapter 9) and the residual global symmetry group of each solution.

Chapter 7

Gauge/gravity duality

Recent research in string theory has culminated in the discovery of an interesting, new class of dualities which relate gravitational theories to quantum field theories, known as gauge/gravity dualities. These dualities provide an exact correspondence between all fields, operators, observables, et cetera of both theories. The true claim of fame of gauge/gravity dualities is that they are in particular strong/weak dualities: whenever the gravitational theory is weakly coupled, the gauge theory is at strong coupling and vice versa. These dualities therefore give us a new computational tool to gain insight into theories at strong coupling, where perturbative calculations fail. This is the spirit behind our work of Chapter 9.

This chapter aims to introduce the concept of a gauge/gravity duality in more detail. We start off with the first hints towards such dualities obtained from fields theories at large N and the holographic nature of the correspondence. The gauge/gravity duality is motivated using the most famous example, the AdS/CFT correspondence discovered by Maldacena in 1997 [43]. We also develop the holographic dictionary employed in Part III of the thesis.

7.1 Large N field theories and holography

As we briefly mentioned in Section 4.3, QCD enjoys asymptotic freedom, meaning that the strong coupling constant decreases at larger energies. At low energies however, the theory is strongly coupled and perturbation theory fails. Therefore, new tools must be sought to perform calculations. One possible trick, invented by 't Hooft, is to treat the number of colours N, equal to three for QCD, as a free parameter. One could hope to solve the theory in the limit $N \to \infty$ and treat the finite N case using a perturbative expansion in $1/N$. In the *'t Hooft limit*, which corresponds to taking $N \to +\infty$ while keeping the *'t Hooft coupling* $\lambda \equiv g^2 N$ constant, it turns out that planar diagrams dominate [44]. That is, a diagram which has Euler number χ carries a factor N^χ. Therefore, the *planar diagrams*, which have $\chi = 2$, dominate in the expansion when taking the limit $N \to \infty$. Other diagrams become suppressed by factors $1/N^2$. Hence, the expansion resembles the genus expansion of perturbative string theory, which we briefly mentioned in Section 5.2.1. This motivates us to identify large N gauge theories with string theories, where the string coupling g_s is associated with the parameter $1/N$. The argument by 't Hooft is very general and this led to the remarkable idea that string theories, possibly including quantum gravity, may be equivalent to field theories.

Moreover, this identification is a particular manifestation of *holography*, meaning that the field theory lives in one dimension of space-time less compared to the gravity theory. The first hints of holography came from the study of black hole thermodynamcis. As well-known in the field of black hole thermodynamics [45], the Bekenstein-Hawking entropy of a black hole depends on the area of its event horizon [46, 47]. As such, Bekenstein argued that the maximal entropy of a region of space depends on its boundary [48]. Based on this, 't Hooft made the interpretation that all phenomena in a $3d$ volume can be explained via degrees of freedom which reside on the $2d$ boundary surface of that volume [49]. One can interpret the $2d$ surface as a 'screen' of bits of information, of which the $3d$ volume is its 'image', which is precisely the idea of a hologram [50].

In gauge/gravity dualities, holography similarly states an equivalence between a gravitational theory in $d+1$ space-time dimensions and a gauge theory in d space-time dimensions. We will introduce the most famous example of the gauge/gravity duality, the AdS/CFT correspondence of Maldacena.

7.2 The Maldacena conjecture

Studies of the connection between field theories at large N and string theory led Maldacena to formulate the AdS/CFT correspondence. We will review, schematically, the argument behind this correspondence based on [10, 13, 21, 24, 51]. The first dualities were found by considering stacks of N coincident branes in superstring or M-theory. The three original AdS/CFT correspondences formulated in the groundbreaking paper of Maldacena are [43]:

$$\text{M-theory on } \mathrm{AdS}_4 \times S^7 \leftrightarrow \text{ SCFT on } N \text{ M2-branes}\,, \tag{7.1}$$

$$\text{M-theory on } \mathrm{AdS}_7 \times S^4 \leftrightarrow \text{ SCFT on } N \text{ M5-branes}\,, \tag{7.2}$$

$$\text{Type IIB string theory on } \mathrm{AdS}_5 \times S^5 \leftrightarrow \text{ SCFT on } N \text{ D3-branes}\,. \tag{7.3}$$

We will consider in more detail Maldacena's conjecture given in the last line. More precisely, we will motivate the conjecture that the following two theories are dual to each other:

$$\text{Type IIB superstring theory on } \mathrm{AdS}_5 \times S^5 \leftrightarrow \mathcal{N}=4, d=4, G=\mathrm{SU}(N) \text{ SYM}\,, \tag{7.4}$$

where one assumes fields are compactified on the internal space S^5. In the duality, one identifies the YM coupling constant with the string coupling by $g_{\mathrm{YM}} = 4\pi g_s$. As preliminary checks of the correspondence, one can verify that the global symmetries match on both sides. As a SCFT, the SYM theory has both Q and S supercharges, such that both sides have 32 real supercharges. Recall from Section 2.4 that the isometry group of an AdS_5 space is $\mathrm{SO}(2,4)$, which is precisely the conformal group in $4d$ as we mentioned in Section 3.1.4. The isometry group of S^5 is $\mathrm{SO}(6) \cong \mathrm{SU}(4)$, which coincides with the gauge group of the right hand side.

Let us now present the arguments presented by Maldacena [43] that led to the correspondence of (7.4). In order to make the argument tractable, readers are encouraged to look at Figure 7.1 while reading the derivation. The correspondence arises by comparing two different points of view on the stack of N coincident D3-branes. Type IIB string theory contains two perturbative excitations: open strings ending on the branes

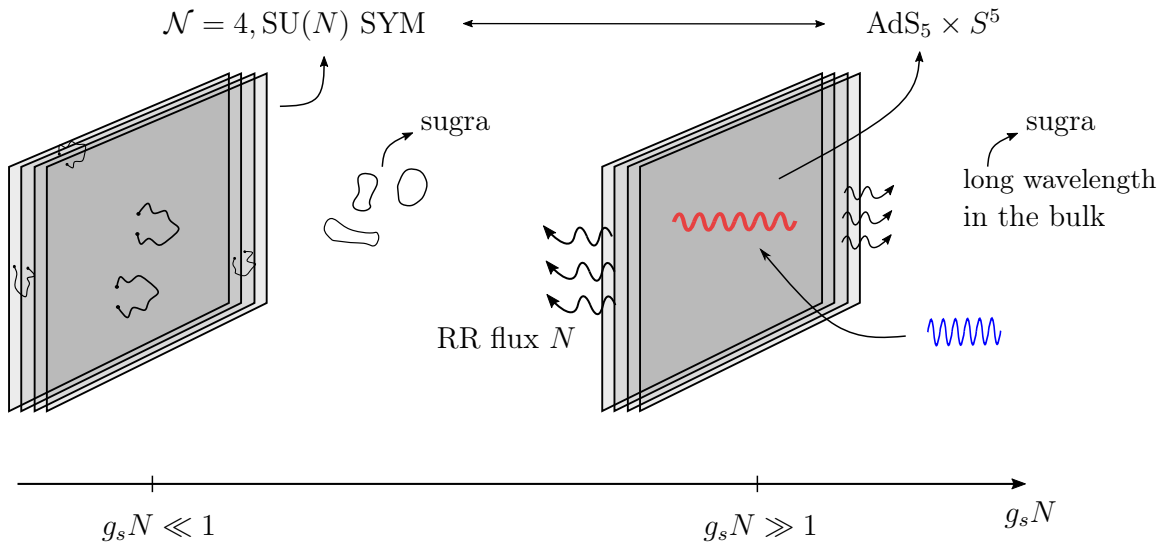

Figure 7.1: Illustration of the argument leading to the Maldacena conjecture. Details are given in the text. Left: open string point of view at $g_s N \ll 1$. Right: closed string point of view at $g_s N \gg 1$.

and describing excitations of the brane, and closed strings, which are interpreted as excitations of empty space and yield a gravitational solution. In this sense, AdS/CFT is a manifestation of a closed string/open string duality.

In the first point of view, which we call the open string point of view, the branes are localized, topological defects in a flat, Minkowski space-time background as gravity is essentially "switched-off" in this picture, as the $10d$ gravitational constant depends on g_s. At energies below the string energy scale, only massless modes are available to be excited. The massless, closed string states living in the bulk (*i.e.*, away from the branes) give a free supergravity multiplet which effectively yields a type IIB sugra action describing their low-energy dynamics. The massless, open strings give a $\mathcal{N} = 4$ vector supermultiplet, with as low-energy Lagrangian that of[1] $\mathcal{N} = 4$, U(N) SYM. In the so-called Maldacena limit[2] $\ell_s \to 0$, these two excitations decouple from each other (their interaction vanishes) and result in a free sugra theory in the bulk plus a gauge theory living on the world-volume of the branes. This is shown at the left in Figure 7.1.

Now, let us adopt a different point of view, which we will refer to as the closed string point of view. In this picture, gravity is relevant and as such, the branes will curve the geometry and yield a non-trivial gravitational solution. Specifically, the result is a black 3-brane, a concept which we briefly introduced in Section 5.2.2. We can write down a classical sugra solution for the extremal black 3-brane. We decompose the coordinates in coordinates x^μ, $\mu = 0, 1, 2, 3$ along the brane, and transverse coordinates y^a, $a = 1, \ldots, 6$. The metric is given by

$$\mathrm{d}s^2 = H(y^a)^{-1/2} \eta_{\mu\nu} \, \mathrm{d}x^\mu \, \mathrm{d}x^\nu + H(y^a)^{1/2} \delta_{ab} \, \mathrm{d}y^a \, \mathrm{d}y^b \,, \tag{7.5}$$

$$= H(y^a)^{-1/2} \eta_{\mu\nu} \, \mathrm{d}x^\mu \, \mathrm{d}x^\nu + H(y^a)^{1/2} (\mathrm{d}r^2 + r^2 \, \mathrm{d}\Omega_5^2) \,, \tag{7.6}$$

[1] A U(N) gauge theory is essentially a SU(N) theory and in fact, in the limit considered here, only the SU(N) part is described [13].

[2] Note that ℓ_s is a dimensionful quantity and we are actually considering the limit of Section 5.2.3. Nevertheless, we will simply refer to this limit as $\ell_s \to 0$ or equivalently, $\alpha' \to 0$.

where $H(y^a)$ is a harmonic function and $r = \sqrt{y_a y^a}$ is the radial coordinate in the transverse direction. For the extremal black brane, we have

$$H(y^a) = 1 + \frac{L^4}{r^4}\,, \tag{7.7}$$

where L is given by

$$L^4 = 4\pi(\alpha')^2 g_s N\,. \tag{7.8}$$

The black 3-brane has a horizon at $r = 0$. Similar to ordinary black holes, approaching the horizon implies that energies are redshifted as seen by an observer at infinity. For this observer, there are hence two different low-energy excitations. The first one are massless particles which propagate in the bulk with a long wavelength. The second kind of excitations consist of any excitation in the theory that is brought arbitrary close to the horizon $r = 0$ and, due to the redshift, becomes a low-energy excitation. Again, these two types of excitations decouple in the low-energy limit and give a free sugra theory in the bulk on the one hand, and the 'near-horizon' (*i.e.*, $r \approx 0$) geometry of the black brane on the other. This near-horizon geometry can be found by approximating $H \approx L^4/r^4$, such that the metric is approximated by

$$\mathrm{d}s^2 \approx \frac{r^2}{L^2}\eta_{\mu\nu}\,\mathrm{d}x^\mu\,\mathrm{d}x^\nu + L^2\left(\frac{1}{r^2}\,\mathrm{d}r^2 + \mathrm{d}\Omega_5^2\right)\,. \tag{7.9}$$

Performing the change of coordinates $z = L^2/r$, this becomes

$$\mathrm{d}s^2 = \frac{L^2}{z^2}\left(\mathrm{d}z^2 + \eta_{\mu\nu}\,\mathrm{d}x^\mu\,\mathrm{d}x^\nu\right) + L^2\,\mathrm{d}\Omega_5^2\,, \tag{7.10}$$

which, upon comparing with equation (2.47), we recognize as the line element of the product space $\mathrm{AdS}_5 \times S^5$. The length scales of the AdS_5 and S^5 spaces are both equal to L. Note that this is indeed similar to an extremal Reissner-Nördstrom black hole, which has an $\mathrm{AdS}_2 \times S^2$ near horizon geometry in $4d$, also known as the Robinson-Bertotti metric [10]. This second viewpoint on the stack of branes is presented at the right of Figure 7.1. In this second picture, the integer N, which appears in the gauge group of the gauge side of the correspondence, is equal to the flux of the five-form $F^{(5)}$ of type IIB string theory through the five-sphere, *i.e.*

$$N = \int_{S^5} F^{(5)}\,. \tag{7.11}$$

Therefore, in both points of view, we have two decoupled theories in the low-energy limit. Both contain supergravity in the bulk, and so we are naturally led to identify the gauge theory from the open string point of view with the type IIB string theory on an $\mathrm{AdS}_5 \times S^5$ background. This is precisely the Maldacena conjecture from (7.4).

So far, we have glossed over the fact that the above two descriptions are only valid in particular regimes of the string coupling g_s. Taking this into account will demonstrate that the AdS/CFT correspondence is in particular a strong/weak duality. Indeed, the open string point of view has a valid perturbative description in the regime $g_s N \ll 1$. The reason is that in string perturbation theory, any additional world-sheet boundary brings in a factor g_s from the genus and a factor N coming from the Chan-Paton trace. On the other hand, the closed string point of view will provide a valid approximation if

the sizes L of the space-times we are dealing with are large compared to the string length scale, such that stringy effects can be neglected. Looking at equation (7.8), and using the fact that $\alpha' = \ell_s^2$, we find that

$$\left(\frac{L}{\ell_s}\right)^4 = 4\pi g_s N \,. \tag{7.12}$$

Hence, we find that a supergravity limit can provide an adequate description of the above solution provided that $g_s N \gg 1$. Therefore, both sides of the AdS/CFT correspondence reign in different regimes of g_s, which is why it is said to be a strong/weak duality. This is represented schematically by Figure 7.2.

There are several versions of the Maldacena conjecture. In its strongest form, the correspondence uses the full string theory on the gravity side, and moreover claims the conjecture to hold for all values of g_s and N. It is, however, desirable to consider weaker forms of the conjecture in which we have more control over the theories. Taking the limit $\alpha' \to 0$ is one example. Another example is the *'t Hooft limit* mentioned earlier in Section 7.1, where one takes the limit $N \to \infty$ with fixed *'t Hooft coupling* $\lambda = g_s N$. The strong/weak aspect of the duality manifests itself in the fact that one naturally works at $\lambda \ll 1$ on the field theory side, but $\lambda \gg 1$ on the gravity side. One can consider an even weaker version by considering the limit $\lambda \to \infty$. In this case, we have an expansion in α' on the gravity side, such that one can work with classical type IIB sugra, while the gauge side now has an expansion in $\lambda^{-1/2}$.

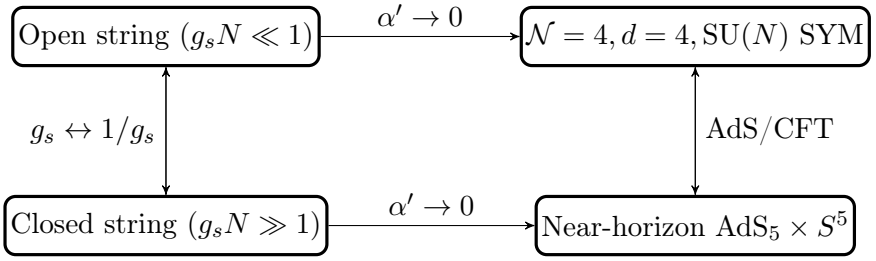

Figure 7.2: Relation between the two different points of view, taking the supergravity limit, and dualities relating the different descriptions.

The other examples of the AdS/CFT correspondence, given in equations (7.1) and (7.2), share most of the features of the correspondence discussed above but are conceptually more involved to formulate and discuss. For example, in the case of (7.1), which will be of relevance to us in Chapter 9, there can be no Yang-Mills gauge group at the CFT side of the correspondence, as the Yang-Mills coupling is dimensionful in $3d$ and hence would break conformal invariance. Moreover, the M-branes, unlike D-branes, do not admit the interpretation of strings attached to them and stretched in between them. As a consequence, the dual field theories are more complicated than the $\mathcal{N} = 4$ SYM theory, and they turn out to be superconformal Chern-Simons theories [52].

7.3 Holographic dictionary

The true strength of dualities is that they stipulate two different theories to be equivalent to one another. In order to turn the gauge/gravity dualities into a computational tool, we have to introduce the *holographic dictionary*, which gives us a precise and explicit

identification between all objects of the gravitational and gauge theories. The dictionary is holographic, since the gauge theory is said to "live on the boundary" of AdS, as we will argue in a moment. The quotation marks indicate that this statement is merely helping us to visualize what is going on, but should be used with care. Like Feynman diagrams, such pictorial statements are only useful to physicists if there is a way to convert them into computations.

To connect AdS/CFT with the ideas of holography, we identify the coordinates x^μ in the bulk with coordinates x^μ in the field theory. The extra coordinate in the gravity theory of AdS (r or z) is identified with the RG scale of the dual field theory, which can be viewed as an evolution coordinate, and one identifies $E \sim 1/z \sim r$ [21]. One can hence consider QFTs obtained from the CFT by integrating out degrees of freedom heavier above a certain energy scale E. If we consider the theory at $E = \infty$ to be the fundamental theory, then this corresponds to $r = \infty$ or $z = 0$, which is the boundary of AdS. This is why it is often said that the CFT "lives at the boundary". Hence we have a consistent holographic interpretation of the AdS/CFT correspondence.

The postulate at the basis of the holographic dictionary offered by AdS/CFT is the identification of the generating function of Green's functions of the gauge theory with the supergravity action in the $\mathrm{AdS}_5 \times S^5$ geometry [53]. This postulate implies that fields ϕ in the bulk must be identified with operators $\mathcal{O}$ in the boundary, which is known as the *field-operator correspondence* [54]. For example, the field dual to the energy-momentum tensor operator in the gauge side of AdS/CFT is the metric, which reinforces the idea of the gauge/gravity duality. In Section 2.4, we mentioned that boundary conditions must be specified for fields living in an AdS space. These boundary conditions will switch on operators in the dual field theory, as we will argue in more detail now.

Let us limit the discussion on the holographic dictionary to a single scalar field ϕ living in AdS_d from now on, as this case is most important for the purpose of holographic RG flows. Consider a scalar field $\phi(x, z)$ in the bulk with boundary condition $\phi(x, z = 0) \equiv \phi_0(x)$. The postulate mentioned above implies that we identify [13]

$$\left\langle e^{\int \mathrm{d}^4 x \ \phi_0(x)\mathcal{O}(x)} \right\rangle_{\mathrm{CFT}} = \mathcal{Z}\left[\phi(x, z = 0) = \phi_0(x)\right] . \tag{7.13}$$

Let us discuss the right hand side in the supergravity limit of the correspondence. The supergravity action[3] is

$$S = \frac{1}{2\kappa^2} \int \mathrm{d}^d x \, \mathrm{d}z \sqrt{|g|} \left(-R + g^{\mu\nu}\partial_\mu\phi\partial_\nu\phi + 2V(\phi)\right) . \tag{7.14}$$

The existence of an AdS vacuum implies the potential V should have at least one critical point $\phi^\star$, through which we can define the length scale of AdS space L via

$$V(\phi^\star) = -\frac{d(d-1)}{2L^2} = \Lambda . \tag{7.15}$$

The cosmological constant was inferred by comparing with our results given in equations (2.33) and (2.39). Note that the potential is negative since the cosmological constant is

[3]We work in Euclidean signature, in order to be consistent with the provided references. However, we will still call the Euclideanized AdS space simply AdS.

negative for AdS. We can expand the potential up to quadratic terms around $\phi^\star$, which we assume without loss of generality to lie at the origin $\phi^\star = 0$. The action reduces to

$$S = \frac{1}{2\kappa^2}\int \mathrm{d}^d x\, \mathrm{d}z \sqrt{|g|}\left(-R + 2\Lambda + g^{\mu\nu}\partial_\mu\phi\partial_\nu\phi + m^2\phi^2\right) . \tag{7.16}$$

We now demand that the AdS metric satisfies the equations of motion for the metric and derive the equation of motion for the scalar field which follows from this requirement. We will present the argument behind this, which we derived independently in order to be able to provide a simplified, tractable version of the exact derivation. Substituting the AdS metric in the above action, we find

$$S \propto \int \mathrm{d}^d x\, \mathrm{d}z \left[\frac{L^{d-1}}{z^{d-1}}(\partial_x\phi)^2 + \frac{L^{d-1}}{z^{d-1}}(\partial_z\phi)^2 + \frac{m^2 L^{d+1}}{z^{d+1}}\phi^2\right] + \dots , \tag{7.17}$$

where we used the shorthand notation $(\partial_x\phi)^2 = \delta^{\mu\nu}\partial_\mu\phi\partial_\nu\phi$, with $\mu = 0, 1\dots, d-1$ and we only explicitly wrote terms relevant for the scalar field dynamics. The terms in between square brackets can be seen as a conventional Lagrangian density for a scalar field $\mathscr{L}_{\text{scalar}}$. The equations of motion are therefore given by the Euler-Lagrange equations, see equation (3.22). We find the result

$$\frac{L^{d-1}}{z^{d-1}}\left(\partial_x^2\phi + \partial_z^2\phi\right) - (d-1)\frac{L^{d-1}}{z^d}\partial_z\phi - \frac{m^2 L^{d+1}}{z^{d+1}}\phi = 0\,, \tag{7.18}$$

By multiplying with z^{d+1}/L^{d-1}, one finds the simpler equation

$$z^2\left(\partial_x^2\phi + \partial_z^2\phi\right) - (d-1)z\partial_z\phi - m^2L^2\phi = 0\,. \tag{7.19}$$

We are interested in the behaviour of solutions near the boundary, as the boundary conditions are crucial according to the postulate mentioned above. Assuming that the scalar field has an asymptotic expansion near the boundary $z = 0$ with a scaling behaviour z^Δ with $\Delta > 0$, we write the following ansatz for ϕ:

$$\phi(x, z) \approx \phi_0(x) z^\Delta\,, \text{ for } z \approx 0\,. \tag{7.20}$$

Substituting this ansatz in the equation of motion gives us

$$(\partial_x^2\phi_0)z^{\Delta+2} + \Delta(\Delta-1)\phi_0 z^\Delta - \Delta(d-1)\phi_0 z^\Delta - m^2L^2\phi_0 z^\Delta = 0\,. \tag{7.21}$$

Near the boundary $z = 0$, we can neglect the $z^{\Delta+2}$ term compared to the other terms. The remaining terms then have ϕ_0 as a common factor. Therefore, we find that solutions behave asymptotically as

$$\phi(x, z) \approx \phi_0^{(-)}(x) z^{\Delta_-} + \phi_0^{(+)}(x) z^{\Delta_+}\,, \text{ for } z \approx 0\,. \tag{7.22}$$

where $\Delta_\pm$ are the roots of

$$\Delta(\Delta - d) = m^2L^2\,, \quad \Delta_\pm = \tfrac{1}{2}\left(d \pm \sqrt{d^2 + 4m^2L^2}\right) . \tag{7.23}$$

A more rigorous derivation of the above relation using the exact solutions can be found in [55]. It can be shown that the postulate from equation (7.13) tells us precisely that, as the notation already suggested, the operator $\mathcal{O}$ which is dual to the field ϕ has scaling dimension Δ given by (7.23). This single entry from the holographic dictionary is the most important one for the application of holographic RG flows. Indeed, the effect of introducing an operator which deforms the CFT depends on the scaling dimension of the operator: recall our discussion on (ir)relevant deformations and the resulting RG flows from Section 4.3. We remark that similar relations hold for particles with non-zero spin, and an overview is provided in [56] and references therein.

Recall that scalar fields in an AdS space-time are allowed to have tachyonic modes (*i.e.*, $m^2L^2 < 0$) up to some value which is known as the BF bound: see the discussion around equation (6.52). We indeed find the BF bound again if we require that the roots $\Delta_\pm$ are real numbers, which implies

$$m^2L^2 \geq -\frac{d^2}{4}\,. \tag{7.24}$$

Recall that scaling dimensions have to satisfy the unitarity bound

$$\Delta \geq \frac{d-2}{2}\,. \tag{7.25}$$

It is clear that the root Δ_+ is guaranteed to satisfy this bound. For generic values of the squared mass, the root Δ_- will not satisfy the unitarity bound, and the above relation specifies the scaling dimension uniquely. However, for a certain range of the squared mass, both roots $\Delta_\pm$ from equation (7.13) satisfy the unitarity bound, such that there is an ambiguity in the dictionary. Indeed, by requiring that Δ_- satisfies the unitarity bound from equation (7.25), we straightforwardly derive that this situation occurs if the squared mass satisfies

$$m^2L^2 \leq \frac{4-d^2}{4}\,. \tag{7.26}$$

As mentioned, in this case, there is an ambiguity in defining the scaling dimension of the dual operator. However, this issue is resolved in the presence of supersymmetry, as we will discuss in more detail in Chapter 9.

7.4 Evidence and prospects of AdS/CFT

It is, as of yet, impossible to provide a proof of Maldacena's conjecture, as we have no complete analytic control over both theories. They have to be treated perturbatively, but both descriptions are valid in different regimes of g_sN. There exist a few quantities which can be treated non-perturbatively, such as anomalies, and compared to the calculations at the gravity side. Besides this, the matching of global symmetries and its representations is a first indication that the duality could be valid. Since the symmetry group is a super-conformal group, the SYM operators are organized in representations of chiral primary states and its descendants. For example, the single-trace operators, mentioned in Section 6.2.1, correspond to single-particle states in the gravity theory, while descendant states are mapped to bound states. The complete matching of representations is beyond the scope of this thesis and can be found in [13, 24].

Regardless of a proof, the true triumph of AdS/CFT is its ability to correctly compute correlation functions of the gauge theory using the gravity theory. Indeed, equation (7.13) allows us to compute correlation functions in the gauge side by employing standard path integral techniques. Differentiating with respect to ϕ_0 brings down a factor $\mathcal{O}$ and sends a ϕ particle into the bulk. The right hand side, in a sugra approximation, allows an expansion in Feynman diagrams. However, in this case, external legs represent the boundary values of scalar fields and are known as bulk-to-boundary propagators. Similarly, we can have bulk-to-bulk and boundary-to-boundary propagators and from them, we can construct generalizations of Feynman diagrams called Witten diagrams which allow us to compute correlation functions. Details on these computations can be found in the references mentioned at the beginning of Section 7.2. As a consequence of the fact that AdS/CFT calculations give correct answers, the general consensus is that the duality is valid, or at least to some extent such that new insights can be gained from it. Moreover, the AdS/CFT correspondence is generalized to many other cases were it turned out to be useful as well.

As we have mentioned earlier, the main motivation for studying AdS/CFT is that it provides a window into strongly coupled field theories. Therefore, we briefly anticipate what new insights and results may be discovered from AdS/CFT to close this chapter. For example, it is expected that the principles of AdS/CFT can be used to learn more about QCD, and this idea is dubbed AdS/QCD [57–59]. However, it is not yet known which gravity theory is dual to QCD, even in the large N limit [60]. Moreover, the absence of conformal symmetry and supersymmetry complicate calculations. Similarly, it is hoped that AdS/CFT might teach us more about condensed matter physics, a concept called AdS/CMT [61–63]. For example, there has been work performed on describing superfluids using so-called holographic superconductors [64, 65]. A thorough introduction to applications of AdS/CFT is given by [60].

While such applications of AdS/CFT are certainly interesting, in this thesis we use the gauge/gravity duality in order to study RG flows of strongly coupled field theories holographically. This was already done in the context of Maldacena's original conjecture, where RG flows induced by deformations of the $\mathcal{N} = 4$ SYM Lagrangian were studied holographically in for example [66, 67]. However, in this thesis we explore this application of AdS/CFT in the different context of four-dimensional gauged supergravities dual to three-dimensional superconformal Chern-Simons field theories. In particular, we work in the theories that were introduced in Chapter 6. This work is presented in Section 6.3.5. As an introduction to the topic, we will first discuss toy models to describe holographic RG flows in an arbitrary number of space-time dimensions in the next chapter.

Part III

Holographic RG flows

Chapter 8

Toy models for holographic RG flows

In the previous chapter, we have explained how AdS/CFT provides a holographic correspondence between a gravitational theory living in an AdS_{d+1} background and a CFT_d without gravity. The claim to fame of holography is that it offers a way to compute field theory quantities by using the gravitational theory. One can consider deforming the theories on both sides. For example, inspired by the ideas of RG flows discussed in Section 4.3, one can deform the CFT by introducing relevant operators with scaling dimension $\Delta < d$ which induce an RG flow. According to our holographic dictionary and field-operator correspondence, this implies a scalar field ϕ is introduced in the gravitational theory which acts as the source term of the relevant operator. Our goal is to describe these RG flows by studying their holographic duals.

As an introduction to holographic RG flows, we will provide two toy models in this chapter which can be discussed analytically. The first involves a single scalar field, which is then generalized to an arbitrary amount of scalar fields with non-trivial kinetic terms. The second toy model is the closest to the situation we will encounter in the next chapter. In both toy models, it turns out that one can find first-order gradient flow equations which simplify the task of finding solutions to the second-order equations of motion. While the toy models are inspired by [10], we give our calculations[1] with, to the best of our knowledge, an unprecedented amount of intermediate steps compared to other sources in order to guide the future explorers of holography through these toy models.

8.1 Single scalar field

We are interested in situations where the RG flow in the field theory side goes from a CFT_d in the UV towards a CFT_d in the IR. We denote these two endpoints of the flow as CFT_{UV} and CFT_{IR} accordingly. The energy scale E, the evolution coordinate of the RG flow, is identified with the 'extra coordinate' r in the $(d+1)$-dimensional dual gravitational theory via $E \sim r$, as explained in the previous chapter. As such, the UV corresponds to $r = +\infty$ and the IR to $r = -\infty$. By the AdS/CFT correspondence, the gravitational theory must have two AdS spaces at these locations. While we will present the toy models in Euclidean signature, we will keep on referring to the Euclidean AdS space (*i.e.*, hyperbolic space) simply as AdS throughout this chapter.

[1] Wherever possible, we checked intermediate steps with code from Mathematica, using for example the `diffgeo.m` package [68] for symbolic GR calculations.

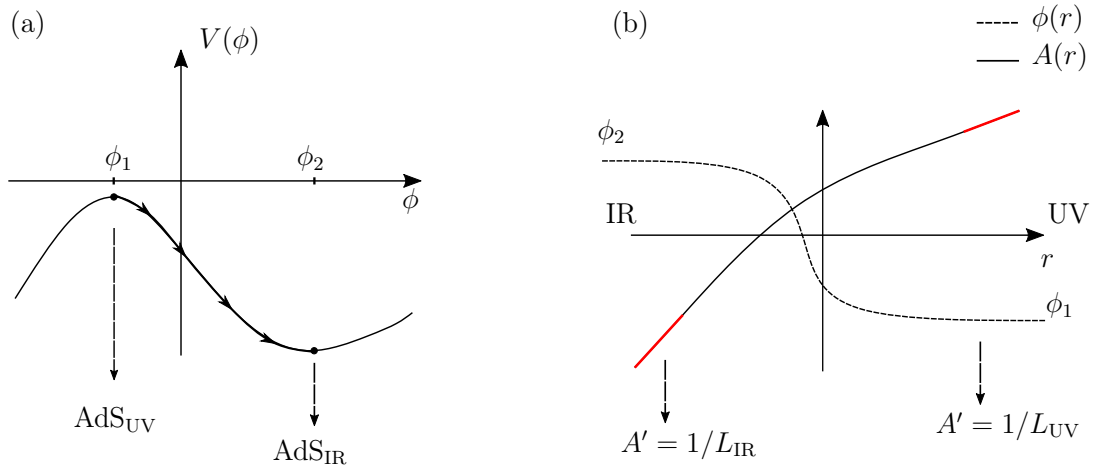

Figure 8.1: Sketch of the single scalar toy model. (a) Scalar potential with two critical points, giving two AdS vacua lying at the UV and the IR. (b) Generic scalar and scale factor profiles as a function of r. The slopes of the scale factor (red) are related to the length scales of AdS.

In the first toy model, we consider a QFT_d obtained by deforming the $\mathrm{CFT}_{\mathrm{UV}}$ by a single relevant operator $\mathcal{O}_\Delta$ dual to a single scalar field ϕ in the bulk, *i.e.*

$$\mathscr{L}_{\mathrm{QFT}} = \mathscr{L}_{\mathrm{CFT}} + \phi_0 \mathcal{O}_\Delta \,, \tag{8.1}$$

where ϕ_0 is the boundary value of ϕ at the UV boundary $r = +\infty$. While the deformation breaks conformal invariance, we will still require the QFT_d to enjoy Poincaré invariance in d space-time dimensions. Due to the gauge/gravity correspondence, the gravity theory must then be invariant under the d-dimensional Poincaré group as well. Since our holographic correspondence identifies the bulk x^μ coordinates with the boundary x^μ coordinates, we make the following general ansatz for the bulk bosonic fields:

$$\mathrm{d}s^2 = e^{2A(r)} \delta_{ij} \, \mathrm{d}x^i \, \mathrm{d}x^j + \mathrm{d}r^2 \,, \quad \phi = \phi(r) \,, \tag{8.2}$$

in which the d-dimensional Poincaré invariance is manifest. The function $A(r)$ is called the *scale factor*. The above ansatz (8.2) is known as the *domain wall* ansatz, and accordingly, its solutions are called domain wall solutions. The action that corresponds to this domain wall ansatz is

$$S = \frac{1}{2\kappa^2} \int \mathrm{d}^d x \, \mathrm{d}z \sqrt{g} \left[-R + \partial_\mu \phi \partial^\mu \phi + 2V(\phi) \right] \,, \tag{8.3}$$

For our purpose, we want the ansatz to describe asymptotically anti-de Sitter space-times, *i.e.* with AdS space-times at $r = \pm\infty$, since the endpoints of the RG flow are CFTs. The scalars, when at these AdS solutions, lie at extrema of the scalar potential. Moreover, the domain wall ansatz at AdS solutions reduces to

$$\mathrm{d}s^2 = e^{2r/L} \delta_{ij} \, \mathrm{d}x^i \, \mathrm{d}x^j + \mathrm{d}r^2 \,. \tag{8.4}$$

One can easily check that via the change of variables[2] $r = -L \ln(z/L)$, the above line element becomes precisely that of an AdS space-time with length L in the form given in

[2]Note that this change of variables is different from the relation $z = 1/r$ used in the previous chapter and in Section 2.4.

equation (2.47). Recall that the value of the scalar potential gives us the length scale and the cosmological constant, as given by equation (7.15).

Therefore, the scalar potential should have multiple critical points $\phi_k^\star$ with corresponding length scales length scales L_k. Given two of such vacua, we would like to find a domain wall solution which interpolates between these vacua, situated at $r = \pm\infty$, respectively. Due to our identification $E \sim r$, we denote the AdS spaces as $\mathrm{AdS}_{\mathrm{UV}}$ and $\mathrm{AdS}_{\mathrm{IR}}$, respectively. Likewise, we label the length of the AdS vacuum at $r = +\infty$ ($r = -\infty$) as L_{UV} (L_{IR}). This situation is sketched in Figure 8.1. The value of the scalar fields at $\mathrm{AdS}_{\mathrm{UV}}$ ($\mathrm{AdS}_{\mathrm{IR}}$) will be denoted by ϕ_1 (ϕ_2).

8.1.1 Equations of motion

We now derive the equations of motion in the above toy model in more explicit details compared the literature (see for example [56]). We will provide the step-by-step derivation of the Klein-Gordon equation in this curved background, in order to make the derivation of the more general case of multiple scalar fields with a non-trivial scalar manifold in Section 8.2 more tractable. The Klein-Gordon equation reads

$$\Box\phi - \frac{\mathrm{d}V}{\mathrm{d}\phi} = 0\,, \tag{8.5}$$

where $\Box = \nabla_\mu\nabla^\mu = g^{\mu\nu}\nabla_\mu\nabla_\nu$. However, the covariant derivative acting on a scalar function reduces to an ordinary partial derivative, and we therefore encounter a term $\nabla_\mu(\partial^\mu\phi)$, for which we can use the result [1]

$$\nabla_\mu V^\mu = \frac{1}{\sqrt{g}}\partial_\mu(\sqrt{g}V^\mu)\,. \tag{8.6}$$

Hence, the scalar equation of motion in curved space-time reads

$$\frac{1}{\sqrt{g}}\partial_\mu\left(\sqrt{g}g^{\mu\nu}\partial_\nu\phi\right) - \frac{\mathrm{d}V}{\mathrm{d}\phi} = 0\,. \tag{8.7}$$

Substituting the domain wall solution, we find the scalar equation of motion

$$\phi'' + dA'\phi' = \frac{\mathrm{d}V(\phi)}{\mathrm{d}\phi}\,, \tag{8.8}$$

where primes denote derivatives with respect to r throughout this chapter. The Einstein equations require a bit more work. First of all, we note that it is easier to work with the Einstein field equations in the form [10]:

$$R_{\mu\nu} = \kappa^2\left(T_{\mu\nu} - \frac{1}{d-1}Tg_{\mu\nu}\right)\,, \tag{8.9}$$

where $T = g^{\mu\nu}T_{\mu\nu}$ is the trace of the energy-momentum tensor. For the domain wall ansatz, the only non-vanishing components of the Riemann tensor are [10]

$$R_{ij}{}^{kl} = -2(A')^2\delta_{ij}^{kl}\,, \tag{8.10}$$

$$R_{ri}{}^{rj} = -(A'' + (A')^2)\delta_i^j\,, \tag{8.11}$$

where we emphasize that we use indices $i, j, \ldots$ for the x^i coordinates on the d-dimensional manifold. From this, one can derive that the only non-vanishing components of the Ricci tensor are [69]

$$R_{ik} = -e^{2A}\left(d(A')^2 + A''\right)\delta_{ik}\,, \tag{8.12}$$
$$R_{rr} = -d(A'' + (A')^2)\,. \tag{8.13}$$

The energy-momentum tensor can be derived from the action, which (for Euclidean signature) is done via the formula [8]

$$T_{\mu\nu} = \frac{2}{\sqrt{g}}\frac{\delta S_M}{\delta g^{\mu\nu}}\,, \tag{8.14}$$

where the matter action S_M is, in our case, given by

$$S_M = \frac{1}{\kappa^2}\int \mathrm{d}^d x\,\mathrm{d}z\sqrt{g}\left(\frac{1}{2}g^{\mu\nu}\partial_\mu\phi\partial_\nu\phi + V(\phi)\right) \equiv \frac{1}{\kappa^2}\int \mathrm{d}^d x\,\mathrm{d}z\sqrt{g}\mathscr{L}_M\,. \tag{8.15}$$

Varying the action, we find[3]

$$\delta S_M = \int \mathrm{d}^d x\,\mathrm{d}z\left[\sqrt{g}\left(\frac{1}{2}\partial_\mu\phi\partial_\nu\phi\right)\delta g^{\mu\nu} + \delta(\sqrt{g})\mathscr{L}_M\right]\,. \tag{8.16}$$

For the second term, we can use the result [1]

$$\delta(\sqrt{g}) = -\tfrac{1}{2}\sqrt{g}g_{\mu\nu}\delta g^{\mu\nu}\,. \tag{8.17}$$

Hence, we find that the energy-momentum tensor of the scalar field is

$$T_{\mu\nu} = -\partial_\mu\phi\partial_\nu\phi + \frac{1}{2}g_{\mu\nu}g^{\rho\sigma}\partial_\rho\phi\partial_\sigma\phi + g_{\mu\nu}V(\phi)\,. \tag{8.18}$$

For the metric of the domain wall solution, one finds

$$T_{\mu\nu} = -\delta^r_\mu\delta^r_\nu(\phi')^2 + \frac{1}{2}g_{\mu\nu}(\phi')^2 + g_{\mu\nu}V(\phi)\,, \tag{8.19}$$

such that the trace is equal to

$$T = \frac{d-1}{2}(\phi')^2 + (d+1)V(\phi)\,. \tag{8.20}$$

Upon using this result for the energy-momentum tensor in equation (8.9) along with the results from equations (8.12) and (8.13), we find that the Einstein equations reduce to

$$A'' + (A')^2 = -\frac{1}{d}\left((\phi')^2 + \frac{2}{d-1}V\right)\,, \tag{8.21}$$
$$A'' + d(A')^2 = -\frac{2}{d-1}V\,. \tag{8.22}$$

By taking the difference between these two equations, we end up with the equation of motion

[3]We ignore the prefactor κ^{-2}, as it simply gets cancelled when we substitute our result for $T_{\mu\nu}$ in equation (8.9).

$$(A')^2 = \frac{1}{d(d-1)}\left((\phi')^2 - 2V(\phi)\right) \tag{8.23}$$

for the scale factor $A(r)$. Equations (8.8) and (8.23) are the coupled set of equations of motion for $\phi(r), A(r)$ to be solved in order to determine the domain wall solution.

These equations of motion are consistent with our earlier discussion of AdS vacua. Indeed, if $\phi^\star$ is a critical point of the potential (*i.e.*, $\mathrm{d}V/\,\mathrm{d}\phi = 0$), then equation (8.8) is trivially satisfied by $\phi(r) = \phi^\star$. Due to the relation between the AdS length scale L and the potential (see equation (7.15)), we find

$$A' = \frac{1}{L}\,, \tag{8.24}$$

which gives $A(r) = r/L$, up to possible integration constants which can be scaled away by a change of variables. This is indeed precisely the metric of AdS as given in equation (8.4).

Let us focus on the solutions of the equations of motion close to the critical points, such that linearization is a good approximation to the full solution. Hence we write

$$\phi(r) = \phi_k^\star + \delta\phi(r)\,, \tag{8.25}$$

$$A'(r) = \frac{1}{L_k} + a'(r)\,, \tag{8.26}$$

and write the potential as

$$V = \frac{1}{2}\left[-\frac{d(d-1)}{L_k^2} + m_k^2(\delta\phi)^2\right]\,, \tag{8.27}$$

around $\phi_k^\star$, and consider the equations of motion (8.8) and (8.23) up to first order in the perturbations $\delta\phi$ and a'. We find that equation (8.23) shows that a' is of second order in $\delta\phi$ and hence negligible. This implies that equation (8.8) results in

$$(\delta\phi)'' + \frac{d}{L_k}h' - m_k^2\delta\phi = 0\,. \tag{8.28}$$

This can easily be solved by the ansatz $\delta\phi \sim e^{\lambda r}$, with characteristic equation

$$\lambda^2 + \frac{d}{L_k}\lambda - m_k^2 = 0\,, \tag{8.29}$$

which has solutions $\lambda_\pm$ given by

$$\lambda_\pm = -\frac{1}{2L_k}\left(d \pm \sqrt{d^2 + 4m^2L_k^2}\right) \equiv -\frac{1}{L_k}\Delta_\pm\,, \tag{8.30}$$

where in the final equation, we have defined

$$\Delta_\pm = \frac{1}{2}\left(d \pm \sqrt{d^2 + 4m_k^2L_k^2}\right)\,. \tag{8.31}$$

This is analogous to the derivation we presented in Section 7.3 which concluded that the scaling dimension of the operator dual to the bulk scalar field is inferred from the

boundary behaviour of the scalar field. Therefore, we again identify[4] $\Delta_k = \Delta_+$ as the scaling dimension of the operator dual to ϕ in the dual field theory.

This identification is consistent with interpreting the domain wall solution as dual to a RG flow in the dual field theory. Indeed, in the UV ($r = +\infty$) and the IR ($r = -\infty$), the solution can be approximated by

$$\phi(r) \approx \phi_k^\star + B_k e^{(\Delta_k - d)\frac{r}{L_k}} + C_k e^{-\Delta_k \frac{r}{L_k}} \,. \tag{8.32}$$

At $r = +\infty$, the B-term is dominant. In order for this perturbation to vanish as we approach the critical point, we therefore have to require that $\Delta_1 < d$, which is consistent with the interpretation that the QFT_d is a relevant deformation of a $\mathrm{CFT}_{\mathrm{UV}}$ (see Section 4.3). At the other endpoint $r = -\infty$, the C-term diverges and has to be put to zero. The B-term now requires that $\Delta_2 > d$, which indeed agrees with the interpretation of an irrelevant deformation such that the RG flow will converge towards the $\mathrm{AdS}_{\mathrm{IR}}$ vacuum.

8.1.2 Irreversibility of holographic RG flows

We will now prove a technically simple to derive, but conceptually deep result which states that holographic RG flows are irreversible. We start from equation (8.8) and take another derivative with respect to r, resulting in

$$A'A'' = \frac{1}{d(d-1)}\phi' \left(\phi'' - \frac{\mathrm{d}V}{\mathrm{d}\phi}\right) \,. \tag{8.33}$$

On the right hand side, we recognize equation (8.8) and upon substitution, we find that

$$A'' = -\frac{(\phi')^2}{d-1} \,. \tag{8.34}$$

One can equivalently derive this result by combining equations (8.21) and (8.22). This simple result tells us that $A'' \leq 0$, *i.e.* A' is a decreasing function of r. Hence, we have that

$$A'(r = -\infty) > A'(r = +\infty) \,. \tag{8.35}$$

Making use of the fact that the $\mathrm{AdS}_{\mathrm{IR}}$ is located at $r = -\infty$ and $\mathrm{AdS}_{\mathrm{UV}}$ at $r = +\infty$, with their length scales related to A' via equation (8.24), this becomes $1/L_{\mathrm{IR}} > 1/L_{\mathrm{UV}}$. By using equation (7.15), we can equivalently state that

$$V_{\mathrm{UV}} > V_{\mathrm{IR}} \,. \tag{8.36}$$

Therefore, we find that holographic RG flows are compelled to flow to a point which lies 'deeper' in the potential landscape. As a consequence, holographic RG flows are necessarily irreversible flows. Irreversibility of RG flows in field theory has been a long-standing problem and was proven first in $2d$ by Zamolodchikov [70]. The proof relies on the existence of a function of the coupling $c(g)$ which is monotonically decreasing along the RG flow. Intuitively, one expects that the amount of degrees of freedom decreases as

[4] We ignore, for the sake of simplicity and clarity in this toy model, the subtlety of the ambiguity of this identification for the case where both roots $\Delta_\pm$ lie above the unitarity bound. This issue is discussed in detail in the next chapter and Appendix B.

we flow from a $\mathrm{QFT}_{\mathrm{UV}}$ to a $\mathrm{QFT}_{\mathrm{IR}}$, as heavier excitation modes of the theory will become integrated out along the RG flow. However, it has been difficult to generalize the proof of the Zamolodchikov c-theorem to higher dimensions [71, 72]. Holography provides us with an alternative way to establish the irreversibility of RG flows via gravity duals of field theories and so-called holographic c-theorems [56].

8.1.3 Gradient flow equations

The equations of motion for the domain wall ansatz, (8.8) and (8.23), constitute a set of non-linear, second order differential equations. However, in special circumstances, there exists a set of first-order ordinary differential equations (gradient flow equations) of which the solutions also solve the full equations of motion. Suppose that there exists some function $W(\phi)$, the superpotential, such that the potential $V(\phi)$ can be written as

$$V(\phi) = \frac{1}{2}\left(\frac{\mathrm{d}W}{\mathrm{d}\phi}\right)^2 - \frac{d}{2(d-1)}W^2\,. \tag{8.37}$$

Then a solution of the system of first-order gradient flow equations

$$\phi' = \frac{\mathrm{d}W}{\mathrm{d}\phi}\,, \quad A' = -\frac{1}{d-1}W \tag{8.38}$$

solves the equations of motion (8.8) and (8.23). For the sake of completeness, we will give the explicit calculations which, to the best of our knowledge, are rarely provided in the literature. First of all, we note that

$$\phi'' = \frac{\mathrm{d}^2W}{\mathrm{d}\phi^2}\phi'\,. \tag{8.39}$$

We take a derivative with respect to ϕ in equation (8.37) to find

$$\frac{\mathrm{d}V}{\mathrm{d}\phi} = \frac{\mathrm{d}^2W}{\mathrm{d}\phi^2}\frac{\mathrm{d}W}{\mathrm{d}\phi} - \frac{d}{d-1}\frac{\mathrm{d}W}{\mathrm{d}\phi}W\,, \tag{8.40}$$

$$= \phi'' - \frac{d}{d-1}\phi' W\,. \tag{8.41}$$

In the last equation, we can make use of the second gradient flow equation of (8.38), which then results in equation (8.8). To prove that solutions of (8.38) imply (8.23), we note that

$$(A')^2 = \frac{1}{d-1}\left(\frac{W^2}{d-1}\right)\,. \tag{8.42}$$

From equation (8.37), we can find that

$$\frac{W^2}{d-1} = \frac{1}{d}\left(-2V + \frac{1}{2}\left(\frac{\mathrm{d}W}{\mathrm{d}\phi}\right)^2\right) = \frac{1}{d}\left(-2V + \frac{1}{2}(\phi')^2\right)\,. \tag{8.43}$$

Combining the above equations then leads to (8.23), as was to be shown.

8.2 Multiple scalar fields

The above, simple toy model of a single scalar field can be generalized to a toy model involving multiple scalar fields ϕ^I which live on a non-trivial scalar manifold with a metric $K_{IJ}(\phi)$. This toy model is of special interest to us, as it is closely related to the situation we will discuss in the next chapter. Indeed, as explained in detail in Section 6.3.5, we will construct holographic RG flows in a $\mathcal{N} = 1, d = 4$ supergravity theory coupled to 7 chiral multiplets, and hence we have to deal with 7 complex scalars which live on a Kähler manifold, such that their kinetic terms depend on a Kähler metric (see Section 6.3.3). Therefore, the metric K_{IJ} used here has to be considered a toy version of the Kähler metric $\mathcal{K}_{\alpha\bar{\beta}}$.

To discuss this toy model, we again start from the domain wall ansatz for the metric $g_{\mu\nu}$ from equation (8.2), but the matter Lagrangian density, defined in equation (8.15), gets generalized to

$$\mathscr{L}_M = \frac{1}{2} K_{AB} g^{\rho\sigma} \partial_\rho \phi^A \partial_\sigma \phi^B + V(\phi) \,, \tag{8.44}$$

Note that we write $V(\phi)$ for notational simplicity, but the potential depends on all scalars ϕ^I. The scalar equations of motion are found from the Euler-Lagrange equations. As intermediate steps, we find

$$\frac{\partial \mathscr{L}_M}{\partial(\partial_\mu \phi^I)} = K_{IL} \partial^\mu \phi^L \,, \quad \frac{\partial \mathscr{L}_M}{\partial \phi^I} = \frac{1}{2} (\partial_I K_{AB}) \partial_\rho \phi^A \partial^\rho \phi^B + \partial_I V \,. \tag{8.45}$$

where we introduced the notation $\partial_I \equiv \partial/\partial\phi^I$. The Euler-Lagrange equations then give

$$\partial_I V = \nabla_\mu \left(K_{IL} \partial^\mu \phi^L \right) - \frac{1}{2} \left(\partial_I K_{AB} \right) \partial_\rho \phi^A \partial^\rho \phi^B \,. \tag{8.46}$$

We again use equation (8.6) to find

$$\partial_I V = K_{IL} \frac{1}{\sqrt{g}} \partial_\mu (\sqrt{g} \partial^\mu \phi^L) + \left(\partial_\mu K_{IL} \right) \partial^\mu \phi^L - \frac{1}{2} \left(\partial_I K_{AB} \right) \partial_\rho \phi^A \partial^\rho \phi^B \,, \tag{8.47}$$

where we emphasize that the covariant derivative ∇_μ is defined with respect to the space-time metric $g_{\mu\nu}$. Upon using our domain wall ansatz for $g_{\mu\nu}$, we find

$$\partial_I V = K_{IL} \left(d(A') \left(\phi^L \right)' + \left(\phi^L \right)'' \right) + \left(\partial_r K_{IL} \right) \left(\phi^L \right)' - \frac{1}{2} \left(\partial_I K_{AB} \right) \left(\phi^A \right)' \left(\phi^B \right)' \,. \tag{8.48}$$

Using the chain rule in the second term, we find that it becomes

$$\partial_I V = K_{IL} \left(d(A') \left(\phi^L \right)' + \left(\phi^L \right)'' \right) + \left(\partial_C K_{IL} \right) \left(\phi^C \right)' \left(\phi^L \right)' - \tfrac{1}{2} \left(\partial_I K_{AB} \right) \left(\phi^A \right)' \left(\phi^B \right)' \,. \tag{8.49}$$

The equation of motion can be simplified if we raise the index I. For this, we multiply the above equation on both sides with K^{IJ}. Now note that

$$\left(\partial_C K_{IL} \right) \left(\phi^C \right)' \left(\phi^L \right)' = \tfrac{1}{2} \left(\partial_C K_{IL} \right) \left(\phi^C \right)' \left(\phi^L \right)' + \tfrac{1}{2} \left(\partial_L K_{IC} \right) \left(\phi^C \right)' \left(\phi^L \right)' \,, \tag{8.50}$$

since C, L are dummy indices. Using this, the final two terms of (8.49) will be combined into a Christoffel symbol, defined with respect to the metric of the scalar manifold, *i.e.*

$$\Gamma^A_{BC}(K) \equiv \frac{1}{2} K^{AD} \left(\partial_B K_{DC} + \partial_C K_{BD} - \partial_D K_{BC} \right) \,. \tag{8.51}$$

We hence end up with the scalar equation of motion

$$\partial^J V = d(A')\left(\phi^J\right)' + \left(\phi^J\right)'' + \Gamma^J_{AB}(K)\left(\phi^A\right)'\left(\phi^B\right)' . \tag{8.52}$$

For the Einstein equations, we can still use equations (8.12) and (8.13). The energy-momentum tensor is now

$$T_{\mu\nu} = -K_{IJ}\partial_\mu\phi^I\partial_\nu\phi^J + \frac{1}{2}K_{IJ}g_{\mu\nu}g^{\rho\sigma}\partial_\rho\phi^I\partial_\sigma\phi^J + g_{\mu\nu}V(\phi)\,, \tag{8.53}$$

which for the domain wall ansatz reduces to

$$T_{\mu\nu} = -K_{IJ}\delta^r_\mu\delta^r_\nu(\phi^I)'(\phi^J)' + \frac{1}{2}K_{IJ}g_{\mu\nu}(\phi^I)'(\phi^J)' + g_{\mu\nu}V(\phi)\,, \tag{8.54}$$

and taking the trace then yields

$$T = \frac{d-1}{2}K_{IJ}\left(\phi^I\right)'\left(\phi^J\right)' + (d+1)V\,. \tag{8.55}$$

One then finds the system of second-order equations

$$A'' + (A')^2 = -\frac{1}{d}\left(K_{IJ}\left(\phi^I\right)'\left(\phi^J\right)' + \frac{2}{d-1}V\right)\,. \tag{8.56}$$

$$A'' + d(A')^2 = -\frac{2}{d-1}V\,, \tag{8.57}$$

Note that the second equation is unchanged with respect to the one scalar case, as we could already anticipate from beforehand. Indeed, this is simply since the scalar kinetic term does not enter this equation. By taking the difference of these equations, one finds

$$(A')^2 = \frac{1}{d(d-1)}\left(K_{IJ}\left(\phi^I\right)'\left(\phi^J\right)' - 2V\right)\,. \tag{8.58}$$

Equations (8.52) and (8.58) generalize the original equations of motion in (8.8) and (8.23) to the many scalar fields toy model. As before, they are second-order equations of motion, but first-order flow equations can be found if V can be written as

$$V = \frac{1}{2}K_{IJ}\partial^I W\partial^J W - \frac{d}{2(d-1)}W^2\,. \tag{8.59}$$

The gradient flow equations are generalized to

$$\left(\phi^I\right)' = \partial^I W = K^{IJ}\partial_J W\,, \quad A' = -\frac{1}{d-1}W\,. \tag{8.60}$$

We prove that a solution of the gradient flow equations also satisfies the second-order equations of motion. We start by taking a covariant derivative with respect to the scalar metric, which is defined to act on a 'vector' X^I as

$$D_I X^J \equiv \partial_I X^J + \Gamma^J_{IA}(K)X^A\,, \tag{8.61}$$

on both sides of equation (8.59). The Christoffel symbols $\Gamma^J_{IA}(K)$ were defined in equation (8.51). For notational simplicity, we drop the explicit K dependence when writing

these Christoffel symbols. As usual, the covariant derivative on a scalar reduces to ordinary partial derivatives, and the metric postulate implies K_{IJ} has vanishing covariant derivative. Hence we find

$$\partial^J V = D^J\left(\partial^A W\right)\partial_A W - \frac{d}{d-1} W \partial^J W \tag{8.62}$$

$$= D^J\left(\partial^A W\right)\partial_A W + dA'\left(\phi^J\right)', \tag{8.63}$$

where we have used the gradient flow equations in the second step. Comparing the above with the scalar equation of motion in (8.58), it is sufficient to show that

$$\left(\phi^J\right)'' + \Gamma^J_{AB}\partial^A W \partial^B W = D^J\left(\partial^A W\right)\partial_A W\,, \tag{8.64}$$

where we again substituted $\left(\phi^A\right)' = \partial^A W$. Let us focus on rewriting $\left(\phi^J\right)''$. First of all, note that

$$\left(\phi^J\right)'' = \frac{\mathrm{d}}{\mathrm{d}r}\left(\phi^J\right)' = \frac{\mathrm{d}}{\mathrm{d}r}\left(\partial^J W\right)\,. \tag{8.65}$$

Using the chain rule on this, we find that

$$\left(\phi^J\right)'' = \partial_A\left(\partial^J W\right)\partial^A W = \partial^J\left(\partial^A W\right)\partial_A W\,, \tag{8.66}$$

where we commuted partial derivatives and raised and lowered dummy indices to obtain the final equality. Substituting in (8.64), we can rephrase that it is sufficient to show that

$$\partial^J(\partial^A W)\partial_A W + \Gamma^J_{AB}\partial^A W \partial^B W = D^J(\partial^A W)\partial_A W\,. \tag{8.67}$$

To show this, we rewrite the right hand side:

$$D^J\left(\partial^A W\right)\partial_A W = K^{JL} D_L\left(\partial^A W\right)\partial_A W \tag{8.68}$$

$$= \partial^J(\partial^A W)\partial_A W + K^{JL}K_{AL}\Gamma^A_{LM}\partial^M W \partial^L W\,, \tag{8.69}$$

which is precisely the left hand side of (8.67) since $K^{JL}K_{AL} = \delta^J_A$. It is less work to show that the Einstein equation of motion is satisfied as well. Indeed, we can completely mimic the derivation for the single scalar case: simply combine the equation

$$(A')^2 = \frac{1}{d-1}\frac{W^2}{d-1}\,, \tag{8.70}$$

obtained from squaring the equation on the right of (8.60), with the equation

$$\frac{W^2}{d-1} = \frac{1}{d}\left(K_{IJ}\left(\phi^I\right)'\left(\phi^J\right)' - 2V\right)\,, \tag{8.71}$$

obtained from rewriting equation (8.59), to immediately find that equation (8.58) is satisfied.

Chapter 9

Holographic RG flows in gauged supergravity

In previous chapters, we have introduced the necessary tools in order to study holographic RG flows in gauged supergravity theories. After the toy models of the previous chapter, we are now ready to tackle theories studied in the literature. We will limit our discussion to maximally supersymmetric four-dimensional gauged supergravity theories which are known to embed into string theory. Hence, we fix $d = 3$ from now on. Moreover, we work in the $\mathbb{Z}_2^3$-invariant truncation which keeps 14 real scalar fields out of the original 70 real scalar fields. As the scalar potential depends on the gauging, the vacuum structure, as well as the holographic RG flows interpolating between them, vary between the different theories we consider.

This chapter is organized as follows. In Section 9.1, we reiterate for completeness the general set-up of the problem at hand. We specify the domain wall ansatz and the first-order gradient flow equations used to construct holographic RG flows. After discussing the main difficulty related to constructing holographic RG flows, we explain the design of our new numerical algorithm, inspired by machine learning principles, to overcome this hurdle. Sections 9.2 – 9.5 discuss each of the four gauged supergravities of interest in detail. We summarize known results from previous studies and, whenever possible, extend this work to the $\mathbb{Z}_2^3$-truncation, which is currently the largest truncation considered in the context of constructing holographic RG flows. Therefore, this chapter aims to present the most thorough overview of work in this field to date. Finally, in Section 9.6, we reflect on our results and possible continuations of our work.

9.1 Set-up and numerical methods

We start this chapter with a general discussion on constructing holographic RG flows, which is relevant for each of the following sections.

9.1.1 General set-up of the problem

Our goal is to construct holographic RG flows in four-dimensional gauged supergravities. We restrict our attention to a specific subset of gauged supergravities which can be obtained via dimensional reduction (see Section 6.3.2) of ten- or eleven-dimensional supergravity (and by extension, string or M-theory). We briefly mentioned these gauged super-

gravities in our discussion from Section 6.3.5. Hence, there exist methods to 'lift' the $4d$ vacua obtained in these supergravities to solutions of the higher-dimensional theories. We have summarized the relations between the gauged supergravities, the higher-dimensional theories and the dual CFTs in Figure 9.1. Detailed information and references for further reading are given in each of the mentioned sections. As we will see, all $3d$ dual field theories are superconformal field theories, discussed in Section 6.2, which are moreover *Chern-Simons* gauge theories. These are so-called topological field theories, where the 3-form of gauge fields A has kinetic terms $A \wedge \mathrm{d}A$. The gauge coupling k, also known as the *Chern-Simons level*, is quantized (*i.e.*, $k \in \mathbb{Z}$) to guarantee gauge invariance. Note that therefore, Chern-Simons theories are necessarily strongly coupled. Note that the dual field theories cannot be *e.g.* a more familiar Yang-Mills theory, since the Yang-Mills coupling becomes dimensionful in three dimensions of space-time, which breaks conformal invariance.

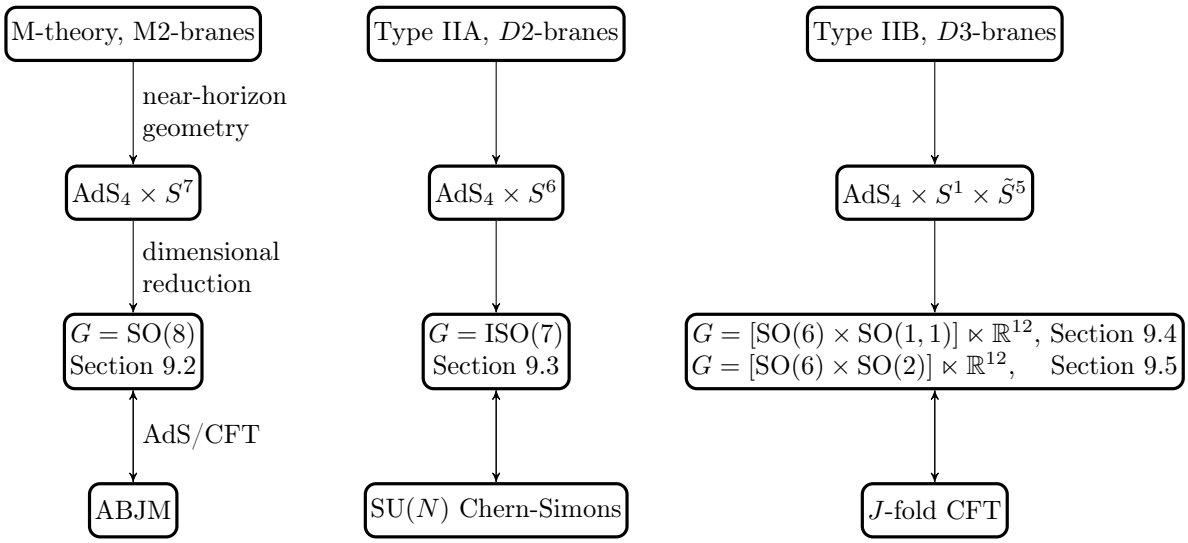

Figure 9.1: Higher-dimensional origin of the four-dimensional gauged supergravities (with gauge groups G) discussed in this chapter, along with their dual field theories.

The domain wall ansatz from which we construct holographic RG flows, already mentioned in Chapter 8, is

$$\mathrm{d}s^2 = e^{2A(r)}\eta_{\mu\nu}\,\mathrm{d}x^\mu\,\mathrm{d}x^\nu + \mathrm{d}r^2\,, \tag{9.1}$$

where $\eta_{\mu\nu}$ is the $3d$ Minkowski metric in order to be consistent with Poincaré invariance of the dual, $3d$ field theory. Two AdS vacua are located at $r = \pm\infty$ in the above coordinate system. Hence, the starting point of constructing holographic RG flows is the identification of the critical points of the scalar potential of interest, as these may serve as endpoints of the flows. Recall that the AdS vacuum at $r = +\infty$ ($r = -\infty$) is referred to as the UV vacuum (IR vacuum), and the irreversibility property, derived in Section 8.1.2, dictates that holographic RG flows go from the UV to the IR. In the $\mathbb{Z}_2^3$-truncation, discussed in Section 6.3.5, the theory can be recast in a $\mathcal{N} = 1, d = 4$ supergravity theory coupled to 7 chiral multiplets introduced in Section 6.3.4. Hence, we retain only 7 complex scalars z_α of which the scalar kinetic terms are non-trivial as the complex scalars live on a Kähler manifold, explained in Section 6.3.3. Employing the $\mathcal{N} = 1, d = 4$ supergravity language allows us to compute the scalar potential in terms of the Kähler potential $\mathcal{K}$, the Kähler metric $\mathcal{K}_{\alpha\overline{\beta}}$ and the superpotential $W(z)$: see equation (6.44). Therefore, the scalar

potential in this specific truncation is a function of 14 real variables. Vacuum solutions correspond to the extrema of this scalar potential. As explained in Section 6.3.6, vacuum solutions with residual supersymmetry correspond to the Kähler covariant extrema of the superpotential. That is, they are solutions of $\mathcal{D}_\alpha W = 0$, with $\mathcal{D}_\alpha$ the Kähler covariant derivative from equation (6.45).

Since the potential is a function of 14 real variables, finding its critical points is a daunting task unless numerical methods are used. One possibility is to use Wolfram Mathematica, a program well suited for symbolic calculations. Following the convention of [73], we label critical points using the first 7 digits[1] of their scalar potential value. That is, a critical point with label $\mathtt{Pn_1n_2n_3n_4n_5n_6n_7}$ has a scalar potential value $V = -n_1n_2.n_3n_4n_5n_6n_7$. Recall that the potential is negative, since we are dealing with AdS vacua and the potential essentially determines the value of the cosmological constant.

Parametrizations and conventions related to the (super)potential and Kähler geometry vary greatly in the literature. We have chosen to, for each gauged supergravity theory separately, adopt the conventions of papers which are most related to our own work. This unfortunately implies that the overall forms of $\mathcal{K}$, W and V vary throughout this chapter. Moreover, we are only interested in supersymmetric vacua, as they are guaranteed to be stable [74, 75]. All known non-supersymmetric vacua are perturbatively unstable in the higher-dimensional theories (see for example [76] for more details). In fact, all non-supersymmetric vacua of string theory are conjectured to be unstable [77], which is why we choose to neglect such vacua in our work.

A second advantage of restricting our attention to supersymmetric vacua is that there exist first-order gradient flow equations which automatically solve the equations of motion obtained from the above ansatz. Such gradient flow equations as solutions to the complete equations of motion were discussed in detail in the toy models of Chapter 8. For the $\mathcal{N} = 1, d = 4$ supergravity theory coupled to chiral multiplets that we consider in this chapter, the gradient flow equations (also called BPS equations) can be derived from equations (6.61) – (6.64). The result is [38, 78]

$$(z^\alpha)' = \mp\sqrt{2}ge^{\mathcal{K}/2}\mathcal{K}^{\alpha\overline{\beta}}\frac{W}{|W|}\overline{\mathcal{D}}_{\overline{\beta}}\overline{W}\,, \quad (\overline{z}^{\overline{\alpha}})' = \mp\sqrt{2}ge^{\mathcal{K}/2}\mathcal{K}^{\alpha\overline{\beta}}\frac{\overline{W}}{|W|}\mathcal{D}_\alpha W\,, \tag{9.2}$$

$$A' = \pm\sqrt{2}ge^{\mathcal{K}/2}|W|\,, \tag{9.3}$$

As before, primes denote derivatives with respect to r. The signs above are related to the freedom in choosing the sign of the radial coordinate in the domain wall ansatz. We will always use the upper sign in these equations. During our work, we have discovered that equation (9.3) is the correct version of the equation that was provided in (6.3) of [78]. However, we have verified that this error does not influence the results of the reference. Note that the metric and the scalars are decoupled in the BPS equations, and this allows one to solve the equations sequentially. That is, one first solves the first line of coupled ordinary differential equations to find the solutions of the scalars $z_\alpha(r)$, from which the profile of $A'(r)$ can be obtained by substituting the values of $z_\alpha(r)$ in the second equation. Below, we will limit our discussion to the solutions of the scalar fields, as the scale factor does not provide independent information.

[1]Note that these are the truncated values, and not the rounded ones.

Note that, due to the BPS equations, we are actually interested in solutions of a dynamical system in the fourteen real scalar fields, with the coordinate r acting as the evolution parameter. Dynamical systems were recapitulated in Section 4.1. Supersymmetric vacua, as Kähler covariant extrema of the superpotential, are fixed points of the above gradient flow equations in the sense that $(z^\alpha)' = 0$ for all α. Hence, we will use the terms 'fixed points' and 'critical points' interchangeably throughout this chapter. Similar to our toy models of Chapter 8, these fixed points correspond to AdS_4 space-times dual to CFT_3 theories. We will only discuss solutions to the BPS equations that interpolate between fixed points, since we have a clear interpretation of such solutions using holography. Unlike ordinary dynamical systems, solutions tending towards infinity are singular and do not admit a viable interpretation [79]. Therefore, the link with dynamical systems should be interpreted in a careful way.

We will split the complex scalars into their real and imaginary parts, and we define $z_\alpha(r) = x_\alpha(r) + iy_\alpha(r)$. We can find BPS equations for $x_\alpha(r), y_\alpha(r)$ by taking the real and the imaginary part of equation (9.2). These equations are numerically integrated using `NDSolve` in Mathematica in order to find the flow solutions. Recall that holographic RG flows must go from the UV to the IR, as explained in Section 8.1.2, since the flows must go 'deeper' into the scalar potential landscape. However, it turns out to be numerically favourable to construct the solutions in the other direction (*i.e.*, from the IR to the UV) and hence the flows go from a deeper value of the potential to a higher value. Therefore, rephrased in the language of RG flows in the dual field theory, we start from an IR CFT and approach a UV CFT by switching on irrelevant deformations (in the sense defined in Section 4.3).

At the gravity side of the gauge/gravity duality, this means that we linearize the BPS equations of the real fields $x_\alpha(r), y_\alpha(r)$, which we will from now on collectively denote by $\phi_a(r)$, $a = 1, \ldots, 14$, around a supersymmetric vacuum $\phi_a^\star$. For this, we have to compute the Jacobian matrix at the fixed point, as explained in Section 4.1. We diagonalize the Jacobian, and obtain its eigenvalues and eigenvectors $(\lambda_a, \boldsymbol{v}_a)$, $a = 1, \ldots, 14$, with bold font denoting 14-dimensional vectors. We refer to an eigenvector of the Jacobian as a *mode*. The initial condition for the flow solutions is written as

$$\boldsymbol{\phi}(r_{\text{in}}) = \boldsymbol{\phi}^\star + \sum_{a=1}^{14} A_a \boldsymbol{v}_a e^{\lambda_a r_{\text{in}}} = \boldsymbol{\phi}^\star + \sum_{a=1}^{14} A_a \boldsymbol{v}_a e^{-\delta_a \frac{r_{\text{in}}}{L}} \,. \tag{9.4}$$

In order to flow away from the fixed point, we will fix $A_a = 0$ for modes with $\lambda_a < 0$ ($\delta_a > 0$). We provide all the linearized BPS equations and the values of the remaining coefficients (*i.e.*, corresponding to $\lambda_a > 0$) used to construct the flows in Appendix A. Above, r_{in} is the initial value at which we evaluate the initial condition. Since we start the flow solution close to the IR ($r = -\infty$), we take $r_{\text{in}} = \ln(10^{-2})$. In the above equation, L is the length scale of the AdS space-time of the critical point, which can be found from the potential value through equation (7.15). In our case, we have[2]

$$L = \sqrt{-\frac{3}{V(z_\alpha^\star)}} \,. \tag{9.5}$$

[2]This equation holds throughout this chapter except for Section 9.3, where the reference that we follow uses conventions such that $V = -12/L^2$.

Moreover, our initial condition also introduced δ_a, defined by

$$\delta_a = -L\lambda_a \,, \tag{9.6}$$

The reason for introducing δ_a is that the operators in the dual field theory which are dual to the scalars ϕ_a will have a scaling dimension Δ_a given by

$$\Delta_a = \delta_a \,, \quad \Delta_a = 3 - \delta_a \,, \tag{9.7}$$

depending on which option satisfies the unitarity bound $\Delta \geq (d-2)/2$, which is $\Delta \geq 1/2$ in our case. This relation between the asymptotic behaviour of the bulk scalar fields and scaling dimensions of operators in the dual field theory was derived in the toy model of Section 8.1.

Recall that the AdS/CFT dictionary translates the squared masses of the scalars in the bulk to scaling dimensions in the dual field theory according to equation (7.23). As discussed in Section 7.3, for a certain range of squared masses m^2L^2, both roots $\Delta_\pm$ of this equation lie above the unitarity bound and the scaling dimension is defined ambiguously by this equation, as there exists two inequivalent ways of quantization. For example, at the SO(8)-invariant vacuum of $G = \mathrm{SO}(8)$ gauged supergravity (see Section 9.2), all scalar fields have a mass $m^2L^2 = -2$, such that the scaling dimension is either $\Delta_+ = 2$ or $\Delta_- = 1$. As it turns out, 35 of these scalars are dual to gauge-invariant scalar bilinears $\mathrm{Tr}\, X^2$, with $\Delta = \Delta_- = 1$, while the other 35 are dual to fermionic bilinears $\mathrm{Tr}\, \lambda^2$, with $\Delta = \Delta_+ = 2$ [60]. In Section 7.3, we mentioned that supersymmetry solves this ambiguity, as the linearized BPS equations specify which scaling dimensions are selected by supersymmetry. We give a more complete discussion of this in Appendix B, where we also compute the masses and the corresponding roots $\Delta_\pm$ for each of the 14 scalar fields at each vacuum discussed in this chapter and we show which scaling dimensions are 'selected' by supersymmetry by linearizing the BPS equations.

Our goal is therefore to find coefficients A_a such that the initial condition for the real fields $\phi_a(r_{\mathrm{in}})$ will result in a flow which in the UV ($r \to +\infty$) approaches a second AdS vacuum. As we have illustrated in Section 4.2, this requires a fine-tuning of the expansion coefficients, which is the main complication especially in the large $\mathbb{Z}_2^3$-truncation we consider in this thesis. To tackle this issue, we have designed and developed an original algorithm which automates the fine-tuning process. All Mathematica code used in this thesis is original and can be found in [80].

9.1.2 A new algorithm to construct holographic RG flows

The design of our algorithm is inspired by the foundations of machine learning (ML) [41]. The core idea behind any ML algorithm is the minimization of a certain *loss function* or error function f, which essentially measures the discrepancy between an output of the algorithm and the correct answer or desired output. The loss function depends on a certain number of parameters which influence the output of the algorithm. Importantly, whenever the loss function is differentiable with respect to these parameters, one can iteratively update the parameters along the gradient of the loss function in order to improve the algorithm output. Such *gradient descent* algorithms are quite popular and well-studied. An example of gradient descent in the context of finding vacua of gauged supergravities is given in [81].

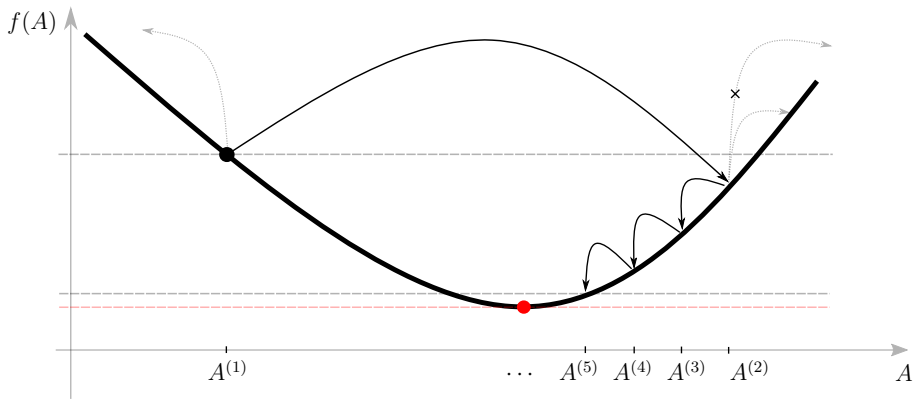

Figure 9.2: Visualization of the step descent algorithm in a one-dimensional parameter space. Starting from an initial parameter $A^{(1)}$ (black dot), the parameter space is explored in the direction of decreasing loss function values towards the minimum of the loss function (red dot).

The ideas behind ML algorithms and gradient descent inspired the following algorithm. We integrate the BPS equations up until $r = r_{\text{max}}$ and denote the endpoint of the constructed solution as z_E^α. The easiest loss function to consider is the Euclidean distance between z_E^α and the 'target' AdS vacuum z_{UV}^α in the UV that we want to reach. Hence, in our algorithm, we will work with the loss function

$$f : \mathbb{R}^n \to \mathbb{R} : (A_1, \ldots, A_n) \mapsto f(A_1, \ldots, A_n) = d_{\text{Eucl}}(z_E^\alpha, z_{\text{UV}}^\alpha)\,, \tag{9.8}$$

where we compute the Euclidean distance from the real fields x^α, y^α, collectively denoted by ϕ^a. Hence, the loss function uses

$$d_{\text{Eucl}}(z_E^\alpha, z_{\text{UV}}^\alpha) = \sqrt{\sum_{a=1}^{14} \left(\phi_E^a - \phi_{\text{UV}}^a\right)^2}\,. \tag{9.9}$$

The algorithm parameters A_i, $i = 1, \ldots, n$ are simply, as the notation suggested, the coefficients appearing in the expansion (9.4) which correspond to the modes which repel us away from the IR AdS vacuum from which we start the solution. In practice, we can rescale the r-coordinate, as the BPS equations constitute a homogeneous dynamical system, thereby giving us the freedom to fix the value of one of these coefficients.

In order to minimize the loss function, we constructed a simpler version of a gradient descent algorithm which we will call the *step descent algorithm*. The step descent algorithm starts from an initial guess for the parameters, say $(A_1^{(1)}, \ldots, A_n^{(1)})$, for which the solution is computed up until $r = r_{(1)}$ and from which an initial value of the loss function is calculated. At each iteration step, we store the current best set of parameter values $(A_1^\star, \ldots, A_n^\star)$ found during the search, *i.e.* with a minimal value of the loss function $f_\star$. At every $r_{(j)}$, we perform the following loop for each of the n parameters A_i. Start each loop with a boolean variable `directionFound`, initialized with `False`, and an initial stepsize s_{in} and let $\hat{u}$ be a unit vector in $\mathbb{R}^n$ pointing in the i-direction (that is, a vector containing zeroes and 1 on the i-th entry). Set an integer variable, `counter`, equal to zero. While the counter is below a specified integer, do:

- If `directionFound` is `False`: compute the solution for the new parameter values $(A_1^\star, \ldots, A_n^\star) \pm s\hat{u}$, with s the current step size, and compute $f_\pm$.

  - If $f_\pm \geq f_\star$: divide the stepsize by a specified factor `sfactor` and increase `counter` by one.
  - If $f_+ < f_\star$ ($f_- < f_\star$), put `sign` $= 1$ (`sign` $= -1$) and put `directionFound` to `True`.

- If `directionFound` is `True`: compute the solution for the new parameter values $(A_1^\star, \ldots, A_n^\star) + s\texttt{sign}\hat{u}$, with s the current step size, and compute f_s.
  - If $f_s \geq f_\star$: divide the stepsize by a specified factor `sfactor` and increase `counter` by one.
  - If $f_s < f_\star$, the parameters are not altered, and the program simply updates the values of $(A_1^\star, \ldots, A_n^\star)$ to the new, improved parameter values.

The above loop is performed for each of the parameters and attempts to decrease the loss function within each cycle. The procedure is visualized in Figure 9.2 for a one-dimensional parameter space. Once all parameters have been fine-tuned, we increase $r_{(j)} \to r_{(j+1)} = r_{(j)} + \Delta r$, construct the flow solution up to $r = r_{(j+1)}$, compute the loss function at $(A_1^\star, \ldots, A_n^\star)$ and start the above loop again.

Now that we have explained the general set-up and our numerical methods, we are ready to present our results.

9.2 SO(8) gauged supergravity

The first $4d$ gauged supergravity we will discuss has gauge group $G = \mathrm{SO}(8)$. Historically, this was the first maximally supersymmetric gauged supergravity discovered by de Wit and Nicolai, which is why this gauged supergravity is also known as the de Wit-Nicolai theory [82, 83]. It can be obtained by performing a dimensional reduction of $11d$ supergravity on $\mathrm{AdS}_4 \times S^7$ [84, 85]. The embedding into $11d$ supergravity was considered in [86]. Note that this is precisely the situation we mentioned in equation (7.1), such that the gauge theory in $11d$ is located on the world-volume of a stack of coincident M2-branes. In this model, the dual field theory is a conformal Chern-Simons field theory, known as the ABJM theory [87], which has gauge group $\mathrm{U}(N)_k \times \mathrm{U}(N)_{-k}$, where k is the Chern-Simons level. Maximal supersymmetry is preserved only if the Chern-Simons level k equals 1 or 2, and since the coupling might be thought of as k^{-1}, the theory is necessarily strongly coupled [88]. Therefore, holography allows us to identify the conformal phases of the dual ABJM theory and probe their strongly coupled RG flows.

To discuss this gauged supergravity and its holographic RG flows, we will follow the conventions of [78]. The superpotential in the $\mathbb{Z}_2^3$-truncation is

$$\begin{aligned} W =& z_1 z_2 z_3 z_4 z_5 z_6 z_7 \\ &+ z_1 z_2 z_3 z_7 + z_1 z_2 z_5 z_6 + z_1 z_3 z_4 z_5 + z_1 z_4 z_6 z_7 + z_2 z_3 z_4 z_6 + z_2 z_4 z_5 z_7 + z_3 z_5 z_6 z_7 \\ &+ z_1 z_2 z_4 + z_1 z_3 z_6 + z_1 z_5 z_7 + z_2 z_6 z_7 + z_2 z_3 z_5 + z_3 z_4 z_7 + z_4 z_5 z_6 + 1 \,. \end{aligned} \tag{9.10}$$

The Kähler potential is

$$\mathcal{K} = -\sum_{\alpha=1}^{7} \log\left(1 - z_\alpha \overline{z}_\alpha\right) \,, \tag{9.11}$$

which means that we are working in 7 copies of the Poincaré disk. The scalar potential is given by

$$V = 2e^{\mathcal{K}} \left(\mathcal{K}^{\alpha\overline{\beta}} \mathcal{D}_\alpha W \overline{\mathcal{D}}_{\overline{\beta}} \overline{W} - 3 W \overline{W} \right) \tag{9.12}$$

In [78], the authors discuss a $\mathrm{SO}(3) \times \mathbb{Z}_2$-invariant subtruncation of the $\mathbb{Z}_2^3$-truncation which retains three complex scalars ζ_a, which can be found from the $\mathbb{Z}_2^3$-truncation if one identifies

$$z_3 = z_4 = z_5 = \zeta_1 \,, \quad z_1 = -\zeta_2 \,, \quad z_2 = z_6 = z_7 = -\zeta_3 \,. \tag{9.13}$$

All our work on holographic RG flows presented in this section therefore directly extends the work of [78].

9.2.1 Supersymmetric vacua

A list of the supersymmetric vacua is provided in Table 9.1, with coordinates given in Section A.1.1. We have numerically computed the location of the $\mathrm{U}(1) \times \mathrm{U}(1)$ critical point which, to the best of our knowledge, has not appeared in the literature before within this truncation. It has been proven explicitly that, apart from the maximally supersymmetric SO(8) vacuum at the origin, all supersymmetric critical points should have $\mathcal{N} \leq 2$ supersymmetry [89], which is indeed the case for the supersymmetric vacua found in the $\mathbb{Z}_2^3$-truncation.

In order to construct holographic RG flows that interpolate between the various AdS vacua of Table 9.1, we have to linearize the BPS equations around the IR vacua. As explained in Section 9.1.1, we can deduce the directions for the initial conditions of the flows from the eigenvectors of the Jacobian of the BPS equations which correspond to positive eigenvalues (negative δ_a's in equation (9.6)). We repeat once again that the number of coefficients to fine-tune in the initial condition is one less than the total number of parameters n in the loss function, or equivalently, total number of positive eigenvalues of the Jacobian. This is due to our freedom to rescale r, such that we can fix the value of one of the coefficients. An overview of the values of δ_a for each critical point is given in Table 9.2.

We remark that the location of the 7 scalars at the susy vacua given in the appendix is not unique, due to a residual symmetry which determines an orbit (in the group-theoretical sense) of the vacua. Hence, we will often construct holographic RG flows that interpolate between AdS vacua which lie at different locations compared to the values of Section A.1.1. In each case, we verified explicitly that the points considered in the flows are susy vacua, *i.e.*, they solve $\mathcal{D}_\alpha W = 0$, with a value of the scalar potential that agrees with the one given in Table 9.2. We will return to the issue of the existence of several 'copies' of the same vacuum in Section 9.2.5.

We are now ready to discuss the holographic RG flows we have constructed in this theory. An overview of the flows that will be discussed is given in Figure 9.3. The arrows in this figure point in the direction of the 'physical' flows: from the UV (higher scalar potential value) to the IR (lower scalar potential value). Numerical solutions are constructed in the opposite direction.

Point	$\mathcal{N}$	**Cont. symmetry**	V	**Refs.**
P0600000	$\mathcal{N}=8$	SO(8)	-6	[83]
P0719157	$\mathcal{N}=1$	G_2	-7.19157	[86]
P0779422	$\mathcal{N}=2$	SU(3) $\times$ U(1)	-7.79422	[90]
P1200000	$\mathcal{N}=1$	U(1) $\times$ U(1)	-12	[91–93]
P1384096	$\mathcal{N}=1$	SO(3)	-13.84096	[41]

Table 9.1: Supersymmetric vacua in the SO(8) gauged supergravity. Potential values are at $g=1$.

Point	δ_a	n
P0600000	$1(\times 14)$	–
P0719157	$-1.4494897(\times 1),\ 0.5917517(\times 6),\ 1.4082482(\times 6),\ 3.449489(\times 1)$	1
P0779422	$-1.561552(\times 1),\ -0.5615528(\times 1),\ 0.666666(\times 3),\ 1(\times 4),$ $1.333333(\times 3),\ 2.5615528(\times 1),\ 3.5615528(\times 1)$	2
P1200000	$-1.8058837(\times 2),\ -1.7320508(\times 1),\ 0.2679491(\times 1),\ 0.6436060(\times 2),\ 1(\times 2),$ $1.3563939(\times 2),\ 1.7320508(\times 1),\ 3.7320508(\times 1),\ 3.8058837(\times 2)$	3
P1384096	$-2.8025410(\times 1),\ -1.7163163(\times 1),\ -0.9632443(\times 2),\ 0.4273831(\times 2),\ 0.7487353(\times 1),$ $1.2512646(\times 1),\ 1.5726168(\times 2),\ 2.9632443(\times 2),\ 3.7163163(\times 1), 4.8025410(\times 1)$	4

Table 9.2: Values of δ_a for the susy vacua in SO(8) gauged supergravity, with the multiplicity given in brackets. The integer n denotes the number of parameters of the loss function.

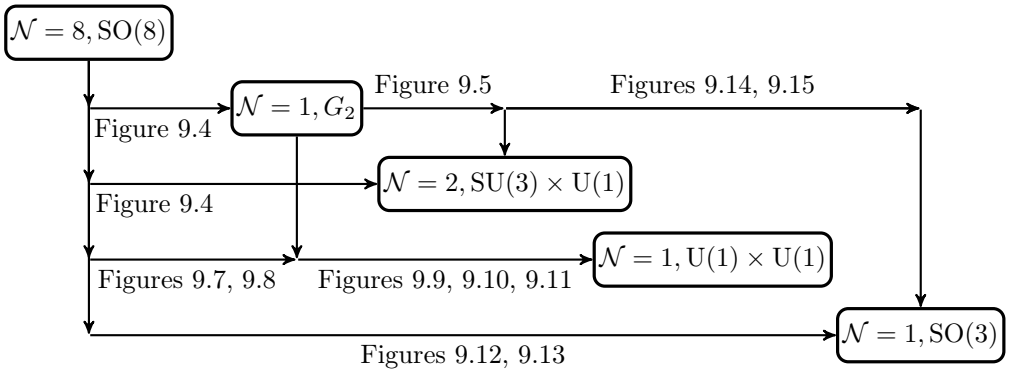

Figure 9.3: Overview of holographic RG flows in the SO(8) theory discussed in this section.

9.2.2 Reconstructing known flows

Let us start our discussion by reconstructing flows that were reported in the literature before within subtruncations of the $\mathbb{Z}_2^3$-truncation to verify that they are still solutions in the larger truncation. From Table 9.2, we see that it is quite straightforward to construct holographic RG flows from the SO(8) vacuum in the UV to the G_2 or $\mathrm{SU}(3) \times \mathrm{U}(1)$ vacua in the IR. Indeed, no coefficients have to be tuned for the G_2 point. For the $\mathrm{SU}(3) \times \mathrm{U}(1)$, the solution is not as sensitive to the undetermined coefficient as other flows, which implies one can easily find a convergent flow from SO(8) to $\mathrm{SU}(3) \times \mathrm{U}(1)$. These 'direct flows' (to be compared with triangular flows later on) to G_2 and $\mathrm{SU}(3) \times \mathrm{U}(1)$, are reconstructed in Figure 9.4. We will always show solutions by plotting the scalars $z_\alpha(r)$ in the complex (x, y)-plane, as well as the evolution of the real fields as function of r. For the latter, we plot the real parts (imaginary parts) using solid lines (dashed lines).

As it is our first encounter with numerical holographic RG flow solutions in this thesis, we have extensively annotated the plots that aim to guide the reader through plots of more complicated flow solutions to come. We emphasize once again that holographic RG flows go from the UV to the IR (*i.e.*, to a more negative value of the scalar potential), but are numerically constructed in the opposite direction. The arrows drawn in the figure point in the direction in which the physical solution will flow. When discussing our flow solutions in the text, our terminology will always relate to this direction for the flow solutions, *e.g.* we say that our flows 'start from the UV' and 'end in the IR'.

By fine-tuning the undetermined coefficient of the $\mathrm{SU}(3) \times \mathrm{U}(1)$ IR vacuum, one can find a so-called *triangular holographic RG flow* between all three aforementioned fixed points. That is, there exists a flow which starts from the SO(8) vacuum in the UV and ends up in the $\mathrm{SU}(3) \times \mathrm{U}(1)$ in the IR, but (as opposed to 'direct flows') comes arbitrarily close to the G_2 vacuum at intermediate values of r. This holographic RG flow was already found in the $\mathrm{SO}(3) \times \mathbb{Z}_2$-truncation [78], and was first constructed in a SU(3)-invariant truncation in [88]. The same flow within our $\mathbb{Z}_2^3$-truncation is shown in Figure 9.5. Let us also use this triangular flow to provide an example of a plot of $A'(r)$, using equation (9.3), shown in Figure 9.6. At the AdS vacua, A' is constant and equal to $A' = 1/L$, as we argued in detail in Chapter 8. Recall that, due to the irreversibility of holographic RG flows, combined with equation (9.5), A' is a monotonically increasing function of r as we go from the UV to the IR, which is indeed the case. Below, we will only discuss solutions by specifying the solutions of the scalar fields $z_\alpha(r)$, as the solution for $A'(r)$ does not convey independent, physically interesting information.

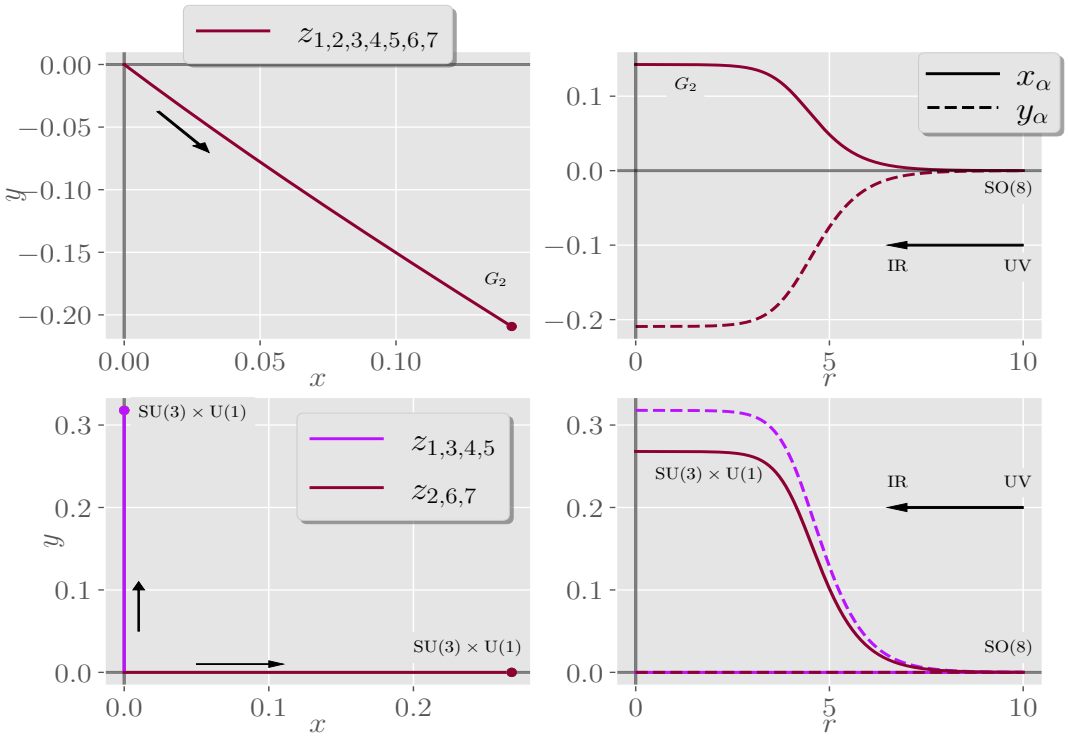

Figure 9.4: Top: Direct flow from the SO(8) vacuum (origin) in the UV to the G_2 vacuum in the IR. Bottom: Direct flow from the SO(8) vacuum (origin) in the UV to the SU(3) × U(1) vacuum in the IR. The arrows denote the direction in which the physical solution will flow: from the UV towards the IR.

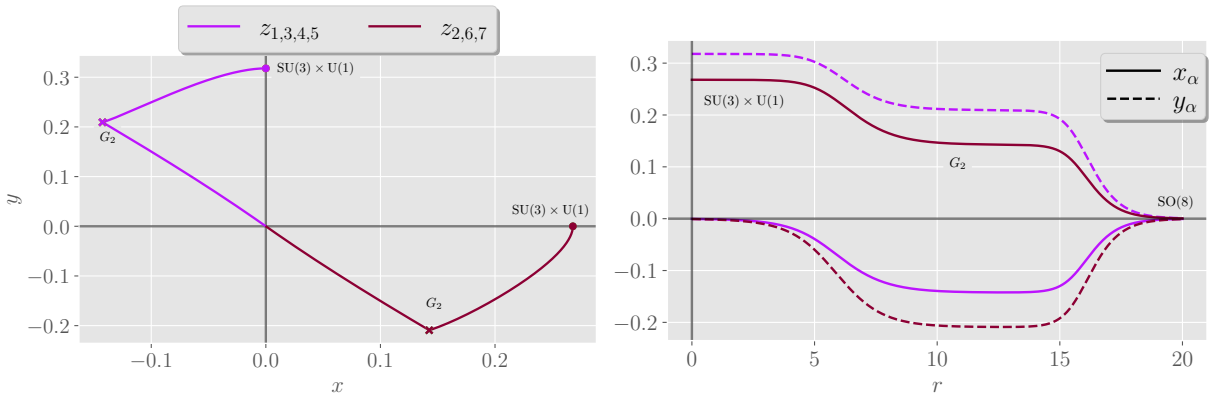

Figure 9.5: Triangular flow from the SO(8) vacuum (origin) in the UV to the G_2 vacuum (crosses) and eventually reaching the SU(3) × U(1) vacuum (dots) in the deep IR.

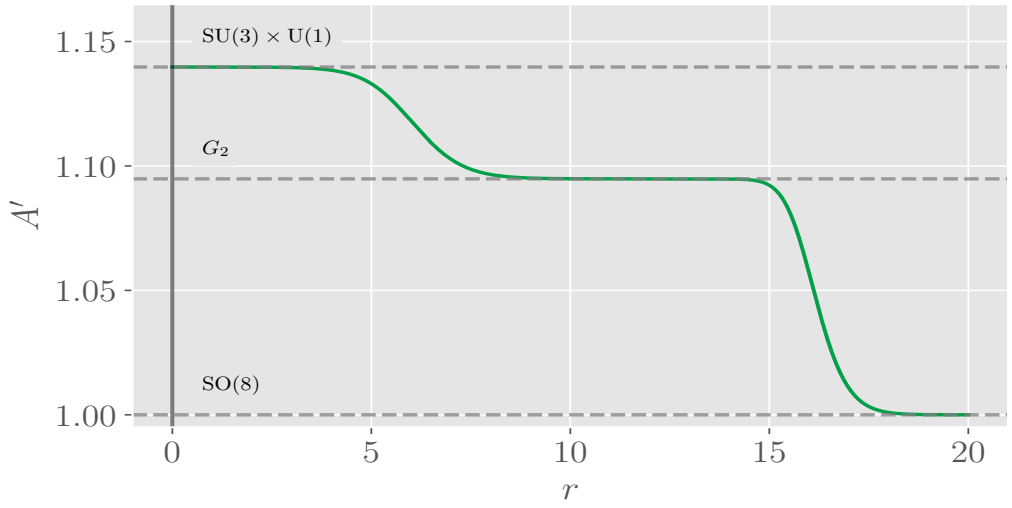

Figure 9.6: Plot of the profile $A'(r)$ related to the solution shown in Figure 9.5. Dashed lines show the value of $1/L$, with L the length scale of the corresponding AdS space-time.

9.2.3 New flows to the U(1) × U(1) vacuum

An interesting aspect of the $\mathbb{Z}_2^3$-truncation is the fact that it also contains the `P1200000` point with a $\mathrm{U}(1) \times \mathrm{U}(1)$ symmetry group, which lies outside of the $\mathrm{SO}(3) \times \mathbb{Z}_2$-truncation of [78]. This opens up new possibilities for holographic RG flows. A flow from the SO(8) point to this $\mathrm{U}(1) \times \mathrm{U}(1)$ point which preserves the $\mathrm{U}(1) \times \mathrm{U}(1)$ symmetry along the flow was already constructed in [93]. We reconstructed this flow, shown in Figure 9.7 below, within the $\mathbb{Z}_2^3$-truncation (note that z_2 and z_6 vanish identically along this flow).

Since the above flow preserves the $\mathrm{U}(1) \times \mathrm{U}(1)$ symmetry, it can be constructed within a $\mathrm{U}(1) \times \mathrm{U}(1)$-invariant truncation which contains only these two susy vacua. However, since our $\mathbb{Z}_2^3$-truncation only imposes invariance under a discrete symmetry group, this truncation admits holographic RG flows which break the continuous symmetry of the endpoints along the flow. We were able to construct such a holographic RG flow, which showcases this new feature of the $\mathbb{Z}_2^3$-truncation. The result is given in Figure 9.8. Indeed, we note that along this flow, the continuous symmetry is completely broken and all 7 complex scalars have a different evolution. To the best of our knowledge, such a phenomenon has not been reported in the literature on holographic RG flows before.

The two flow solutions just discussed start from the SO(8) vacuum in the UV. However, we were also able to find holographic RG flows which start from the G_2 vacuum in the UV and again end in the $\mathrm{U}(1) \times \mathrm{U}(1)$ vacuum in the IR. As before, there exist several, inequivalent flow solutions. First of all, we can require the flow to preserve a continuous symmetry group along the flow. Such a solution is given in Figure 9.9. However, we are again able to explicitly break the continuous symmetry along the flow, and an example of such a flow is given in Figure 9.10. In fact, we have found multiple, inequivalent versions of this latter flow which interpolate between different copies of the G_2 vacuum in the UV (recall that a residual symmetry determines an orbit for the critical points, resulting in these 'copies'). Indeed, another example of the same flow, which starts from a different G_2 vacuum, is given in Figure 9.11. These flows are inequivalent also in the sense that both approach the G_2 vacuum differently. That is, while the solution of z_5 merges with z_6 before approaching the G_2 vacuum in Figure 9.11, z_5 merges with z_2 and z_7 in Figure

9.11.

Due to the irreversibility of holographic RG flows, only the SU(3) × U(1) vacuum can serve as UV endpoint besides the SO(8) and G_2 vacua, if the U(1) × U(1) vacuum is the IR endpoint of the flow. However, we have not been successful in finding a flow from the SU(3) × U(1) vacuum in the UV to the U(1) × U(1) vacuum in the IR. We will report on these attempts and the insights gained from our numerical explorations in Section 9.2.5.

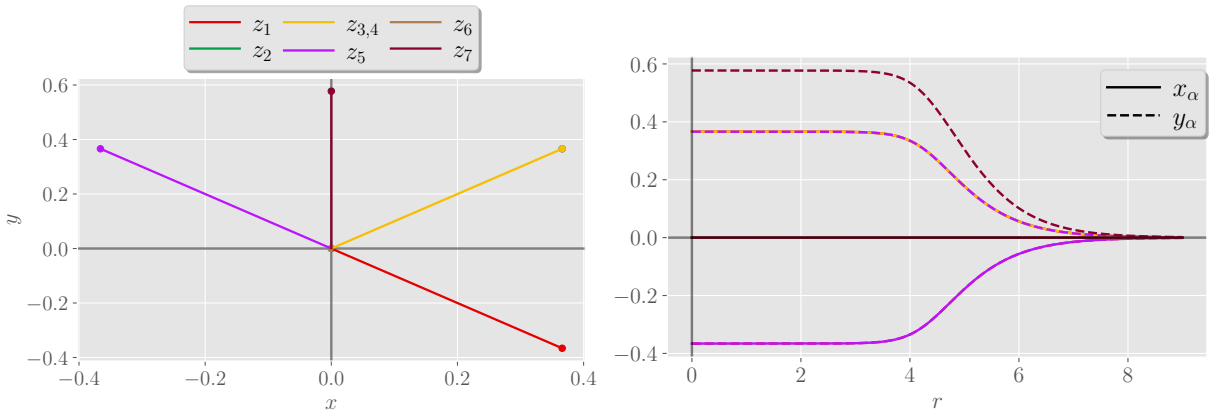

Figure 9.7: Flow from the SO(8) vacuum (origin) in the UV to the U(1) × U(1) vacuum (dots) in the IR, which was found in [93].

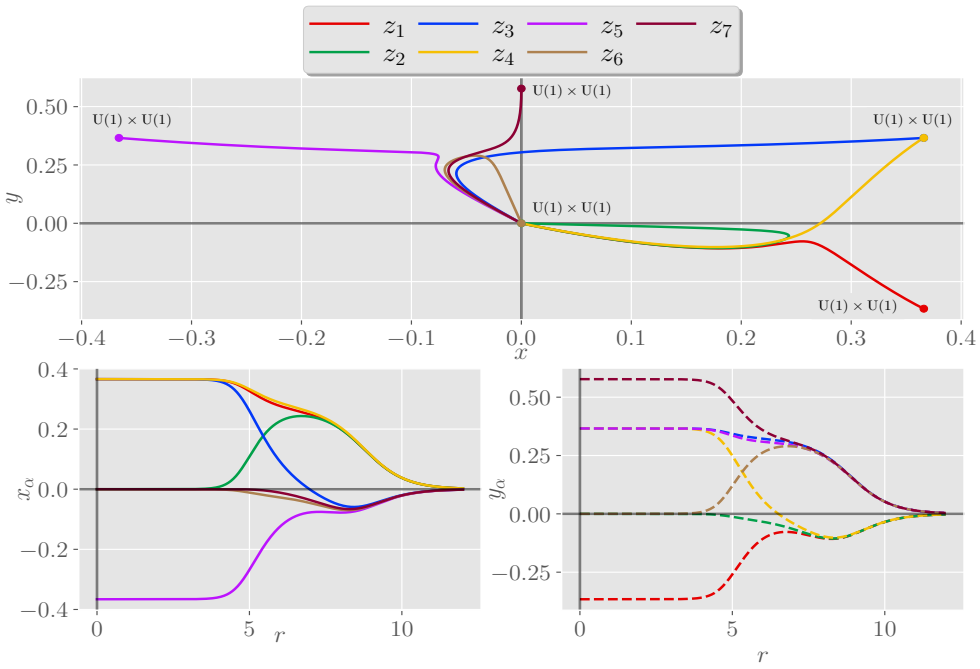

Figure 9.8: Flow from the SO(8) vacuum (origin) in the UV to the U(1) × U(1) vacuum (dots) in the IR, where the continuous symmetry is broken along the flow.

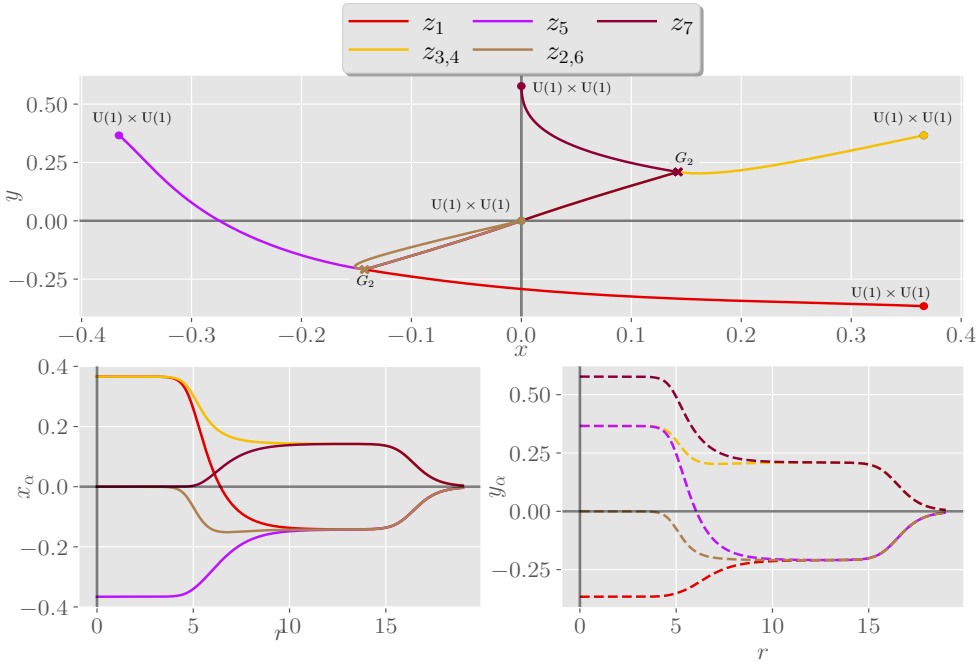

Figure 9.9: Flow from the SO(8) vacuum (origin) in the UV to the G_2 vacuum (crosses) and eventually reaching the $\mathrm{U}(1) \times \mathrm{U}(1)$ vacuum in the IR and preserving the $\mathrm{U}(1) \times \mathrm{U}(1)$ symmetry.

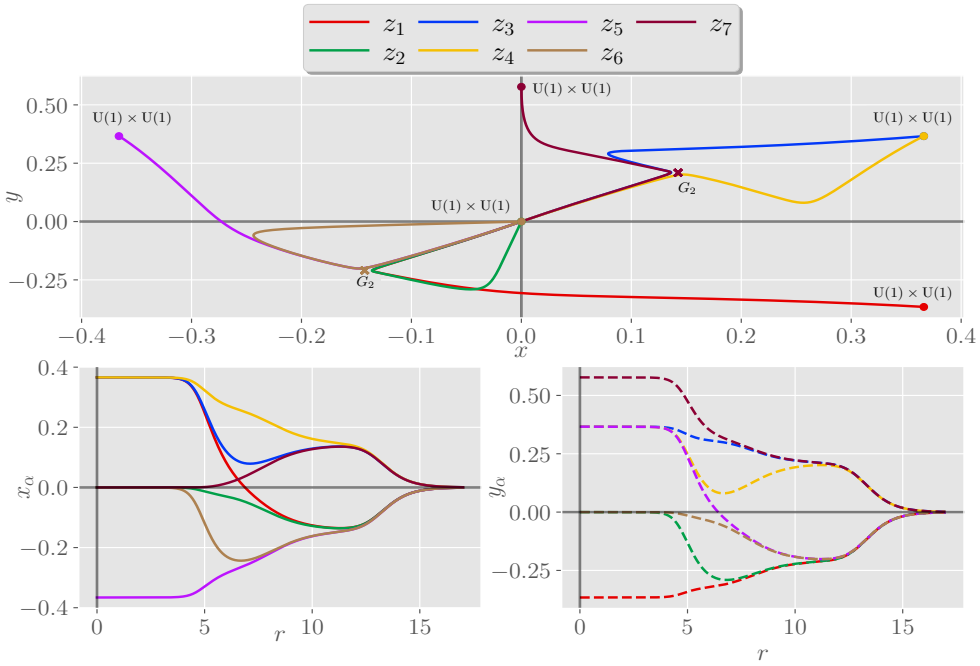

Figure 9.10: Triangular flow from the SO(8) vacuum (origin) in the UV to the G_2 vacuum (crosses) and to the $\mathrm{U}(1) \times \mathrm{U}(1)$ vacuum (dots) in the deep IR.

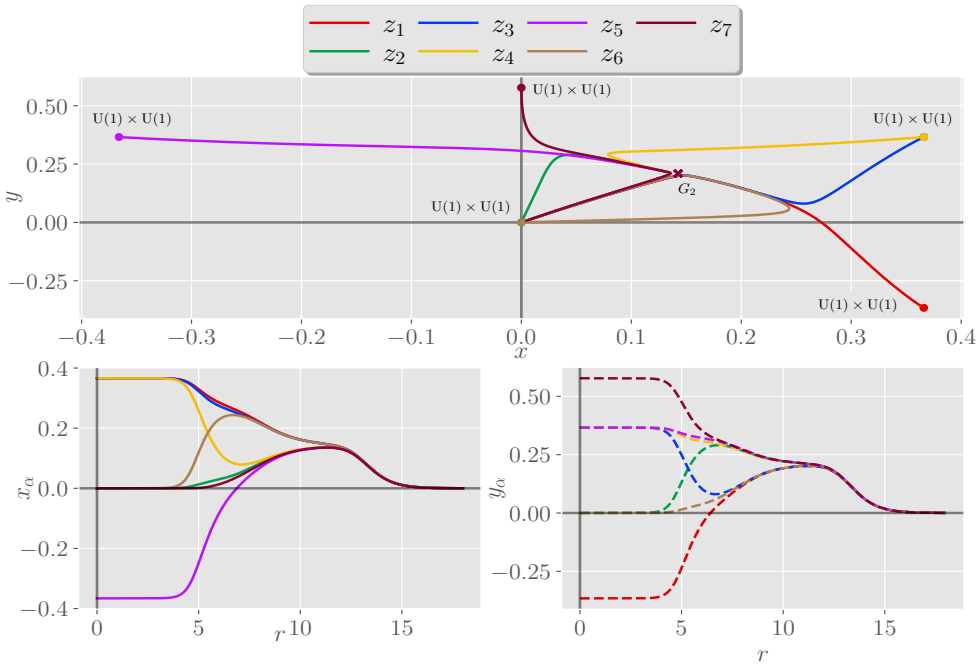

Figure 9.11: An inequivalent triangular flow from the SO(8) vacuum (origin) in the UV to the G_2 vacuum (cross) and to the U(1) × U(1) vacuum (dots) in the deep IR.

9.2.4 New flows to the SO(3) vacuum

The supersymmetric vacuum which lies 'deepest' in the potential landscape (and hence in RG scale) is the vacuum preserving a SO(3) symmetry group. We reconstructed the previously found flow [78] from the SO(8) vacuum in the UV to the SO(3) vacuum in the IR, which is shown in Figure 9.12. As before, the linearized BPS equations within the $\mathbb{Z}_2^3$-truncation allow us to break the continuous symmetry along the flow. We were able to find such a flow, and this new result is shown in Figure 9.13.

We were also able to construct flows from the G_2 vacuum in the UV to the SO(3) vacuum in the IR. In [78], the authors constructed triangular RG flows which start from the SO(8) critical point in the UV, approach the G_2, and eventually reach the SO(3) vacuum in the IR. We verified that a similar RG flow can be constructed within the larger $\mathbb{Z}_2^3$-truncation considered here. The result is shown in Figure 9.14. However, in the truncation discussed in this reference, there are only two irrelevant operators which can be turned on in the IR. The two additional irrelevant modes which appear in our larger truncation both break the symmetry of the SO(3) critical point along the flow (see Section A.1.2). The two coefficients of these modes therefore parametrize a family of triangular flows which are connected to the flow of Figure 9.14. One example of a flow coming from this family, with 'maximal' symmetry breaking (*i.e.*, both additional irrelevant modes are switched on) is given in Figure 9.15.

We have attempted to construct flows that start from either the SU(3) × U(1) vacuum or the U(1) × U(1) vacuum in the UV and reach the SO(3) vacuum in the IR but we did not find any results regarding these flows. The insights gained from our explorations are discussed in the next section.

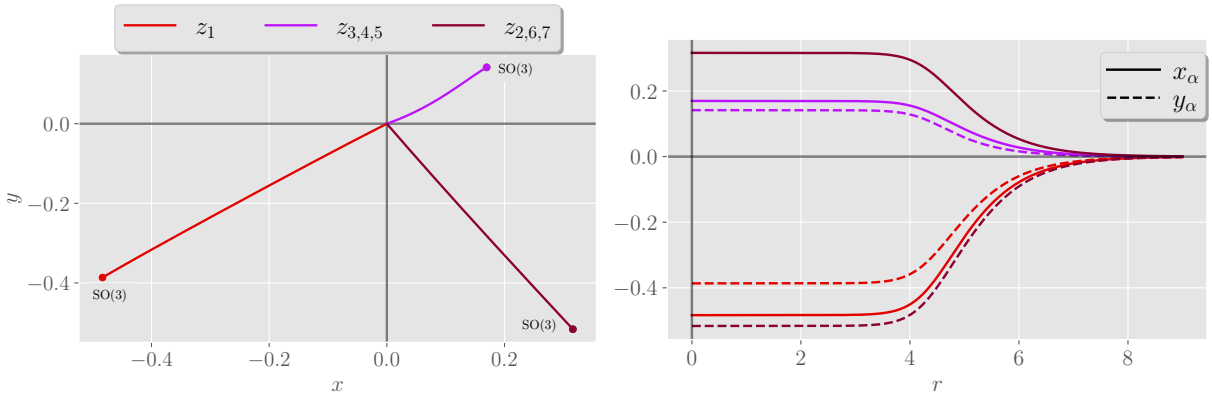

Figure 9.12: Flow from the SO(8) vacuum (origin) in the UV to the SO(3) vacuum (dots) in the IR which preserves the SO(3) symmetry.

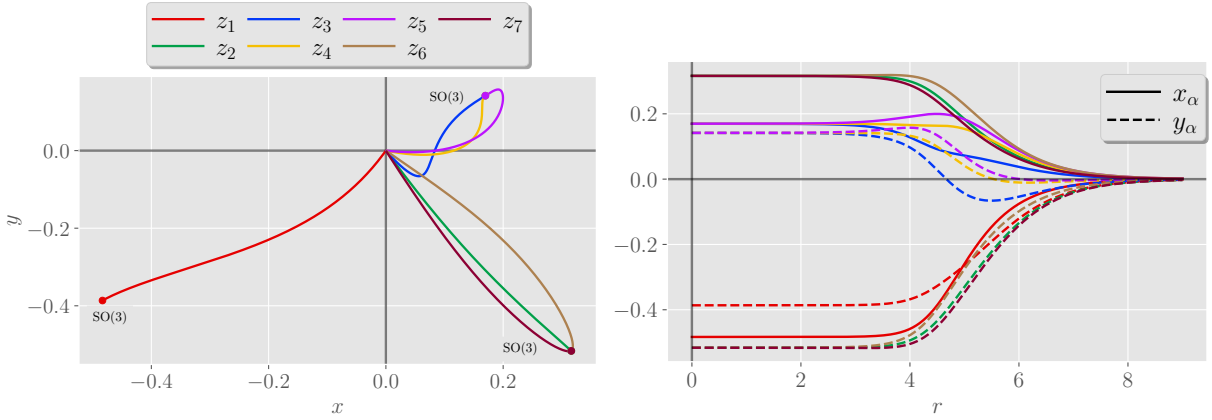

Figure 9.13: Flow from the SO(8) vacuum (origin) in the UV to the SO(3) vacuum (dots) in the IR, where the continuous symmetry is broken along the flow.

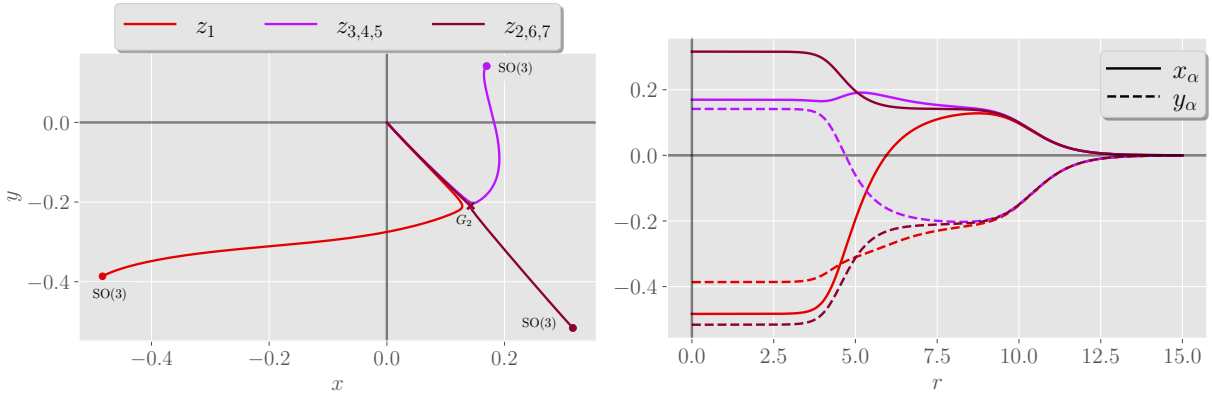

Figure 9.14: Flow from the SO(8) vacuum (origin) in the UV to the G_2 vacuum (cross) and eventually reaching the SU(3) × U(1) vacuum (dots) in the IR which preserves the SO(3) symmetry.

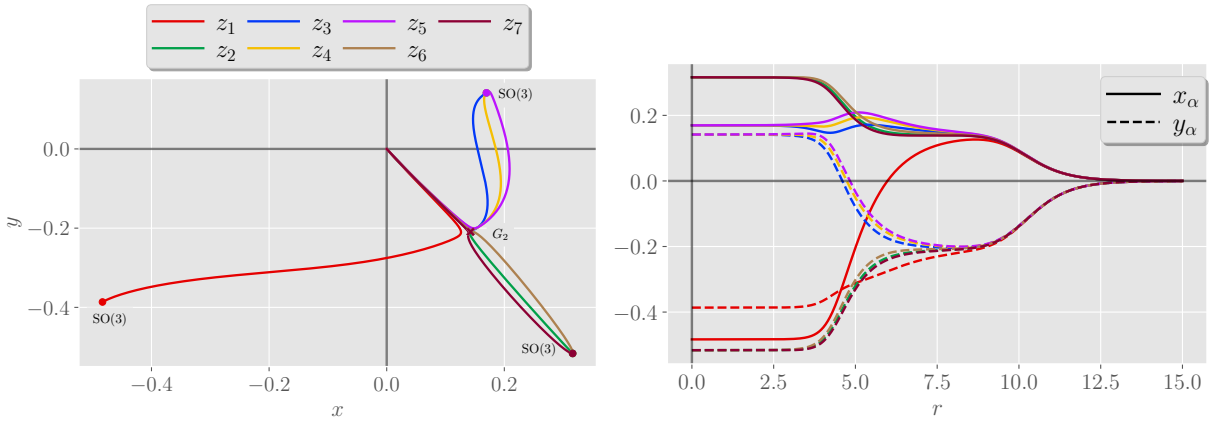

Figure 9.15: Flow from the SO(8) vacuum (origin) in the UV to the G_2 vacuum (cross) and eventually reaching the SU(3) × U(1) vacuum (dots) in the IR, where the continuous symmetry group is maximally broken.

9.2.5 On conjectured flows and the plethora of vacua

In the previous sections, we showed various new flows between some of the vacua of this SO(8) gauged supergravity theory. However, we were unsuccessful in constructing new flows interpolating between some of the vacua which lie 'deeper' in RG scale (more negative potential value), as already mentioned a few times. A priori, there is no argument that forbids the existence of these flows, and therefore, it is worth sharing our insights on this issue gained from our numerical explorations.

An example of a flow which, at first sight, seems likely to connect the SU(3) × U(1) vacuum in the UV to the U(1) × U(1) vacuum in the IR is given in Figure 9.16. Unleashing our algorithm to this situation and optimizing the algorithm parameters (*i.e.*, the step sizes s and Δr) yielded the flow in this figure as 'best' attempt (*i.e.*, minimal loss function). The flow diverges away from the target vacuum as soon as we continue the fine-tuning using our algorithm and go to larger values of r. The same conclusion holds for the flow from the SU(3) × U(1) in the UV to the SO(3) vacuum in the IR, which was not found in [78] and was conjectured by the authors to exist within the $\mathbb{Z}_2^3$-truncation in this reference. While we are unable to conclude that such flows do not exist, our numerical explorations at least demonstrate that finding these flows is much harder compared to finding flows which originate from the SO(8), G_2 or SU(3) × U(1) vacua in the UV.

To fully appreciate why constructing flows between vacua at a deeper RG scale is much harder to achieve, we emphasize once again that all critical points come in different 'copies'. That is, the location of each critical point as given in Appendix A.1.1 is certainly not unique, except for the SO(8) vacuum at the origin. Other locations can be related to the location given in the appendix by acting with a symmetry group on the vector of complex scalars $(z_1, \ldots, z_7)$, and therefore, we speak of the *orbit* of the critical point. These copies are leftovers from the symmetry breaking, as indeed the scalar potential has (loosely speaking) a similar shape as the Mexican hat potential. However, instead of a continuous orbit, the vacua have a discrete orbit, since we are only considering a subspace of the scalar manifold. This situation is visualized in Figure 9.17.

While rigorously determining this residual symmetry group goes beyond the scope of this thesis, we have performed a rough, preliminary scan for these different copies starting

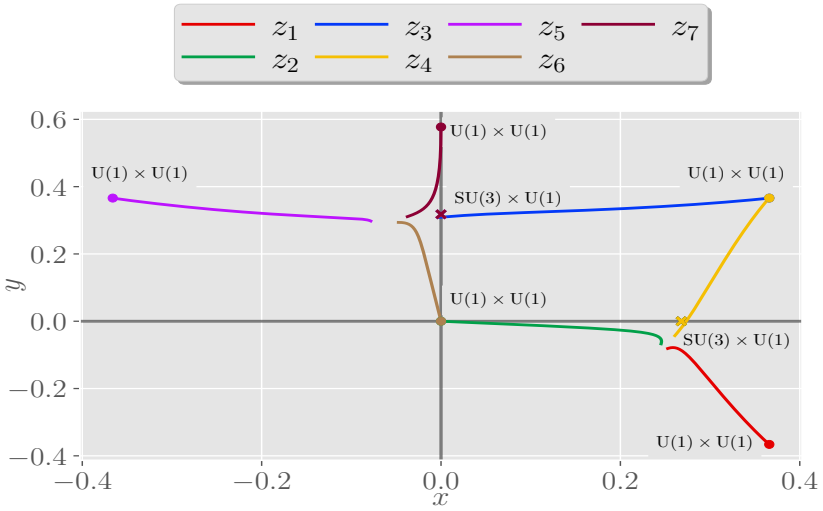

Figure 9.16: An attempt to construct a flow from the SU(3) × U(1) vacuum in the UV to the U(1) × U(1) vacuum in the IR.

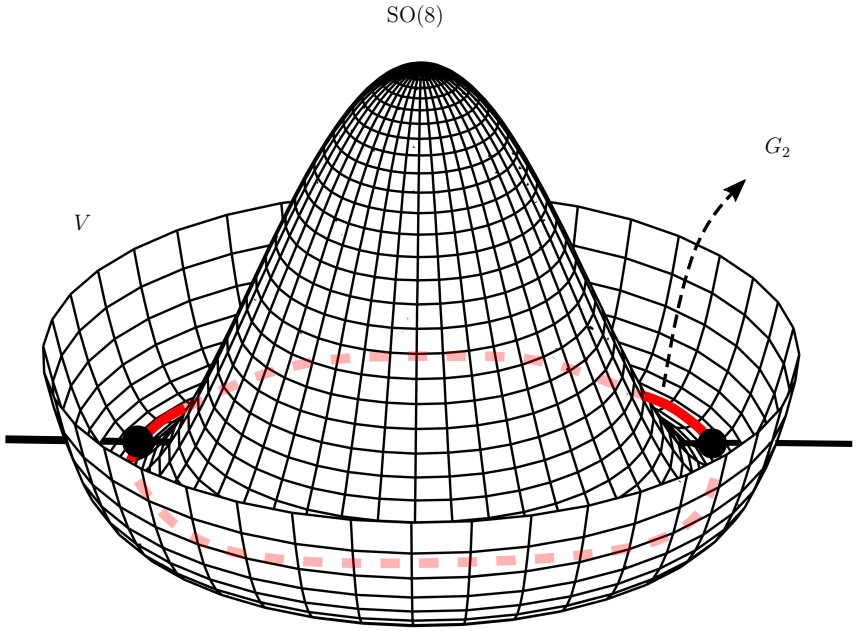

Figure 9.17: Visualization of the scalar potential V and the SO(8) and G_2 vacua. Since the G_2 breaks the continuous symmetry, it has a continuous orbit (red) within the 70-dimensional scalar manifold. However, since we only consider a 14-dimensional subspace of the scalar manifold (black line), only a few points of this orbit are vacua within our truncation (black dots). Figure adapted from [94].

from the location given in the appendix to quantify our statements. We looked for a symmetry group of discrete transformations that map each susy vacuum to another susy vacuum with the same value of the scalar potential. Since susy vacua solve $\mathcal{D}_\alpha W = 0$, we used the symmetries of the superpotential from equation (9.10) as our guide to find these discrete symmetries. We looked into permutations of the scalars, sign flips $z_\alpha \to -z_\alpha$ and taking the complex conjugate. It turns out that 168 permutations leave the superpotential invariant, and one can show that this subgroup is isomorphic to PSL(3, 2). Indeed, in [78], the authors remark that the 7 complex scalars of the $\mathbb{Z}_2^3$-truncation can be identified with the points on the Fano plane, which has PSL(3, 2) as symmetry group. Out of all $2^7 = 128$ possible sign combinations for the 7 scalars, we find that the superpotential is left invariant only if $(z_1, \ldots, z_7)$ is replaced by

$$
\begin{aligned}
&(-z_1, -z_2, -z_3, \quad z_4, \quad z_5, \quad z_6, -z_7)\\
&(-z_1, -z_2, \quad z_3, \quad z_4, -z_5, -z_6, \quad z_7)\\
&(-z_1, \quad z_2, -z_3, -z_4, -z_5, \quad z_6, \quad z_7)\\
&(-z_1, \quad z_2, \quad z_3, -z_4, \quad z_5, -z_6, -z_7)\\
&(\quad z_1, -z_2, -z_3, -z_4, \quad z_5, -z_6, \quad z_7)\\
&(\quad z_1, -z_2, \quad z_3, -z_4, -z_5, \quad z_6, -z_7)\\
&(\quad z_1, \quad z_2, -z_3, \quad z_4, -z_5, -z_6, -z_7)
\end{aligned}
$$

Therefore, starting from each susy critical point as given in Appendix A.1.1, we obtain all copies of that critical point and its complex conjugate obtained from these permutations, sign flips, and their combined transformations. We then check which copies solve the equation $\mathcal{D}_\alpha W = 0$ and count the number of different copies that are obtained in this way. These numbers are reported in Table 9.3. Note that these estimates provide only a lower bound on the number of distinct copies, as it is possible that other copies exist which are not within the orbit we have established above (the only exception being, of course, the unique SO(8) vacuum).

With these lower bounds, it is now clear that finding flows between vacua at deeper scalar potential values is a gargantuan task. For example, to find the flow conjectured in [78], going from SU(3) × U(1) to SO(3), one has to consider more than 25 000 pairs of copies of these vacua. For a flow from U(1) × U(1) to SO(3), this becomes more than 300 000 pairs. Keeping in mind that these flows have to be constructed numerically by a careful fine-tuning of parameters, we can only appreciate the complexity of this task.

Point	**Lower bound**
P0600000	1
P0719157	16
P0779422	56
P1200000	672
P1384096	448

Table 9.3: Lower bounds on number of distinct copies of each of the critical points.

9.3 ISO(7) gauged supergravity

The second four-dimensional gauged supergravity of interest has an isometry group of a 7-dimensional Euclidean space $\mathrm{ISO}(7) \equiv \mathrm{SO}(7) \ltimes \mathbb{R}^7$ as gauge group [95–97]. This theory has an additional parameter c, since the 7 translations (*i.e.*, $\mathbb{R}^7$ in the above semi-direct product) are said to be dyonically gauged. In a purely electric gauging, like the SO(8) gauging from the previous section, we only consider the 28 'electric' vector fields that enter the Lagrangian of the $\mathcal{N} = 8, d = 4$ theory. However, one can also consider their dual vector fields, which are called 'magnetic'. By introducing these new vector fields, covariant derivatives acquire a new term proportional to the magnetic vector field, with proportionally constant c. This constant c determines the ratio between the (electric) gauge coupling g and the magnetic gauge coupling m, *i.e.* $c = m/g$. While this seems suggestive that there exists an entire family of gaugings parametrized by c, it turns out that there are only two inequivalent members corresponding to $c = 0$ and $c \neq 0$ [98]. The coupling of scalars to the magnetic vectors introduces additional terms in the scalar potential. Since the dyonically gauged case (*i.e.*, $c \neq 0$) has therefore a rich structure of AdS vacua, it provides the ideal arena for the study of holographic RG flows. We will hence restrict our attention to dyonically gauged ISO(7) supergravity and, without loss of generality, we put $c = 1$.

Let us briefly remark here that it is possible to dyonically gauge the SO(8) supergravity theory from the previous section. These deformed theories are often called ω-deformed SO(8) supergravity in the literature, as there exists a continuous family of distinct gaugings parametrized by ω [99–101]. However, it has not been possible so far to identify a higher-dimensional origin of the parameter ω. In fact, there exist no-go theorems which state that it is impossible to obtain these theories from ten or eleven dimensions [102], which is why we restricted our attention to the electric gauging (*i.e.*, $\omega = 0$) of SO(8) supergravity theory.

Unlike the SO(8) case, it is known how to obtain the dyonic ISO(7) gauged supergravity theory from higher dimensions. This theory arises from dimensional reduction of type IIA supergravity on a S^6 internal manifold [103, 104]. Therefore, the AdS vacua of the $4d$ theory uplift to $\mathrm{AdS}_4 \times S^6$ backgrounds. Massive type IIA supergravity on these backgrounds is dual to superconformal Chern-Simons theories with gauge group $\mathrm{SU}(N)$, and low Chern-Simons level k, which is identified with the magnetic coupling m in the supergravity theory.

For our discussion, we will adopt the conventions of [105]. The Kähler potential is

$$\mathcal{K} = -\sum_{\alpha=1}^{7} \log(2\,\mathrm{Im}(z_\alpha))\,, \tag{9.14}$$

such that we will be working in 7 copies of the upper half-plane. The superpotential is[3]

$$W = 2m + 2g(z_1 z_2 z_3 + z_1 z_6 z_7 + z_2 z_7 z_5 + z_3 z_5 z_6 + (z_1 z_5 + z_2 z_6 + z_3 z_7) z_4)\,, \tag{9.15}$$

and the scalar potential is given by

$$V = 4e^{\mathcal{K}} \left(\mathcal{K}^{\alpha\overline{\beta}} \mathcal{D}_\alpha W \overline{\mathcal{D}}_{\overline{\beta}} \overline{W} - 3 W \overline{W} \right)\,. \tag{9.16}$$

[3]This superpotential coincides with the one obtained from Section 6.3.5 using Table 6.2 and equations (6.49), (6.50) up to a permutation of the complex scalars. However, we stick to the conventions of the mentioned reference to facilitate the comparison between our work and the reference.

9.3.1 Supersymmetric vacua

A list of the supersymmetric vacua is provided in Table 9.4, with coordinates given in Section A.2.1. We remark that an additional supersymmetric vacuum was found within a $\mathbb{Z}_2^2$-invariant truncation, which keeps 22 real scalar fields rather than 14, in [38]. During our work, we discovered that the precision of the numerical values given for the `P2569710` and `P3561023` points in [105] is quite poor. Since it is desirable to minimize numerical errors in our computations as much as possible, we computed the location of the critical point independently. The values are reported in the appendix with an improved accuracy compared to [105]. The values of δ_a are provided in Table 9.5 below. As we are working within the larger $\mathbb{Z}_2^3$-truncation compared to [105], these values provide a direct extension of their work.

We will now discuss some of the holographic RG flows constructed in this theory. An overview of the known flows is given in Figure 9.18. For previously found flows reported in the literature, it is not possible to break the continuous symmetry group along the flow similar to the flows of the previous section. This is shown by the linearized BPS equations, given in Section A.2.1. As such, we do not discuss these flows in this thesis.

Point	$\mathcal{N}$	**Cont. symmetry**	V	**Refs.**
`P1998705`	$\mathcal{N}=1$	G_2	-19.98705	[106–108]
`P2078460`	$\mathcal{N}=2$	$\mathrm{SU}(3)\times\mathrm{U}(1)$	-20.78460	[109]
`P2327730`	$\mathcal{N}=3$	$\mathrm{SO}(4)$	-23.27730	[89]
`P2379560`	$\mathcal{N}=1$	$\mathrm{SU}(3)$	-23.79560	[96]
`P2569710`	$\mathcal{N}=1$	$\mathrm{U}(1)$	-25.69710	[105]
`P3561023`	$\mathcal{N}=1$	$\mathrm{U}(1)$	-35.61023	[105]

Table 9.4: Supersymmetric vacua in the ISO(7) gauged supergravity. Potential values are at $g, m, c = 1$.

Point	$\boldsymbol{\delta_a}$	n
`P1998705`	$1-\sqrt{6}(\times1),\ 1-\frac{1}{\sqrt{6}}(\times6),\ 1+\frac{1}{\sqrt{6}}(\times6),\ 1+\sqrt{6}(\times1)$	–
`P2078460`	$\frac{1-\sqrt{17}}{2}(\times1),\ \frac{3-\sqrt{17}}{2}(\times1),\ \frac{2}{3}(\times3),\ 1(\times4),\ \frac{4}{3}(\times3),\ \frac{1+\sqrt{17}}{2}(\times1),\ \frac{3+\sqrt{17}}{2}(\times1)$	2
`P2327730`	$-\sqrt{3}(\times1),\ 1-\sqrt{3}(\times2),\ 2-\sqrt{3}(\times1),\ 1(\times6),\ \sqrt{3}(\times1),\ 1+\sqrt{3}(\times2),\ 2+\sqrt{3}(\times1)$	3
`P2379560`	$1-\sqrt{6}(\times2),\ 0(\times2),\ \frac{1}{3}(\times3),\ \frac{5}{3}(\times3),\ 2(\times2),\ 1+\sqrt{6}(\times2)$	2
`P2569710`	-1.7271365, -1.7169275, -1.0440791, -0.2418020, 0.7083131, 0.8775354, 0.8888917, 1.1111082, 1.1224645, 1.2916868, 2.2418021, 3.0440791, 3.7169276, 3.7271365	4
`P3561023`	-2.1201597, -1.9726403, -1.6337960, -1.0225228, -1.0050748, 0.4696956, 0.6036253, 1.3963756, 1.5303052, 3.0050758, 3.0225238, 3.6337969, 3.9726413, 4.1201607	5

Table 9.5: Values of δ_a for the susy vacua in ISO(7) gauged supergravity, with multiplicity given in brackets. For `P2569710` and `P3561023`, all δ_a have multiplicity one. The integer n denotes the number of parameters of the loss function.

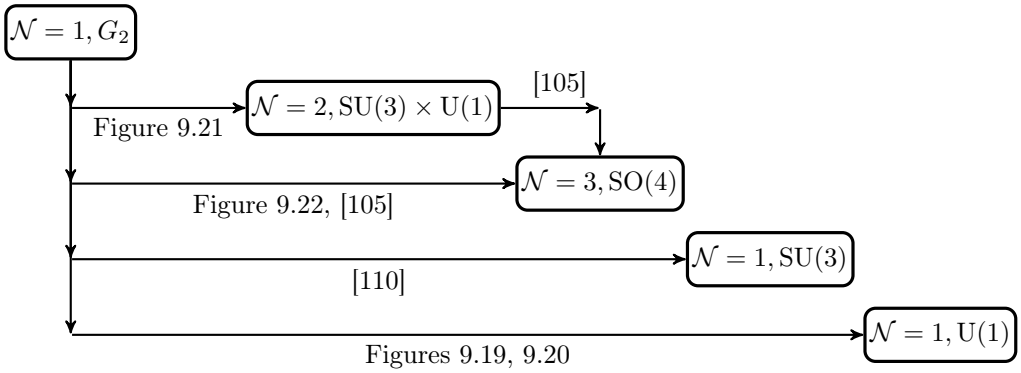

Figure 9.18: Overview of known holographic RG flows in the ISO(7) theory.

9.3.2 New flows to the `P2569710` vacuum

Previous studies on holographic RG flows in this theory involved truncations with continuous symmetry groups, most notably SU(3) [110] and SO(3) [105]. Therefore, these truncations do not contain the U(1) invariant `P2569710` and `P3561023` vacua. Hence there have been, as far as we know, no studies about holographic RG flows which reach these vacua. Our main goal in this theory was to fill this gap, since our $\mathbb{Z}_2^3$-truncation does contain these vacua. We have successfully constructed new holographic RG flows ending at the `P2569710` vacuum in the IR. We constructed a flow that originates from the G_2 vacuum in the UV, and preserves a U(1) symmetry along the flow. The result is shown in Figure 9.19. In Section 9.2, we observed that solutions can break the continuous symmetry group along the flow in the $\mathbb{Z}_2^3$-truncation. It turns out that this is also possible for the flow ending at the `P2569710` vacuum. In Figure 9.20, we present such a flow where the continuous U(1) symmetry is broken along the flow, before it gets restored as we approach the U(1) vacuum in the IR.

We would like to briefly compare these flows to previously known flows that also originate from the G_2 vacuum in the UV and which we reconstructed in the larger $\mathbb{Z}_2^3$-truncation. We show a flow from the G_2 vacuum that reaches the $\mathrm{SU}(3) \times \mathrm{U}(1)$ vacuum in the IR in Figure 9.21, and a flow which reaches the SO(4) vacuum in the IR in Figure 9.22. Note that for these solutions, the initial 'velocity' of the flow (which, numerically, starts from the IR) is pointing towards the target vacuum (in the UV). This is not the case for the flow of Figure 9.19: the complexity of this flow requires some scalars (such as z_3 and z_7) to perform an excursion through the scalar manifold before eventually approaching the UV vacuum. Such flows are difficult to construct with our algorithm, as it uses the distance between the endpoint of the flow and the desired UV target as loss function to minimize. This is presumably the reason why we were not able to find a flow that ends in the deeper U(1) vacuum, `P3561023`.

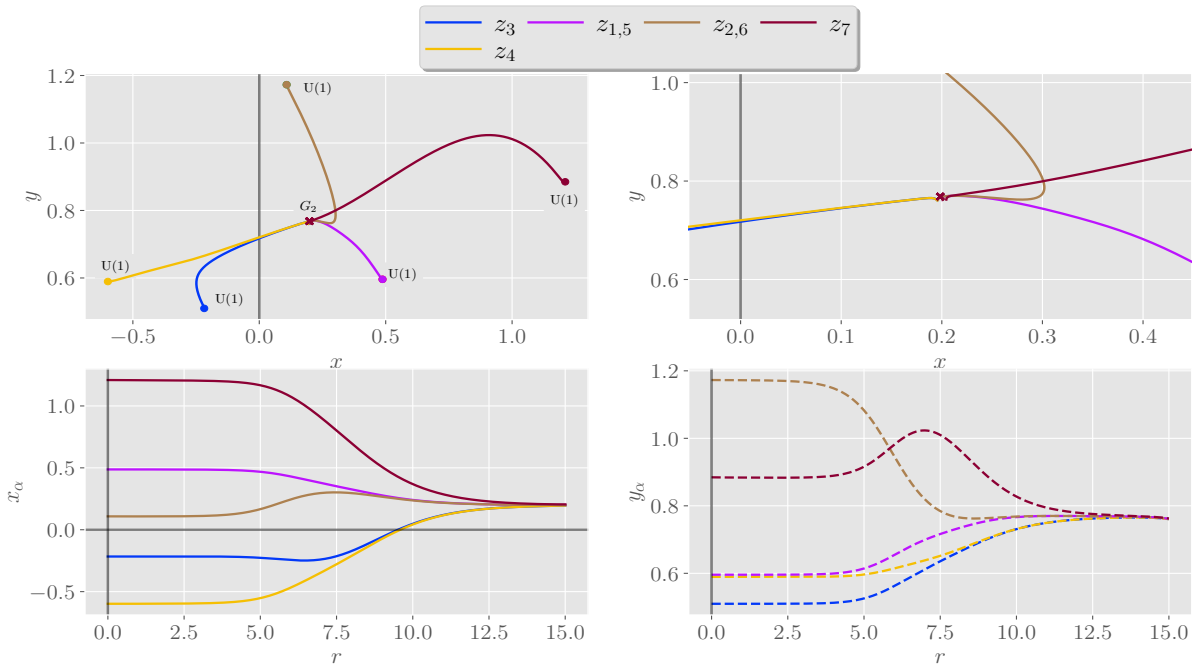

Figure 9.19: Flow from the G_2 vacuum (cross) in the UV to the U(1) vacuum `P2569710` (dots) in the IR. The flow itself preserves U(1) symmetry.

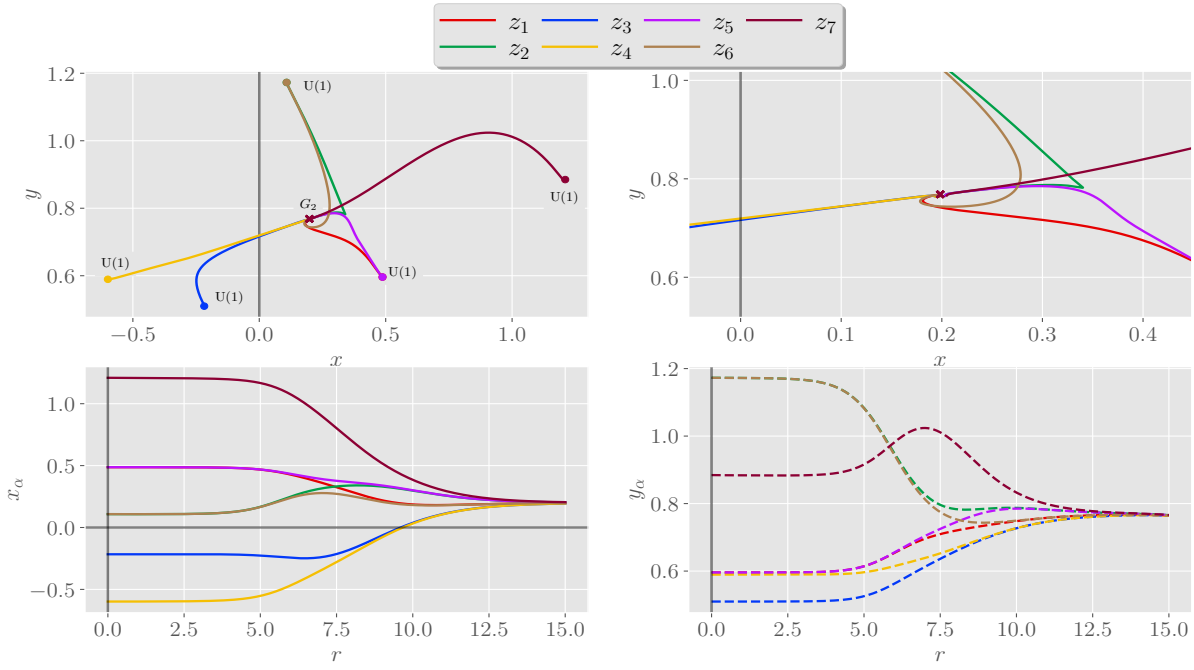

Figure 9.20: Flow from the G_2 vacuum (cross) in the UV to the U(1) vacuum `P2569710` (dots) in the IR. The flow itself breaks the U(1) symmetry.

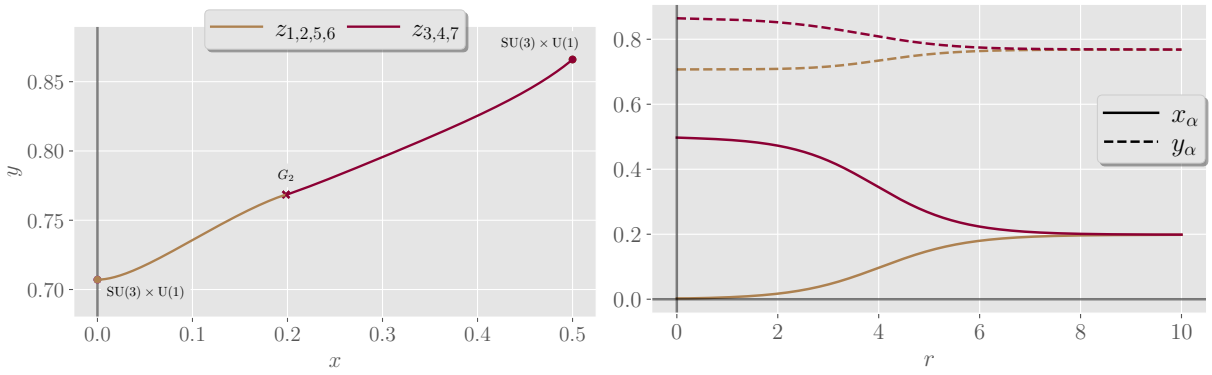

Figure 9.21: Flow from the G_2 vacuum (cross) in the UV and reaching the $\mathrm{SU}(3)\times\mathrm{U}(1)$ vacuum (dots) in the IR.

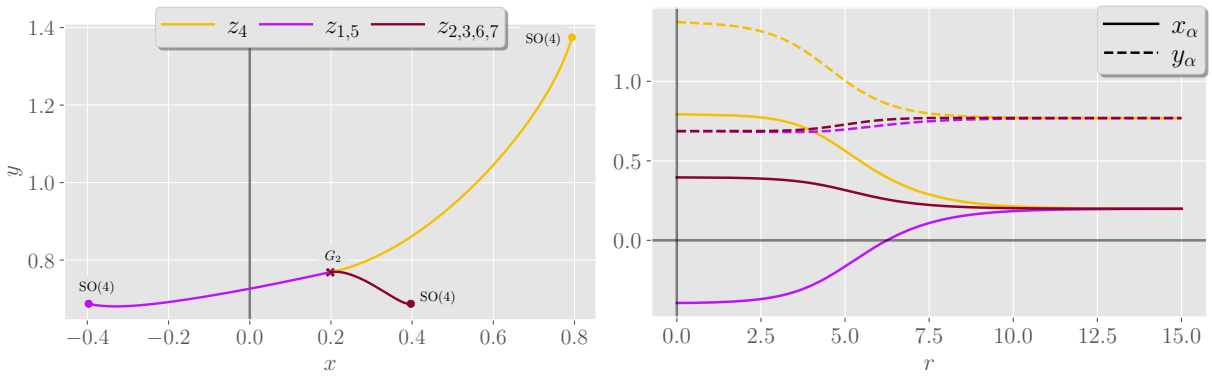

Figure 9.22: Flow from the G_2 vacuum (cross) in the UV and reaching the SO(4) vacuum (dots) in the IR.

9.3.3 Plethora of vacua

Given our discussion of Section 9.2.5, one may wonder whether the vacua of this gauged supergravity similarly have several 'copies' due to symmetries. This is indeed the case, and therefore, we performed the analysis explained in Section 9.2.5 within this theory. It turns out that the subgroup of permutations that leave the superpotential invariant is again the unique (up to isomorphism) group PSL(3, 2) and there are 7 sign flips giving copies of the vacua, which in the current parametrization are

$$\begin{aligned}
&(-z_1, -z_2, -z_3, \quad z_4, \quad z_5, \quad z_6, -z_7)\\
&(-z_1, -z_2, \quad z_3, \quad z_4, -z_5, -z_6, \quad z_7)\\
&(-z_1, \quad z_2, -z_3, -z_4, -z_5, \quad z_6, \quad z_7)\\
&(-z_1, \quad z_2, \quad z_3, -z_4, \quad z_5, -z_6, -z_7)\\
&(\quad z_1, -z_2, -z_3, -z_4, \quad z_5, -z_6, \quad z_7)\\
&(\quad z_1, -z_2, \quad z_3, -z_4, -z_5, \quad z_6, -z_7)\\
&(\quad z_1, \quad z_2, -z_3, \quad z_4, -z_5, -z_6, -z_7)\,,
\end{aligned}$$

such that the same symmetry group leaves the superpotential invariant. We have determined how many distinct copies can be found by applying this symmetry group. The lower bounds on these numbers are given in Table 9.6. As in the SO(8) theory, there are many pairs of vacua that can serve as endpoints of RG flows for vacua lying deeper in RG scale, complicating the construction of solutions.

Point	**Lower bound**
P1998705	8
P2078460	56
P2327730	168
P2379560	56
P2569710	1344
P3561023	1344

Table 9.6: Lower bounds on number of distinct copies of each of the critical points in the ISO(7) theory.

9.4 $[\mathbf{SO}(6) \times \mathbf{SO}(1,1)] \ltimes \mathbb{R}^{12}$ gauged supergravity

The final two gauged supergravities can be discussed in parallel to some extent as they are, loosely speaking, related to each other by a sign flip. Indeed, the only difference between the two gauge groups is one compact or non-compact generator (giving SO(2) or SO(1, 1), respectively). Additionally, the two superpotentials, following the parametrization given in equations (6.49) and (6.50), are the same up to a sign flip in the $\tilde{b}$-term. While this implies that the vacua structures are different, both theories share some general properties. For example, the gauging is of dyonic type, like the ISO(7) gauged supergravity of the previous section. The $4d$ gauged supergravity is obtained from dimensional reduction of type IIB supergravity on a $S^1 \times \tilde{S}^5$ internal manifold, where $\tilde{S}^5$ is known as a squashed five-sphere [111, 112]. The $4d$ vacua uplift to $10d$ so-called S-fold background solutions

of type IIB supergravity [113]. Loosely speaking, they can be constructed from quotients of degenerate solutions (Janus solutions), where the string coupling diverges at infinity [114]. The AdS_4 vacua are dual to CFTs which are constructed from field theories that are localized on the interface between two $\mathcal{N} = 4$ SYM theories (see Section 6.2.1) [115]. That is, on the two sides of the interface, we have $\mathcal{N} = 4$ SYM theories, but the gauge coupling has different values on both sides [116]. From such theories, we can build new $\mathcal{N} = 4$ SCFTs by introducing Chern-Simons interactions, which are known as J-fold constructions [117]. These theories are dual to the AdS_4 vacua that we find.

The dyonic ISO(7), $[\mathrm{SO}(6)\times\mathrm{SO}(1,1)]\ltimes\mathbb{R}^{12}$ and $[\mathrm{SO}(6)\times\mathrm{SO}(2)]\ltimes\mathbb{R}^{12}$ gaugings are particular examples of $\mathrm{CSO}(p,q,r)$ gaugings, which have an 'electric' subalgebra $\mathfrak{cso}(p,q,r)$ and a 'magnetic' subalgebra $\mathfrak{cso}(p',q',r')$ [118]. The gauge group is then of the form

$$[\mathrm{SO}(p,q)\times\mathrm{SO}(p',q')]\ltimes N\,, \tag{9.17}$$

with N nilpotent. For $p+q=7$, we find the $\mathrm{ISO}(p,q)$ gaugings, of which the ISO(7) model with $p=7, q=0$ and $p'=q'=0$ is an example. The two remaining supergravity theories correspond to the above ansatz, with $p=6, q=0$ and $p'=q'=1$ or $p'=2, q'=0$. These models can be embedded into type IIA (type IIB) supergravity if $p+q$ is odd (even), which is consistent with earlier remarks.

To discuss the $4d$ supergravity theory, we follow the conventions of [111, 112], which coincide with the conventions used in Section 6.3.5. Hence, the superpotential is obtained from equations (6.49) and (6.50) with the values from Table 6.2, from which the scalar potential can be computed using equation (6.44).

In both supergravity theories, rather than distinct points as in the previous sections, one finds that the AdS vacua actually constitute families of vacua. That is, they are parametrized by continuous parameters and lie on so-called flat directions of the scalar potential [111]. Therefore, contrary to the SO(8) and ISO(7) supergravities, the locations of the vacua now depend on continuous parameters. Note that this situation is different from the 'copies' of vacua we discussed before, as the mass spectra change when we move along these flat directions. Moreover, the residual symmetry of vacua becomes enhanced at certain, special points along these flat directions.

9.4.1 Supersymmetric vacua

A list of the supersymmetric vacua is provided in Table 9.7, with their locations given in Section A.3.1. In this section, we use `F` instead of `P` to emphasize that all vacua that we consider are part of a family of supersymmetric solutions. We refer to both `F0300000` families of vacua collectively as "the IR", and to the `F0289794` vacuum as "the UV". The endpoints of our flows will be denoted by their χ, φ or $\chi_{1,2,3}$ coordinates, respectively. Moreover, we refer to the UV as the UV plane, as this UV family of vacua is parametrized by two independent coordinates due to the constraint $\chi_1+\chi_2+\chi_3=0$. Note that this is unlike the situation in the IR, where χ and φ parametrize two lines instead of a plane.[4] For generic points in both the UV as well as the IR, there is a residual $\mathrm{U}(1)\times\mathrm{U}(1)$ global symmetry. This symmetry becomes enhanced at special points, as discussed in Section A.3.1. The values of δ_a at vacua relevant for the flow solutions are given in Table 9.8. We note that these values change as we change the parameters χ, φ and $\chi_{1,2,3}$.

[4]This statement is valid for the $\mathbb{Z}_2^3$-truncation of the thesis. In a larger truncation, such as the one considered in [111], all points in a (χ,φ)-plane correspond to AdS vacua.

Family	$\mathcal{N}$	**Cont. symmetry**	V	**Refs.**
F0289794($\chi_{1,2,3}$)	$\mathcal{N}=1$	$\mathrm{U}(1)^2, \mathrm{SU}(2)\times\mathrm{U}(1), \mathrm{SU}(3)$	-2.897944	[112]
F0300000(χ)	$\mathcal{N}=2$	$\mathrm{U}(1)^2, \mathrm{SU}(2)\times\mathrm{U}(1)$	-3	[112, 119, 120]
F0300000(φ)	$\mathcal{N}=2,4$	$\mathrm{U}(1)^2, \mathrm{SU}(2)\times\mathrm{U}(1), \mathrm{SO}(4)$	-3	[111]

Table 9.7: Supersymmetric vacua of the $[\mathrm{SO}(6)\times\mathrm{SO}(1,1)]\ltimes\mathbb{R}^{12}$ gauged supergravity. Potential values are at $g=c=1$. Symmetry enhancements occur at special values for the parameters $\chi, \chi_{1,2,3}$ and φ given in the appendix.

Family	δ_a	n
F0289794($\chi_{1,2,3}=0$)	$-1.44949\ (\times2), 0\ (\times2), 0.333333\ (\times3),$ $1.66667\ (\times3), 2\ (\times2), 3.44949\ (\times2)$	–
F0289794($\chi^\star_{1,2,3}$)	$-1.44949\ (\times2), 0\ (\times2), 0.327182\ (\times1), 0.33179\ (\times2),$ $1.66821\ (\times2), 1.67282\ (\times2), 2\ (\times2), 3.44949\ (\times2)$	–
F0300000($\chi=0$)	$-1.56155\ (\times2), -0.561553\ (\times2), 0\ (\times2), 1\ (\times2),$ $2\ (\times2), 2.56155\ (\times2), 3.56155\ (\times2)$	4
F0300000($\chi=0.01$)	$-1.56155\ (\times2), -0.561553\ (\times2), -0.0004\ (\times1), 0\ (\times1), 0.9996\ (\times1),$ $1.0004\ (\times1), 2\ (\times1), 2.0004\ (\times1), 2.56155\ (\times2), 3.56155\ (\times2)$	5

Table 9.8: Values of δ_a for the susy vacua, with multiplicity given in brackets. The integer n denotes the number of parameters of the loss function.

9.4.2 New holographic RG flows

Given the above set-up of families of vacua both in the UV and the IR, one can wonder whether holographic RG flows exist going from any point of the UV plane to any point in the IR. While a complete answer to this question is beyond the scope of the thesis, our goal is to provide a preliminary exploration on this matter.

In [112], the authors give one holographic RG flow which starts from the origin $\chi_{1,2,3}=0$ of the UV plane and ends at the origin $\chi=0$ in the IR. We reproduced this flow in Figure 9.23. We remark that the real scalar fields $x_{1,2,3}$ are not exactly at zero, but since these values are very small compared to the values at the critical points, we attribute this to numerical errors. This flow has a SU(3) symmetry in the UV and a $\mathrm{SU}(2)\times\mathrm{U}(1)$ symmetry in the IR. In our work, we were able to construct a new flow which originates from a different UV vacuum that has $\mathrm{SU}(2)\times\mathrm{U}(1)$ symmetry and ends at the same IR vacuum, such that the $\mathrm{SU}(2)\times\mathrm{U}(1)$ symmetry is preserved along the flow and in the endpoint. The result is shown in Figure 9.24. The UV vacuum is located at

$$\chi^\star_{1,3}\approx 0.02029767\,,\quad \chi^\star_2\approx -0.0405452\,. \tag{9.18}$$

Besides, we found a new flow which ended at a different vacuum in the IR. This new flow is given in Figure 9.25 and ends at $\chi=0.01$. To construct this flow, we changed our loss function to use a Euclidean distance for the 14 scalar fields excluding $x_{1,2,3}$, summed together with $|x_1+x_2+x_3|$, to adapt the algorithm to the current situation. We remark that at $\chi=0.01$, the loss function gets an additional parameter which likely allows flows to break the continuous symmetry: see Section A.4.2. We have, however, not explicitly computed such a flow solution.

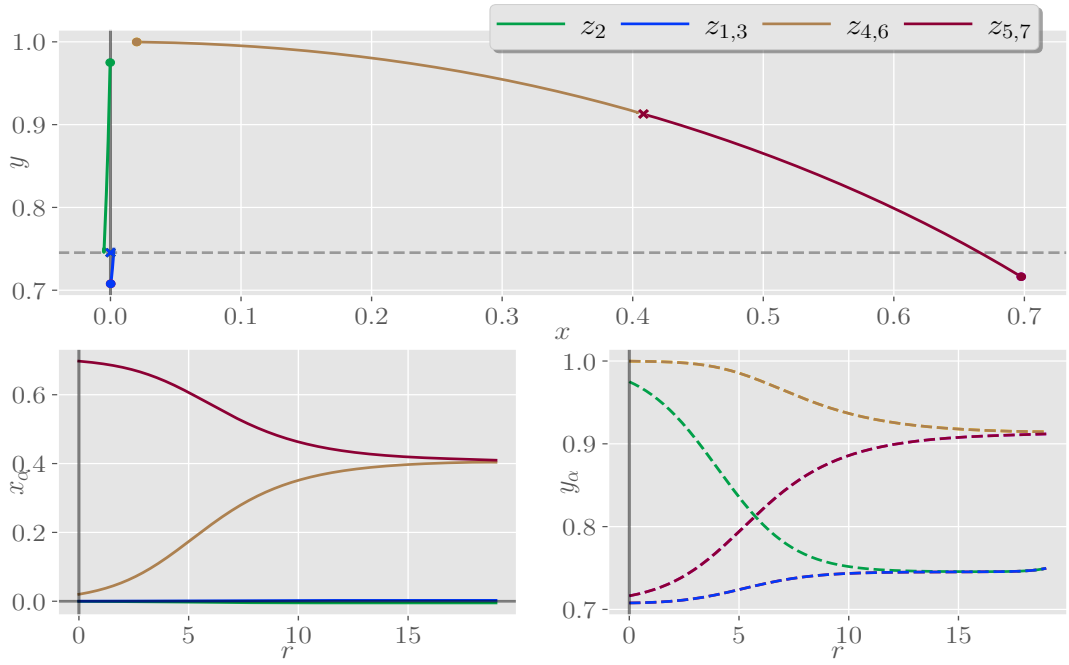

Figure 9.23: Flow from the $\chi_{1,2,3} = 0$ vacuum in the UV with SU(3) symmetry to the $\chi = 0$ vacuum with SU(2) × U(1) symmetry in the IR.

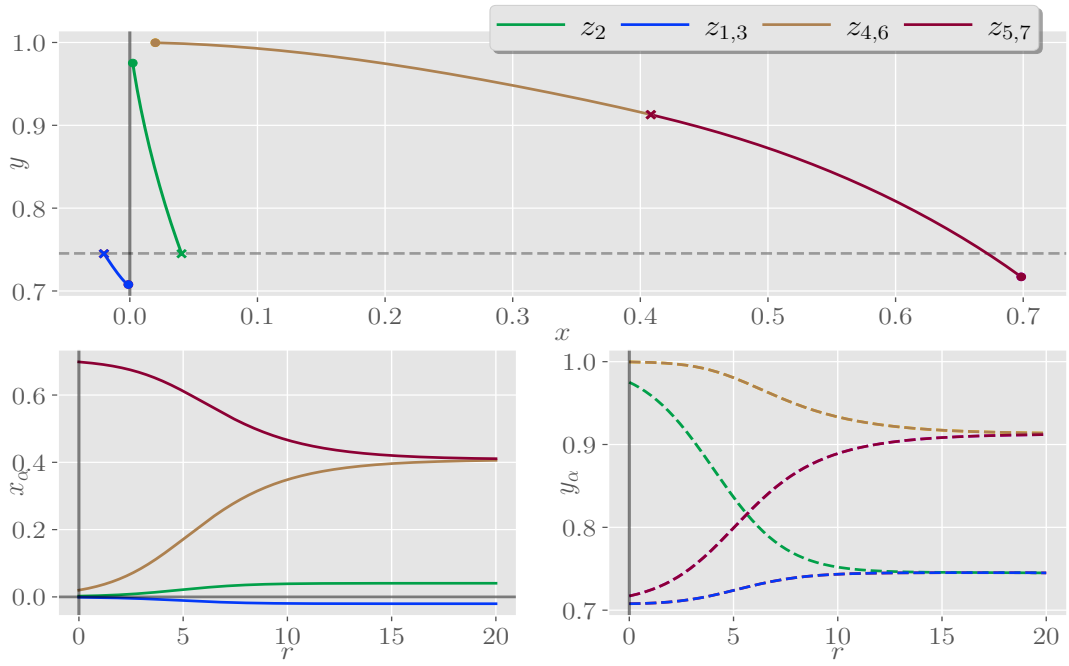

Figure 9.24: Flow from the $\chi^\star_{1,2,3}$ vacuum with SU(2) × U(1) symmetry in the UV to the $\chi = 0$ vacuum with SU(2) × U(1) symmetry in the IR.

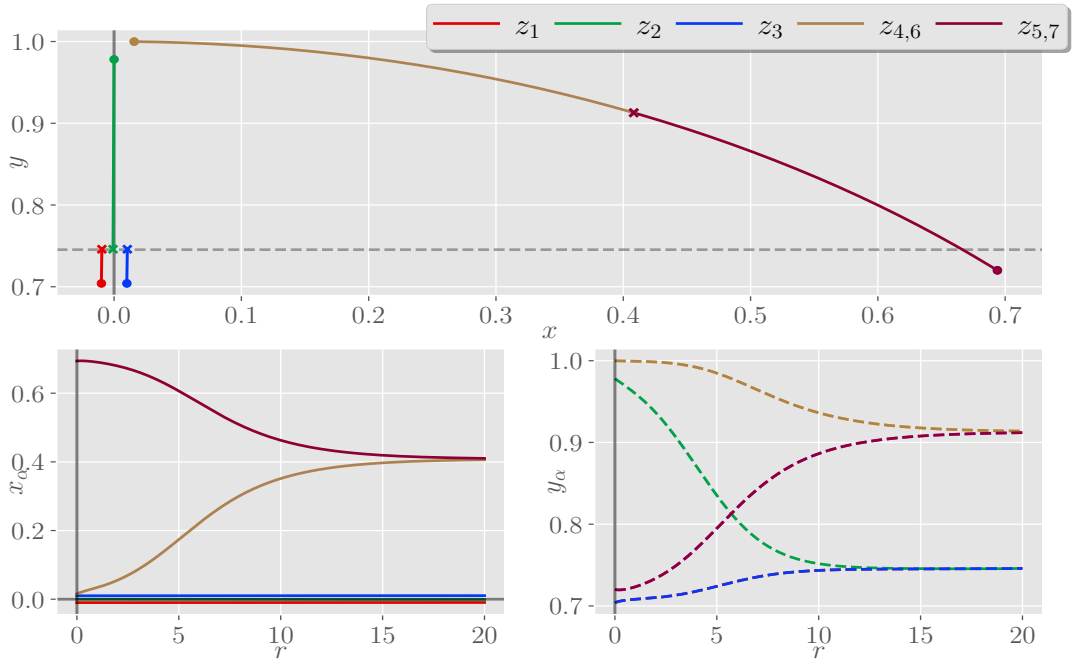

Figure 9.25: Flow from a vacuum with $\mathrm{U}(1)\times\mathrm{U}(1)$ symmetry in the UV to the $\chi = 0.01$ vacuum with $\mathrm{U}(1) \times \mathrm{U}(1)$ symmetry in the IR.

9.5 $[\mathbf{SO}(6) \times \mathbf{SO}(2)] \ltimes \mathbb{R}^{12}$ gauged supergravity

Our introduction of this final $4d$ gauged supergravity of interest to us can be brief, as most of the notable features were already discussed in the previous section. As in the previous section, this gauged supergravity has flat directions for its scalar potential. However, these directions are, loosely stated, located outside of our $\mathbb{Z}_2^3$-truncation. That is, out of the families of vacua, only a single point is seen as a vacuum solution within our $\mathbb{Z}_2^3$-truncation.

A list of the supersymmetric vacua is provided in Table 9.9, with their locations specified in Section A.4.1. We have discovered that the `P0758297` critical point has been reported erroneously in [39]. Instead, the correct critical point can be obtained, as we have verified, by taking the complex conjugate of the 7 scalars provided in equation (3.19) in [39]. The values of δ_a at the critical points are given in Table 9.10. It is clear that, within the $\mathbb{Z}_2^3$-truncation, there is only a single holographic RG flow that can be constructed, going from the SO(3) vacuum in the UV to the U(1) vacuum in the IR. However, we were not able to construct this flow with our algorithm such that the construction of this flow is left for future work. From the linearized BPS equation of Section A.4.2, we conjecture that there exist two kinds of flows, depending whether or not the continuous symmetry is broken along the flow.

Point/family	$\mathcal{N}$	Cont. symmetry	V	Refs.
P0752907	$\mathcal{N}=1$	SO(3)	-7.52907	[39]
P0758297	$\mathcal{N}=1$	U(1)	-7.58297	[39]

Table 9.9: Supersymmetric vacua in $[\mathrm{SO}(6)\times\mathrm{SO}(2)]\ltimes\mathbb{R}^{12}$ gauged supergravity. Potential values are at $g=c=1$.

Point	δ_a	n
P0752907	$-3.03142, -2.14466, -2.14466, -1.88118, 0.333333, 0.333333, 0.663692,$ $1.33631, 1.66667, 1.66667, 3.88118, 4.14466, 4.14466, 5.03142$	–
P0758297	$-2.93747, -2.53094, -1.95438, -1.86799, -0.406614, 0.692894, 0.724684,$ $1.27532, 1.30711, 2.40661, 3.86799, 3.95438, 4.53094, 4.93747$	5

Table 9.10: Values of δ_a for the susy vacua. All values have multiplicity 1. The integer n denotes the number of parameters of the loss function.

9.6 Discussion and outlook

We now discuss the results that we have presented in the previous sections, reflect about our work and comment on possible continuations.

9.6.1 Discussion of results

Our results include several new holographic RG flows which give us new information regarding RG flows of the dual field theories. In the SO(8) theory, we have studied flows that reach the $\mathrm{U}(1)\times\mathrm{U}(1)$ vacuum for the first time, as earlier work considered truncations that did not capture this critical point. For similar reasons, we were able to construct a new holographic RG flow reaching one of the deeper U(1) vacua of the ISO(7) gauged supergravity. While the $\mathbb{Z}_2^3$-truncation was already considered in [112] for the $[\mathrm{SO}(6)\times\mathrm{SO}(1,1)]\ltimes\mathbb{R}^{12}$ supergravity, we constructed two new flows with less residual symmetry that were not considered in this reference.

Besides completely new flows, we discussed new, inequivalent flows which are related to flows found earlier and interpolate between the same IR and UV vacua. These are based on our observation that, in the $\mathbb{Z}_2^3$-truncation, solutions can break the continuous symmetry along the flow. Moreover, we discovered that there even exist multiple, inequivalent ways to break this symmetry by flowing towards different copies of the same vacua. Our explorations therefore indicate a rich and intricate structure of holographic RG flows, which gives us a glimpse of the RG flow structure of the dual field theories. One may therefore be interested in further investigation of these inequivalent holographic RG flows. Such a study would give information on which patterns of symmetry breaking will (not) be observed in the dual field theories. On the other hand, we have presented arguments that indicate that such a task will be intimidating to say the least. Indeed, in Section 9.2.5, we argued that the susy vacua have many copies, leading to an enormous amount of possible flows to consider and classify.

9.6.2 Future work

We were not able to find some of the holographic RG flows and hence future work can build on the work presented here to fill this gap. In particular, we have only partially explored the flows in the theory of Section 9.4, which possibly contains an interesting structure due to the flat directions of the scalar potential. However, one needs to adjust and improve our algorithm. Indeed, we have remarked in Section 9.3.2 that complicated flows have a rather unpredictable flow pattern, which makes our algorithm design inadequate to capture them. This becomes an even greater issue in the two final gauged supergravities we discussed. Indeed, the SO(8) and ISO(7) models have vacua which attract and stabilize solutions and reduce the sensitive dependence of solutions on the initial conditions. In particular, these are the SO(8) and G_2 vacua, which attract solutions from almost all directions. Further comments on possible improvements of our numerical methods will be discussed in Section 9.6.3.

In this thesis, we have restricted our attention to four-dimensional gauged supergravity. One may extend our methods and work to other dimensions of space-time. For example, five-dimensional gauged supergravities have received attention in the literature, as they are linked with the most well-known example of AdS/CFT explained in Section 7.2. In this case, AdS/CFT and holographic RG flows allow us to probe deformations of $\mathcal{N} = 4$ SYM [67, 121]. All tricks presented in this thesis can again be applied: consistent truncations, first-order flow equations in terms of a superpotential and so on. Indeed, the general ideas behind holographic RG flows are captured adequately by the toy models we discussed in Chapter 8, which were formulated in an arbitrary number of space-time dimensions. Another attractive feature of the $5d$ theories is the fact that there are only 42 scalar fields, as opposed to 70 in $4d$, as the scalar manifold is $E_{6,6}/\mathrm{Usp}(8)$ [10]. Therefore, consistent truncations maintain more of the original physics and give even more insightful approximations compared to the $4d$ studies. Selected papers on holographic RG flows in $5d$ gauged supergravity include [122–125].

A final possible direction to extend our work is to study holographic RG flows that interpolate between non-supersymmetric AdS vacua. We have limited our discussion to supersymmetric vacua, as they are guaranteed to be stable vacua and since we can numerically integrate the 'simple' (on a conceptual level) BPS equations from equation (9.2) to find flow solutions. Unlike changing the dimension, studying non-susy AdS vacua therefore requires completely different tools and brings additional challenges into the story. However, this is certainly an interesting direction to pursue, as many field theories of interest to us are non-supersymmetric. Some examples were briefly discussed in Section 7.4. We hope that AdS/CFT can deliver us a deeper understanding of these theories and equip us with a tool to probe their currently inaccessible strongly coupled regimes.

9.6.3 Comparison of numerical methods and future algorithms

As explained above, our numerical algorithm was successful in the construction of new holographic RG flows. Let us compare the performance of our newly designed step descent algorithm with methods currently in use in the literature on holographic RG flows. Recent papers, most notably [112], made use of a brute-force search method. That is, these methods explore the full parameter space and look for regular flows, steadily improving the accuracy of the search until, eventually, the code finds an interpolating flow between

AdS vacua. A comparison between the two methods is given in Table 9.11. The clearest

Brute-force methods	**Step descent algorithm**
− Days to weeks computation time	+ Hours to a day computation time
− Waste of computational resources	+ Targeted search
− Not adjustable	+ Adjustable and improvable
+ In principle guaranteed to find flows	− Not guaranteed to converge

Table 9.11: Comparison between algorithms to construct holographic RG flows currently being used in the literature and the algorithm designed in this thesis.

advantage of our targeted search algorithm compared to the brute-force methods is that it reduces the required amount of computation time and computational resources.[5] However, a major drawback is that the step descent algorithm is not guaranteed to converge when starting from any initial ansatz. On the other hand, a brute-force method should (at least in principle) eventually find the correct initial condition to construct a flow. This drawback is a common phenomenon encountered in gradient descent algorithms, our source of inspiration for the step descent algorithm. Indeed, this main issue may be attributed to a loss function that has a shape similar to Figure 9.26. In essence, our algorithm converges to a local minimum of the loss function, which is different from the true minimum we want to find.

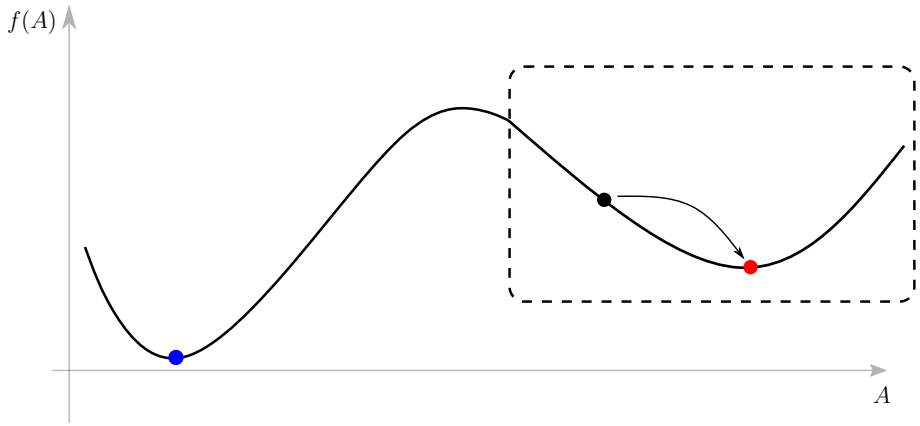

Figure 9.26: Visualization of a major drawback of gradient descent algorithms. The algorithm converges to a local minimum (red) lying close to the initial guess (black) and is unable to find the true minimum (blue).

Let us speculate about possible solutions to this problem. First of all, recall that our algorithm uses a step descent rather than gradient descent, such that we explore the parameter space in a less efficient way compared to gradient descent algorithms. Therefore, a first improvement would be to adjust our algorithm to include a proper gradient descent, which may improve our odds of finding the true minimum. Moreover, the step sizes s and Δr are unaltered during the search. If we implement code which adapts the step sizes according to the amount of convergence, the speed and performance

[5]The estimate of computational time for brute-force methods is based on private communication with Colin Sterckx related to the work of [112], assuming sequential computations, and on personal experience using a basic brute-force method which we implemented ourselves.

of the algorithm will be drastically improved. Furthermore, we could alter the loss function used in the algorithm. Indeed, our simple Euclidean distance-based loss function does not properly quantify how 'close' a solution is to the desired solution. For example, the flows constructed in Figures 9.19 and 9.20 required some of the scalars to start off (in the IR) along directions which are not directly aimed at the UV target. Indeed, solutions that 'shoot' in the direction of the UV target blow up at later integration times. Finding this flow required us to reduce the step sizes of the algorithm to correct this tendency to converge towards such undesired solutions. This is likely the main reason why we were not able to construct other holographic RG flows, and we believe this could be prevented by a more clever design of the loss function. Indeed, this has been demonstrated by the flow reported Figure 9.25, which we found by using a different loss function adapted to the problem at hand. Throughout our explorations, we have already experimented with other designs for the loss function. Firstly, we replaced the Euclidean distance by a hyperbolic distance, which is actually the 'correct' metric since we are working in hyperbolic spaces. However, quite surprisingly and still unexplained, this worsened the convergence of the algorithm compared to the 'wrong' Euclidean metric. Secondly, we considered a loss function which compared the value of A' (see equation (9.3)) at the end of the flow solution with the UV target. Again, this did not improve convergence. In short, the design of the loss function should be refined for future work, but it is unclear what possibilities may yield better results.

9.6.4 Machine learning meets theoretical physics

Our results and discussions suggest to direct future research on holographic RG flows towards more cleverly designed algorithms which remind us of machine learning methods. It is our personal opinion that targeted search algorithms, when upgraded to proper machine learning algorithms, will prove to be more fruitful compared to brute-force methods. Since our work essentially boils down to finding fine-tuned flow solutions of dynamical systems in a phase space with many dimensions, this puts our work into a bigger picture for future research. Indeed, future work (without restricting our attention to the specific case of holographic RG flows) may benefit from exploring the intersection of machine learning methods with theoretical or computational physics. In fact, this development has already been started recently in this field, as machine learning algorithms are employed to find vacuum solutions [41]. Expanding this intersection of knowledge domains is certainly an exciting prospect which may influence the whole body of physics in general.

Appendix A

Critical points and linearized BPS equations

We specify the locations of the vacua in the $\mathbb{Z}_2^3$-truncation using the conventions specified in Sections 9.2 – Section 9.5. Recall that a vacuum with label $\mathtt{Pn_1n_2n_3n_4n_5n_6n_7}$ has potential value $V = -n_1 n_2 . n_3 n_4 n_5 n_6 n_7$.

A.1 SO(8) gauged supergravity

A.1.1 Locations of critical points

P0600000: $\mathcal{N} = 8, \mathrm{SO}(8)$

$$z_1 = z_2 = z_3 = z_4 = z_5 = z_6 = z_7 = 0 \tag{A.1}$$

P0719157: $\mathcal{N} = 1, G_2$

$$z_1 = z_2 = z_3 = z_4 = z_5 = z_6 = z_7 = \frac{3 + \sqrt{3} - 3^{1/4}}{4} \left(1 - i 3^{-1/4} \sqrt{2 + \sqrt{3}}\right) \tag{A.2}$$

P0779422: $\mathcal{N} = 2, \mathrm{SU}(3) \times \mathrm{U}(1)$

$$z_1 = z_3 = z_4 = z_5 = i\sqrt{5 - 2\sqrt{6}}\,, \quad z_2 = z_6 = z_7 = 2 - \sqrt{3} \tag{A.3}$$

P1200000: $\mathcal{N} = 1, \mathrm{U}(1) \times \mathrm{U}(1)$

$$z_1 = -z_5 = 0.3660254(1 - i)\,, \quad z_2 = z_6 = 0 \tag{A.4}$$
$$z_3 = z_4 = 0.3660254(1 + i)\,, \quad z_7 = 0.5773502i \tag{A.5}$$

P1384096: $\mathcal{N} = 1, \mathrm{SO}(3)$

$$z_1 = -0.4833214 - 0.3864057i, \tag{A.6}$$
$$z_2 = z_6 = z_7 = 0.3162021 - 0.5162839i \tag{A.7}$$
$$z_3 = z_4 = z_5 = 0.1696359 + 0.1415740i \tag{A.8}$$

A.1.2 Linearized BPS equations

P0719157: $\mathcal{N} = 1, G_2$

$$\begin{aligned} x_{1,2,3,4,5,6,7} &= 0.142565 + 0.223702 A_1 e^{2.24423 r} \\ y_{1,2,3,4,5,6,7} &= -0.209269 - 0.304654 A_1 e^{2.24423 r} \end{aligned}$$

The top figure of Figure 9.4 was created with $A_1 = 1$.

P0779422: $\mathcal{N} = 2, \mathrm{SU}(3) \times \mathrm{U}(1)$

$$\begin{aligned} x_{1,3,4,5} &= 0 && && + 0.301579 A_2 e^{0.905142 r}, \\ y_{1,3,4,5} &= 0.317837 && - 0.389262 A_1 e^{2.517 r} && \\ x_{2,6,7} &= 0.267949 && - 0.362353 A_1 e^{2.517 r} && \\ y_{2,6,7} &= 0 && && + 0.460507 A_2 e^{0.905142 r} \end{aligned}$$

The bottom figure of Figure 9.4 was created with $(A_1, A_2) = (1, 0)$. Figure 9.5 was created with $(A_1, A_2) = (1, -0.1020462419)$.

P1200000: $\mathcal{N} = 1, \mathrm{U}(1) \times \mathrm{U}(1)$

$$\begin{aligned} x_1 &= 0.366025 && - 0.0472688 A_1 e^{3.61177 r} && - 0.217087 A_2 e^{3.61177 r} && + 0.319801 A_3 e^{3.4641 r} \\ y_1 &= -0.366025 && - 0.0587983 A_1 e^{3.61177 r} && - 0.270037 A_2 e^{3.61177 r} && - 0.319801 A_3 e^{3.4641 r} \\ x_2 &= 0 && + 0.318184 A_1 e^{3.61177 r} && - 0.419622 A_2 e^{3.61177 r} && \\ y_2 &= 0 && - 0.539002 A_1 e^{3.61177 r} && - 0.451521 A_2 e^{3.61177 r} && \\ x_3 &= 0.366025 && - 0.211878 A_1 e^{3.61177 r} && && + 0.319801 A_3 e^{3.4641 r} \\ y_3 &= 0.366025 && + 0.263558 A_1 e^{3.61177 r} && && + 0.319801 A_3 e^{3.4641 r} \\ x_4 &= 0.366025 && + 0.211878 A_1 e^{3.61177 r} && && + 0.319801 A_3 e^{3.4641 r} \\ y_4 &= 0.366025 && - 0.263558 A_1 e^{3.61177 r} && && + 0.319801 A_3 e^{3.4641 r} \\ x_5 &= -0.366025 && - 0.0472688 A_1 e^{3.61177 r} && - 0.217087 A_2 e^{3.61177 r} && - 0.319801 A_3 e^{3.4641 r} \\ y_5 &= 0.366025 && - 0.0587983 A_1 e^{3.61177 r} && - 0.270037 A_2 e^{3.61177 r} && + 0.319801 A_3 e^{3.4641 r} \\ x_6 &= 0 && - 0.500922 A_1 e^{3.61177 r} && - 0.419622 A_2 e^{3.61177 r} && \\ y_6 &= 0 && + 0.342372 A_1 e^{3.61177 r} && - 0.451521 A_2 e^{3.61177 r} && \\ x_7 &= 0 && && && \\ y_7 &= 0.57735 && && && + 0.426401 A_3 e^{3.4641 r} \end{aligned}$$

The A_1-mode breaks the symmetry. Figure 9.7 was created with $A_1 = A_2 = 0$ and $A_3 = -1$. Figure 9.8 was created with

$$(A_1, A_2, A_3) = (0.099671, -0.1007, -0.1317)\,. \tag{A.9}$$

Figure 9.9 was created with $A_1 = 0$, $A_2 = 0.1$ and $A_3 = -0.110952124$. Figure 9.10 was created with $A_1 = A_2 = 0.1$, and $A_3 = -0.162581999$. Figure 9.11 was created with $A_1 = A_2 = -0.1$ and $A_3 = -0.162581999$.

P1384096: $\mathcal{N} = 1, \mathrm{SO}(3)$

$$
\begin{aligned}
x_1 &= -0.483321 + 0.168488A_1e^{6.0197r} + 0.366609A_2e^{3.68655r} \\
y_1 &= -0.386406 - 0.215774A_1e^{6.0197r} + 0.321566A_2e^{3.68655r} \\
x_2 &= 0.316202 + 0.012542A_1e^{6.0197r} - 0.240569A_2e^{3.68655r} + 0.202913A_3e^{2.06899r} - 0.203681A_4e^{2.06899r} \\
y_2 &= -0.516284 + 0.0162529A_1e^{6.0197r} + 0.38121A_2e^{3.68655r} + 0.191427A_3e^{2.06899r} - 0.192151A_4e^{2.06899r} \\
x_3 &= 0.169636 + 0.360345A_1e^{6.0197r} - 0.17284A_2e^{3.68655r} + 0.0191429A_3e^{2.06899r} - 0.462658A_4e^{2.06899r} \\
y_3 &= 0.141574 - 0.421996A_1e^{6.0197r} - 0.1449A_2e^{3.68655r} + 0.0180324A_3e^{2.06899r} - 0.43582A_4e^{2.06899r} \\
x_4 &= 0.169636 + 0.360345A_1e^{6.0197r} - 0.17284A_2e^{3.68655r} - 0.483894A_3e^{2.06899r} + 0.485726A_4e^{2.06899r} \\
y_4 &= 0.141574 - 0.421996A_1e^{6.0197r} - 0.1449A_2e^{3.68655r} - 0.455825A_3e^{2.06899r} + 0.45755A_4e^{2.06899r} \\
x_5 &= 0.169636 + 0.360345A_1e^{6.0197r} - 0.17284A_2e^{3.68655r} + 0.464752A_3e^{2.06899r} - 0.0230679A_4e^{2.06899r} \\
y_5 &= 0.141574 - 0.421996A_1e^{6.0197r} - 0.1449A_2e^{3.68655r} + 0.437792A_3e^{2.06899r} - 0.0217297A_4e^{2.06899r} \\
x_6 &= 0.316202 + 0.012542A_1e^{6.0197r} - 0.240569A_2e^{3.68655r} - 0.00802724A_3e^{2.06899r} + 0.194008A_4e^{2.06899r} \\
y_6 &= -0.516284 + 0.0162529A_1e^{6.0197r} + 0.38121A_2e^{3.68655r} - 0.00757286A_3e^{2.06899r} + 0.183026A_4e^{2.06899r} \\
x_7 &= 0.316202 + 0.012542A_1e^{6.0197r} - 0.240569A_2e^{3.68655r} - 0.194886A_3e^{2.06899r} + 0.00967311A_4r^{2.06899r} \\
y_7 &= -0.516284 + 0.0162529A_1e^{6.0197r} + 0.38121A_2e^{3.68655r} - 0.183854A_3e^{2.06899r} + 0.00912556A_4e^{2.06899r}
\end{aligned}
$$

The A_3 and A_4 modes break the continuous symmetry. Figure 9.12 was created with $A_3 = A_4 = 0$, $A_2 = 1$ and $A_1 = 0.1$. Figure 9.13 was created with $A_3 = A_4 = 0.3$, $A_2 = 1$ and $A_1 = 31.5$. Figure 9.14 was created with $A_3 = A_4 = 0$, $A_2 = 1$ and fine-tuning $A_1 = 1.7686$. Figure 9.15 was created with $A_2 = 1$, $A_3 = A_4 = 0.15$ and fine-tuning $A_1 = 9.278570$.

A.2 ISO(7) gauged supergravity

A.2.1 Locations of critical points

P1998705: $\mathcal{N} = 1, G_2$

$$z_1 = z_2 = z_3 = z_4 = z_5 = z_6 = z_7 = \frac{1}{4 \cdot 2^{1/3}}(1 + i\sqrt{15}), . \tag{A.10}$$

P2078460: $\mathcal{N} = 2, \mathrm{SU}(3) \times \mathrm{U}(1)$

$$z_1 = z_2 = z_5 = z_6 = \frac{i}{\sqrt{2}}, \quad z_3 = z_4 = z_7 = \frac{1}{2}\left(1 + i\sqrt{3}\right). \tag{A.11}$$

P2327730: $\mathcal{N} = 3, \mathrm{SO}(4)$

$$z_1 = -\overline{z}_2 = -\overline{z}_3 = -\tfrac{1}{2}\overline{z}_4 = z_5 = -\overline{z}_6 = -\overline{z}_7 = \frac{1}{2^{4/3}}\left(-1 + i\sqrt{3}\right) \tag{A.12}$$

P2379560: $\mathcal{N} = 1, \mathrm{SU}(3)$

$$z_1 = z_2 = z_5 = z_6 = \frac{1}{4}\left(\sqrt{3} + i\sqrt{5}\right), \quad z_3 = z_4 = z_7 = \frac{1}{4}\left(-1 + i\sqrt{15}\right) \tag{A.13}$$

P2569710: $\mathcal{N} = 1, \mathrm{U}(1)$

$$\begin{aligned} z_1 &= z_5 = 0.4874331 + 0.5960593i \\ z_2 &= z_6 = 0.1081762 + 1.1727984i, \\ z_3 &= -0.2177695 + 0.5098402i \\ z_4 &= -0.5988588 + 0.5894185i, \\ z_7 &= 1.210100 + 0.8849423i \end{aligned} \tag{A.14}$$

P3561023: $\mathcal{N} = 1, \mathrm{U}(1)$

$$\begin{aligned} z_1 &= z_5 = -0.1102603 + 0.7629108i \\ z_2 &= z_6 = 0.8364390 + 0.3907021i \\ z_3 &= -0.4021216 + 0.3120032i \\ z_4 &= -0.9448821 + 1.4405741i \\ z_7 &= 0.7401864 + 1.1525653i \end{aligned} \tag{A.15}$$

A.2.2 Linearized BPS equations

P2078460: $\mathcal{N} = 2, \mathrm{SU}(3) \times \mathrm{U}(1)$

$$\begin{aligned} x_{1,2,5,6} &= 0 && && -0.34556 A_2 e^{0.739045 r} \\ y_{1,2,5,6} &= 0.707107 && +0.421613 A_1 e^{2.05512 r} && \\ x_{3,4,7} &= 0.5 && -0.15518 A_1 e^{2.05512 r} && +0.36137 A_2 e^{0.739045 r} \\ y_{3,4,7} &= 0.866025 && +0.268779 A_1 e^{2.05512 r} && +0.208637 A_2 e^{0.739045 r} \end{aligned}$$

The expansion preserves the symmetry at the critical point. Figure 9.21 is made with

$$(A_1, A_2) = (1, -0.21555924645)\,. \tag{A.16}$$

P2327730: $\mathcal{N} = 3, \mathrm{SO}(4)$

$$\begin{aligned} x_{1,5} &= -0.39685 && +0.104502 A_1 e^{2.41233 r} && -0.557678 A_2 e^{1.01957 r} && -0.557678 A_3 e^{1.01957 r} \\ y_{1,5} &= 0.687365 && +0.390007 A_1 e^{2.41233 r} && +0.149429 A_2 e^{1.01957 r} && +0.149429 A_3 e^{1.01957 r} \\ x_{2,3,6,7} &= 0.39685 && -0.104502 A_1 e^{2.41233 r} && +0.321975 A_3 e^{1.01957 r} && \\ y_{2,3,6,7} &= 0.687365 && +0.390007 A_1 e^{2.41233 r} && && +0.086273 A_3 e^{1.01957 r} \\ x_4 &= 0.793701 && -0.142753 A_1 e^{2.41233 r} && +0.086273 A_2 e^{1.01957 r} && +0.086273 A_3 e^{1.01957 r} \\ y_4 &= 1.37473 && +0.0382504 A_1 e^{2.41233 r} && +0.321975 A_2 e^{1.01957 r} && +0.321975 A_3 e^{1.01957 r} \end{aligned}$$

Figure 9.22 was made with parameters

$$(A_1, A_2, A_3) = (3.5709160396, -0.2920101, -0.2920101)\,. \tag{A.17}$$

We note that triangular RG flows can be constructed by requiring $A_2 \neq A_3$ while fine-tuning. Such flows were reported in [105].

P2379560: $\mathcal{N} = 1, \mathrm{SU}(3)$

$$\begin{aligned} x_{1,2,5,6} &= 0.433013 && -0.0846158 A_1 e^{2.04114 r} && -0.17883 A_2 e^{2.04114 r} \\ y_{1,2,5,6} &= 0.559017 && 0.479722 A_1 e^{2.04114 r} && +0.444676 A_2 e^{2.04114 r} \\ x_{3,4,7} &= -0.25 && && +0.164449 A_2 e^{2.04114 r} \\ y_{3,4,7} &= 0.968246 && 0.130164 A_1 e^{2.04114 r} && \end{aligned}$$

We have not shown any flows which start from this critical point in the IR. A flow between this vacuum and the G_2 vacuum is known [110]. However, since our expansion preserves the symmetry of the critical point, there are no interesting new features (*e.g.*, symmetry breaking along flows) within the larger $\mathbb{Z}_2^3$-truncation.

P2569710: $\mathcal{N} = 1, \mathrm{U}(1)$

$x_1 = 0.487433$	$+ 0.0805976 A_1 e^{2.52742 r}$	$- 0.583761 A_2 e^{2.51248 r}$	$- 0.217792 A_3 e^{1.52786 r}$	$+ 0.101019 A_4 e^{0.353844 r}$
$y_1 = 0.596059$	$- 0.436001 A_1 e^{2.52742 r}$	$- 0.119631 A_2 e^{2.51248 r}$	$+ 0.142738 A_3 e^{1.52786 r}$	$+ 0.0851004 A_4 e^{0.353844 r}$
$x_2 = 0.108176$	$+ 0.0491102 A_1 e^{2.52742 r}$	$+ 0.315758 A_2 e^{2.51248 r}$	$+ 0.249373 A_3 e^{1.52786 r}$	$+ 0.0745267 A_4 e^{0.353844 r}$
$y_2 = 1.1728$	$- 0.0991282 A_1 e^{2.52742 r}$	$+ 0.212624 A_2 e^{2.51248 r}$	$- 0.352276 A_3 e^{1.52786 r}$	$+ 0.0266824 A_4 e^{0.353844 r}$
$x_3 = -0.21777$	$- 0.0702244 A_1 e^{2.52742 r}$		$- 0.302592 A_3 e^{1.52786 r}$	$- 0.764726 A_4 e^{0.353844 r}$
$y_3 = 0.50984$	$- 0.547589 A_1 e^{2.52742 r}$		$+ 0.150666 A_3 e^{1.52786 r}$	$+ 0.0775593 A_4 e^{0.353844 r}$
$x_4 = -0.598859$	$- 0.0564274 A_1 e^{2.52742 r}$		$+ 0.57109 A_3 e^{1.52786 r}$	$- 0.358423 A_4 e^{0.353844 r}$
$y_4 = 0.589419$	$- 0.443772 A_1 e^{2.52742 r}$		$- 0.020298 A_3 e^{1.52786 r}$	$- 0.0187729 A_4 e^{0.353844 r}$
$x_5 = 0.487433$	$+ 0.0805976 A_1 e^{2.52742 r}$	$+ 0.583761 A_2 e^{2.51248 r}$	$- 0.217792 A_3 e^{1.52786 r}$	$+ 0.101019 A_4 e^{0.353844 r}$
$y_5 = 0.596059$	$- 0.436001 A_1 e^{2.52742 r}$	$+ 0.119631 A_2 e^{2.51248 r}$	$+ 0.142738 A_3 e^{1.52786 r}$	$+ 0.0851004 A_4 e^{0.353844 r}$
$x_6 = 0.108176$	$+ 0.0491102 A_1 e^{2.52742 r}$	$- 0.315758 A_2 e^{2.51248 r}$	$+ 0.249373 A_3 e^{1.52786 r}$	$+ 0.0745267 A_4 e^{0.353844 r}$
$y_6 = 1.1728$	$- 0.0991282 A_1 e^{2.52742 r}$	$- 0.212624 A_2 e^{2.51248 r}$	$- 0.352276 A_3 e^{1.52786 r}$	$+ 0.0266824 A_4 e^{0.353844 r}$
$x_7 = 1.2101$	$+ 0.164504 A_1 e^{2.52742 r}$		$- 0.146936 A_3 e^{1.52786 r}$	$+ 0.402256 A_4 e^{0.353844 r}$
$y_7 = 0.884942$	$- 0.22444 A_1 e^{2.52742 r}$		$+ 0.171483 A_3 e^{1.52786 r}$	$+ 0.266689 A_4 e^{0.353844 r}$

Note that the A_2-mode breaks the symmetry of the fixed point ($z_1 = z_5$, $z_2 = z_6$). Figure 9.19 was made with

$$(A_1, A_2, A_3, A_4) = (1, 0, 0.15615488023200016, -0.01011)\,, \tag{A.18}$$

while Figure 9.20 was made with

$$(A_1, A_2, A_3, A_4) = (1, 0.005, 0.1561553522550902, -0.01011)\,. \tag{A.19}$$

P3561023: $\mathcal{N} = 1, \mathrm{U}(1)$

$$
\begin{array}{llll}
x_1 = -0.11026 & +0.386828A_1e^{3.65229r} & +0.0461372A_2e^{3.39817r} & +0.0364767A_3e^{2.81446r} \\
 & -0.0888923A_5e^{1.73139r} & & \\
y_1 = 0.762911 & -0.194545A_1e^{3.65229r} & -0.401245A_2e^{3.39817r} & +0.121247A_3e^{2.81446r} \\
 & +0.0874768A_5e^{1.73139r} & & \\
x_2 = 0.836439 & -0.226951A_1e^{3.65229r} & +0.302688A_2e^{3.39817r} & -0.131328A_3e^{2.81446r} \\
 & +0.409767A_5e^{1.73139r} & & \\
y_2 = 0.390702 & -0.114444A_1e^{3.65229r} & +0.17518A_2e^{3.39817r} & +0.492662A_3e^{2.81446r} \\
 & -0.0226078A_5e^{1.73139r} & & \\
x_3 = -0.402122 & -0.657371A_1e^{3.65229r} & -0.120826A_2e^{3.39817r} & +0.0019231A_3e^{2.81446r} \\
y_3 = 0.312003 & -0.0387341A_1e^{3.65229r} & +0.240211A_2e^{3.39817r} & +0.664027A_3e^{2.81446r} \\
x_4 = -0.944882 & +0.00348252A_1e^{3.65229r} & +0.199985A_2e^{3.39817r} & +0.030437A_3e^{2.81446r} \\
y_4 = 1.44057 & -0.104856A_1e^{3.65229r} & +0.289221A_2e^{3.39817r} & -0.0055178A_3e^{2.81446r} \\
x_5 = -0.11026 & +0.386828A_1e^{3.65229r} & +0.0461372A_2e^{3.39817r} & +0.0364767A_3e^{2.81446r} \\
 & -0.0888923A_5e^{1.73139r} & & \\
y_5 = 0.762911 & -0.194545A_1e^{3.65229r} & -0.401245A_2e^{3.39817r} & +0.121247A_3e^{2.81446r} \\
 & +0.0874768A_5e^{1.73139r} & & \\
x_6 = 0.836439 & -0.226951A_1e^{3.65229r} & +0.302688A_2e^{3.39817r} & -0.131328A_3e^{2.81446r} \\
 & +0.409767A_5e^{1.73139r} & & \\
y_6 = 0.390702 & -0.114444A_1e^{3.65229r} & +0.17518A_2e^{3.39817r} & +0.492662A_3e^{2.81446r} \\
 & -0.0226078A_5e^{1.73139r} & & \\
x_7 = 0.740186 & +0.0402257A_1e^{3.65229r} & -0.482697A_2e^{3.39817r} & -0.0264938A_3e^{2.81446r} \\
y_7 = 1.15257 & +0.222625A_1e^{3.65229r} & -0.0138388A_2e^{3.39817r} & +0.0736079A_3e^{2.81446r}
\end{array}
$$

$$
\begin{array}{ll}
 & -0.0364767A_4e^{1.76145r} \\
 & \\
 & -0.323186A_4e^{1.76145r} \\
 & \\
 & +0.540451A_4e^{1.76145r} \\
 & \\
 & +0.0256776A_4e^{1.76145r} \\
 & \\
 & +0.679593A_5e^{1.73139r} \\
 & +0.0263984A_5e^{1.73139r} \\
 & -0.264003A_5e^{1.73139r} \\
 & +0.152541A_5e^{1.73139r} \\
 & -0.320631A_4e^{1.76145r} \\
 & \\
 & -0.323186A_4e^{1.76145r} \\
 & \\
 & +0.540451A_4e^{1.76145r} \\
 & \\
 & +0.0256776A_4e^{1.76145r} \\
 & \\
 & -0.0365176A_5e^{1.73139r} \\
 & +0.27424A_5e^{1.73139r}
\end{array}
$$

We have not been able to find holographic RG flows from this critical point. We expect that, as was the case for the other U(1) critical point, there exists a flow which preserves the U(1) symmetry (by putting $A_4 = 0$) and a flow which breaks the U(1) symmetry (by putting $A_4 \neq 0$).

A.3 $[\mathbf{SO}(6) \times \mathbf{SO}(1,1)] \ltimes \mathbb{R}^{12}$ gauged supergravity

A.3.1 Locations of critical points

F0289794($\chi_{1,2,3}$): The critical point is located at

$$z_{1,2,3} = c\left(-\chi_{1,2,3} + i\frac{\sqrt{5}}{3}\right), \quad z_4 = z_5 = z_6 = z_7 = \frac{1}{\sqrt{6}}(1 + i\sqrt{5}). \tag{A.20}$$

Here, $\chi_{1,2,3}$ are constant parameters and are subject to the constraint $\chi_1 + \chi_2 + \chi_3 = 0$. A generic solution preserves a $\mathrm{U}(1)^2$ symmetry. This symmetry becomes enhanced to $\mathrm{SU}(2) \times \mathrm{U}(1)$ if we have a pairwise identification between the χ_i parameters, and gets even further enhanced to SU(3) at $\chi_{1,2,3} = 0$.

F0300000(χ): The critical point is located at

$$\begin{aligned} z_1 = -\overline{z}_3 = c\left(-\chi + i\frac{1}{\sqrt{2}}\right), \quad z_2 = ic, \quad z_4 = z_6 = i, \\ z_5 = z_7 = \frac{1}{\sqrt{2}}(1+i). \end{aligned} \tag{A.21}$$

A generic solution preserves only $\mathrm{U}(1)^2$, while this symmetry becomes enhanced to $\mathrm{SU}(2)\times\mathrm{U}(1)$ at $\chi=0$.

F0300000(φ): The critical point is located at

$$z_1 = z_2 = \frac{ic\sqrt{\varphi^2+1}}{\sqrt{2}}\,, \quad z_3 = ic\,, \quad z_4 = z_5 = \frac{1}{\sqrt{2}}(1+i)\,,$$
$$z_6 = -\overline{z}_7 = \frac{1}{\sqrt{\varphi^2+1}}(-\varphi+i)\,. \tag{A.22}$$

A generic solution again only preserves $\mathrm{U}(1)^2$ and $\mathcal{N}=2$. At $\varphi=0$, this becomes enhanced to $\mathrm{SU}(2)\times\mathrm{U}(1)$ and $\mathcal{N}=2$, while at $\varphi=1$, this enhances to $\mathrm{SO}(4)$ and $\mathcal{N}=4$. We remark that F0300000($\varphi=0$) represents the same critical point as F0300000($\chi=0$).

A.3.2 Linearized BPS equations

F0300000($\chi=0$): $\mathcal{N}=2, \mathrm{SU}(2)\times\mathrm{U}(1)$

$x_{1,3}=0$		$+0.552092A_2e^{0.561553r}$		
$y_{1,3}=0.707107$	$-0.905646A_1e^{1.56155r}$			
$x_2=0$		$-A_2e^{0.561553r}$		$-A_4e^{1.56155r}$
$y_2=1$	$-A_12.71828^{1.56155r}$		$-A_3e^{0.561553r}$	
$x_{4,6}=0$			$+0.780776A_3e^{0.561553r}$	
$y_{4,6}=1$				$+1.28078A_4e^{1.56155r}$
$x_{5,7}=0.707107$	$+0.353553A_1e^{1.56155r}$	$-0.353553A_2e^{0.561553r}$	$-0.353553A_3e^{0.561553r}$	$+0.353553A_4e^{1.56155r}$
$y_{5,7}=0.707107$	$-0.353553A_1e^{1.56155r}$	$-0.353553A_2e^{0.561553r}$	$+0.353553A_3e^{0.561553r}$	$+0.353553A_4e^{1.56155r}$

Flows were obtained by putting $A_1=-1$. Figure 9.23 was found in [112] with parameter values

$$(A_2, A_3, A_4) = (0.00429589502, 0.3421361222342497, -0.15669397894)\,. \tag{A.23}$$

We obtained Figure 9.24 by fine-tuning the parameters to the values

$$(A_1, A_2, A_3) = (-0.027605720061501006, 0.3397537432343989, -0.30789650806929986)\,. \tag{A.24}$$

F0300000($\chi = 0.01$): $\mathcal{N} = 2, \mathrm{U}(1) \times \mathrm{U}(1)$

$$
\begin{aligned}
x_1 &= -0.01 && && && -0.473483A_3e^{0.561553r} && +0.052623A_4e^{0.561553r} \\
y_1 &= 0.707107 && +0.452416A_1e^{1.56155r} && -0.126687A_2e^{1.56155r} \\
x_2 &= 0 && -0.253456A_1e^{1.56155r} && -0.389575A_2e^{1.56155r} && +0.428808A_3e^{0.561553r} && -0.0476578A_4e^{0.561553r} \\
y_2 &= 1 && +0.249775A_1e^{1.56155r} && -0.069943A_2e^{1.56155r} && && -0.483821A_4e^{0.561553r} \\
x_3 &= 0.01 && && && -0.473483A_3e^{0.561553r} && +0.052623A_4e^{0.561553r} \\
y_3 &= 0.707107 && +0.452416A_1e^{1.56155r} && -0.126687A_2e^{1.56155r} \\
x_4 &= 0 && && && +0.377756A_4e^{0.561553r} && -0.706824A_5e^{0.00039984r} \\
y_4 &= 1 && +0.32462A_1e^{1.56155r} && +0.498958A_2e^{1.56155r} \\
x_5 &= 0.707107 && +0.00260258A_1e^{1.56155r} && +0.324928A_2e^{1.56155r} && +0.303213A_3e^{0.561553r} && -0.375812A_4e^{0.561553r} \\
& && && && && -0.0141308A_5e^{0.00039984r} \\
y_5 &= 0.707107 && +0.355838A_1e^{1.56155r} && +0.226014A_2e^{1.56155r} && +0.303213A_3e^{0.561553r} && +0.308414A_4e^{0.561553r} \\
& && && && && -0.0141308A_5e^{0.00039984r} \\
x_6 &= 0 && && && +0.377756A_4e^{0.561553r} && +0.706824A_5e^{0.00039984r} \\
y_6 &= 1 && +0.32462A_1e^{1.56155r} && -0.498958A_2e^{1.56155r} \\
x_7 &= 0.707107 && +0.00260258A_1e^{1.56155r} && +0.324928A_2e^{1.56155r} && +0.303213A_3e^{0.561553r} && -0.375812A_4e^{0.561553r} \\
& && && && && +0.0141308A_5e^{0.00039984r} \\
y_7 &= 0.707107 && +0.355838A_1e^{1.56155r} && +0.226014A_2e^{1.56155r} && +0.303213A_3e^{0.561553r} && +0.308414A_4e^{0.561553r}
\end{aligned}
$$

Note that A_5 breaks the symmetry of the critical point. In fact, it is likely possible to break the symmetry along the flow (*i.e.*, put $A_5 \neq 0$ such that $z_4 \neq z_6$ and $z_5 \neq z_7$ along the flow). However, we did not verify this statement by creating a full solution, up until the UV vacuum. Figure 9.25 was created with parameters (putting $A_5 = 0$)

$$(A_1, A_2, A_3, A_4) = (-7.662078398570975, 4.673264742920671, 0.05936499004466509, 0.5543896161564815)\,. \tag{A.25}$$

A.4 $[\mathbf{SO}(6) \times \mathbf{SO}(2)] \ltimes \mathbb{R}^{12}$ gauged supergravity

A.4.1 Locations of critical points

P0752907: $\mathcal{N} = 1, \mathrm{SO}(3)$

$$z_1 = z_2 = z_3 = \frac{1}{\sqrt{3}}\left(2 + i\sqrt{5}\right)\,, \tag{A.26}$$

$$z_4 = z_5 = z_6 = \frac{1}{108^{1/4}}\left(-1 + i\sqrt{5}\right)\,, \quad z_7 = \frac{1}{108^{1/4}}\left(5 + i\sqrt{5}\right)\,, \tag{A.27}$$

P0758297: $\mathcal{N} = 1, \mathrm{U}(1)$
Note that this location is the corrected version of the location provided in [39].

$$
\begin{aligned}
z_1 &= \frac{\kappa}{\sqrt{6}}e^{\frac{\pi}{3}i}\,, \quad z_2 = z_3 = \frac{\sqrt{3+\kappa^2}}{4\sqrt{2}} + i\frac{\sqrt{3(-1+\kappa^2)}}{4\sqrt{2}} \\
z_4 &= \frac{\kappa - 2}{2\sqrt{3}\sqrt[4]{2\kappa^2 - 5}} + i\frac{\sqrt[4]{\frac{7\kappa^2}{2}} - 8}{\kappa}\,, \quad z_5 = z_6 = \frac{\sqrt{\kappa}}{\sqrt[4]{6}}e^{\frac{2\pi}{3}i}\,, \qquad \text{(A.28)} \\
z_7 &= \frac{\sqrt{\kappa^2+2}\sqrt[4]{2\kappa^2-5}}{\sqrt{6}(2-\kappa)} + i\frac{\sqrt[4]{\frac{7\kappa^2}{2}} - 8}{\kappa}\,, \quad \kappa \equiv \sqrt{\sqrt{13} - 1} \approx 1.6141720\,. \qquad \text{(A.29)}
\end{aligned}
$$

A.4.2 Linearized BPS equations

P0758297: $\mathcal{N} = 1, \mathrm{U}(1)$

$$
\begin{aligned}
x_1 = {} & 0.329491 - 0.0105981 A_1 e^{4.67016 r} + 0.531815 A_2 e^{4.02385 r} - 0.0581137 A_4 e^{2.96984 r} + 0.250936 A_5 e^{0.64646 r} \\
y_1 = {} & 0.570696 + 0.0486849 A_1 e^{4.67016 r} + 0.1631 A_2 e^{4.02385 r} + 0.344803 A_4 e^{2.96984 r} - 0.591551 A_5 e^{0.64646 r} \\
x_2 = {} & 0.418537 + 0.0837058 A_1 e^{4.67016 r} - 0.364737 A_2 e^{4.02385 r} - 0.582028 A_3 e^{3.10719 r} + 0.0183412 A_4 e^{2.96984 r} \\
& - 0.259639 A_5 e^{0.64646 r} \\
y_2 = {} & 0.38797 + 0.0491905 A_1 e^{4.67016 r} + 0.00108551 A_2 e^{4.02385 r} - 0.0271857 A_3 e^{3.10719 r} + 0.603269 A_4 e^{2.96984 r} \\
& + 0.244692 A_5 e^{0.64646 r} \\
x_3 = {} & 0.418537 + 0.0837058 A_1 e^{4.67016 r} - 0.364737 A_2 e^{4.02385 r} + 0.582028 A_3 e^{3.10719 r} + 0.0183412 A_4 e^{2.96984 r} \\
& - 0.259639 A_5 e^{0.64646 r} \\
y_3 = {} & 0.38797 + 0.0491905 A_1 e^{4.67016 r} + 0.00108551 A_2 e^{4.02385 r} + 0.0271857 A_3 e^{3.10719 r} + 0.603269 A_4 e^{2.96984 r} \\
& + 0.244692 A_5 e^{0.64646 r} \\
x_4 = {} & -0.164316 - 0.409271 A_1 e^{4.67016 r} + 0.341085 A_2 e^{4.02385 r} + 0.0372728 A_4 e^{2.96984 r} - 0.383014 A_5 e^{0.64646 r} \\
y_4 = {} & 0.637235 + 0.357766 A_1 e^{4.67016 r} + 0.438277 A_2 e^{4.02385 r} + 0.057542 A_4 e^{2.96984 r} + 0.206638 A_5 e^{0.64646 r} \\
x_5 = {} & -0.405889 - 0.454195 A_1 e^{4.67016 r} - 0.119006 A_2 e^{4.02385 r} - 0.153763 A_3 e^{3.10719 r} + 0.0651159 A_4 e^{2.96984 r} \\
& + 0.227142 A_5 e^{0.64646 r} \\
y_5 = {} & 0.70302 + 0.242622 A_1 e^{4.67016 r} - 0.208615 A_2 e^{4.02385 r} - 0.369948 A_3 e^{3.10719 r} + 0.0860953 A_4 e^{2.96984 r} \\
& - 0.00888242 A_5 e^{0.64646 r} \\
x_6 = {} & -0.405889 - 0.454195 A_1 e^{4.67016 r} - 0.119006 A_2 e^{4.02385 r} + 0.153763 A_3 e^{3.10719 r} + 0.0651159 A_4 e^{2.96984 r} \\
& + 0.227142 A_5 e^{0.64646 r} \\
y_6 = {} & 0.70302 + 0.242622 A_1 e^{4.67016 r} - 0.208615 A_2 e^{4.02385 r} + 0.369948 A_3 e^{3.10719 r} + 0.0860953 A_4 e^{2.96984 r} \\
& - 0.00888242 A_5 e^{0.64646 r} \\
x_7 = {} & 1.5392 + 0.330155 A_1 e^{4.67016 r} - 0.0230995 A_2 e^{4.02385 r} - 0.230127 A_4 e^{2.96984 r} + 0.0543129 A_5 e^{0.64646 r} \\
y_7 = {} & 0.637235 + 0.209394 A_1 e^{4.67016 r} + 0.0133712 A_2 e^{4.02385 r} + 0.261208 A_4 e^{2.96984 r} + 0.191916 A_5 e^{0.64646 r}
\end{aligned}
$$

We did not find a flow starting from this point. We observe that the A_4 mode breaks the symmetry at the fixed point, and hence there likely exists two inequivalent solutions, depending on whether or not they break the symmetry along the flows.

Appendix B

Scalar masses and scaling dimensions

Recall that the scaling dimensions of operators in the dual field theory can be obtained from the masses of the bulk scalar fields. They are related to the roots $\Delta_\pm$ of

$$m^2 L^2 = \Delta(\Delta - 3)\,, \tag{B.1}$$

which were given in equation (7.23). For most values of the squared masses, the scaling dimension is equal to the root Δ_+, as Δ_- lies below the unitarity bound ($\Delta \geq (d-2)/2$) and can therefore not be interpreted as the scaling dimension of an operator. However, if the squared masses are within a certain negative range, both roots $\Delta_\pm$ lie above the unitarity bound, and there is an ambiguity in defining the scaling dimension of the dual operator. As we argued in Section 7.3, this range is

$$-\frac{d^2}{4} \leq m^2 L^2 \leq \frac{4-d^2}{4}\,. \tag{B.2}$$

For our purpose, the dual field theories are formulated in $d = 3$, such that the bound becomes

$$-2.25 \leq m^2 L^2 \leq -1.25\,. \tag{B.3}$$

The ambiguity is resolved by the presence of supersymmetry, such as in the case considered in Chapter 9. Indeed, by linearizing the BPS equations, the eigenvalues of the Jacobian matrix are related to the scaling dimensions that are selected by supersymmetry. In this appendix, we compute the mass spectra at each of the vacua considered in Chapter 9 and compute the corresponding roots $\Delta_\pm$. The masses $m^2 L^2$ can be obtained from the eigenvalues of the mass matrix $\mathcal{M}$ with entries

$$\mathcal{M}^a{}_c = \frac{1}{2}\mathcal{K}^a{}_b \partial^b \partial_c V\,, \tag{B.4}$$

where indices a refer to the 14 real scalar fields, which we denoted by ϕ_a in Chapter 9, and $\mathcal{K}_{ab}$ is the 14×14 matrix specifying the kinetic terms for the fields ϕ_a. We specify which of these roots is selected by the linearized BPS equations, for which we refer readers to Tables 9.2, 9.5, 9.8 and 9.10. The values of δ_a give the selected scaling dimension by the relation

$$\Delta_a = \delta_a\,, \quad \Delta_a = 3 - \delta_a\,, \tag{B.5}$$

depending on which option satisfies the unitarity bound. These results are specified in Tables B.1 – B.4 below for each of the considered sugra theory.

P0600000	m^2L^2				-2		
	Δ_+				2		
	Δ_-				**1**		
P0719157	m^2L^2		$-2.24158(\times6)$	$-1.42509(\times6)$	$1.55051(\times1)$	$6.44949(\times1)$	
	Δ_+		1.59175	2.40825	**3.44949**	**4.44949**	
	Δ_-		**1.40825**	**0.59175**	-0.44949	-1.44949	
P0779422	m^2L^2	$-2.22222(\times3)$	-2 $(\times4)$	$-1.55556(\times3)$	$-1.12311(\times1)$	2 $(\times2)$	$7.12311(\times1)$
	Δ_+	1.66667	2	2.33333	**2.56155**	**3.56155**	**4.56155**
	Δ_-	**1.33333**	**1**	**0.66666**	0.43845	-0.56155	-1.56155
P1200000	m^2L^2	$-2.22938(\times2)$	$-2.19615(\times1)$	-2 $(\times2)$	$-1.51659(\times2)$	$-0.73205(\times1)$	
	Δ_+	1.64361	**1.73205**	2	2.35639	**2.73205**	
	Δ_-	**1.35639**	1.26795	**1**	**0.64361**	0.26795	
P1384096	m^2L^2	$2.73205(\times1)$	$3.06709(\times2)$	$8.19615(\times1)$	$8.67887(\times2)$		
	Δ_+	**3.73205**	**3.80588**	**4.73205**	**4.80588**		
	Δ_-	-0.73205	-0.80588	-1.73205	-1.80588		
	m^2L^2	$-2.24473(\times2)$	$-2.18813(\times1)$	$-1.68560(\times1)$	$-1.09949(\times2)$	$-0.10892(\times2)$	
	Δ_+	**1.57262**	1.74874	2.25126	**2.57262**	**2.96324**	
	Δ_-	1.42738	**1.25126**	**0.74874**	0.42738	0.03676	
	m^2L^2	$2.66206(\times1)$	$3.81757(\times2)$	$8.09469(\times1)$	$8.65678(\times1)$	$16.2619(\times1)$	
	Δ_+	**3.71632**	**3.96324**	**4.71632**	**4.80254**	**5.80254**	
	Δ_-	-0.71632	-0.96324	-1.71632	-1.80254	-2.80254	

Table B.1: Masses of the 14 scalar fields at vacua of SO(8) gauged supergravity. The two roots $\Delta_\pm$ are obtained using equation (B.2). Grey-coloured values of Δ_- are below the unitarity bound and hence do not correspond to scaling dimensions in the dual theory. Boldface values of $\Delta_\pm$ denote modes that are selected by the linearized BPS equations.

P1998705	m^2L^2		$-2.24158(\times 6)$	$-1.42509(\times 6)$	$1.55051(\times 1)$	6.44949		
	Δ_+		1.59175	2.40825	$\mathbf{3.44949}$	$\mathbf{4.44949}$		
	Δ_-		$\mathbf{1.40825}$	$\mathbf{0.591752}$	-0.44949	-1.44949		
P2078460	m^2L^2	$-2.22222(\times 3)$	$-2 \quad (\times 4)$	$-1.55556(\times 3)$	$-1.12311(\times 1)$	$2 \quad (\times 2)$	$7.12311(\times 1)$	
	Δ_+	1.66666	2	2.33333	$\mathbf{2.56155}$	$\mathbf{3.56155}$	$\mathbf{4.56155}$	
	Δ_-	$\mathbf{1.33333}$	$\mathbf{1}$	$\mathbf{0.66666}$	0.43845	-0.56155	-1.56155	
P2327730	m^2L^2	$-2.19615(\times 1)$	$-2 \quad (\times 6)$	$-0.73205(\times 3)$	$2.73205(\times 3)$	$8.19615(\times 1)$		
	Δ_+	$\mathbf{1.73205}$	2	$\mathbf{2.73205}$	$\mathbf{3.73205}$	$\mathbf{4.73205}$		
	Δ_-	1.26795	$\mathbf{1}$	0.26795	-0.73205	-1.73205		
P2379560	m^2L^2	$-2.22222(\times 3)$	$-2 \quad (\times 2)$	$-0.88888(\times 3)$	$0 \quad (\times 2)$	$1.55051(\times 2)$	$6.44949(\times 2)$	
	Δ_+	$\mathbf{1.66666}$	2	$\mathbf{2.66666}$	$\mathbf{3}$	$\mathbf{3.44949}$	$\mathbf{4.44949}$	
	Δ_-	1.33333	$\mathbf{1}$	0.333333	0	-0.44949	-1.44949	
P2569710	m^2L^2	-2.20661	-2.10747	-2.09876	-1.87655	-1.86254	-1.69973	-1.62323
	Δ_+	1.70831	1.87754	1.88889	2.11111	2.12246	$\mathbf{2.24180}$	2.29169
	Δ_-	$\mathbf{1.29169}$	$\mathbf{1.12246}$	$\mathbf{1.11111}$	$\mathbf{0.88889}$	$\mathbf{0.87754}$	0.75820	$\mathbf{0.70831}$
	m^2L^2	0.13418	0.783875	2.66477	2.71014	4.22234	8.09862	8.16441
	Δ_+	$\mathbf{3.04408}$	$\mathbf{3.24180}$	$\mathbf{3.71693}$	$\mathbf{3.72714}$	$\mathbf{4.04408}$	$\mathbf{4.71693}$	$\mathbf{4.72714}$
	Δ_-	-0.04408	-0.24180	-0.71693	-0.72714	-1.04408	-1.71693	-1.72714
P3561023	m^2L^2	-2.24908	-2.23926	-1.44651	-1.18847	0.01525	0.06807	2.30308
	Δ_+	$\mathbf{1.53027}$	1.60361	2.39637	$\mathbf{2.53030}$	$\mathbf{3.00507}$	$\mathbf{3.02252}$	$\mathbf{3.63380}$
	Δ_-	1.46973	$\mathbf{1.39639}$	$\mathbf{0.60363}$	0.46970	-0.00507	-0.02252	-0.63380
	m^2L^2	3.86395	4.02540	4.11312	4.61524	7.57068	9.80923	10.8556
	Δ_+	$\mathbf{3.97264}$	$\mathbf{4.00508}$	$\mathbf{4.02252}$	$\mathbf{4.12016}$	$\mathbf{4.6338}$	$\mathbf{4.97264}$	$\mathbf{5.12016}$
	Δ_-	-0.97264	-1.00508	-1.02252	-1.12016	-1.63380	-1.97264	-2.12016

Table B.2: Masses of the 14 scalar fields at vacua of ISO(7) gauged supergravity. The two roots $\Delta_\pm$ are obtained using equation (B.2). Grey-coloured values of Δ_- are below the unitarity bound and hence do not correspond to scaling dimensions in the dual theory. Boldface values of $\Delta_\pm$ denote modes that are selected by the linearized BPS equations.

F0289794($\chi_{1,2,3}=0$)	m^2L^2	$-2.22222(\times3)$	-2 $(\times2)$	$-0.88888(\times3)$	0 $(\times3)$	$1.55051(\times2)$ $6.44949(\times2)$
	Δ_+	**1.66666**	**2**	**2.66666**	**3**	**3.44949** **4.44949**
	Δ_-	1.33333	1	0.33333	0	-0.44949 -1.44949
F0289794($\chi^\star_{1,2,3}$)	m^2L^2		$-2.22171(\times2)$	$-2.22013(\times2)$	-2 $(\times2)$	$-0.88529(\times2)$
	Δ_+		**1.66821**	**1.67282**	**2**	**2.66821**
	Δ_-		1.33179	1.32718	1	0.33179
	m^2L^2		$-0.87445(\times1)$	0 $(\times2)$	$1.55051(\times2)$	$6.44949(\times2)$
	Δ_+		**2.67282**	**3**	**3.44949**	**4.44949**
	Δ_-		0.32718	0	-0.44949	-1.44949
F0300000($\chi=0$)	m^2L^2	-2 $(\times4)$	$-1.12311(\times2)$	0 $(\times2)$	2 $(\times4)$	$7.12311(\times2)$
	Δ_+	**2**	**2.56155**	**3**	**3.56155**	**4.56155**
	Δ_-	**1**	0.438447	0	-0.561553	-1.56155
F0300000($\chi=0.01$)	m^2L^2		$-2.00040(\times1)$	-2 $(\times1)$	$-1.99960(\times2)$	$-1.12311(\times2)$
	Δ_+		1.99960	**2**	**2.00040**	2.56155
	Δ_-		**1.00040**	1	**0.99960**	0.43845
	m^2L^2		0 $(\times1)$	$0.00120(\times1)$	2 $(\times4)$	$7.12311(\times2)$
	Δ_+		**3**	**3.00040**	**3.56155**	**4.56155**
	Δ_-		0	-0.00040	-0.56155	-1.56155

Table B.3: Masses of the 14 scalar fields at vacua of $[\mathrm{SO}(6)\times\mathrm{SO}(1,1)]\ltimes\mathbb{R}^{12}$ gauged supergravity. The two roots $\Delta_\pm$ are obtained using equation (B.2). Grey-coloured values of Δ_- are below the unitarity bound and hence do not correspond to scaling dimensions in the dual theory. Boldface values of $\Delta_\pm$ denote modes that are selected by the linearized BPS equations. The values of $\chi^\star_{123}$ are given in equation (9.18).

P0752907	m^2L^2		$-2.22321(\times1)$	$-2.22222(\times2)$	$-1.55059(\times1)$	$-0.88888(\times2)$	$3.42004(\times1)$	
	Δ_+		1.66369	**1.66666**	2.33631	**2.66666**	**3.88118**	
	Δ_-		**1.33631**	1.33333	**0.66369**	0.333333	-0.881184	
	m^2L^2		$4.74423(\times2)$	$9.18240(\times1)$	$10.2209(\times1)$	$11.0335(\times2)$	$18.2838(\times1)$	
	Δ_+		**4.14466**	**4.88118**	**5.03142**	**5.14466**	**6.03142**	
	Δ_-		-1.14466	-1.88118	-2.03142	-2.14466	-3.03142	
P0758297	m^2L^2	-2.21279	-2.19952	-1.64889	-1.59858	-1.42805	1.38518	3.35737
	Δ_+	1.69289	1.72468	2.27532	2.30711	**2.40661**	3.40661	3.86799
	Δ_-	**1.30711**	**1.27532**	**0.72468**	**0.69289**	0.59339	-0.40661	-0.86799
	m^2L^2	3.77399	6.93661	9.09334	9.56617	9.68275	13.9985	17.4411
	Δ_+	**3.95438**	**4.53094**	**4.86799**	**4.93747**	**4.95438**	**5.53094**	**5.93747**
	Δ_-	-0.95438	-1.53094	-1.86799	-1.93747	-1.95438	-2.53094	-2.93747

Table B.4: Masses of the 14 scalar fields at vacua of $[\mathrm{SO}(6) \times \mathrm{SO}(2)] \ltimes \mathbb{R}^{12}$ gauged supergravity. The two roots $\Delta_\pm$ are obtained using equation (B.2). Grey-coloured values of Δ_- are below the unitarity bound and hence do not correspond to scaling dimensions in the dual theory. Boldface values of $\Delta_\pm$ denote modes that are selected by the linearized BPS equations.

Bibliography

[1] S. M. Carroll. *Spacetime and geometry.* Cambridge University Press, 2019.

[2] B. P. Abbott et al. "Observation of Gravitational Waves from a Binary Black Hole Merger". In: *Phys. Rev. Lett.* 116 (6 Feb. 2016), p. 061102. DOI: 10.1103/PhysRevLett.116.061102.

[3] R. Abbott et al. "Observation of Gravitational Waves from Two Neutron Star-Black Hole Coalescences". In: *The Astrophysical Journal Letters* 915.1 (June 2021), p. L5. DOI: 10.3847/2041-8213/ac082e.

[4] B. P. Abbott et al. "GW170817: Observation of Gravitational Waves from a Binary Neutron Star Inspiral". In: *Phys. Rev. Lett.* 119 (16 Oct. 2017), p. 161101. DOI: 10.1103/PhysRevLett.119.161101.

[5] R. Azulay et al. "First M87 Event Horizon Telescope Results. I. The Shadow of the Supermassive Black Hole". In: *Astrophys.J.Lett* 875.1 (2019), pp. 1–17. ISSN: 2041-8205.

[6] K. Akiyama et al. "First Sagittarius A* Event Horizon Telescope Results. I. The Shadow of the Supermassive Black Hole in the Center of the Milky Way". In: *The Astrophysical Journal Letters* 930.2 (2022), p. L12.

[7] J. A. Wheeler and K. Ford. *Geons, black holes and quantum foam: a life in physics.* W. W. Norton & Company, 2010.

[8] S. M. Carroll. *Lecture notes on general relativity.* arXiv: gr-qc/9712019.

[9] S. Dodelson. *Modern cosmology.* Elsevier, 2003.

[10] D. Z. Freedman and A. Van Proeyen. *Supergravity.* Cambridge university press, 2012.

[11] F. Mandl and G. Shaw. *Quantum field theory.* John Wiley & Sons, 2010.

[12] J. Fuchs and C. Schweigert. *Symmetries, Lie algebras and representations: A graduate course for physicists.* Cambridge University Press, 2003.

[13] O. Aharony et al. "Large N field theories, string theory and gravity". In: *Physics Reports* 323.3 (2000), pp. 183–386. ISSN: 0370-1573. DOI: https://doi.org/10.1016/S0370-1573(99)00083-6.

[14] D. Poland, S. Rychkov, and A. Vichi. "The conformal bootstrap: Theory, numerical techniques, and applications". In: *Rev. Mod. Phys.* 91 (1 Jan. 2019), p. 015002. DOI: 10.1103/RevModPhys.91.015002.

[15] S. Ribault. "Minimal lectures on two-dimensional conformal field theory". In: *SciPost Phys. Lect. Notes* (2018), p. 1. DOI: 10.21468/SciPostPhysLectNotes.1. arXiv: 1609.09523 [hep-th].

[16] S. H. Strogatz. *Nonlinear dynamics and chaos: with applications to physics, biology, chemistry, and engineering.* CRC press, 2018.

[17] D. Skinner. "Quantum field theory II". In: *Lecture notes, Part III of the Mathematical Tripos, University of Cambridge* (2018).

[18] S. P. Martin. "A Supersymmetry Primer". In: *Perspectives on Supersymmetry*. World Scientific, July 1998, pp. 1–98. DOI: 10.1142/9789812839657_0001. arXiv: hep-ph/9709356 [hep-ph].

[19] M. Maggiore. *Gravitational waves: Volume 1: Theory and experiments*. OUP Oxford, 2007.

[20] A. Shomer. *A pedagogical explanation for the non-renormalizability of gravity*. 2007. DOI: 10.48550/ARXIV.0709.3555. arXiv: 0709.3555 [hep-th].

[21] K. Becker, M. Becker, and J. H. Schwarz. *String theory and M-theory: A modern introduction*. Cambridge university press, 2006.

[22] D. Tong. *Lectures on String Theory*. 2009. DOI: 10.48550/ARXIV.0908.0333.

[23] A. Strominger and C. Vafa. "Microscopic origin of the Bekenstein-Hawking entropy". In: *Physics Letters B* 379.1-4 (June 1996), pp. 99–104. DOI: 10.1016/0370-2693(96)00345-0.

[24] E. D'Hoker and D. Z. Freedman. *Supersymmetric Gauge Theories and the AdS/CFT Correspondence*. 2002. DOI: 10.48550/ARXIV.HEP-TH/0201253.

[25] G. 't Hooft and M. Veltman. "One loop divergencies in the theory of gravitation, Annales Poincare". In: *Phys. Theor. A* 20 (1974), p. 69.

[26] M. H. Goroff, A. Sagnotti, and A. Sagnotti. "Quantum gravity at two loops". In: *Physics Letters B* 160.1 (1985), pp. 81–86. ISSN: 0370-2693. DOI: https://doi.org/10.1016/0370-2693(85)91470-4.

[27] J. Polchinski. *Dualities of Fields and Strings*. 2014. DOI: 10.48550/ARXIV.1412.5704.

[28] C. Montonen and D. Olive. "Magnetic monopoles as gauge particles?" In: *Physics Letters B* 72.1 (1977), pp. 117–120. ISSN: 0370-2693. DOI: https://doi.org/10.1016/0370-2693(77)90076-4.

[29] E. Witten. "Five-branes and M-theory on an orbifold". In: *Nuclear Physics B* 463.2-3 (Mar. 1996), pp. 383–397. DOI: 10.1016/0550-3213(96)00032-6.

[30] S. R. Coleman and J. Mandula. "All Possible Symmetries of the S Matrix". In: *Phys. Rev.* 159 (1967). Ed. by A. Zichichi, pp. 1251–1256. DOI: 10.1103/PhysRev.159.1251.

[31] R. Haag, J. T. Lopuszanski, and M. Sohnius. "All Possible Generators of Supersymmetries of the S Matrix". In: *Nucl. Phys. B* 88 (1975), p. 257. DOI: 10.1016/0550-3213(75)90279-5.

[32] W. Nahm. "Supersymmetries and their Representations". In: *Nucl. Phys. B* 135 (1978), p. 149. DOI: 10.1016/0550-3213(78)90218-3.

[33] E. Cremmer, B. Julia, and J. Scherk. "Supergravity Theory in Eleven-Dimensions". In: *Phys. Lett. B* 76 (1978), pp. 409–412. DOI: 10.1016/0370-2693(78)90894-8.

[34] The M.C. Escher Company B.V. *Gallery - Mathematical*. 2022. URL: https://mescher.com/gallery/mathematical (visited on 06/10/2022).

[35] B. de Wit, H. Samtleben, and M. Trigiante. "The maximal $D = 4$ supergravities". In: *Journal of High Energy Physics* 2007.06 (June 2007), pp. 049–049. DOI: 10.1088/1126-6708/2007/06/049.

[36] B. de Wit, H. Samtleben, and M. Trigiante. "On Lagrangians and gaugings of maximal supergravities". In: *Nuclear Physics B* 655.1-2 (Apr. 2003), pp. 93–126. DOI: 10.1016/s0550-3213(03)00059-2.

[37] M. Trigiante. "Gauged supergravities". In: *Physics Reports* 680 (Mar. 2017), pp. 1–175. DOI: 10.1016/j.physrep.2017.03.001.

[38] N. Bobev et al. "New AdS_4 vacua in dyonic ISO(7) gauged supergravity". In: *Journal of High Energy Physics* 2021.2 (Feb. 2021). DOI: 10.1007/jhep02(2021)215.

[39] N. Bobev, F. F. Gautason, and J. van Muiden. *Holographic 3d $\mathcal{N} = 1$ Conformal Manifolds*. 2021. DOI: 10.48550/ARXIV.2111.11461.

[40] P. Breitenlohner and D. Z. Freedman. "Stability in gauged extended supergravity". In: *Annals of Physics* 144.2 (1982), pp. 249–281. ISSN: 0003-4916. DOI: https://doi.org/10.1016/0003-4916(82)90116-6.

[41] I. M. Comsa, M. Firsching, and T. Fischbacher. "SO(8) supergravity and the magic of machine learning". In: *Journal of High Energy Physics* 2019.8 (Aug. 2019). DOI: 10.1007/jhep08(2019)057.

[42] D. Z. Freedman and S. S. Pufu. "The holography of F-maximization". In: *Journal of High Energy Physics* 2014.3 (Mar. 2014). DOI: 10.1007/jhep03(2014)135.

[43] J. Maldacena. "The large N limit of superconformal field theories and supergravity". In: *International journal of theoretical physics* 38.4 (1999), pp. 1113–1133.

[44] G. 't Hooft. "A Planar Diagram Theory for Strong Interactions". In: *Nucl. Phys. B* 72 (1974). Ed. by J. C. Taylor, p. 461. DOI: 10.1016/0550-3213(74)90154-0.

[45] R. M. Wald. "The Thermodynamics of Black Holes". In: *Living Reviews in Relativity* 4.1 (July 2001). DOI: 10.12942/lrr-2001-6.

[46] S. W. Hawking. "Particle Creation by Black Holes". In: *Commun. Math. Phys.* 43 (1975). Ed. by G. W. Gibbons and S. W. Hawking. [Erratum: Commun.Math.Phys. 46, 206 (1976)], pp. 199–220. DOI: 10.1007/BF02345020.

[47] J. D. Bekenstein. "Black Holes and Entropy". In: *Phys. Rev. D* 7 (8 Apr. 1973), pp. 2333–2346. DOI: 10.1103/PhysRevD.7.2333.

[48] J. D. Bekenstein. "Entropy bounds and black hole remnants". In: *Phys. Rev. D* 49 (4 Feb. 1994), pp. 1912–1921. DOI: 10.1103/PhysRevD.49.1912.

[49] G. 't Hooft. *Dimensional Reduction in Quantum Gravity*. 1993. DOI: 10.48550/ARXIV.GR-QC/9310026.

[50] L. Susskind. "The world as a hologram". In: *Journal of Mathematical Physics* 36.11 (Nov. 1995), pp. 6377–6396. DOI: 10.1063/1.531249.

[51] J. Polchinski. *Introduction to Gauge/Gravity Duality*. 2010. DOI: 10.48550/ARXIV.1010.6134.

[52] J. H. Schwarz. "Superconformal Chern-Simons Theories". In: *Journal of High Energy Physics* 2004.11 (Nov. 2004), pp. 078–078. DOI: 10.1088/1126-6708/2004/11/078.

[53] S. Gubser, I. Klebanov, and A. Polyakov. "Gauge theory correlators from non-critical string theory". In: *Physics Letters B* 428.1-2 (May 1998), pp. 105–114. DOI: 10.1016/s0370-2693(98)00377-3.

[54] E. Witten. "Anti-de Sitter space and holography". In: *Advances in Theoretical and Mathematical Physics* 2 (1998), pp. 253–291. arXiv: hep-th/9802150 [hep-th].

[55] M. Fukuma, S. Matsuura, and T. Sakai. "Holographic Renormalization Group". In: *Progress of Theoretical Physics* 109.4 (Apr. 2003), pp. 489–562. DOI: 10.1143/ptp.109.489.

[56] D. Z. Freedman et al. "Renormalization group flows from holography supersymmetry and a c-theorem". In: *Advances in Theoretical and Mathematical Physics* 3 (1999), pp. 363–417. arXiv: hep-th/9904017 [hep-th].

[57] M. R. Pahlavani and R. Morad. *Application of AdS/CFT in Nuclear Physics*. 2014. DOI: 10.48550/ARXIV.1403.2501.

[58] Y. Kim, I. J. Shin, and T. Tsukioka. "Holographic QCD: Past, present, and future". In: *Progress in Particle and Nuclear Physics* 68 (Jan. 2013), pp. 55–112. DOI: 10.1016/j.ppnp.2012.09.002.

[59] J. Erlich et al. "QCD and a Holographic Model of Hadrons". In: *Physical Review Letters* 95.26 (Dec. 2005). DOI: 10.1103/physrevlett.95.261602.

[60] O. DeWolfe. *TASI Lectures on Applications of Gauge/Gravity Duality*. 2018. DOI: 10.48550/ARXIV.1802.08267.

[61] S. A. Hartnoll. "Lectures on holographic methods for condensed matter physics". In: *Classical and Quantum Gravity* 26.22 (Oct. 2009), p. 224002. DOI: 10.1088/0264-9381/26/22/224002.

[62] S. Sachdev. "Condensed Matter and AdS/CFT". In: *From Gravity to Thermal Gauge Theories: The AdS/CFT Correspondence*. Springer Berlin Heidelberg, 2011, pp. 273–311. DOI: 10.1007/978-3-642-04864-7_9.

[63] S. A. Hartnoll, C. P. Herzog, and G. T. Horowitz. "Building a Holographic Superconductor". In: *Physical Review Letters* 101.3 (July 2008). DOI: 10.1103/physrevlett.101.031601.

[64] N. Bobev et al. "Minimal holographic superconductors from maximal supergravity". In: *Journal of High Energy Physics* 2012.3 (Mar. 2012). DOI: 10.1007/jhep03(2012)064.

[65] R. Cai et al. "Introduction to holographic superconductor models". In: *Science China Physics, Mechanics & Astronomy* 58.6 (May 2015), pp. 1–46. DOI: 10.1007/s11433-015-5676-5.

[66] E. Akhmedov. "A remark on the AdS/CFT correspondence and the renormalization group flow". In: *Physics Letters B* 442.1-4 (Dec. 1998), pp. 152–158. DOI: 10.1016/s0370-2693(98)01270-2.

[67] L. Girardello et al. "Novel local CFT and exact results on perturbations of $\mathcal{N} = 4$ super Yang Mills from AdS dynamics". In: *Journal of High Energy Physics* 1998.12 (Dec. 1998), pp. 022–022. DOI: 10.1088/1126-6708/1998/12/022.

[68] M. Headrick. *Mathematica packages by Matthew Headrick*. 2015. URL: https://people.brandeis.edu/~headrick/Mathematica/ (visited on 06/11/2022).

[69] P. Karndumri. "On Holographic RG Flows". PhD thesis. SISSA, Trieste, 2011.

[70] A. B. Zamolodchikov. "Irreversibility of the Flux of the Renormalization Group in a 2D Field Theory". In: *JETP Lett.* 43 (1986), pp. 730–732.

[71] J. L. Cardy. "Is There a c Theorem in Four-Dimensions?" In: *Phys. Lett. B* 215 (1988), pp. 749–752. DOI: 10.1016/0370-2693(88)90054-8.

[72] Z. Komargodski and A. Schwimmer. "On renormalization group flows in four dimensions". In: *Journal of High Energy Physics* 2011.12 (Dec. 2011). DOI: 10.1007/jhep12(2011)099.

[73] T. Fischbacher. *The Encyclopedic Reference of Critical Points for SO(8)-Gauged $\mathcal{N} = 8$ Supergravity Part 1: Cosmological Constants in the Range $-\Lambda/g^2 \in [6; 14.7)$*. 2011. DOI: 10.48550/ARXIV.1109.1424.

[74] G. Gibbons, C. Hull, and N. Warner. "The stability of gauged supergravity". In: *Nuclear Physics B* 218.1 (1983), pp. 173–190. ISSN: 0550-3213. DOI: https://doi.org/10.1016/0550-3213(83)90480-7.

[75] M. Duff, B. Nilsson, and C. Pope. "Kaluza-Klein supergravity". In: *Physics Reports* 130.1 (1986), pp. 1–142. ISSN: 0370-1573. DOI: https://doi.org/10.1016/0370-1573(86)90163-8.

[76] E. Malek, H. Nicolai, and H. Samtleben. "Tachyonic Kaluza-Klein modes and the AdS swampland conjecture". In: *Journal of High Energy Physics* 2020.8 (Dec. 2020). DOI: 10.1007/jhep08(2020)159.

[77] H. Ooguri and C. Vafa. *Non-supersymmetric AdS and the Swampland*. 2016. DOI: 10.48550/ARXIV.1610.01533.

[78] N. Bobev, T. Fischbacher, and K. Pilch. "Properties of the new $\mathcal{N} = 1$ AdS_4 vacuum of maximal supergravity". In: *JHEP* 01 (2020), p. 099. DOI: 10.1007/JHEP01(2020)099. arXiv: 1909.10969 [hep-th].

[79] S. S. Gubser. "Curvature Singularities: the Good, the Bad, and the Naked". In: (2000). DOI: 10.48550/ARXIV.HEP-TH/0002160.

[80] T. Wouters. *Holographic RG flows in gauged supergravity*. 2022. URL: https://github.com/ThibeauWouters/Holographic-RG-flows-in-gauged-supergravity.

[81] T. Fischbacher. "The many vacua of gauged extended supergravities". In: *General Relativity and Gravitation* 41.2 (Dec. 2008), pp. 315–411. DOI: 10.1007/s10714-008-0736-z.

[82] B. de Wit and H. Nicolai. "$\mathcal{N} = 8$ supergravity with local $SO(8) \times SU(8)$ invariance". In: *Physics Letters B* 108.4 (1982), pp. 285–290. ISSN: 0370-2693. DOI: https://doi.org/10.1016/0370-2693(82)91194-7.

[83] B. De Wit and H. Nicolai. "$\mathcal{N} = 8$ supergravity". In: *Nuclear Physics B* 208.2 (1982), pp. 323–364. ISSN: 0550-3213. DOI: https://doi.org/10.1016/0550-3213(82)90120-1.

[84] B. De Wit and H. Nicolai. "The consistency of the S^7 truncation in $d = 11$ supergravity". In: *Nuclear Physics B* 281.1 (1987), pp. 211–240. ISSN: 0550-3213. DOI: https://doi.org/10.1016/0550-3213(87)90253-7.

[85] H. Nicolai and K. Pilch. "Consistent truncation of $d = 11$ supergravity on $AdS_4 \times S^7$". In: *Journal of High Energy Physics* 2012.3 (Mar. 2012). DOI: 10.1007/jhep03(2012)099.

[86] B. de Wit, H. Nicolai, and N. Warner. "The embedding of gauged $\mathcal{N} = 8$ supergravity into $d = 11$ supergravity". In: *Nuclear Physics B* 255 (1985), pp. 29–62. ISSN: 0550-3213. DOI: https://doi.org/10.1016/0550-3213(85)90128-2.

[87] O. Aharony et al. "$\mathcal{N} = 6$ superconformal Chern-Simons-matter theories, M2-branes and their gravity duals". In: *JHEP* 10 (2008), p. 091. DOI: 10.1088/1126-6708/2008/10/091. arXiv: 0806.1218 [hep-th].

[88] N. Bobev et al. "Holographic, $\mathcal{N} = 1$ supersymmetric RG flows on M2 branes". In: *Journal of High Energy Physics* 2009.09 (Sept. 2009), pp. 043–043. DOI: 10.1088/1126-6708/2009/09/043.

[89] A. Gallerati, H. Samtleben, and M. Trigiante. "The $\mathcal{N} > 2$ supersymmetric AdS vacua in maximal supergravity". In: *Journal of High Energy Physics* 2014.12 (Dec. 2014). DOI: 10.1007/jhep12(2014)174.

[90] N. Warner. "Some new extrema of the scalar potential of gauged $\mathcal{N} = 8$ supergravity". In: *Physics Letters B* 128.3 (1983), pp. 169–173. ISSN: 0370-2693. DOI: https://doi.org/10.1016/0370-2693(83)90383-0.

[91] T. Fischbacher. "Fourteen new stationary points in the scalar potential of SO(8)-gauged $\mathcal{N} = 8, D = 4$ supergravity". In: *Journal of High Energy Physics* 2010.9 (Sept. 2010). DOI: 10.1007/jhep09(2010)068.

[92] T. Fischbacher. "Numerical tools to validate stationary points of -gauged supergravity". In: *Computer Physics Communications* 183.3 (Mar. 2012), pp. 780–784. DOI: 10.1016/j.cpc.2011.11.022.

[93] T. Fischbacher, K. Pilch, and N. P. Warner. *New Supersymmetric and Stable, Non-Supersymmetric Phases in Supergravity and Holographic Field Theory*. 2010. arXiv: 1010.4910 [hep-th].

[94] W. Commons. *Mexican hat potential polar — Wikimedia Commons, the free media repository*. 2020. URL: https://commons.wikimedia.org/wiki/File:Mexican_hat_potential_polar.svg (visited on 06/03/2022).

[95] C. M. Hull. "New gauging of $\mathcal{N} = 8$ supergravity". In: *Phys. Rev. D* 30 (4 Dec. 1984), pp. 760–764. DOI: 10.1103/PhysRevD.30.760.

[96] A. Guarino and O. Varela. "Dyonic ISO(7) supergravity and the duality hierarchy". In: *Journal of High Energy Physics* 2016.2 (Feb. 2016). DOI: 10.1007/jhep02(2016)079.

[97] G. Dall'Agata, G. Inverso, and M. Trigiante. "Evidence for a Family of SO(8) Gauged Supergravity Theories". In: *Phys. Rev. Lett.* 109 (20 Nov. 2012), p. 201301. DOI: 10.1103/PhysRevLett.109.201301.

[98] G. Dall'Agata, G. Inverso, and A. Marrani. "Symplectic deformations of gauged maximal supergravity". In: *Journal of High Energy Physics* 2014.7 (July 2014). DOI: 10.1007/jhep07(2014)133.

[99] J. Tarrio and O. Varela. "Electric/magnetic duality and RG flows in AdS_4/CFT_3". In: *Journal of High Energy Physics* 2014.1 (Jan. 2014). DOI: 10.1007/jhep01(2014)071.

[100] A. Guarino. "On new maximal supergravity and its BPS domain-walls". In: *Journal of High Energy Physics* 2014.2 (Feb. 2014). DOI: 10.1007/jhep02(2014)026.

[101] B. de Wit and H. Nicolai. "Deformations of gauged SO(8) supergravity and supergravity in eleven dimensions". In: *Journal of High Energy Physics* 2013.5 (May 2013). DOI: 10.1007/jhep05(2013)077.

[102] K. Lee, C. Strickland-Constable, and D. Waldram. *New gaugings and non-geometry*. 2015. DOI: 10.48550/ARXIV.1506.03457.

[103] A. Guarino, D. L. Jafferis, and O. Varela. "String theory origin of dyonic $\mathcal{N} = 8$ supergravity and its Chern-Simons duals". In: *Physical Review Letters* 115.9 (Dec. 2015). DOI: 10.1103/physrevlett.115.091601.

[104] A. Guarino and O. Varela. "Consistent $\mathcal{N} = 8$ truncation of massive IIA on S^6". In: *JHEP* 12 (2015), p. 020. DOI: 10.1007/JHEP12(2015)020. arXiv: 1509.02526 [hep-th].

[105] A. Guarino, J. Tarrio, and O. Varela. "Flowing to $\mathcal{N} = 3$ Chern-Simons-matter theory". In: *JHEP* 03 (2020), p. 100. DOI: 10.1007/JHEP03(2020)100. arXiv: 1910.06866 [hep-th].

[106] K. Behrndt and M. Cvetic. "General $\mathcal{N} = 1$ supersymmetric flux vacua of (massive) type IIA string theory". In: *Phys. Rev. Lett.* 95 (2005), p. 021601. DOI: 10.1103/PhysRevLett.95.021601. arXiv: hep-th/0403049.

[107] A. Borghese, A. Guarino, and D. Roest. "All G_2 invariant critical points of maximal supergravity". In: *JHEP* 12 (2012), p. 108. DOI: 10.1007/JHEP12(2012)108. arXiv: 1209.3003 [hep-th].

[108] D. Cassani and A.-K. Kashani-Poor. "Exploiting $\mathcal{N} = 2$ in consistent coset reductions of type IIA". In: *Nucl. Phys. B* 817 (2009), pp. 25–57. DOI: 10.1016/j.nuclphysb.2009.03.011. arXiv: 0901.4251 [hep-th].

[109] A. Guarino, D. L. Jafferis, and O. Varela. "String Theory Origin of Dyonic $\mathcal{N} = 8$ Supergravity and Its Chern-Simons Duals". In: *Phys. Rev. Lett.* 115.9 (2015), p. 091601. DOI: 10.1103/PhysRevLett.115.091601. arXiv: 1504.08009 [hep-th].

[110] A. Guarino, J. Tarrio, and O. Varela. "Romans-mass-driven flows on the D2-brane". In: *Journal of High Energy Physics* 2016.8 (Aug. 2016). DOI: 10.1007/jhep08(2016)168.

[111] N. Bobev, F. F. Gautason, and J. van Muiden. "The holographic conformal manifold of 3d $\mathcal{N} = 2$ S-fold SCFTs". In: *JHEP* 07.221 (2021), p. 221. DOI: 10.1007/JHEP07(2021)221. arXiv: 2104.00977 [hep-th].

[112] A. Guarino and C. Sterckx. "S-folds and holographic RG flows on the D3-brane". In: *JHEP* 06 (2021), p. 051. DOI: 10.1007/JHEP06(2021)051. arXiv: 2103.12652 [hep-th].

[113] A. Guarino, C. Sterckx, and M. Trigiante. "$\mathcal{N} = 2$ supersymmetric S-folds". In: *Journal of High Energy Physics* 2020.4 (Apr. 2020). DOI: 10.1007/jhep04(2020)050.

[114] B. Assel and A. Tomasiello. "Holographic duals of 3d S-fold CFTs". In: *Journal of High Energy Physics* 2018.6 (June 2018). DOI: 10.1007/jhep06(2018)019.

[115] A. Guarino and C. Sterckx. "S-folds and (non-)supersymmetric Janus solutions". In: *Journal of High Energy Physics* 2019.12 (Dec. 2019). DOI: 10.1007/jhep12(2019)113.

[116] E. D'Hoker, J. Estes, and M. Gutperle. "Interface Yang-Mills, supersymmetry, and Janus". In: *Nuclear Physics B* 753.1-2 (Oct. 2006), pp. 16–41. DOI: 10.1016/j.nuclphysb.2006.07.001.

[117] N. Bobev et al. "Janus and J-fold solutions from Sasaki-Einstein manifolds". In: *Physical Review D* 100.8 (Oct. 2019). DOI: 10.1103/physrevd.100.081901.

[118] G. Inverso, H. Samtleben, and M. Trigiante. "Type II supergravity origin of dyonic gaugings". In: *Physical Review D* 95.6 (Mar. 2017). DOI: 10.1103/physrevd.95.066020.

[119] A. Guarino, C. Sterckx, and M. Trigiante. "$\mathcal{N} = 1$ supersymmetric S-folds". In: *Journal of High Energy Physics* 2020.4 (Apr. 2020). DOI: 10.1007/jhep04(2020)050.

[120] A. Giambrone et al. "Global properties of the conformal manifold for S-fold backgrounds". In: *Journal of High Energy Physics* 2021.6 (June 2021). DOI: 10.1007/jhep06(2021)111.

[121] N. Evans and M. Petrini. "AdS RG-flow and the super-Yang-Mills cascade". In: *Nuclear Physics B* 592.1-2 (Jan. 2001), pp. 129–142. DOI: 10.1016/s0550-3213(00)00593-9.

[122] A. Khavaev and N. P. Warner. "A class of supersymmetric RG flows from five-dimensional supergravity". In: *Physics Letters B* 495.1-2 (Dec. 2000), pp. 215–222. DOI: 10.1016/s0370-2693(00)01228-4.

[123] K. Pilch and N. P. Warner. "$\mathcal{N} = 2$ supersymmetric RG flows and the IIB dilaton". In: *Nuclear Physics B* 594.1-2 (Jan. 2001), pp. 209–228. DOI: 10.1016/s0550-3213(00)00656-8.

[124] N. Bobev, D. Cassani, and H. Triendl. "Holographic RG flows for four-dimensional $\mathcal{N} = 2$ SCFTs". In: *Journal of High Energy Physics* 2018.6 (June 2018). DOI: 10.1007/jhep06(2018)086.

[125] I. Arav et al. "Marginal deformations and RG flows for type IIB S-folds". In: *Journal of High Energy Physics* 2021.7 (July 2021). DOI: 10.1007/jhep07(2021)151.

Index

B_n, 20
C_n, 20
D_n, 20
$\frac{n_Q}{\mathcal{N}}$-BPS, 43
$\mathbb{Z}_2^3$-invariant truncation, 52
$\mathfrak{gl}(n)$, 18
$\mathfrak{sl}(n)$, 20
$\mathfrak{so}(2n)$, 20
$\mathfrak{so}(2n+1)$, 20
$\mathfrak{sp}(n)$, 20
't Hooft coupling, 57, 61
't Hooft limit, 57, 61
R-symmetry, 43
S-duality, 38
p-brane, 37
p-form, 11

abelian, 18
action, 23
algebra, 17
anti-commutator, 23
anti-de Sitter, 14
anti-symmetrization, 11
atlas, 8
    maximal, 8

beta-function, 31
BPS bound, 43
BPS solution, 43, 55

canonical form, 12
Cartan subalgebra, 18
central charges, 43
character, 21
chart, 8
    compatible, 8
Chern-Simons, 77
    level, 77
chiral fermions, 41
chiral multiplet, 51
chiral primary operator, 45
chiral projection, 41
Christoffel symbols, 13
Clifford algebra, 23
commutator, 13
conformal field theory, 25
conformal primary operator, 26
conformal supercharge, 44
Conformal symmetry, 22
connection, 12
    Christoffel, 13
    coefficients, 12
    Levi-Civita, 13
    spin, 46
consistent truncation, 48, 52
contraction, 11
coordinate basis, 9
coordinate indices, 46
coordinate system, 8
cosmological constant, 14
cotangent space, 10
covariant derivative
    in GR, 12
    in QFT, 24
    Kähler, 51
curvature tensor, 13

Dp-branes, 37
descendant operators, 26, 44
dimensional reduction, 48
domain wall, 67
dual vector space, 10
duality, 38
dynamical system, 28
dyonic gauging, 95

Einstein equation, 14
Einstein metric, 15
Einstein space-time, 15
Einstein summation convention, 9
Einstein-Hilbert action, 14
electric gauging, 95
energy-momentum tensor, 14
Euler-Lagrange equations, 23
exponential mapping, 19
extended supersymmetry, 42
exterior derivative, 11

field strength, 24
field-operator correspondence, 62
fixed point, 29
flow, 28
frame fields, 46

gamma matrices, 23
gauge coupling, 24
gauge field, 24
gauge symmetry, 23
gauged supergravity, 51
geodesic, 13
    equation, 13
gradient descent, 80
gravitino, 47
gravitons, 35
group, 17

heterotic string theory, 36
highest-weight representation, 20
holographic dictionary, 61
holography, 58
holomorphic superpotential, 50
horizon, 16

ideal, 20
internal manifold, 36, 48
irrelevant operator, 32

Jacobian matrix, 29

Kaluza-Klein compactification, 48
Kähler, 49
    manifold, 49
    metric, 49
    potential, 49
Kähler covariant derivative, 51
Kähler covariant extrema, 54

Lagrangian density, 23
length scale, 15
Lie algebra, 18
    classical, 20
    exceptional, 21
    orthogonal, 20
    symplectic, 20
Lie bracket, 18
Lie group, 19
line element, 11
linearization, 29
local frame, 46
local frame indices, 46
loss function, 80

M-theory, 39
Majorana conjugate, 41
Majorana spinor, 41
manifold, 8
marginal operator, 32
matter multiplets, 50
maximally supersymmetric, 43
maximally symmetric space-time, 14
metric, 11
metric compatible, 13
minimal substitution, 24
Minkowski space-time, 12
mode, 79
multiplet, 20

non-abelian gauge theory, 24

operator product expansion, 27
orbit, 92

phase space, 28
planar diagram, 57
Planck length, 36
Planck mass, 36
Poincaré disk, 50
Poincaré group, 22
Poincaré patch, 16
Poincaré plane, 49

rank, 10
    of a gamma matrix, 40
    of a Lie algebra, 18

of a tensor, 10
real forms, 21
Regge slope, 35
regularization, 25
relevant operator, 32
renormalizable, 25
renormalization, 25
renormalization group, 31
representation, 19
irreducible, 20
Ricci scalar, 14
Ricci tensor, 13
Riemann tensor, 13
running coupling constant, 31

saddle point, 29
scalar manifold, 49
scalar potential, 51
scale factor, 67
scale transformations, 22
scaling dimension, 26
semisimple elements, 18
short representation, 45
signature, 12
Lorentzian, 12
simple, 20
simple supersymmetry, 42
single-trace operators, 45
special conformal transformations, 22
spin connection, 46
spinor fields, 23
spinor indices, 23
step descent algorithm, 81
string theory, 35
strong/weak duality, 38
structure constants, 18
subalgebra, 18
super Yang-Mills, 45
superalgebra, 42
superconformal algebra, 44
superconformal field theories, 44
superconformal primary operator, 44
supergravity limit, 38
supermultiplets, 34
superstring theories, 36
supersymmetry, 34
supersymmetry transformations, 43
symmetrization, 11
symmetry, 17

tachyonic modes, 54
tangent space, 9
tensor, 10
torsion tensor, 12
triangular holographic RG flow, 85

unitarity bound, 26

vacua, 54
vacuum energy, 14

wedge product, 11
Weyl fields, 41
Weyl weight, 44
world-line, 13
world-sheet, 37
world-volume, 37

Yang-Mils theory, 24

Institute for Theoretical Physics
Celestijnenlaan 200D box 2415
3001 LEUVEN, BELGIË
tel. +32 16 32 72 32
www.kuleuven.be